NIST GCR 22-917-51

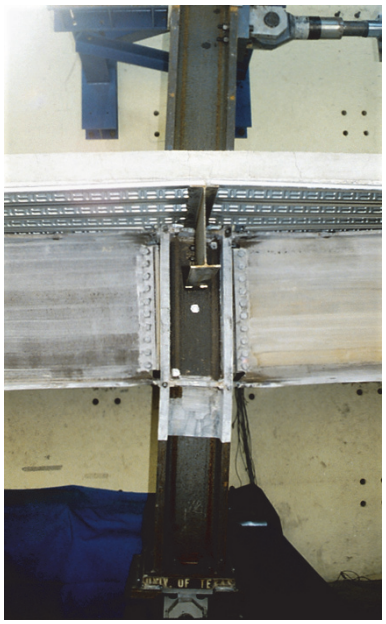

Research Plan for the Study of Pre-Northridge Earthquake PJP-welded Column Splices and Weak Panel Zones

Applied Technology Council

This publication is available free of charge from:
https://doi.org/10.6028/NIST.GCR.22-917-51

nehrp

NIST
National Institute of Standards and Technology
U.S. Department of Commerce

Disclaimer

This report was prepared for the Engineering Laboratory of the National Institute of Standards and Technology (NIST) under Contract 1333ND20PNB730779. The contents of this publication do not necessarily reflect the views and policies of NIST.

This report was produced by the Applied Technology Council (ATC). While endeavoring to provide practical and accurate information, the Applied Technology Council, the authors, and the reviewers assume no liability for, nor express or imply any warranty with regard to, the information contained herein. Users of information contained in this report assume all liability arising from such use.

Unless otherwise noted, photos, figures, and data presented in this report have been developed or provided by ATC staff or consultants engaged under contract to provide information as works for hire. Any similarity with other published information is coincidental. Photos and figures cited from outside sources have been reproduced in this report with permission. Any other use requires additional permission from the copyright holders.

Certain commercial software, equipment, instruments, or materials may have been used in the preparation of information contributing to this report. Identification in this report is not intended to imply recommendation or endorsement by NIST, nor is it intended to imply that such software, equipment, instruments, or materials are necessarily the best available for the purpose.

NIST policy is to use the International System of Units (metric units) in all its publications. In this report, however, information is presented in U.S. Customary Units (inch-pound), as this is the preferred system of units in the U.S. engineering industry.

Cover image – Experiment from the SAC Steel Project of a steel moment frame beam-to-column connection exhibiting weak panel zone behavior (Engelhardt et al., 2000).

NIST GCR 22-917-51

Research Plan for the Study of Pre-Northridge Earthquake PJP-welded Column Splices and Weak Panel Zones

Prepared for
U.S. Department of Commerce
Engineering Laboratory
National Institute of Standards and Technology
Gaithersburg, MD 20899-8600

By
Applied Technology Council
201 Redwood Shores Parkway, Suite 240
Redwood City, CA 94065

This publication is available free of charge from:
https://doi.org/10.6028/NIST.GCR.22-917-51

September 2022

U.S. Department of Commerce
Gina M. Raimondo, Secretary

National Institute of Standards and Technology
Laurie E. Locascio, Under Secretary of Commerce for Standards and Technology and Director

Participants

National Institute of Standards and Technology

John (Jay) Harris, Research Structural Engineer
Earthquake Engineering Group, Materials and Structural Systems Division, Engineering Laboratory
www.NEHRP.gov

Applied Technology Council

201 Redwood Shores Parkway, Suite 240
Redwood City, California 94065
www.ATCouncil.org

Program Management

Jon A. Heintz
Ayse Hortacsu
Chiara McKenney (Project Manager)

Project Technical Committee

James O. Malley (Project Director)
Masume Dana
Amit Kanvinde
Larry Kruth
Duane Miller
Robert Pekelnicky
Thomas Sabol
Chia-Ming Uang

Working Group

Aditya Jhunjhunwala
Mathew Reynolds

Preface

In 2020, the National Institute of Standards and Technology (NIST) awarded Contract 1333ND20PNB730779 to the Applied Technology Council to develop a long-range research plan to study the seismic behavior of pre-Northridge Earthquake column splices with partial joint penetration (PJP) groove welds and weak panel zones (ATC-153 project). The resulting plan is a summary of needed experimental and computational research tasks that are designed to result in the development of state-of-the-art evaluation criteria and guidance on retrofit and repair solutions.

The Applied Technology Council is indebted to the leadership of James Malley, Project Director, to the members of the Project Technical Committee, consisting of Masume Dana, Amit Kanvinde, Larry Kruth, Duane Miller, Robert Pekelnicky, Thomas Sabol, and Chia-Ming Uang, for their contributions in developing this report, and to the Project Working Group consisting of Aditya Jhunjhunwala and Mathew Reynolds.

The Applied Technology Council also gratefully acknowledges John (Jay) Harris (Acting NEHRP Director and NIST Project Manager) for his input and guidance in the preparation of this report, Chiara McKenney for ATC project management, and Ginevra Rojahn for ATC report production services.

Ayse Hortacsu
ATC Director of Projects

Jon Heintz
ATC Executive Director

Table of Contents

List of Figures

List of Tables

Chapter 1
Introduction

Many steel moment frame buildings designed between the 1960s and 1990s include column splices and beam-to-column connections that are seismically vulnerable. The 1994 earthquake in Northridge, California exposed these deficiencies and led to improved seismic design and construction practices for new steel moment frames. Nonetheless, almost 30 years after the earthquake, there are still major gaps in the guidance that structural engineers use to evaluate and retrofit existing steel moment frame buildings that were designed before practices were improved. Thousands of such buildings, which are commonly referred to as *pre-Northridge,* remain in use today, including some high-rise buildings and facilities that serve essential functions in earthquakes (FEMA, 2000d).

This report defines the scope of a comprehensive, long-range research plan to better understand the seismic behavior of two major vulnerabilities of pre-Northridge steel moment frames: column splices constructed with partial joint penetration groove welds (*PJP column splices*) and weak panel zones in beam-to-column moment connections. The plan includes experiments and analyses related to fracture mechanics, subassemblage-level behavior, and system-level performance. Tasks in the research plan are designed to culminate in improved modeling and evaluation criteria that can be readily incorporated into future editions of ASCE/SEI 41, *Seismic Evaluation and Retrofit of Existing Buildings*, and AISC 342, *Seismic Provisions for Evaluation and Retrofit of Existing Structural Steel Buildings*. The tasks are also designed to result in the development of practical seismic retrofit and post-earthquake repair solutions.

1.1 Definition of the Problem

Column splice connections and panel zones (Figure 1-1) are integral to the resistance of earthquake forces in steel moment frames; failure of either component has the potential to compromise structural safety.

Column splices in a moment frame transfer loads from the upper column sections to lower column sections. Pre-Northridge PJP column splices (Figure 1-2) rely on PJP welds to transfer these forces, but the welds of the era are brittle and prone to fracture in earthquakes. Weld fracture can occur suddenly and trigger failure of the entire splice joint, which in turn can cause large drifts or loss of axial load-carrying capacity of the columns, potentially leading to collapse.

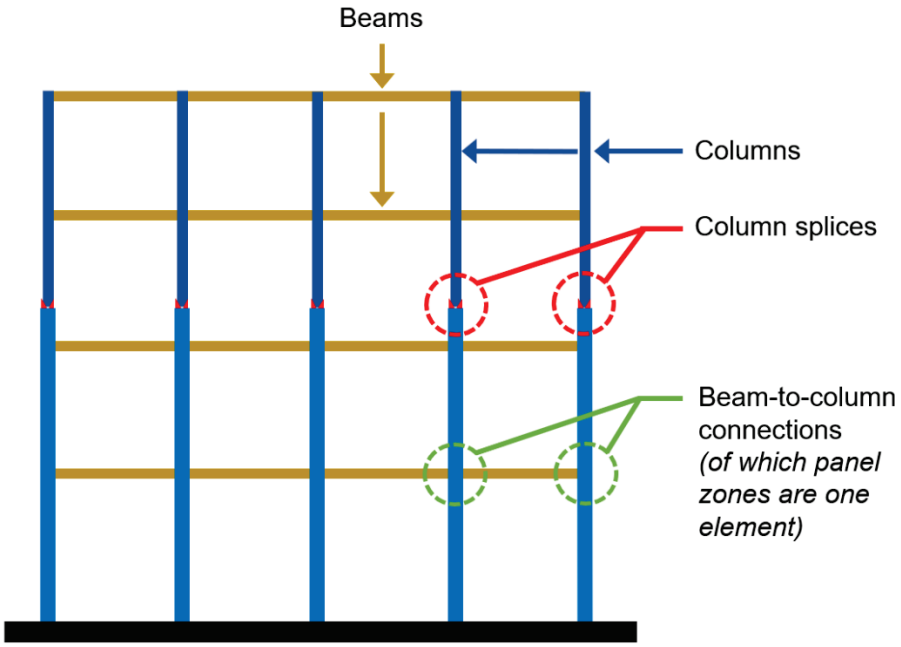

Figure 1-1 Steel moment frame elevation with column splices and beam-to-column connections indicated.

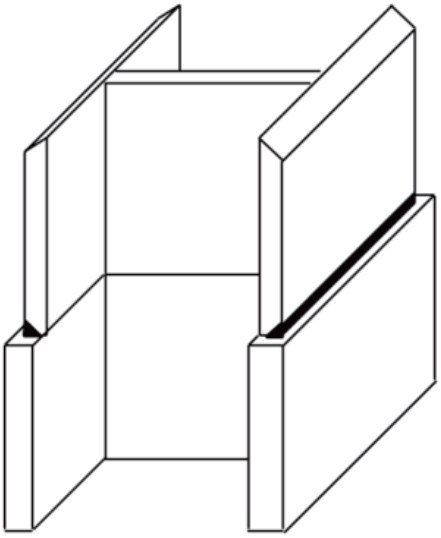

Figure 1-2 Typical pre-Northridge PJP column splice (NIST, 2017).

No column splice fractures were reported in buildings damaged by the Northridge Earthquake (FEMA, 2000c). However, there is little documentation of inspections that explicitly checked the column splices for damage, and it is possible that in some cases, the damage at the beam-to-column connections protected the column splices. Column splice fractures were observed in the 1995 Kobe Earthquake (AIJ, 1995), and analytical studies suggest that pre-Northridge PJP column splices are a concern that requires further investigation, especially due to their brittle failure mode.

Panel zones transfer the beam end moments to the columns (Figure 1-3). By definition, panel zones that are *weak* yield in earthquakes before the adjacent beams yield. Though the deformation of a pre-Northridge weak panel zone itself is ductile, it can trigger bending in the column flanges and fracture the brittle complete joint penetration (CJP) groove weld connecting the beam flange to the column flange (Figure 1-4). Fracture of this weld is one of the most common types of earthquake damage observed in pre-Northridge moment frames (Figure 1-5). The details of the interaction between the panel zone and its adjacent components are not well understood.

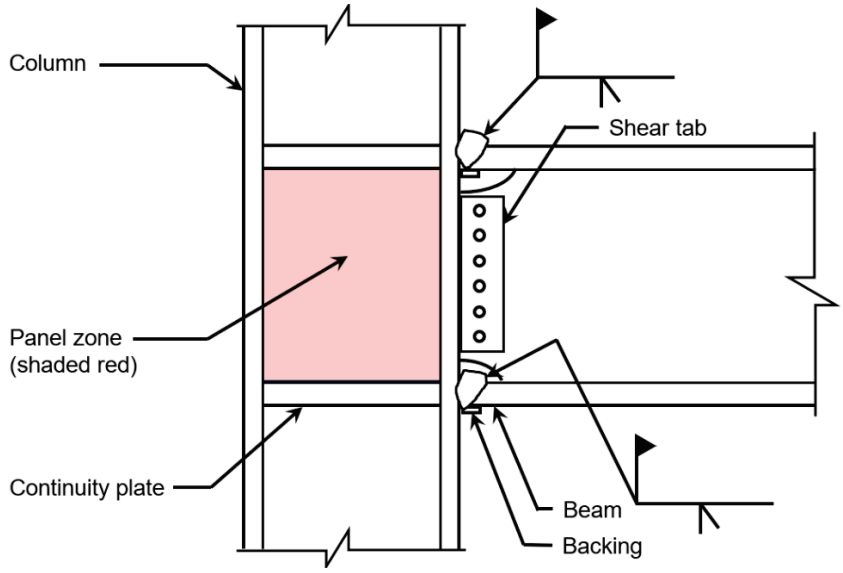

Figure 1-3 A typical pre-Northridge beam-to-column moment connection. The panel zone is the portion of the column between the beam flange elevations.

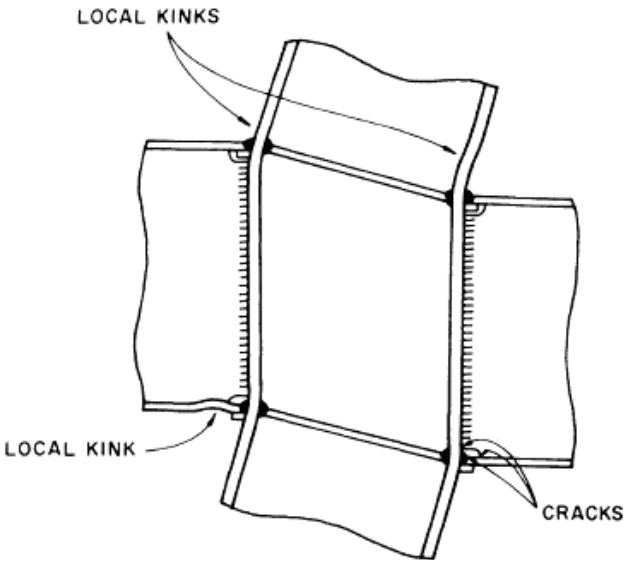

Figure 1-4 Column behavior when subjected to large panel zone displacements (Krawinkler et al., 1971).

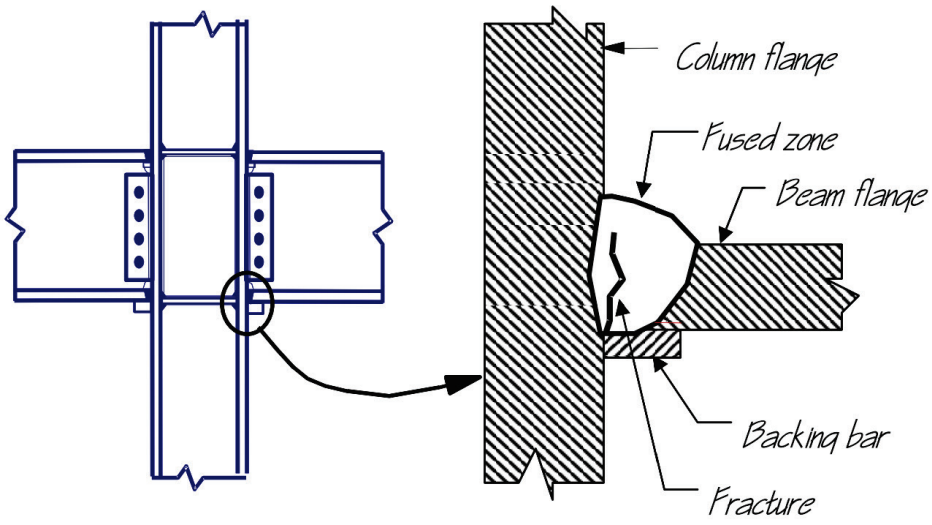

Figure 1-5 Typical location of fracture initiation in a pre-Northridge beam-to-column connection detail (FEMA, 2000c).

Pre-Northridge buildings with PJP column splices and weak panel zones remain prevalent in the U.S. building stock, but most of these buildings have not been evaluated or retrofitted. In the pre-Northridge era, many major buildings in seismic regions of the United States were constructed with steel moment frames. Some pre-Northridge buildings currently serve as essential facilities, such as hospital buildings, emergency command centers, and government office buildings. Most high-rise and some mid-rise buildings constructed in the United States during the pre-Northridge era are steel moment frames. To a lesser extent, steel moment frames were also used in low-rise assembly occupancy buildings built during this period (FEMA, 2000d). In addition to the overall large number of these buildings and potential seismic safety risk they pose, the use of some for essential functions and large occupancies mean that damage to these buildings in an earthquake could have a pronounced effect on recovery.

Until 1994, engineers assumed that steel moment frames would exhibit ductile behavior and perform well in earthquakes. The observations of brittle weld fractures in the 1994 Northridge Earthquake and 1995 Kobe Earthquake alarmed the structural engineering community and served as the impetus for the major improvements in seismic design and construction of steel moment frames that occurred in the late 1990s (FEMA, 2000c). The project to develop the recommended improvements, known as the *SAC Project*, was funded by the Federal Emergency Management Agency (FEMA) and managed by a joint venture between the Structural Engineers Association of California (SEAOC), the Applied Technology Council (ATC), and California Universities for Research in Earthquake Engineering (CUREe). The SAC Project was a multi-phase, multi-year effort of experimental and computational studies on the performance of steel moment frame connections of various configurations. The SAC Project had far-reaching implications on design and

construction of new steel moment frame buildings, including the improved design of column splices and panel zones. However, limited funding was available to develop recommendations for evaluation, retrofit, and post-earthquake repair. Existing PJP column splices and weak panel zones were not thoroughly researched in the SAC Project, nor was evaluation or retrofit guidance for them developed as part of the project.

Evaluation guidance for PJP column splices and beam-to-column moment connections with weak panel zones remains limited to this day, and current practices are inconsistent across the structural engineering community. Engineers evaluating pre-Northridge moment frames buildings could be applying conservative assumptions that lead to excessive retrofit costs or unconservative assumptions that do not adequately address the risk. Though inclusion of a check for column splice fracture potential is planned for the forthcoming 2023 edition of ASCE/SEI 41 (via AISC 342-22), the evaluation criteria lack the refinement that fundamental research can provide. For panel zones, no measures to-date have been developed to evaluate the parameters that contribute to fracture.

Engineers currently lack practical guidance for cost-effective retrofit solutions for these components, and if they are damaged in a future earthquake, there is no repair guidance readily available to engineers. Practical retrofit guidance is crucial to support risk mitigation; post-earthquake repair guidance is critical to support post-earthquake recovery.

Insufficient fundamental research into the seismic behavior of pre-Northridge PJP column splices and weak panel zones is the major roadblock to developing the guidance for modeling, evaluation, retrofit, and post-earthquake repair of PJP column splices and weak panel zones. The critical need for research is especially pronounced for PJP column splices because there has only been one experiment on pre-Northridge column splices (Bruneau and Mahin, 1991), and the consequence of splice failure would be severe, with a potential for structural collapse.

The present state of knowledge and research gaps that should be addressed are described in more detail in other parts of this report. Concise summaries are provided in Section 4.2 for column splices and Section 5.2 for panel zones. Comprehensive summaries are provided in Appendix A for column splices and in Appendix B for panel zones.

1.2 Pre-Northridge and Post-Northridge Terms

This report describes steel moment frame design and construction practices as either *pre-Northridge* or *post-Northridge*. These terms are used to delineate between the eras for simplicity and because they are commonly used in the steel design and construction profession.

The term *pre-Northridge* is used to refer to typical design and construction practices for welded steel moment frames from the 1960s until the 1994 Northridge Earthquake. Some connections of that era are susceptible to fracture due to inherent flaws in the detailing and the lack of consistent quality assurance and quality control requirements at the time of construction.

The term *post-Northridge* is used to refer to the design and construction practices for welded steel moment frames after they were improved based on observations from the 1994 Northridge Earthquake and recommendations from the SAC Project. Welded connections use either CJP welds that meet the design and construction requirements for demand-critical welds in accordance with AISC 341, *Seismic Provisions for Structural Steel Buildings*, or PJP welds that meet the requirements of Section E3.6g of AISC 341. These welding provisions were developed specifically in response to the fractures observed in the Northridge Earthquake. Some national consensus standards (e.g., ASCE/SEI 41) have adopted the terms *compliant* and *non-compliant* to delineate between welds that do and do not comply with AISC 341.

Some elements of pre-Northridge connection configurations and detailing are still allowed by present design standards for structures expected to have low seismic demands. Pre-Northridge connections are still constructed in some parts of the United States.

1.3 Project Approach

In developing this research plan, an extensive literature review of relevant existing information was conducted. Based on the information collected, key issues related to the performance of pre-Northridge column splices and weak panel zones were identified (Chapter 2). These issues form the basis of computational and experimental research outlined in this plan.

Major activities in this research plan are organized into PJP column splice studies, weak panel zone studies, and system studies addressing both components. The plan also includes an effort at the start of the program to identify archetype buildings to form the basis for the selection of subassemblages and systems to be studied (Chapter 3). The archetypes are intended to represent the range of structural characteristics that are associated with pre-Northridge PJP column splices and weak panel zones.

Although the activities of the research plan have been structured and specifically identified, it is understood that the program will evolve as implementation occurs. Wherever possible, innovative ideas for new experimental and analytical approaches should be encouraged to resolve technical issues that cannot be addressed with present techniques or could not have been foreseen with present knowledge.

Activities in the research plan could be combined with research activities supporting NIST GCR 11-917-13, *Research Plan for the Study of Seismic Behavior and Design of Deep, Slender Wide Flange Structural Steel Beam-Column Members* (NIST, 2011b).

1.4 Overview of Research Plan

The objectives of the research program described in this plan are to gain a comprehensive understanding of the seismic behaviors of pre-Northridge PJP column splices and weak panel zones and to use that understanding to inform practical guidance for engineers, including state-of-the-art modeling and evaluation criteria, guidance on retrofit solutions, and guidance on post-earthquake repair solutions.

Figure 1-6 is a flowchart for the anticipated major workflows of the overall research plan. The plan begins with the identification of archetype building configuration designs (Section 3.1) and preliminary system-level analyses (Section 3.2) that will form the basis for the experimental and computational studies described in Chapters 4 through 6. Significant integration and collaboration will be required between the experimental and computational investigations, with each informing the other. The computational investigations will consist of continuum finite element (CFE) analysis work to evaluate system behavior using component-specific configurations and frame analyses. The repair and retrofit portions of the programs will be integrated into the experimental and computational studies for both the column splice and panel zone research work. As a result, it is not expected that the experimental or computational plans will be completely developed prior to commencement of the research program. Rather, the plan will evolve to reflect important findings from the program as they are generated.

Once the major findings and recommendations for both the column splice and panel zone studies are completed, the second phase of the system-level investigation plans will take place (Chapter 6). Advanced computational models will be used to address the range of configurations, connection details, and other parameters that were common in the pre-Northridge era (Section 6.2). These studies will build on the results and recommendations from the column splice studies (Chapter 4) and panel zones studies (Chapter 5). System-level experimental studies (Section 6.3), including both hybrid and shake table testing, are proposed to capture overall system behavior. As with the column splice and panel zone studies, it is anticipated that there will be extensive integration of the system-level studies to maximize the value of the overall program.

Upon completion of the system-level studies, a final set of recommendations, products, and implementation plans will be developed and shared with the structural engineering community (see Section 7.7).

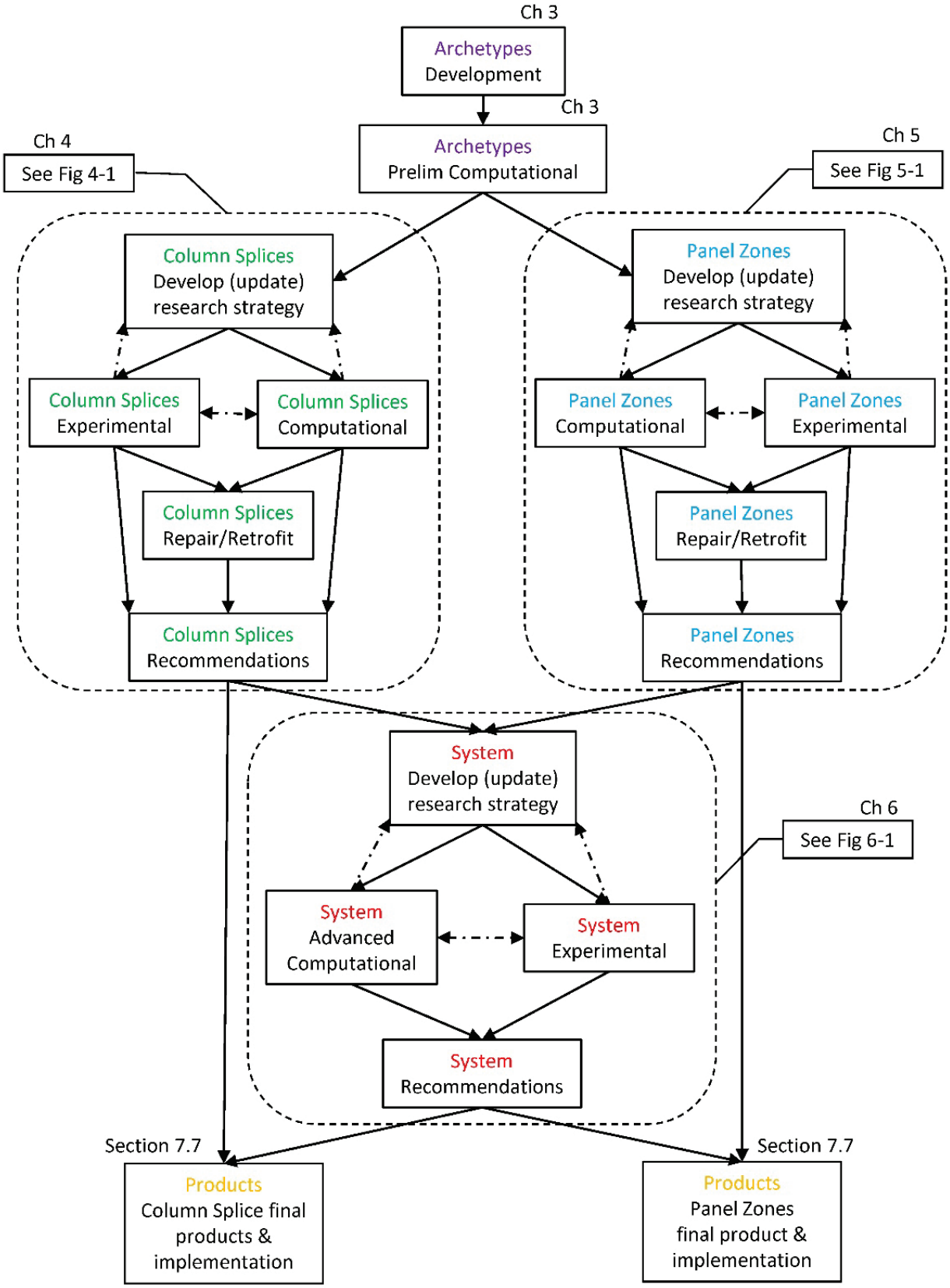

Figure 1-6 Overview of overall research plan.

1.5 Report Organization and Content

This research plan summarizes available information, defines key areas of need, provides recommendations for additional study and testing, and provides an order of magnitude estimate of the approximate level of effort. The plan is intended to be coordinated with other National Earthquake Hazard Reduction Program (NEHRP) partner agencies, representative industry organizations, and national model building codes and standards development organizations.

The remaining chapters of this report are organized as follows:

- Chapter 2 identifies key issues related to the performance of pre-Northridge PJP column splices and weak panel zones.
- Chapter 3 describes the identification of archetype buildings and preliminary system analyses on these buildings.
- Chapter 4 outlines recommendations for studying pre-Northridge PJP column splice behavior.
- Chapter 5 outlines recommendations for studying pre-Northridge weak panel zone behavior.
- Chapter 6 outlines recommendations for studying overall system behavior and performance for both PJP column splices and weak panel zones.
- Chapter 7 summarizes the recommended tasks, approximate schedule, and budget to conduct the research plan and lists key collaborators that should be involved the research.

Comprehensive summaries of relevant research are provided in Appendix A for pre-Northridge PJP column splices and Appendix B for pre-Northridge panel zones. Appendix C summarizes important characteristics that can be included in the CFE simulations in the research program.

Lists of acronyms and key terms used throughout the report, along with references and project participants, are provided at the end of the report.

Chapter 2

Key Issues

This chapter provides a summary of key issues to consider in the research. Each issue represents a parameter that influences seismic behavior or informs analysis methods. Addressing the knowledge gaps present in these issue areas will serve the development of evaluation, retrofit, and post-earthquake repair guidance.

Critical to understanding and modeling seismic behavior of a component is understanding how it fails or causes failure. Based on past earthquake performance and experimental testing, failure modes for pre-Northridge PJP column splices and weak panel zones are understood as follows:

- **PJP column splices**: Fracture can initiate in the PJP weld, fusion zone, heat-affected zone (HAZ), or area near the weld access hole. The weld is especially prone to fracture due material properties (Section 2.2; Section 3.1.7) and because the root of the weld is unfused. Failure is sudden, with little to no inelastic response prior to fracture initiation, and can result in failure of the entire splice connection.
- **Weak panel zones**: Unless the panel zone has high slenderness, which is uncommon in practice, weak panel zones themselves do not fail; rather, flexible behavior of the weak panel zone triggers failure of another component in the beam-to-column connection. Weak panel zones deform in shear when they yield, and in cases where the panel zone is classified as weak, this occurs before the beams develop plastic hinges. Though the inelastic deformation is ductile, it can cause local column flange bending at the corners of the panel zone, called *kinking*, and high strains between the beam and column flanges. The high local strain demands can cause the welded joint between the beam and column flanges to fracture, as was observed after the Northridge Earthquake.

Exploration of the following key issues are expected to help the investigators characterize and model behavior of PJP column splices and weak panel zones:

- Section and member slenderness
- Weld parameters and local detailing practices
- Effect of composite slabs, restraint, and boundary conditions
- Ratio of beam-to-column flexural strength
- Column splice detailing

- Effect of panel zone behavior on beam-to-column connection demands
- Modeling of inelastic response in beam-to-column connections

Many of the issues are interrelated and require consideration through a combination of component-specific activities (i.e., column splice or beam-to-column connection testing) and system-based activities. Other issues are more specific to a single activity of the recommended research plan. Key background on each issue is provided in this chapter.

2.1 Section and Member Slenderness

Beam and column section slenderness (i.e., width-to-thickness ratios) impact the ductility of steel moment frame systems. High local slenderness ratios can lead to local buckling and strength degradation. The current provisions, AISC 341, *Seismic Provisions for Structural Steel Buildings*, and ASCE/SEI 41, recognize this by including limitations on performance parameters that depend on width-to-thickness ratios for both wide flange and hollow structural shape sections. Prior to the Northridge Earthquake, there were few restrictions on the member and section slenderness ratios in the *Uniform Building Code*. As a result, it is expected that the beam and column configurations utilized in most pre-Northridge moment frames do not meet present standards and are a limiting factor on the ductility of these frames.

The strong-axis dominance of deep, slender wide-flange column sections makes them more susceptible to weak axis failure modes (e.g., flexural buckling, lateral torsional buckling). Recent tests (Ozkula, et al., 2021; NIST, 2021) demonstrate the reduced column flexural ductility that results from high member slenderness ratios, especially under significant axial loading. These test results are expected to result in changes to AISC 341 that will further restrict the use deep column special moment frames.

2.2 Weld Parameters and Local Detailing Practices

Pre-Northridge PJP column splices and weak panel zones are both associated with weld fractures. Many of the fractures in moment frame beam-to-column connections observed after the Northridge Earthquake initiated within the beam-flange-to-column-flange CJP joints, often near the *root pass,* the first weld pass in the welded joint. Weld procedures, filler metal properties, and local detailing practices, which all varied over the course of the pre-Northridge era, influence the susceptibility of the welds to fractures.

The weld placement procedure affects the weld properties. The earliest applications of welded moment connections in the 1950s used shielded metal arc welding (SMAW), also known as stick welding, for both shop and field welding operations. In the late 1960s, flux core arc welding (FCAW) replaced SMAW for most field operations including beam-flange-to-column-flange CJP welds and column splice

PJP welds. Until the mid-1990s, self-shielded FCAW welding was used in most field conditions. Shop welding applications, such as for web doubler plates and continuity plates in panel zone regions, may have been made with either FCAW or gas metal arc welding (GMAW) processes, depending on the preference of the fabrication shop (FEMA, 2000b).

Seismic performance of a welded joint is impacted by characteristics of the *filler metal*, metal added in the welding process to fill the joint. The various types of filler metal used in the pre-Northridge era are associated with low *notch toughness*, a measure of fracture resistance commonly measured using a Charpy-V notch (CVN) test. Notch toughness is affected by chemistry of the filler metal, welding position, level of heat input, travel speed, and deposition rate used during placement. A combination of these factors, along with the local state of stress and strain demand, impacts the ability of the weld to deliver the forces through the joint. Pre-Northridge filler metals predate notch toughness requirements, and the limited Charpy-V notch test data collected after the Northridge Earthquake indicated a toughness range of 6 to 15 foot-pounds at 70ºF for beam-flange-to-column-flange joints. This is significantly less than current requirements for similar welds in post-Northridge moment frames, which must be at least 40 foot-pounds at 70ºF. Little data is available on the notch toughness of column splice joints, but it is expected that these welds have higher toughness that the beam-flange-to-column-flange welds due to the welding position, deposition rate, and typical electrode.

Local detailing practice also impacts the performance of pre-Northridge beam-flange-to-column-flange and column splice welded joints. In the beam-to-column joints, the proper placement of weld backing and run-off tabs should have been made per AWS D1.1, *Structure Welding Code – Steel*, requirements of the time. However, some observations have been made of run-off tabs turned 90 degrees from the axis of the weld to act as weld dams, resulting in undesirable characteristics at the ends of the welds. In addition, weld backing left in place, which was allowed by AWS D1.1 at the time of the Northridge Earthquake, creates a natural stress riser that increases the susceptibility of the welds to fracture. Since the Northridge Earthquake, the requirements have changed: run-off tabs are removed, and weld backing is not left in place without additional work. To meet the present requirements, a reinforcing fillet weld is placed between the column flange and the bottom of the backing bar at the top flange weld, and at the bottom flange weld, the backing bar is removed. The root pass is backgouged to sound weld metal to remove any potential flaws or defects in the root pass. Then a reinforcing fillet weld is placed between the bottom of the weld and the face of the column flange.

2.3 Effects of Composite Slabs, Restraint, and Boundary Conditions

Using boundary conditions and restraints that capture realistic system-level behavior are important for experimental testing to produce accurate results. The effect of composite slab construction on beam-to-column connection behavior is not well understood but could be significant due to the difference in neutral axis depth and restraint provided to the beam and column members by the slab.

Most experimental testing of beam-to-column moment connections has not included composite slabs, so the effects on panel zone behavior are not known. In a composite slab system, shear connectors between the beam top flange and the concrete slab result in a shift of the neutral axis. The use of a composite slab system may impact panel zone behavior and affect the likelihood of weak panel zone deformation in various ways:

- Shifting of the neutral axis results in an increased strain demand in the joint at the bottom of the beam flange during seismic loading. This increased strain, dependent on the level of sustained composite action, may make fracture more likely.
- The presence of a concrete slab may increase the effective depth of the panel zone due to bearing of the concrete slab on the column flange.
- Restraint of beams and columns by the composite slab can increase the amount of force transmitted through the beam-flange-to-column-flange welded joints. Well-restrained systems prevent member-level instabilities that cause premature strength degradation, which results in sustained levels of force transmitted through the beam-to-column connections. A well-restrained system also reduces out-of-plane deformations which may contribute to the beam-flange-to-column-flange weld demand.

Beams and columns in a moment frame are typically expected to experience reverse curvature bending under lateral loading. However, this has been found to not always be the case in the results of nonlinear response history analyses (NLRHA). Unless the gravity loads acting on the beams are significant, it is reasonable to assume that the inflection points occur near the midspan of the beams and mid-height of the columns if the distribution of flexural stiffness from the adjacent beams is uniformly distributed. When a beam-to-column connection subassembly is extracted for experimental testing, it is a common practice that that assumption be used for the design of test specimens and the associated boundary conditions. It should be noted, however, that the typical test setup used would allow the beam to shorten due to beam local and lateral buckling, while in reality such shortening would be limited by the system restraint in the axial direction of the beam (Yu and Uang, 2000). Consequently, the typical subassembly test setup is likely to exaggerate the amount

of strength degradation. Providing a simple support to simulate the inflection point also may not provide torsional (warping) restraint that exists in real conditions.

Most experimental testing of beam-to-column moment connections use an exterior column configuration with a beam framing in on only one side. It is less common to test an interior column, which has beams framing in on both in-plane sides. External column configurations do not capture the panel zone behavior of the interior column configurations, which typically have double the shear transmitted through the panel zone.

System-level boundary conditions (i.e., the column base fixity) have minimal effect beyond the first story of a frame.

2.4 Ratio of Beam-to-Column Flexural Strength

Frame configurations with columns that have more flexural strength that the beams connecting into it force flexural hinging to occur in the beams rather than the columns. Beam hinging is accompanied by the development of strain-hardened plastic moment at or near the column faces, which is transmitted through the connection to the column. In current provisions, strong column-weak beam (SCWB) requirements encourage this behavior, but many pre-Northridge moment frames predate this requirement, and in some cases the beams may be stronger than the column. Column yielding before beam yielding can create a weak story mechanism and generate instability of the structure.

Though columns that are weak relative to the connected beams are associated with undesirable performance, a fortuitous result of frames with shallow columns and a beam-to-column flexural strength ratio larger than 1.0 is that the column flange thicknesses tend to be thicker. This can minimize the fracture demand by decreasing flange local bending.

In the later years of the pre-Northridge era, pressures to economize moment frames caused a reduction in number of moment frame bays. At the same time, deep column sections became more common to address building code drift limits and the SCWB criterion. These frames may be prone to deep-column instabilities (Elkady and Lignos, 2018; Wu et al., 2018; Ozkula et al., 2021).

2.5 Column Splice Detailing

In pre-Northridge era, columns were typical spliced using PJP welds to join the flanges. Splice performance is influenced by variations in the detailing of the connection, including the size of the flange welds, configuration of the root pass, and web connection type.

Flange penetration (Figure 2-1) is the size of the PJP weld relative to the thickness of the upper column flange. It is often described as a percentage or fraction of the flange thickness. Penetration is typically in the 25% to 50% range for pre-Northridge splice connections. As a result, large unfused sections are common. Under applied loads (e.g., tension in the flange), the unfused section acts as a stress riser and increases the stresses at the root pass. This unfused region, coupled with the low toughness of the filler metal used in the pre-Northridge era (Section 2.2), suggest fracture of the connection at low loads (i.e., flange stresses in the 10 to 25 ksi range). NLRHA shows that these stresses have a high probability of exceedance, even under moderate earthquake loads.

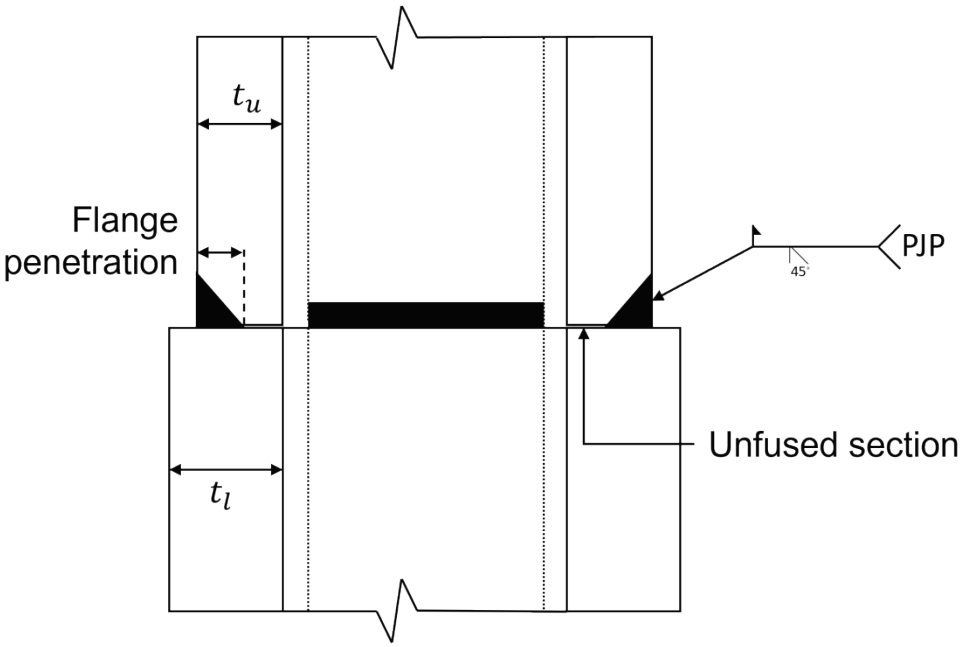

Figure 2-1 Typical pre-Northridge splice detail illustrating key parameters.

The PJP weld is either one-sided or two-sided, a difference which affects the configuration of the root pass. Very thick flanges and webs may have used two-sided preparation, but it is expected that in most cases, a one-sided preparation was used.

The web connection is typically another PJP weld or a bolted connection.

2.6 Effect of Panel Zone on Beam-to-Column Connection Demands

Because panel zone behavior can trigger failure of other parts of the beam-to-column connection, understanding the realistic effects of panel zones on connection demands is crucial. Behavior of the panel zone depends on its strength relative to other components in the beam-to-column connection.

A strong panel zone is one where most of the inelastic behavior occurs in the beam(s). This scenario has the highest potential for the beam to develop its maximum probable plastic moment strength. The same phenomenon can occur where post-yield hardening of the beam flanges may result in eventual panel zone yielding after the beam flange force has increased to a sufficient level. This condition requires sufficient beam restraint to prevent beam instability prior to inelastic hardening of the flanges.

If the panel zone is weak relative to the beam(s) framing into the connection, it can act as the primary source of hysteric energy absorption in the system. In some scenarios, post-yield hardening of the panel zone may result in delayed onset of inelastic behavior in the beam.

In modern design, the part of the beam(s) adjacent to the beam-to-column connection is intended as the primary location of inelastic behavior. Depending on the strength of the panel zone, the panel zone may act as a secondary location of inelastic behavior. When both components participate, the overall inelastic strains are less concentrated in one single component which should generate better seismic performance.

2.7 Modeling of Inelastic Response in Beam-to-Column Connections

Current modeling methods can capture some level of inelastic response in steel moment frame beam-to-column connections but advancing modeling methods is critical to improve evaluation procedures for weak panel zones. The local interaction between the panel zone deformations with the adjoining beam and column members, specifically at the welded joints between the beam and column flanges, is a key issue to investigate in the research program. Current modeling techniques cannot capture the column kinking effect associated with weak panel zones.

Two reports serve as valuable resources for developing more refined modeling guidance:

- NEHRP Seismic Design Technical Brief No. 4, *Nonlinear Structural Analysis for Seismic Design, A Guide for Practicing Engineers* (NIST, 2011b) summarizes approaches for modeling inelastic effects, including flexural plastic hinging, shear yielding, connection failure, and member instabilities due to local or lateral-torsional buckling.
- NIST GCR 17-917-46v2*, Guidelines for Nonlinear Structural Analysis for Design of Buildings, Part IIa – Steel Moment Frames* (NIST, 2017) provides modeling guidelines for steel moment frames.

Inelastic structural component models can be classified by the way that inelastic behavior is distributed through the member cross-section and along its length (NIST, 2011b). Figure 2-2 is a comparison of five idealized model types for simulating the inelastic response of beams, columns, and beam-to-column connections.

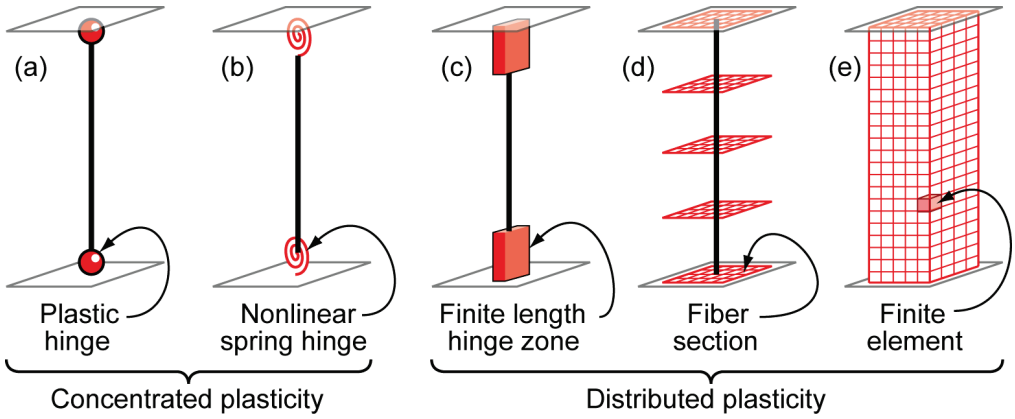

Figure 2-2 Comparison of different component simulation models (NIST, 2011).

Concentrated plasticity models elements that are essentially zero length that simulate the moment-rotation relationship of a steel component. Distributed plasticity models include finite length hinge models with designated hinge zones at the member ends. Member cross-sections are characterized through either nonlinear moment-curvature relationships or explicit fiber-section integrations, based on the assumption that plane sections remain plane.

The NIST *Guidelines* (NIST, 2017) include in-depth discussion of panel zones modeling in Section 3.4. Focus is on the ductile response expected of post-Northridge design, but much of the information also applies to the response and modeling of the pre-Northridge panel zones, which are anticipated to behave in a ductile manner. The modeling techniques range from simplified models to concentrated shear models to finite-size kinematics models. Simplified models generally assume elastic panel zone response that use centerline dimensions with variable length rigid end zones to estimate the panel stiffness. Concentrated shear models can be used when the panel zone is expected to go into the nonlinear range with a tri-linear response model curve for shear force versus deformation. A number of finite-size kinematics and flexibility models have been proposed such as the scissor model, the kinematic constraint model, and the Krawinkler model (Figure 2-3). Common to all three approaches are: (1) the assumption that the panel zone can only deform in shear; (2) the panel zone response is controlled by a single shear spring that can be elastic or inelastic; and (3) inelastic deformation in the connected beams and columns is modeled independently in the member models. The specific implementation details often differ, including how rigorously the panel zone assemblies (or constraint relationships) capture large deformation and rotation response. In all three models, the shear strength and

stiffness of the panel zone must be translated from a shear-force-shear-deformation relationship to an equivalent moment-rotation relationship (NIST, 2017).

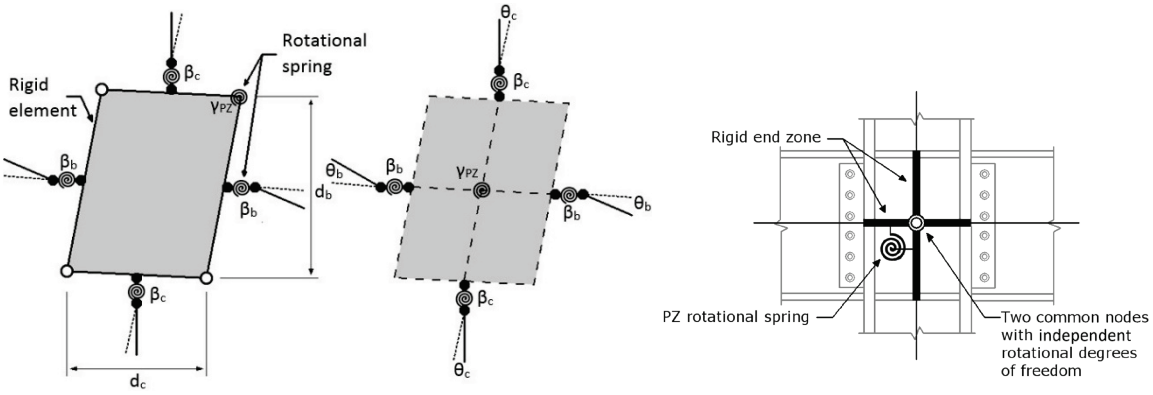

Figure 2-3 Idealized panel zone models that capture finite-size and panel deformations: (a) "Krawinkler model" constructed with rigid elements, (b) kinematic constraint model, (c) "scissor model" constructed with rigid end offsets and double node (NIST, 2017).

Item (3) is a significant limitation in modeling the response of pre-Northridge moment frame connections, because panel zones with significant shear yielding will have a local discontinuity with the deformations of the surrounding beams and column in the model.

Appendix A of the NIST *Guidelines* (NIST, 2017) specifically addresses the modeling of pre-Northridge (i.e., fracture-critical) connections such as the beam-to-column connection and column splices. The summary provides a discussion of state-of-the-art approaches to modeling the beam-to-column connections to reflect both the anticipated fracture and post-fracture response. Anticipated fracture initiation modeling is based on classical fracture mechanics concepts and is combined with the experimental results on full-scale connections with recommendations on both median and lower-bound estimates provided. Hinge modeling approaches include both typical concentrated hinge and fiber hinges with the fiber hinge approaches being able to model the degradation of pre-Northridge moment connection tests more closely. Appendix A of the NIST *Guidelines* (NIST, 2017) provides similar guidance for the modeling of PJP column splice welds but recognizes that these models are based on limited testing results.

Chapter 3

Identification of Archetype Buildings and Preliminary Computational Studies

This chapter describes a recommended plan to identify a set of archetype pre-Northridge steel moment frame buildings and perform preliminary computational studies using those archetypes to inform the range of parameters that should be explored in the rest of the research plan. These tasks form the foundation of the research program and should be conducted first. Archetypes should cover a range of characteristics consistent with those found in steel moment frames built in the United States between the 1960s and the early 1990s.

3.1 Identification of Archetype Buildings

Identified archetype buildings should reflect typical building configurations, detailing, and code requirements of moment frame systems in the pre-Northridge era. These characteristics evolved due to changes in construction technology, building code design requirements, design tools such as structural analysis software, and architectural considerations. The investigators identifying the archetypes should closely review historical background resources when designing the archetype buildings to make sure that the buildings are representative of the existing building stock in the United States and have characteristics that typically occur contemporaneously. The archetypes should preserve the coherence between building configuration, connection detailing, material selection, and weld characteristics at the point-in-time of interest.

To ensure that the research addresses the wide range of typical building configurations, column splices, and beam-to-column moment connections representative of pre-Northridge moment frames, an effort should be made to collect existing building drawings of steel moment frame buildings across the pre-Northridge era in regions of moderate to high seismicity in the United States. Documentation of seismic evaluations and retrofit designs should also be collected to inform the later stages of the research program focused on applying the fundamental research to practice and developing retrofit guidance. Field investigations of existing pre-Northridge moment frame buildings could also be conducted.

Identified archetype buildings should represent key stages of steel moment frame design over the timeline of the pre-Northridge era. The steel moment frames that were damaged in the Northridge Earthquake evolved from earlier steel moment frame design in the United States. Introduction of new technologies and economic pressures resulted in some of the characteristics of pre-Northridge detailing that were later found to be deficient (FEMA, 2000g).

The earliest steel moment frames employed riveted connections between beams and columns. Column splices were made with riveted plates placed over the top and bottom column sections. In the 1950s, high strength bolts began to replace rivets in beam-to-column connections and column splices. During this era before welding, the entire frame was encased in concrete for fire protection, which added strength and stiffness.

When welding became common in the late 1950s, bolted clip angles or "T" sections in the beam-to-column connection were replaced by plates that were welded to the column during fabrication and bolted to the beam in the field.

Field welding emerged in the early 1960s, making it possible for the beam flanges and webs to be welded directly to the column. Field welding of columns splices also became the norm, typically with PJP welds ranging from about one-third to just over one-half the thickness of the thinner column flange and web. PJP column splices were regularly constructed until 1994.

In the late 1960s, based on tests performed at University of California, Berkeley (Popov and Pinkney, 1969; Popov and Stephen, 1970), the beam-to-column connection web weld was eliminated to reduce costs, and it became typical to bolt the beam web to the column. Some of these connections have a *weak panel zone*, which can yield in shear before the adjacent beams yield in flexure. This specific beam-to-column moment connection was most associated with damage in the Northridge Earthquake, and it is commonly referred as "the pre-Northridge connection." This connection detail is, however, just one of several beam-to-column moment connections constructed in the pre-Northridge era (Section 3.1.4).

How overall frame geometry evolved over time is important context for developing the archetypes. New technologies and economic pressures resulted in some of the characteristics of moment frame geometry that contribute to the vulnerability of pre-Northridge buildings.

In the 1950s and 1960s, all beam-to-column connections were rigid, resulting in a three-dimensional space frame. In the 1970s and 1980s, economic pressure to reduce labor and materials pushed engineers to specify fewer moment frame connections. Moment frames were first limited to the perimeter lines, and then the number of frame bays along each line decreased. Beam and column sections in the moment

frames became larger to compensate for the smaller number of moment frames. The lower redundancy and larger member sizes may have led to lower performance of these moment connections compared to the smaller shapes used in the University of California, Berkeley tests in the 1960s. Present design standards do not allow such extrapolation beyond available tests.

In the 1980s, the availability of structural frame analysis computer programs made more complicated geometries possible to evaluate. As a result, irregularities within the moment frame lines that increase seismic vulnerability (e.g., building setbacks; discontinuous or offset columns) became more common.

Welding and inspection requirements of the pre-Northridge era also were not as stringent as modern requirements, which were developed as a result of the connection fractures that occurred in the Northridge Earthquake. On the West Coast and other regions of high seismic activity, pre-Northridge connections continued to be designed and constructed after the Northridge Earthquake until the late 1990s, when the code provisions changed to address the deficiencies observed in the earthquake. In regions of low seismic activity, the connections can still be used.

More in-depth historical background and information for representative buildings that have been used in other projects can be found in other documents:

- FEMA 355C, *State of the Art Report on Systems Performance of Moment Steel Frame Buildings in Earthquakes* (FEMA, 2000e) outlines model buildings designed for the SAC Project that could form the basis of one or more of the archetypes buildings.
- FEMA 355E, *State of the Art Report on Past Performance of Steel Moment-Frame Buildings in Earthquakes* (FEMA, 2000g) describes the construction changes in moment frames, documents much of the testing of pre-Northridge connections, tracks how building codes have changed over time, presents summaries of the performance of steel buildings in past earthquakes, and provides detailed discussion on the performance of moment frame buildings in the Northridge Earthquake, including a number of case studies. One or more of these case study buildings could form the basis of one or more of the archetype buildings.
- "Seismic performance of tall steel framed buildings built between 1960 and 1994" (Pekelnicky and Malley, 2019) describes transitions in structural configuration, column splice and beam-to-column connection details, and welding procedures.

The set of archetype buildings should encompass a range of design variables that address the key issues related to the behavior of pre-Northridge frames presented in

Chapter 2. The important design variables that should be considered are described in the sections that follow.

3.1.1 Structural Configuration

Structural configuration affects the behavior of a moment frame. The variables can influence building period, base shear, overturning moment, and lateral drift, which in turn impact local member demands such as shear and flexural forces, axial load ratio, and the formation of plastic hinges. There are several variables in particular that should be considered:

- **Plan configuration.** Frames with low redundancy concentrate seismic resisting elements into a few frames or bays within planar frames. Most early moment frames were space frames with all columns moment connected in both directions, resulting in high redundancy. Later in the pre-Northridge era, most buildings used perimeter moment frames, which have lower redundancy. In some cases, just one bay of moment frames on each building face was used. The set of archetype buildings should include examples of space frames, perimeter frames, and partial perimeter frames.
- **Number of bays and bay width.** The number of bays and bay width will affect the range of axial load in the end columns of steel moment frames. The number of bays should range from 2 to 8. Typical bay widths of between 20 feet and 30 feet have been used in some recent studies (FEMA, 2009; NIST, 2010).
- **Number of stories and story height.** Tall steel buildings (up to about fifty stories) in regions of high seismicity were often designed using steel moment frames. Few exceeded thirty-five stories, however. For this reason, it is recommended that the archetype buildings range in height from one to thirty-five stories. A range of story heights for typical floors between 13 and 16 feet should be considered, recognizing that the first floor of most steel buildings is taller, in some cases upwards of 20 feet.

3.1.2 Building Stiffness and P-Delta Effects

A range of building stiffnesses should be considered in the set of archetype buildings to be consistent with the building stock of the various eras. Early steel moment frame designs did not consider P-Delta effects or only did so in an approximate manner, so the systems are typically more flexible than modern designs. While explicit drift limits were not introduced into codes until the 1980s, some engineers did provide stiffness checks that controlled the frame sizing.

Variation in the tributary floor area affects P-Delta considerations. A range of tributary areas should be considered in the archetype building designs. This is

consistent with the recommendation to include building plan configurations with both high and low redundancy.

3.1.3 Level of Seismic Design Loading

Codes in effect through the 1994 Northridge Earthquake used Seismic Zones to determine seismic design parameters. The level of seismic design loading used in the archetype buildings should be consistent with the design requirements in effect at the chosen site for the point-in-time being considered.

Current structural design requirements are keyed to Seismic Design Categories. In general, special steel moment frames are required in Seismic Design Categories D, E, and F. Most site locations should be chosen based on the present code definitions for Seismic Design Categories D and higher. However, consideration should also be given to including archetype buildings in regions of lower seismic demand, because pre-Northridge connections are still permitted in Seismic Design Categories B and C. In the SAC Project, buildings with identical structural configurations were designed for three different seismic exposures. Such an approach could also be employed for these archetypes.

In addition, design locations will dictate the selection and scaling of appropriate sets of ground motion records to represent the seismic hazard at the selected location. Ground motion selection should consider both far-field and near-fault site characteristics at a range of locations and intensities. A range of ground motion durations should also be used.

3.1.4 Column Splice and Beam-to-Column Connection Type

For PJP column splices, the factors that varied over the pre-Northridge era were the amount of flange penetration, the filler metal properties, and the welding processes. Generally, flange penetration increased over time from about one third of the thickness of the flanges in the shape above the splice to half of the thickness of the flange plus one eighth of an inch. Welding processes started with SMAW and transitioned to FCAW in the early 1960s. The toughness of the filler metal varied over that time as well. In some cases, web connections included a bolted splice to facilitate erection (Figure 3-1). In most cases, however, a PJP weld similar to the column flange joint was used.

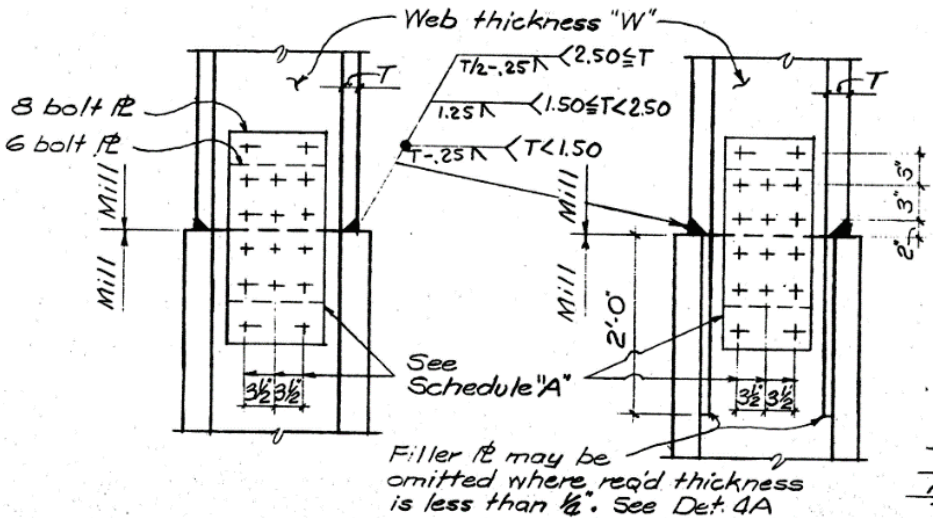

Figure 3-1 Existing column splice detail (Nudel et al., 2015).

The beam-to-column connection details used between the 1950s and 1994 also transitioned in both detail configuration and welding procedures. Prior to the 1950s, rivets were the primary joining element between members of steel frame structures. In the 1950s, bolting (including high strength bolts) replaced rivets. By the early 1960s, most buildings were connected with high strength bolted connections with top and bottom flange plates to develop the moment resistance (Figure 3-2).

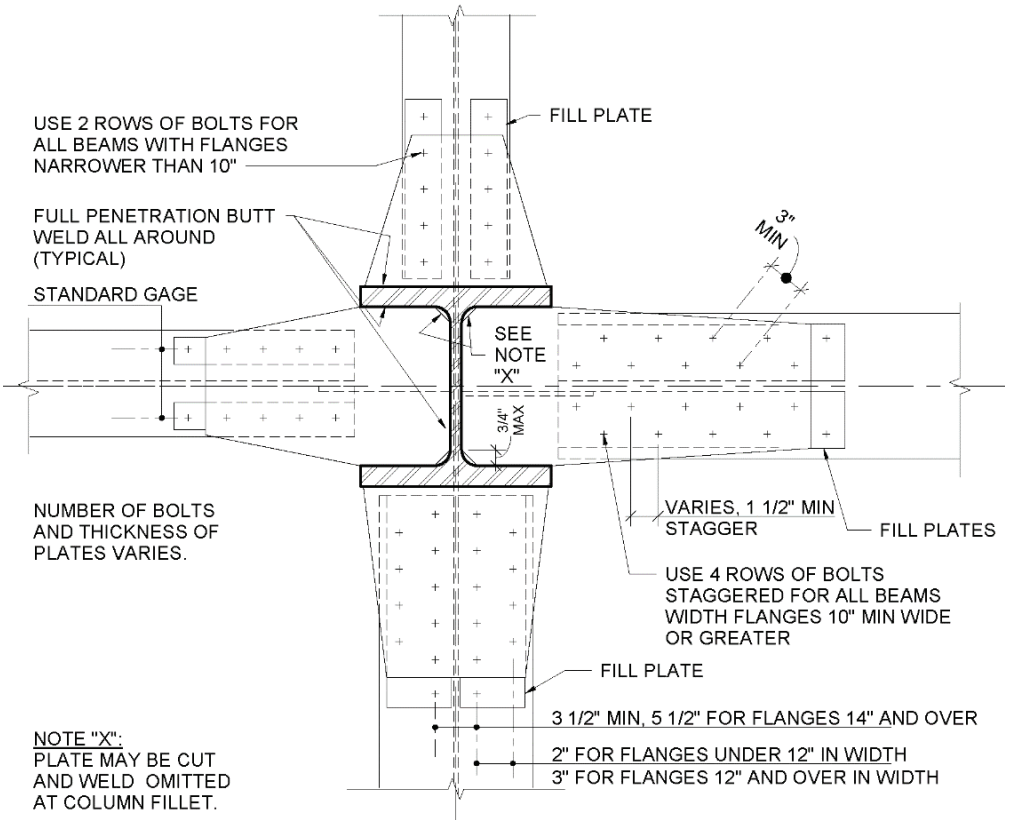

Figure 3-2 Four-way high strength bolted moment connection.

As field welding became an option, the beam flanges and web were welded to the column flanges for strong axis connections and to continuity plates for weak axis connections. This detail has been designated as *Welded Unreinforced Flange - Welded Web* or WUF-W (Figure 3-3). Like the column splices, the welding approach originally used SMAW and then transitioned to FCAW by the early 1970s.

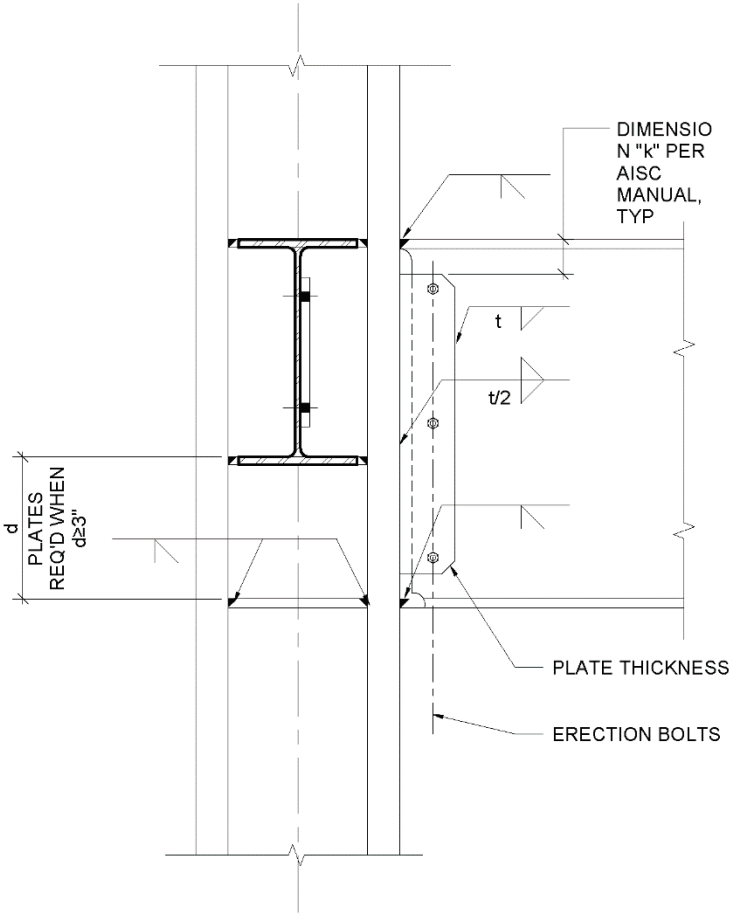

Figure 3-3 Example of strong axis WUF-W connection.

In the late 1960s, based on tests performed at University of California, Berkeley (Popov and Pinkney, 1969; Popov and Stephen, 1970), the WUF-W connection was modified to allow the web to be bolted to the beam. The web connection was typically designed with a single row of high strength bolts connected to a shear tab that was shop welded to the column with fillet welds. The elimination of the web weld in the field reduced the cost of this connection, making it more desirable, and design practice quickly adopted this detail starting in the early 1970s. This detail (Figure 3-4), known as the WUF-B, became the standard connection and is now commonly referred as "the pre-Northridge connection." This is the connection detail that was most commonly damaged in the Northridge Earthquake.

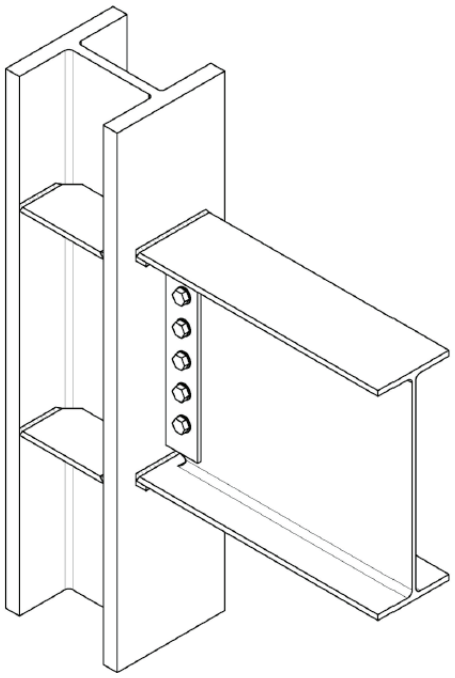

Figure 3-4 WUF-B connection (NIST, 2016).

As there is some demonstrated difference in performance between the WUF-W and WUF-B connections, this parameter should be part of the identification of the archetype buildings to be investigated. Consideration should also be given to the four-way bolted moment connection details that were prevalent starting in the 1950s.

3.1.5 Ratio of Beam-to-Column Flexural Strength

The ratio of beam-to-column flexural strength affects the distribution of yielding in steel moment frames. Since building codes did not require consideration of this ratio, commonly referred to as strong column-weak beam (SCWB), prior to the 1990s, many pre-Northridge buildings have columns that are weak relative to the beams. Older designs with four-way beam connections to all columns, with columns engaged both strong-way and weak-way, likely have low ratios, while perimeter frames and partial perimeter frames with wide-flange columns engaged strong-way will likely have ratios near 1.0 (late 1980s and early 1990s). The axial force in the column used to check this ratio also varied over time.

3.1.6 Panel Zone Design

Strength of panel zones can impact local demands on connection elements and global response of the frame. While minor inelastic deformation in panel zones can be beneficial to the behavior of steel moment frames, excessive panel zone deformation negatively impacts frame response by limiting the inelastic deformation capacity of beam-to-column connections.

Since the mid-1990s, assessment requirements for existing buildings have been based on what is known as *balanced panel zone design*, which means approximately matching the relative strengths between the panel zone and the forces generated by the yield capacity of the connecting beams. Prior to the mid-1980s, there was no code-required explicit check of panel zone design strength, though some engineering firms did include a check of the shear demand from code lateral forces. This approach was formalized in the 1988 *Uniform Building Code* with a requirement of checking the panel zone strength for a factor of 1.85 times the force generated by the code base shear. As with other parameters of interest, the archetype building panel zone capacities should be developed consistent with design practice of the time.

3.1.7 Material Properties

Many of the earliest steel moment frames were built using the ASTM A6 specification (33 ksi yield stress). By the 1950s, the ASTM A36 specification became typical for steel beams and column shapes. ASTM A36 members had a nominal minimum yield strength of 36 ksi but were usually stronger. ASTM A572 Grade 50 steel became widely used in the early 1980s. Many engineers in the 1980s and into the 1990s specified beams of A36 steel and columns of A572 Grade 50 to help satisfy the SCWB design requirement. However, at that time, many steel producers made only one material that satisfied both the A36 and A572 Grade 50 specifications (what came to be known as *dual certified*), so the desired SCWB design may not have been realized. The effect of designs using dual grade steels should be considered when identifying archetypes from this era. Present shape material production is dominated by ASTM A992, which was introduced partly in response to the findings from the Northridge Earthquake. Information on the expected yield strength of steel materials through various eras can be found in ASCE/SEI 41. AISC 341-16 (AISC, 2016) has a similar table for the expected yield strength for presently produced steel shapes and plate material.

Weld properties, including process (SMAW to FCAW), strength, and toughness have changed over time. Nominal strength of typical structural filler metals ranged from 60 to 70 ksi. Filler metal was “matched” to the shape and plate materials to be welded, with the 60 ksi weld metal matching A36 material and 70 ksi material matching 50 ksi minimum strength materials steels such as A572 Grade 50 and A992. Weld metal toughness values are related to specified values based on specification requirements for project applications. In almost all pre-Northridge welding applications for both column splices and beam-to-column connections, there was no specified filler metal minimum toughness. When specified in present practice, filler metal toughness specifications include a specified minimum CVN level for the foot-pounds of energy absorbed at one or more specified testing temperatures. In the present AISC *Specifications*, all welds in the seismic force-resisting system must

meet a minimum weld toughness of 20 foot-pounds at 0ºF. For demand-critical welds, the filler metal must also meet 40 foot-pounds at 70ºF.

Chapters 4 and 5 include discussions on how the experimental programs need to consider the availability of shape, plate, and filler metal. It may not be possible to provide shape material that can simulate the properties of previous production, requiring the use of built-up plates as an alternative. It is expected that all the filler metals in different eras can still be specified, or a reasonably close substitute can be found.

3.1.8 Column Base Connections

Bases of columns located at the bottom story of a moment frame are often a source of significant inelastic response, so explicit consideration of column-to-base connection conditions is necessary in assessment of building performance. In most engineering designs, pinned base connections are assumed for buildings without basements. Design of buildings with basements often consider the continuity of columns to the foundation level, but still assume a pinned connection at the basement. Since some design configurations and base conditions are assumed to be fixed, both conditions should be included in the archetype design space. Distinction between exposed base plate connections and embedded connections should be made. Limit states, including bearing capacity of the concrete foundation and the supporting soils and the degree of rotational fixity provided by different base connections, should be considered in assessment of archetype building designs.

3.1.9 Design of Gravity Framing

Past NLRHA studies of moment frames have shown that gravity framing affects the distribution of yielding within moment frames and could help mitigate the potential for collapse caused by lateral dynamic instability (FEMA, 2009). Archetype buildings should consider typical gravity framing systems. Gravity columns will be more prevalent in more recent pre-Northridge moment frame buildings that rely on perimeter or partial perimeter frames. Gravity frame design did not consider seismic forces or detailing requirements, so standard non-seismic design procedures should be followed. In most applications, the beam-to-gravity-column connection is likely a shear tab. Assessments of these buildings should consider the presence of the gravity system, including consideration of the connections and capacity of gravity column splices. Tests by Liu and Astaneh-Asl (2000) for the SAC Project provide useful information on the force and rotation capacity of shear tab connections.

3.2 Preliminary Computational Studies on Archetype Buildings

After the archetypes are identified, preliminary computational studies should be conducted. Archetype buildings should be analyzed using simulation models that

have been calibrated based on currently available information from past analytical and experimental studies. Preliminary system-level computational research will contribute to the identification of high priority issues that affect the behavior of pre-Northridge moment frame systems, specifically the PJP column splices and weak panel zones. The results of these studies will inform the development of the research tasks on these two topics as described in Chapters 4 and 5. Preliminary computational studies are expected to serve several purposes:

- Provide a range of representative design parameters (e.g., column load, ratio of beams to column flexural strength, connection details) for use in establishing parameters for experimental testing of column splices and beam-to-column subassemblages.
- Identify which of the archetype design variables have significant impact on the behavior of pre-Northridge moment frame systems.
- Identify limitations in currently available standards and guidelines for modeling column splices and beam-to-column connections in pre-Northridge moment frame systems.
- Address limitations in state-of-the-art simulation models for capturing the post-fracture behavior of column splices and weak panel zones.

3.2.1 Simplified Models

A number of critical issues related to nonlinear response can be identified with simplified building models. Two-dimensional, one-bay models have been utilized to investigate system-level response parameters by varying a number of design variables such as: SCWB ratio; number of stories and bays; second-order (P-Delta) effects; and the effect of gravity framing (NIST, 2010). The advantage of using simplified models is reduced computational effort. Simplified models can also be used to evaluate ground motion input parameters and investigate dynamic instability for different ground motion sets.

Simplified modeling recommendations for steel structural components should be based on:

- NIST GCR 17-917-46v2, *Guidelines for Nonlinear Structural Analysis for Design of Buildings* (NIST, 2017),
- ASCE/SEI 41-23, *Seismic Evaluation and Retrofit of Existing Buildings* (ASCE, expected 2023), and
- AISC 342-22, *Seismic Provisions for Evaluation and Retrofit of Existing Structural Steel Buildings* (AISC, expected 2022).

3.2.2 Building Prototype Models

Building prototype models are full building nonlinear models of the archetype buildings. These detailed models should be used to explore parametric variations on building characteristics and their effect on response. Two-dimensional and three-dimensional models of the archetype buildings should be developed.

Three-dimensional models are necessary for considering three-dimensional effects, including coupling of axial load and biaxial bending at end columns, the effect of the gravity framing on nonlinear response, and the effect of varying foundation modeling approaches. However, due to lack of available experimental information on three-dimensional effects, preliminary computational studies should emphasize two-dimensional models. Modeling of slab effects, panel zone response, column bases, and splices is essential.

Nonlinear building prototype models should incorporate strength and stiffness, deterioration of beams and columns, and account for second-order effects. State-of-the-art component simulation models that have been calibrated with available experimental data from past experimental studies should be employed for this purpose.

Two types of nonlinear archetype building models should be developed. The first includes the bare steel frame only (i.e., no consideration of the composite action and gravity framing). The second incorporates the slab and other elements in order to quantify the effects of additional restraint. Preliminary modeling assumptions for this purpose are summarized in Lignos et al. (2011a). A distinction should be made for composite beams that are part of interior or exterior connections.

Column splices and panel zones should be modeled nonlinearly. Panel zone modeling can be calibrated over the course of the research program using experimental data from subassemblage-based research.

Models should also include explicit consideration of column-to-base connection restraint. A distinction should be made between exposed base plate versus embedded column base connections.

Chapter 4

Research Plan for Studying PJP Column Splice Behavior

This chapter describes a recommended plan for studying the seismic behavior of PJP column splices in pre-Northridge moment frames. A concise summary of research knowledge gaps is also provided.

The recommended research requires both experimental and computational studies. Experimental testing is anticipated to include large-scale testing of column splice subassemblies conforming to identified archetype buildings (Section 3.1), as well as related subcomponent and ancillary testing. Computational studies will be used to extend the range of investigated parameters.

The ultimate goals of the research are to develop a decision framework regarding PJP column splice evaluation procedures coherent with the provisions with ASCE/SEI 41 for moment frames, to outline retrofit design requirements, and to propose practical mitigation and repair solutions.

4.1 Overall Research Strategy

The research on PJP column splices should focus on four main areas:

Area 1: *Assessment of component response with regard to fracture initiation and propagation.* A range of unretrofitted and retrofitted details should be investigated. A probabilistic or fragility-based characterization of fracture response with respect to applied demands should be developed.

Area 2: *Characterization of component demands.* Unlike deformation-controlled components such as plastic hinges within beam-to-column connections, PJP column splices tend to be load-controlled (i.e., dominated by a combination of axial force and moment). Characterization of these demands is essential from the standpoint of developing appropriate loading protocols for component testing and simulation.

Area 3: *Assessment of system response considering the interactions between the splices and the frame*. This will provide insight on the effect of retrofit strategies and implications of non-intervention.

Area 4: *Practice-oriented tools and guidance for simulation*. These tools should reflect the scientific knowledge developed in Areas 1, 2, and 3.

Performance-based engineering principles can support the development of decision support frameworks for column splice risk mitigation, which should be practice-oriented and consider retrofit costs and occupant disruption. The developed tools should be based on performance-based principles applied at the system level.

Strong coupling exists between component and system response (i.e., fracture in a column splice may influence overall frame response and the demands in other components). Consequently, the first three research areas overlap and are informed by each other. They should be developed as such, rather than in a serial manner. To this end, the computational and experimental tasks should be conducted in close coordination with each other. Subsequent sections of this chapter describe the experimental and computational plans, each of which contains various tasks. Figure 4-1 below schematically illustrates the anticipated interconnections among these tasks.

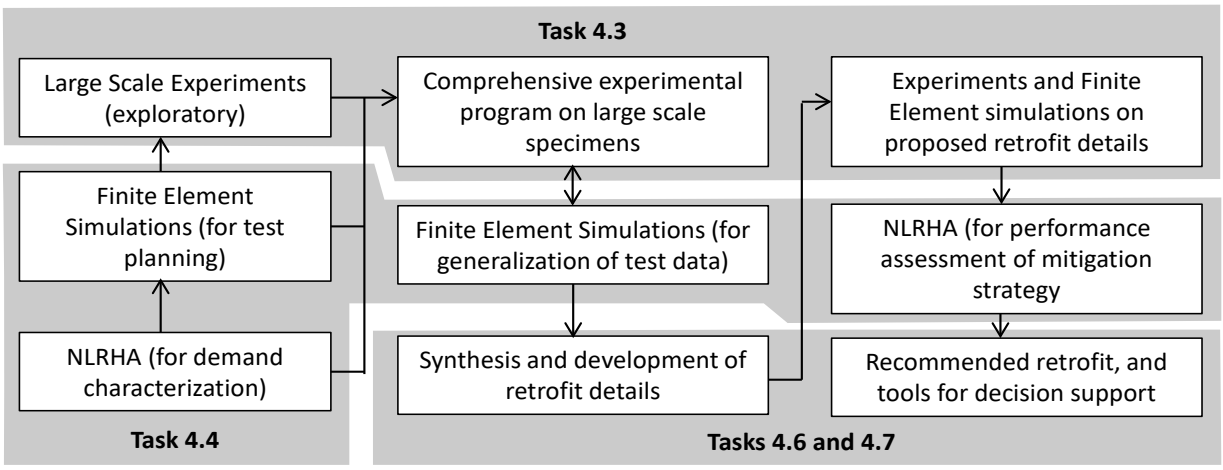

Figure 4-1 Anticipated interconnections between research tasks.

The archetype building designs identified at the start of the project should be used in the PJP column splice studies described in this chapter. The process for identifying the archetype buildings, which involves close study of the historical background and an effort to collect existing building information representative of pre-Northridge design in the United States, is described in Section 3.1. Findings from the preliminary computational studies (Section 3.2) should be used to inform the direction of the column splice studies.

4.2 Prior Research on Behavior of PJP Column Splices

Appendix A is a comprehensive summary of prior research on PJP column splices in the context of the research program objectives. The more concise summary provided in this section focuses on knowledge gaps identified in the literature review and how they relate to the identified research areas.

4.2.1 PJP Column Splice Component Response

Experimental data on pre-Northridge PJP splices are sparse and do not fully represent the range of details and materials that were prevalent in construction practices from the 1960s to 1990s. A large-scale test on a PJP column splice was performed by Bruneau and Mahin (1991), but only one level of flange penetration (50%) was represented, and there was a smooth transition of weld between the thicker and the thinner flange. Additionally, this test was conducted in four-point bending, and therefore does not include the effect of either axial force or shear. More recent tests by Shaw et al. (2015) were directed towards PJP splices with large penetration (i.e., more than 85%) and notch-tough weld filler metal representative of post-Northridge construction practice. Moreover, none of these tests consider effects of biaxial bending that are common in field conditions. Finally, no experimental data are available on retrofitted PJP column splice connections.

Various researchers (Nuttayasakul, 2000; Stillmaker et al., 2016) have conducted finite element simulations to assess fracture toughness demands in PJP splice connections. These studies have been complementary to the experimental programs outlined above: Nuttayasakul (2000) simulated the experimental specimens of Bruneau and Mahin (1991), whereas Stillmaker et al. (2016) simulated the experimental specimens of Shaw et al. (2015). As a result, these suffer from similar limitations as the experimental programs in terms of details considered. Stillmaker et al. (2016) examined flange penetrations in the range of 50% to 90% and developed regressed relationships to relate fracture toughness demands to the applied flange stresses.

Prior component simulations lack investigation into several important topics:

- Splice behavior under the full range of typical flange penetrations
- Absence of weld transition between the flanges (which results in a large decrease in section area)
- Effect of stress gradients, both in-plane and out-of-plane
- Effects associated with crack propagation, including crack arrest (e.g., during crack transition between flange and web) and interaction with other splice components such as bolted or welded web plates

The SAC Project included material testing on base and weld materials from pre-Northridge moment frames (Fisher et al., 1995; Kaufmann et al., 1996, 1997). The data provide important estimates of material toughness as well as constitutive properties. However, the samples used for these studies were not extracted from PJP column splice connections. Welding processes, deposition rates, weld passes, and heat input would have differed from the samples. Moreover, CVN values must be paired with other parameters not included in the SAC testing such as critical stress

intensity factor of the weld material (K_{IC}) to develop a quantitative fracture mechanics framework.

4.2.2 PJP Splice Demand Assessment

Recent work (Galasso et al., 2015; Nudel et al., 2013; Shaw et al., 2015; Shen et al., 2010; Song et al., 2020) has addressed demands in splices with the objective of estimating the risk of fracture. The demand assessment conducted by these studies, when considered along with research on component response outlined above, motivates the research program outlined in this document. However, the research plan should address numerous knowledge gaps in demand assessment.

The first gap is in the area of selection of buildings, locations, and ground motions that represent pre-Northridge conditions. The existing research focuses only on a narrow set of generic frames and on post-Northridge construction (with the exception of Nudel et al., 2013).

The second knowledge gap relates to the physical phenomena represented by the simulations. The existing work considers only two-dimensional models and does not consider the effect of fracture or failure of other components. Validated, user-friendly technologies are needed to simulate post-fracture response of structural components that could affect demands in the splices and overall frame response. These technologies are essential for the development of the decision support framework outlined in Section 4.7.3.

4.2.3 Knowledge Gaps in the Area of Retrofit Details

Various details have been proposed by engineers to retrofit PJP column splices that are susceptible to fracture. Examples include addition of fin plates to flanges and complete replacement of PJP welds with CJP welds. In large part, these designs are based on engineering intuition and simplified calculations that have not been validated by testing or fracture mechanics simulations. As a result, the efficacy of retrofit details has not yet verified experimentally. The only study in this area was by the Structural Engineers Association of Northern California (SEAONC) University Research Program (Tam et al., 2021) that addressed stress demands in fin-plate retrofit details through CFE modeling.

4.3 Experimental Research Plan

The experimental research is the most significant component of the column splice research for several reasons:

- There is only one known experiment (Bruneau and Mahin, 1991) on pre-Northridge splice details, in which a splice was subjected to pure bending.

- In general, there are fewer experiments of column splices compared to other moment frame details.
- There has been no experimental investigation of retrofit strategies for column splice details.

4.3.1 Objectives

There are four objectives of the experimental research plan:

Objective 1: Physical demonstration of splice fracture in pre-Northridge details and behavior characterization in terms of Engineering Demand Parameters (EDPs) for splice capacity and potential retrofit details.

Objective 2: Validation of the CFE models for splice simulation, such that along with these models, a comprehensive dataset of splice fracture will be generated.

Objective 3: Building on Objectives 1 and 2, the development of tools to predict fracture of given splice details and corresponding fragilities (i.e., probability of fracture for given the EDPs).

Objective 4: Support and validate the development of frame analysis procedures that incorporate splice fracture and post-fracture response.

4.3.2 Experimental Strategy

The experimental and computational plan should be conducted in a coordinated manner. The NLRHA (Section 4.4.1) should inform the loading to apply in the PJP column splice experiments. The experimental data should inform and validate the CFE simulations (Section 4.4.2) and the NLRHA simulations by providing preliminary data on splice performance and assessment of retrofit strategies (Section 4.4.3). Broadly, the experiments should focus on attaining fracture in the PJP details and be designed to preclude other types of failure.

To ensure consistency between the various sets of tests, and coherence with the CFE simulations, the archetypes used to plan CFE simulations should guide the experiments. For each category of PJP splice detail, experiments should include large-scale specimens for assessment of component response, scaled subcomponent specimens for more effective validation of CFE models and analysis of local effects, and coupon scale specimens for material characterization.

4.3.3 Large-scale Subassemblage Specimens

The large-scale specimens should include the PJP column splice and connected columns over the entire story height (Figure 4-2). The testing of large-scale subassemblage specimens is important because there are many size effects in welded connections susceptible to fracture. These size effects range from pure fracture

mechanics scaling, material sampling (Beremin et al., 1983), and variations in microstructure between different scales due to different heat dissipation and the number of weld passes.

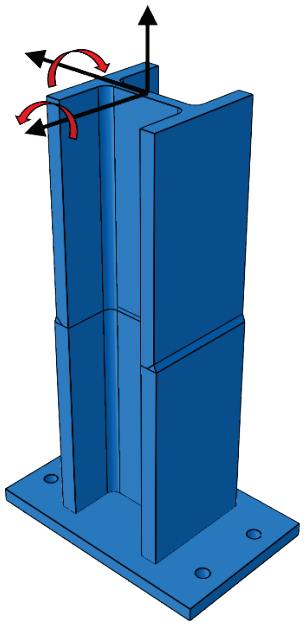

Figure 4-2 Sample schematic for large scale subassemblage test specimen.

Parameter Sets

The selection strategy for parameters for the subassemblage experiments and the CFE simulations (Section 4.4.2) is presented in Section 4.5. These include member size pairs, splice details in terms of flange penetrations and web connection, material selection for filler and base metals, and parameters that could inform the retrofit details. These parameter sets will be detail-dependent and cannot be envisioned until the research plan is underway. The large-scale tests should aim to interrogate these parameters in such a manner that the complementary CFE simulations are used to interpolate, rather than extrapolate the splice performance. Given the randomness in fracture, especially brittle fracture, the large-scale experiment test matrix should feature an appropriate number of replicate specimens to characterize the uncertainty in response.

Specimen Fabrication

Welding practices and positions, erection procedures, materials, and column sections should be consistent with the selected archetype for assessment of existing splice details. Material selection should be informed by the guidance in Section 3.1.7, which outlines the various material grades and properties used in pre-Northridge construction. Welding Procedure Specifications (WPS) should be developed in

collaboration with the American Institute of Steel Construction (AISC). Procedure Qualification Records (PQR) assemblies should be fabricated and tested to ensure that the parameters of the WPS are met and provide performance consistent with the identified archetypes. It is important to accurately replicate the welding practices of the time, including their deficiencies. Appropriate WPS should be developed for the retrofit details to provide optimal performance.

Nondestructive testing (e.g., ultrasonic (UT), magnetic particle) should be conducted before experimentation to ensure the absence of unintended flaws, and consistency with the expected detail and unfused section size.

Specimens for characterization of material properties, including coupon specimens for fracture and toughness properties, should be extracted from fabricated splice details.

Boundary Conditions and Loading Protocols

General considerations for boundary conditions and loading protocols are outlined in Section 4.5. The loading should be applied in a closed loop control, with appropriately tuned control algorithms. However, given the complexity and expense of applying 6-degrees of freedom loading to large-scale specimens, rational simplifications could be made.

Vertical ground motions are likely to have high frequencies and loading rates; representing them effectively in large-scale experimental setups may be challenging.

4.3.4 Subcomponent Tests

Subcomponent tests should be used to verify modeling approaches. These smaller-scale tests complement the large-scale subassembly tests that aggregate many effects, like material constitutive response, fracture response, material sampling, and the balance between fracture and specimen strain energy. Subcomponent tests can be used to verify the effectiveness of models in a way that large-scale tests cannot.

Subcomponents tests could include pull-plate specimens representative of PJP flange details with or without retrofit subjected to monotonic or cyclic loading, or tee-stub specimens. Guidelines for fabrication, parameter selection, and data documentation are similar to those for the large-scale tests.

4.3.5 Ancillary Tests

The large-scale and subcomponent scale tests should be complemented by ancillary experiments, such as mechanical, spectrochemical, and fractographical studies. The purposes are to ensure that the tested materials conform to expectations, to inform the CFE and NLRHA simulations (in terms of constitutive as well as fracture properties such that they utilize measured, rather than specified properties) and to facilitate

generalization of test results. The data from ancillary tests should complement conventional data from mill certificates.

Fractographical studies should be conducted on selected fracture specimens across all scales of testing, with the objective of determining the mode (ductile or cleavage) and the location of fracture initiation and subsequent propagation. The studies should include visual and photographic observations (e.g., chevron patterns), as well as scanning electron microscopy.

Materials samples should be taken from each archetype tested in the large-scale and subcomponent tests, and key properties should be documented:

- Base material of the columns, at locations through the flange and at the web, running along the length of the member:
    - Material tensile and yield strength
    - Material elongation over specified gage length
    - CVN data for the lower shelf, transition, and upper shelf regions
    - Spectrochemical analysis
- Weld assemblies tested per AWS 5.20, *Specification for Carbon Steel Electrodes for Flux Cored Arc Welding*:
    - Material tensile and yield strength
    - Material elongation over specified gage length
    - CVN data for the lower shelf, transition, and upper shelf regions
    - Spectrochemical analysis

The following experiments should be conducted on the PQR assembly and dummy large-scale specimen detail (i.e., mockups of splice details constructed using similar plates and weld materials):

- In weld material and key locations in the HAZ in the longitudinal direction: Measure CVN curve and standard fracture mechanics K_{IC} or J_{IC} specimens, following standards such as ASTM E399 or ASTM E1820.
- In weld material: Measure CVN data (capturing lower shelf, transition, and upper shelf region) and standard fracture mechanics K_{IC}/J_{IC} specimens.
- Macro-etch specimens to document grain size and spatial distribution of microstructures over the weld material and the HAZ.

Some ancillary tests may be conducted before or concurrently with the large-scale tests (e.g., material testing), whereas some will need to be conducted after the

large-scale tests (e.g., fractography). This program of experiments should be conducted for each archetype used in the large-scale and subcomponent tests.

4.3.6 Data Recovery and Documentation

Prior to each experiment, physical data about the as-fabricated specimen geometry should be gathered, including measurements of welds, member sizes, and unfused section sizes. A combination of photography, nondestructive testing, and 3D scanning can be used to gather this information. Fractography, such as Scanning Electron Microscopy, should be used to identify modes of fracture and microstructures. All WPS and other relevant welding parameters should be documented.

During the experiments, observations should be documented on fracture initiation, propagation, and post-fracture response of the column splice subassemblage. To complement these observations, there are several important types of data to gather during the experiment:

- Loads and deformations at each actuator, corresponding to each controlled degrees of freedom
- Local deformation in key regions of the specimens, particularly at the splice connections where fracture is expected to initiate and propagate
- High speed photography and videography, particularly of the splice region to capture crack propagation
- Recordings of ambient temperatures and specimen temperatures in the vicinity of the area of expected fracture
- Strain gage data to examine local deformation patterns, infer stress flows, and validate CFE studies

4.4 Computational Research Plan

The computational research plan for pre-Northridge PJP column splices is critical because the risk of PJP column splice failure must be assessed in the context of system response, including collapse, and there are significant interactions between component and frame response, especially after partial or full fracture of the splice; these will influence performance.

It is envisioned that each of these simulations will be validated rigorously against appropriate experimental data sets, including new experiments that may be proposed expressly for this purpose. The components of the computational plan should be developed in a coordinated manner, explicitly considering the physical interactions between the splice and system, as well as coupling between the results of each

component of the computational plan and the physical response obtained from the experiments (Section 4.3).

The computational research plan should address several areas:

- Building or frame response that drives demands in PJP column splice connections
- PJP column splice component response under these demands
- Building or frame response, to assess the impact of potential risk mitigation strategies

4.4.1 Analysis Strategy for NLRHA for Demand Assessment

The primary objective of the NLRHA for demand assessment is the characterization of seismic demands in splice connections that may be used to conduct subassemblage-level experiments and finite element simulations.

The first step should be to identify and develop appropriate EDPs that are indicators of PJP column splice performance and failure. Unlike beam-to-column connections and other deformation-controlled components, for which interstory drift and interstory drift histories have been established to be effective indicators of failure, EDPs for splices are not well established. There are several issues to consider:

- Interstory drifts and deformation may not be suitable indicators of splice fracture. Axial forces, shears, and moments about both axes may be more suitable indicators. However, this could vary across various building designs and splice details.
- Local stresses may be most correlated with splice fracture but they require more sophisticated simulations, and the stresses will vary between configurations.
- Cyclic history effects may be important in terms of localized strain reversals even if the members and splices remain elastic at the global scale.

Once the EDPs are identified, the NLRHA should simulate them in a probabilistic sense for different levels of seismic hazard, accounting for variability in ground motions and structural properties. The EDPs should then be correlated with aspects of frame design, member sizing, and other important parameters of the configurations.

Physical Phenomena and Effects to be Simulated in the NLRHA

The NLRHA should simulate member forces (i.e., axial, biaxial moment, and biaxial shear) and deformation histories with accuracy, so that they can be used to calculate the EDPs. Previous studies have shown that the stresses in splices are driven by a combination of high moments in the central region of the column due to higher mode effects (e.g., single curvature bending), and axial tension or loss of compression due

to frame overturning effects. The NLRHA should simulate the physical phenomena that may inform the EDPs:

- *Inelastic response considering yielding of beams as well as columns under combined bending and axial forces:* This includes damage deterioration modes, including fracture of beam-to-column connections and the flexibility of base connections. Especially in the columns, simulation of distributed plasticity and axial force-bending moment (P-M) interaction is important.
- *Geometric nonlinearity, including P-Delta and member P-δ effects*: The latter are especially important to simulate, especially if they amplify single curvature bending of columns.
- *Finite joint sizes and panel zone flexibility.*
- *Vertical accelerations:* Research by Song et al. (2020) indicated that consideration of vertical accelerations has a significant effect on the fracture fragility of PJP splice connections, especially for high-rise moment frames.
- *Three-dimensional response*: This should include the effects of biaxial shaking, along with the vertical shaking.

Other issues may be important and should be included or ruled out through exploratory simulations or reasoning. Simulation of all factors may not be necessary in every NLRHA simulation if the effects can be demonstrated to only have a modest influence. Examples of such issues are: the effects of flexible diaphragms and torsional coupling; isolated or unsupported columns in atriums that may excite single curvature bending; and splices in gravity frames (including bolted splices).

Splice behavior affected by fracture in other splices should also be considered, but it may not be possible to capture this behavior before the experimental research is underway. Some NLRHA procedures should be updated to incorporate this type of feedback or coupling between various analysis and testing tasks.

Building Selection

The overall strategy for building selection should be addressed using the considerations in Section 3.1. In the specific context of PJP column splice computational studies, there are additional factors to consider in the selection of parameters:

- Seismic demands in PJP splices may not be as drift sensitive as other components, such as panel zones.
- Studies by Galasso et al. (2015) and Shen et al. (2010) indicate that in low- to mid-rise buildings, the demands in splices are typically controlled by bending of the columns. In these buildings, higher mode effects are not dominant; however,

the deviation of column bending from perfect double curvature as well as the location of splices (e.g., not at the center of the column) contribute to the risk of fracture.

- The risk of fracture has been shown to be higher in frames where both higher-mode effects, which induce single-curvature bending in columns, are present along with column tension or a reduction in net compression.
- The differences in loading and other phenomena between space frames, perimeter frames, and partial perimeter frames should be considered.

Outputs from NLRHA

The outputs should be developed in a manner that will facilitate application to experiments and finite element simulations, either directly or through the development of loading protocols. There are several key outputs:

- Characterization of splice demands in terms of the appropriate EDPs
- Representation of these EDPs in a probabilistic manner, considering uncertainties in the ground motions and structural modeling
- Based on this probabilistic representation, development of loading histories and protocols for use in the experiments and finite element simulations

Pseudo-dynamic tests may be required for some of the experimental specimens. The NLRHA simulations and the platform they are developed on should be capable of integrating the experimental and analytical components required for such simulation.

4.4.2 Analysis Strategy for CFE Simulation

The primary objective of the CFE simulations is to establish the fracture potential of a given splice configuration, given a set of EDPs determined through NLRHA simulations. These CFE simulations should be conducted in a complementary manner to the experiments. There are several objectives of the CFE simulation:

- Generalize the results of the physical experiments to untested configurations
- Develop physical intuition regarding internal stress distributions, fracture toughness demands and modes of response
- Facilitate sensitivity and reliability studies
- Support optimal planning of the component experiments and the NLRHA.

Appendix C provides guidance for development of the CFE simulations.

4.4.3 Analysis Strategy for NLRHA Simulations for Assessment of Mitigation Strategies

The primary objective of the NLRHA simulations for mitigation strategy assessment is to examine the effectiveness of the proposed mitigation strategies. The plan for developing these mitigation strategies by synthesizing the experimental and computational findings is presented in Section 4.7. To assess the mitigation strategies, the NLRHA will assess, in a probabilistic sense, the post-mitigation response of the selected buildings. In terms of building selection and ground motion selection and scaling, the NLRHA should be like those outlined for demand assessment in Section 4.4.1. However, a few differences are envisioned:

- The NLRHA should be focused on assessing system performance, with an emphasis on collapse.
- The simulations should simulate the fracture of splices and related effects, including partial or full fracture, the loss of shear capacity in the case of complete fracture, and subsequent phenomena such as unseating and reseating.
- The simulations should reflect results from experiments for both unretrofitted and retrofitted splices, including the post-fracture response as inferred from the CFE simulations and experiments.
- Mitigation strategies other than splice retrofit could be suggested (e.g., supplemental damping devices).

Ideally, the NLRHA models developed should be validated against shake table studies. However, such studies may not be entirely within the scope of research, unless they can be significantly scaled down. NLRHA models could be validated using existing data sets (e.g., from shake table studies or field reconnaissance) or with other experiments.

4.5 Parameter Selection, Boundary Conditions and Loading Protocols for Experiments and CFE Simulations

The overall aim of the experimental and computational programs (Sections 4.3 and 4.4) is to examine the fracture potential of splices across a range of configurations, material parameters, and loadings, as identified in the archetype buildings (Section 3.1). Interrogating each of these parameter sets experimentally is infeasible experimentally, and also challenging through CFE simulations. Consequently, this section provides guidance for the selection and prioritization of parameters and should be used judiciously to formulate experimental as well as CFE simulation matrices. Various parameters should be investigated:

- *Member size pairs:* Selection of column size pairs should consider the overall geometry and flange sizes, accounting for prevalence in construction practice and feasibility of welding the flange sizes together.
- *Flange penetration:* A range should be examined analytically. Section A.1.3 provides pre-Northridge PJP splice column details that use a range of flange penetrations.
- *Additional parameters pertaining to splice details*: For example, if web/erection plates are welded or bolted.
- *A range of base material and filler material combinations*: Fracture and constitutive properties should be studied. Section A.4.2 summarizes materials used for the splice details over the eras.

The parameter sets should include retrofit details that will be proposed based on the results of the experimental as well as simulation studies. It is not possible to envision the parameters associated with these details at this time. However, the simulations should be complementary to the experiments on retrofit details, in the same manner as the simulations on pre-Northridge details are complementary to the corresponding experiments.

Appendix A provides discussion on material selection and detailing practices in the period from 1960 to 1994. Most combinations of the parameters should be investigated through CFE to establish individual and coupled parameter effects. For the experiments, a smaller subset of parameters should be carefully selected to reflect the most prevalent details and conditions as inferred from the survey of practitioners.

Finally, the parameter sets should be consistent in terms of reflecting particular eras or archetypes of construction, with coherence between members, materials, welding practices, and PJP column splice details. Most existing buildings are air-conditioned, and test temperatures should generally reflect the operating temperatures of the buildings. However, in some cases (i.e., if columns are exposed), consideration should be given to how lower temperatures may decrease fracture toughness.

The boundary conditions and loading protocols for the large-scale tests and CFE should be informed by the demand analysis from the NLRHA simulations, as well as evaluation of pilot tests. In the most general interpretation, the boundary conditions will have the following features:

- Mixed boundary conditions (i.e., a combination of forces) as well as deformations applied at the ends. Applying only forces or deformations may not be effective for obtaining the EDPs. For example, axial forces may be sensitive to minor variations in column stiffness and for such degrees of freedom load control may be more appropriate. Similarly, post-fracture response may be controlled by displacement histories rather than forces. For large-scale tests, the

use of pseudo-dynamic tests (to understand response under specific ground motions) as well as protocol-based testing is recommended.

- Independent application of the 6-degrees of freedom loading at each end of the splice simulation model. This may be adapted to only one end, appropriately accounting for rigid body modes.
- Consideration of load cyclicity, loading rate, as well as load non-proportionality to achieve the appropriate EDPs, including cyclic effects.

Within this general interpretation, appropriate simplifications might be made to facilitate convenient application or to study specific effects. There are several possible simplifications that could be made in some situations with proper justification:

- use of two-dimensional loading
- the use of monotonic loading instead of cyclic loading
- application of regular cycles instead of irregular cycles
- application of proportional loading instead of non-proportional loading.

4.6 Development of Strategies for Repair

The experiments (Section 4.3) provide an opportunity to develop strategies for repair of failed PJP column splices. Each experiment conducted as part of the study should result in a connection fracture. The research plan should include the development of strategies for repair of such fractures. These strategies will depend on the specific mode of fracture observed (e.g., fracture of the flange versus fracture of the entire cross section) and features of post-fracture response (e.g., misalignment of the columns above and below the splice after fracture). In this context, the examination of splice fractures from the pseudo-dynamic tests, which represent full-building response, will be informative. The repair strategies should be developed through consultations with an advisory panel of steel fabricators and practitioners. The repair strategies should specifically consider anticipated performance in future earthquakes, gravity load paths and shoring to maintain structural safety, and degree of disruption due the repair.

It is not possible to envision the specific repair strategy until the mode of fracture is known; thus, potential repairs will be developed as part of the research program.

Once the repair strategies are developed, selected large-scale specimens with splice fracture should be repaired using strategies and retested in a manner similar to the original experiments (i.e., featuring similar loadings and boundary conditions) to assess the performance. In cases where it is unsafe to experimentally examine the repair strategies (e.g., if the repair must be conducted under high axial loads), finite

element simulations could be used to examine the response of such repairs, provided the simulations have been validated using experiments on similar details.

4.7 Development of Improved Evaluation and Retrofit Design Recommendations

The final task of the PJP column splice studies is to develop a practice-oriented, performance-based based decision support framework for pre-Northridge PJP column splice risk mitigation. This task has three parts: evaluation procedures, recommended retrofit practices, and guidance for decision support.

4.7.1 Development of Best Practices for Evaluation

Best practices for evaluation of existing PJP column splices should be developed. The final outcome should be a methodology that returns the probability of various modes of failure (e.g., fracture initiation, propagation, complete failure) of a given splice in a building, for a given seismic loading. The developed guidelines should address types of demand analysis with different levels of sophistication, including linear static, nonlinear static pushover, linear dynamic and NLRHA. Similarly, for capacity analysis, the approaches should include simplified formulas and equations (i.e., those that express critical stress in terms of detail geometry, root penetration, and material toughness), as well as best practices for linear and nonlinear finite element analysis. These practices should be developed such that they are practical to apply through mainstream structural analysis software. It is especially important to characterize and quantify the expected degree of uncertainty and error associated with each type of analysis, such that potential users may make informed tradeoffs between desired accuracy and computation time. Additionally, it is desirable to use the tools and methods described in Section 4.4.3 to simulate splice fracture and its impact on overall building performance.

4.7.2 Recommendation of Retrofit Practices

Based on the experimental and simulation data, recommendations for retrofit details should be developed. A primary focus of these details should be inclusion into AISC 342. Consequently, these should be developed in a format that facilitates adoption by the appropriate code committee. Further, these recommended details should feature a range of interventions, from minimally invasive to full replacement. The recommended details should prescribe all aspects of design, including geometry, materials, weld procedures and other fabrication procedures. The recommendations should also clearly provide limits within which the details are qualified to provide expected performance. Finally, the details should be accompanied by fragilities (similar to those that will be developed for existing PJP splice details) such that the probability of failure of each retrofit detail may be assessed and used within performance-based frameworks. Similar to Section 4.7.1, the tools for retrofitted

building performance assessment should also be used to evaluate retrofit recommendations.

4.7.3 Guidance for Decision Support and Acceptance Criteria

The evaluation practices and retrofit recommendations should be integrated within a performance-based framework to develop sample decision trees, based on desired outcomes. It is important to note here that many factors (e.g., remaining life of the building, condition of existing splices, building performance after splice fracture, local hazard) will influence selection of the most appropriate retrofit strategy. Optimal decisions may not be trivial, and could even include non-intervention or measures such as introduction of supplemental damping (i.e., no splice retrofit). To address this, the research should develop guidelines for interpreting continuous probabilities of failure into discrete risk mitigation decisions. This may include the development of acceptance criteria that triggers specific retrofit recommendations for certain performance levels. Where possible, software tools (or aids) should be provided for the decision support framework that can automate calculation of failure probabilities and other decision variables based on outputs from simulation software.

Chapter 5

Research Plan for Studying Weak Panel Zone Behavior

This chapter describes a recommended plan for studying the seismic behavior of weak panel zones in pre-Northridge beam-to-column moment connections. A concise history of panel zone design and short summary of research knowledge gaps are also provided.

The recommended research requires both experimental and computational studies. Experimental testing is anticipated to include large-scale testing of beam-to-column subassemblies conforming to identified archetype buildings (Section 3.1) and related ancillary testing. Computational studies will be used to extend the range of investigated parameters.

The ultimate goals of the research are to develop a decision framework regarding weak panel zone evaluation procedures coherent with the provisions with ASCE/SEI 41 for moment frames, outline retrofit design requirements, and propose feasible retrofit and repair solutions.

5.1 Overall Research Strategy

The research on weak panel zones should focus on three main areas:

Area 1: *Characterization of the panel zone force-deformation demand for steel moment frames constructed in the pre-Northridge era*. Existing models in ASCE/SEI 41 and the literature should be incorporated or expanded upon to investigate the deformation demand of weak panel zones. These expanded force-deformation relationships can be leveraged by engineers tasked with the nonlinear modeling of these structures. The influence of panel zone deformations to the fracture demand imposed on the beam-flange-to-column-flange CJP welds will also be essential for developing performance predictions of different connection types.

Area 2: *Characterization of the ultimate shear deformation capacity of the panel zone prior to failure of the connection as influenced by connection configuration and geometry, material strength, and filler metal toughness*. Past research has identified that weak panel zones may contribute to premature connection failure; conversely, it has been demonstrated that connections utilizing modern detailing can leverage the weak panel zone to

realize a stable hysteretic behavior. The characterization should help distinguish between these two extremes.

Area 3: *Exploration of retrofit strategies.* After the panel zone force-deformation response and ultimate shear deformation capacity are established, retrofit strategies should be explored. These strategies, at the connection level, may include increasing the shear deformation capacity by replacing the beam-flange-to-column-flange CJP weld, or by strengthening the panel zone. Based on the available shear capacity and connection configuration, other system-level strategies may be required, including adding isolation or viscous damping systems. It is not the intent of this research program to explore system-level retrofits, but the proposed decision framework developed in this program should consider this type of strategy.

The research will incorporate both experimental and computational tasks. It is anticipated that these tasks will not necessarily be serialized as they may be used to inform each other. In the final stages of the research program, both the experimental and computational results will be leveraged to propose and predict the response of retrofitted connections. The new body of knowledge will then synthesize to form a cohesive decision framework regarding the deformation capacity of weak panel zones, when retrofit is required, and what retrofit solutions are viable. Figure 5-1 is the proposed research workflow showing interrelations between tasks.

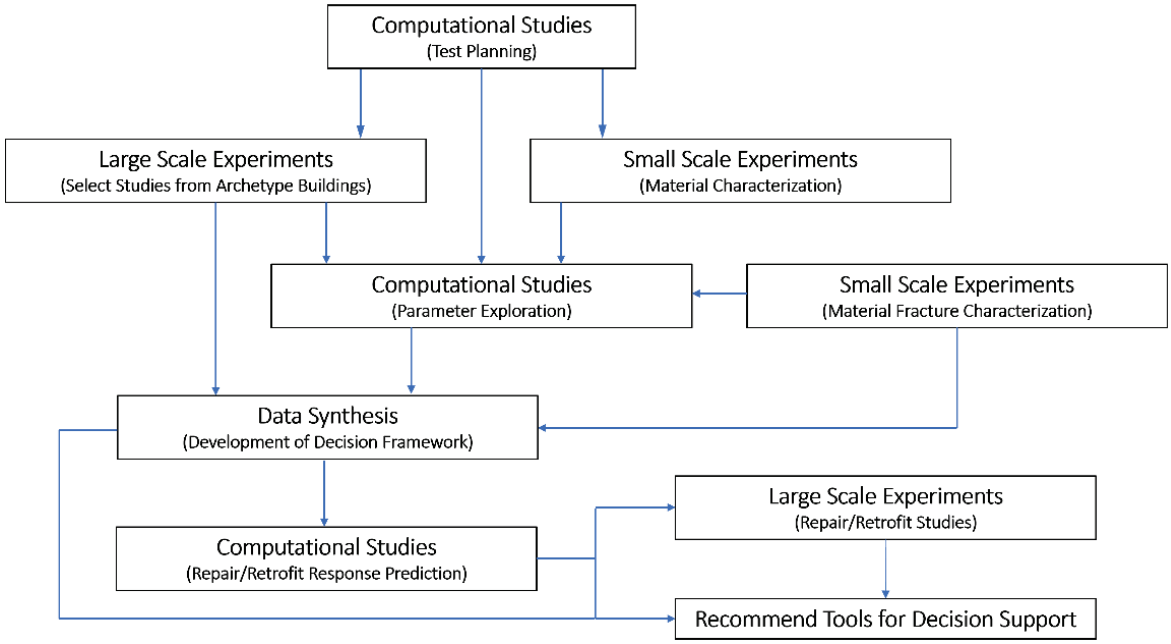

Figure 5-1 Research workflow.

The archetype building designs identified at the start of the project will be used in the panel zone studies described in this chapter. The process for developing the archetype buildings, which involves close study of the historical background and an effort to

collect existing building information representative of pre-Northridge design in the United States, is described in Section 3.1. Findings from the preliminary computational studies (Section 3.2) should be used to inform the direction of the panel zone studies.

5.2 Prior Research on Behavior of Panel Zones

Appendix B is a comprehensive summary of prior research on panel zones in the context of the research program objectives. The more concise summary provided in this section focuses on history of panel zone design and knowledge gaps in the main research areas.

The design requirements of panel zones in the pre-Northridge era resulted in scenarios that can cause significant panel zone yielding when subjected to a seismic demand. When the majority of the inelastic behavior is anticipated in the panel zone such that it becomes the primary ductile mechanism, it is called a *weak* panel zone. This is contrasted to connections with a *strong* panel zone, which use the flexural hinging in the beam as the primary source of ductility. A panel zone designed to share the ductility demands with the beam is referred to as *balanced*.

Before the 1988 *Uniform Building Code* (UBC), design requirements were limited, with engineers following different recommendations. For example, the 1980 *Recommended Lateral Force Requirements and Commentary* published by SEAOC suggested panel zones be designed for the shear produced by the nominal plastic moment capacity for each beam framing into the column. This recommendation and others used prior to the 1988 UBC may result in a weak panel zone. The 1988 UBC required that the panel zone shear be designed for 1.85 times the prescribed seismic force for working stress design with an upper bound of 80% of the nominal plastic moment capacity of the beams framing into the column. Also, during this era, a more liberal panel zone design strength that considers the contribution from column flanges was adopted. The combination of these two design requirements is prone to produce a weak panel zone. Following the 1994 Northridge Earthquake, the 1997 AISC *Seismic Provisions* and its two supplements amended the design provisions such that the panel zone is designed for the probable maximum moment generated by the beams. This moment includes factors that account for the expected versus nominal strength of the material and cyclic strain hardening of the beams as well as other factors that increase the forces into the joint. These later requirements do not produce weak panel zones.

Early research on panel zones conducted in the 1960s and 1970s identified that panel zones may possess significant inelastic potential, but high shear deformations in the panel zone of a beam-to-column joint result in kinking of the column flange. These kinks have since been postulated to contribute to premature failure of the beam-

flange-to-column flange CJP weld of typical WUF connections (Section 3.1.4). Other typical moment connection details may have similar issues. Also, several researchers developed force-deformation models of the panel zone during this time period. This includes work done by Krawinkler in the early 1970s that forms the basis of the inelastic panel zone strength used in the current AISC *Specifications*. Since the 1970s, researchers have extended these force-deformation models to expand their scope to heavy column sections and a wider range of connection aspect ratios.

After the 1994 Northridge Earthquake, a significant amount of research was conducted on the behavior of moment frames as part of the SAC Project. The work in this period led to substantial changes in the design of seismic moment frame connections and defines a transition between the pre-Northridge and post-Northridge type connections. Post-Northridge moment connections improve the connection by using filler metals with specified toughness, amended weld details, and connection parameters that have been identified to achieve at a minimum story drift angle during testing.

Experimental testing of moment connections with weak panel zones otherwise following post-Northridge practices has shown good hysteretic performance. This testing has shown that column flange kinking due to large panel zone shear deformations may not lead to premature fracture if the beam-flange-to-column-flange CJP weld is well-detailed with notch-tough filler metal. There are no known experimental programs that sought to directly remedy a weak panel zone, but several retrofit strategies have been explored that indirectly influence the panel zone. Included in some of the experiments were connections that were rewelded using notch-tough filler metal.

Several researchers have explored using ductile fracture metrics to quantify the fracture potential of the beam-flange-to-column-flange CJP welds. These ductile fracture metrics were developed to overcome limitations of proportional loading that quantification of a pre-existing flaw required in traditional linear elastic or elastic plastic fracture mechanics. These simplified metrics demonstrated that a weak panel zone generates a higher fracture potential when compared to a similar specimen using a balanced or strong panel zone. A limitation of these metrics is that they are limited to relative comparisons only and cannot be used to predict fracture. Modern calibrated ductile fracture mechanics models like the Cyclic Void Growth Model (CVGM) can be utilized to overcome the issues with the earlier fracture metrics.

5.3 Experimental Research Plan

Experimental studies should be designed to explore a wide range of parameters and be complemented by the computational research program. The experimental research

is fundamental to inform the computational models, which should be leveraged to extend the parametric range from the experimental program.

Figure 5-2 and Figure 5-3 show common configurations of full-scale testing setups for interior moment frame subassemblages with and without incorporating a composite slab. Material testing for data reduction and further computational model calibrations should also be conducted.

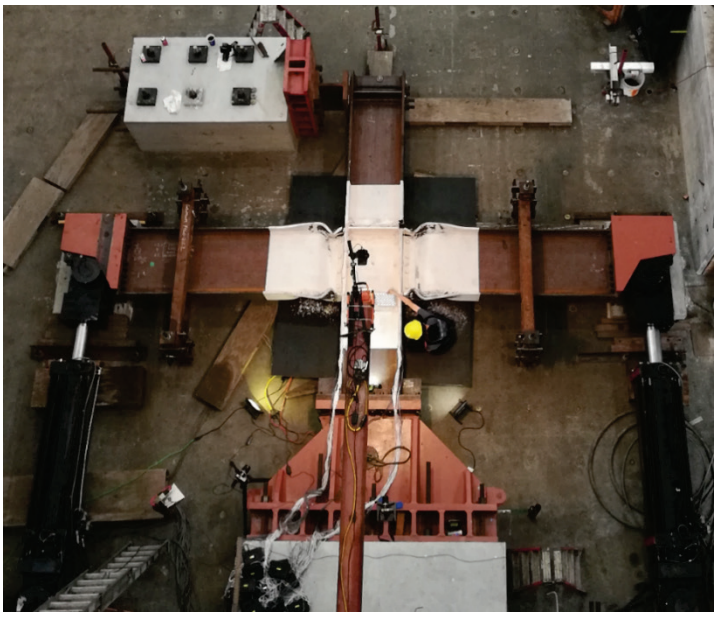

Figure 5-2 Sample interior frame test specimen.

Figure 5-3 Sample interior frame test specimen with composite slab (NIST, 2016).

5.3.1 Objectives

There are two objectives of the experimental research plan:

Objective 1: Understand the role that panel zone deformations have on the beam-flange-to-column-flange CJP welds and develop an estimate of the ultimate panel zone deformation capacity prior to failure of the pre-Northridge moment connection.

Objective 2: Investigate viable retrofit strategies for connections identified with weak panel zones. The subassemblage experimental testing should include large-scale testing of retrofitted beam-to-column moment connections.

5.3.2 Key Parameters

Test specimens should be selected to correspond to the identified archetype buildings (Section 3.1). Connections should be typical of space frames, perimeter frames, and partial perimeter frames. Other key parameters include: design era, member sizes, panel zone aspect ratios, configuration of beam-to-column subassembly, connection details, weld details, steel grades, presence of composite slab, boundary conditions, and loading protocols.

Design Era

In addition to those pre-Northridge moment frames designed per 1988 and 1991 UBC, which encourage weak panel zone behavior, frames designed prior to the adoption of formal panel zone criteria should be investigated. Although no formal panel zone criteria were present in those design codes, some designers implemented their own standards of practice for the connections. These may have originated from the recommendations in earlier editions of the SEAOC *Recommended Lateral Force Requirements and Commentary*. Investigations should respect design provisions during their respective era for other elements of the frames: for example, the requirements pertaining to stiffening elements within the moment connection.

Member Sizes and Panel Zone Aspect Ratios

The test program should explore a range of beam and column sizes. The relative depth between the column depth and beam depth defines the aspect ratio of the panel zone. The panel zone aspect ratio controls the relative proportion of bending versus shear in the panel zone. This is expected to be an important parameter affecting the nature of column kinking. Other important parameters like thickness of the column flanges can be varied by selecting columns of increasing weights. Moment frame span-to-depth ratios should be selected to conform to the archetype buildings.

Configuration of Subassembly

For ease of connection testing, it is common that a one-sided test specimen be used, simulating an exterior moment connection. While such configuration is appropriate when the testing objective is to investigate the robustness of beam-flange-to-column flange CJP welds, it is more appropriate for panel zone research that a two-sided beam-to-column subassembly be used. Simulating an interior moment connection will typically double the shear in the panel zone. This configuration also allows the investigation of the effect of panel zone deformation on four instead of two beam-flange-to-column flange CJP joints in one test.

Connection Details

Beam-to-column connections should include details where the beam flanges and web are welded to the column flange (WUF-W) connections and versions with a bolted web (WUF-B) connection. Additionally, connections with and without stiffeners (i.e., continuity plates and doubler plates) based on the design requirements and common engineering practice at the time should be considered.

Weld Details

It is anticipated that the beam-flange-to-column flange CJP weld details and filler metal toughness will bear the most significant influence on the panel zone shear deformation capacity (Section 2.2). To predict the usable shear deformation capacity of existing weak panel zones, appropriate filler metal and welding process representative of the construction practice at the time should be simulated. Careful consideration should be made to the detailing of the existing welds, including the profile of weld access hole, tack-welding of the left-in-place steel backing, run-off tabs, and weld end dams. It is preferable that simulated field welding be conducted by a certified welder with a prior experience with the E70T-4 welding process. The WPS should reflect the practice of the construction era and follow the applicable provisions from the AWS. Welded joints should be inspected by a certified inspector, and the results should be documented.

It should be noted that the simulated connection details are intended to be representative of those in many existing pre-Northridge steel moment frames, and the quality assurance, including UT inspection, was not as stringent as it is in post-Northridge practice. Care should be taken to produce welds of similar quality to welds made in the field at the time the archetype buildings were originally constructed. The investigator should devise methods to achieve this and avoid laboratory-quality welds. It is anticipated that the investigator will coordinate with the advisory panel of the project during specimen construction to achieve this.

Shape Materials

Material grades of test specimens should match those of the identified archetype buildings. Depending on the era, this may be A36 steel for the beams and columns, although investigators should be aware of the prevalence of dual grade steels since the early 1980s. More information regarding material specification is provided in Section 3.1.7. If the preferred material is not available for testing, the investigator should consider different approaches to reconcile any differences in the material tested versus the archetypes.

Composite Slab

To simplify specimen construction, composite slabs are often ignored in moment connection tests. Since the slab may alter the depth of the panel zone and change the force demand in the CJP welds, the investigator needs to justify that the slab effect can be ignored if the concrete slab is not to be included in most of the test specimens. This justification should be done by performing a comparative study at the beginning of the experimental program.

Boundary Conditions

The boundary conditions of the simulated subassemblage should reasonably reflect those observed in a contiguous moment frame building. One common practice is to assume that inflection points exist in the midspan of the beams and mid-height of the columns. This is representative of first-mode response and is anticipated to be an adequate representation for this study. The presence of axial load would affect the panel zone strength, stiffness, and deformation capacity. For ease of testing, this effect is seldomly included, but it should be investigated in this program to ensure a complete decision framework.

Loading Protocols

Cyclic loading of the moment frame subassembly is essential to develop representative demands and deformations. Chapter K of AISC 341 (AISC, 2016a) provides a standard loading protocol for prequalification of post-Northridge moment connections. This story drift angle-based loading protocol can be used for this research unless an alternate loading protocol is proposed by the investigator. If needed, a near-field loading protocol developed for the SAC Project also can be used (FEMA, 2000a). Testing should continue to large inelastic deformations such that the cyclic response near collapse can be evaluated.

5.3.3 Ancillary Testing

Ancillary experimental testing should be conducted to characterize the steel and filler metal properties. These properties will be used in the computational research studies

and to compute actual material properties during data reduction. Testing should include cyclic testing of samples to determine the yielding and post-yielding behavior when subjected to representative strain ranges. In addition, measurements of fracture toughness should be performed to develop a calibrated fracture model. The investigators should perform sufficient testing to establish the variability of material strength and toughness.

See Appendix C for a description of the required material properties for the anticipated CFE simulations.

5.3.4 Data Recovery and Documentation

The large-scale testing and ancillary testing should be thoroughly documented in a systematic manner to facilitate post-processing.

Prior to each experiment, Material Testing Reports (MTR) and the WPS should be compiled for each specimen component. Geometrical properties of the steel members and welds, including the actual dimensions of the rolled steel shapes and welds, should be documented.

During the experiments, several data collection measures should be put in place to allow for documentations of important data:

- Load and displacement at the actively controlled degrees of freedom should be recorded.
- Restrained degrees of freedom should be sufficiently instrumented to confirm their restraint.
- Specimens should be sufficiently instrumented to recover the panel zone deformation. This is often done with two transducers extending between the corners of the panel zone. The investigators should consider techniques to isolate secondary deformations that may influence the data. Additional transducers can be used to record other deformations, for example to extract the constituent components of the story drift.
- Specimens should be instrumented with strain gauges to enrich the experimental observations at the local level.
- High resolution photographs should be taken of the specimens throughout testing to document their performance. It is common to paint the specimens to provide a visual indication of yielding.

Ancillary test results should be used to show alignment with the MTRs and provide information regarding the strength of the weld metal.

5.4 Computational Research Plan

The computational research will be instrumental in testing a broad range of parameters to define the panel zone force-deformation relationship and ultimate shear capacity. The finite element models can also be implemented to validate proposed retrofitted schemes prior to experimental testing. There are two objectives of the computational research plan:

Objective 1: Establish a calibrated CFE modeling methodology that includes a set of representative nonlinear cyclic material properties, an accurate representation of the boundary conditions and specimen geometry, and a validated methodology to predict fracture of the beam-flange-to-column-flange CJP weld.

Objective 2: Leverage the developed CFE models to expand on the experimental test matrix.

A guide to developing accurate CFE modeling is provided in Appendix C.

5.4.1 Parameter Selection

The first test parameters should match the experimental tests based on the identified archetype buildings. The second cohort is meant to fill in the gaps of the experimental test matrix and to systematically test the relevant parameters. These may include a variation of beam and column sizes, column flange and web thickness, thickness of continuity plates and doubler plates, material properties, and the inclusion of a composite concrete slab.

5.4.2 Perform CFE of Beam-to-Column Subassemblages

The computational research should include CFE analyses using an established computer program (e.g., ABAQUS). Geometric and material nonlinearity should be appropriately captured by the analysis. Investigators should choose appropriate finite elements and may utilize techniques of refined sub models using solid elements. Models should include boundary conditions and restraint that match those used in the experimental program and of the archetype buildings. It is envisioned that the loading protocol will match Chapter K of AISC 341, although other loading protocols may also be considered. Modeling of fracture within a CFE analyses should be performed with a regime of sufficient complexity to capture the non-proportional stress state at the beam-flange-to-column-flange CJP weld.

5.4.3 Assessment of Computational Research Results

The assessment of the computational research should primarily focus on establishing the panel zone shear deformation capacity prior to connection strength degradation caused by the fracture of beam-flange-to-column flange CJP welds, such that findings from experimental testing can be generalized. This effort should include a

wide range of parameters so that their sensitivities can be established. This should include establishing an average and lower bound response. The developed finite element methodology can be assessed by comparing the performance of the retrofitted specimens tested as part of the experimental program to their simulated counterparts. Finally, the panel zone shear deformation capacity and behavior should be compared to provisions in the AISC *Specifications* and ASCE/SEI 41.

5.5 Development of Strategies for Retrofit and Repair

One of the final tasks of the panel zones studies is to develop a practice-oriented, performance-based based decision support framework for repair and retrofit.

5.5.1 Retrofit Evaluation

Because a weak panel zone may exacerbate brittle fracture of beam-flange-to-column flange CJP welds in a pre-Northridge connection, there is a need to develop measures to mitigate such effect. FEMA 351 (FEMA, 2000b) is a report developed by the SAC Project for retrofitting pre-Northridge connections. Two approaches are provided: the simplified approach and the systematic approach. The simplified approach involves modifications made to individual connections, while the systematic approach also includes measures that add either supplemental lateral force-resisting elements (e.g., braced frames, shear walls) or response modification devices (e.g., base isolation, energy dissipation devices) to the existing building. In practice, it is not uncommon that both connection modification and system modification be used simultaneously to retrofit a pre-Northridge steel moment frame building (e.g., Malley et al., 2009). In this proposed research, the focus is on retrofit of pre-Northridge connections with weak panel zones. Since panel zone response is directly related to the potential for fracture of beam-flange-to-column-flange CJP welds (especially at the bottom flange), retrofit procedures for the CJP welds should also investigated.

After sufficient progress is made by investigators performing the experimental and computation research, an evaluation strategy for retrofit should be proposed. The anticipated decision framework should incorporate the prevailing variables and focus on structural configurations identified in the set of archetype buildings.

5.5.2 Retrofit

Informed by the evaluation criteria developed by performing the experimental and computation research tasks, the investigators should consider possible retrofit strategies. FEMA 351 (FEMA, 2000b) and the AISC *Steel Design Guide 12* (AISC, 1999b) provide retrofit schemes, but they were not specifically developed to address the weak panel zone issue. Strengthening weak panel zones is seldom done in practice. Typically, access to panel zones is impaired by gravity beams that frame into the connections in the perpendicular direction and the presence of a concrete

slab. Any retrofit strategy considered by the investigators should address access issues. To ensure that the proposed schemes are achievable, the investigators should seek guidance from practicing engineers prior to their proposed study. Retrofit strategies may take several approaches. The first one is to physically strengthen the panel zone in order to reduce the inelastic deformations. The second scheme is to improve beam-to-column joints, especially welded joints that are vulnerable to brittle fracture, while allowing the existing panel zone to undergo large inelastic deformations. The latter approach has been implemented in practice (e.g., Kim et al., 2015).

5.5.3 Repair

Pre-Northridge connections with weak panel zones will be damaged in the experiments, and these damaged specimens should be used to investigate repair methods. Depending on the failure mode, FEMA 352 (FEMA 2000c) provides detailed procedures to repair damaged connections. It is expected that some schemes used for repair are also applicable for retrofit.

5.6 Development of Improved Evaluation Recommendations

Based on results from the experimental and computational studies, a practice-oriented decision framework should be developed. This framework will form the basis of a seismic evaluation procedure that addresses the effect of weak panel zones on pre-Northridge beam-to-column moment connections. It is expected that a panel zone model that considers all the important parameters will be proposed. As a subset of this decision framework, and in the context of ASCE/SEI 41, a refined decision framework should be developed in a format that facilitates an easy adoption by the code committee to AISC 342.

Chapter 6

Research Plan for Studying System Behavior

This chapter describes a recommended plan for studying the behavior of pre-Northridge moment frame buildings at the system level, specifically as they relate to the issues of PJP column splice and weak panel zone performance. It outlines program objectives and necessary computational and experimental strategies for investigating system-level performance to serve the development of evaluation and retrofit design recommendations. Studies described in this chapter include system-level experimental research and advanced computational research. Preliminary computational system studies on the archetype buildings, to take place in an early stage of the research program, are presented in Section 3.2.

6.1 Overall Research Strategy

System-level investigations are intended to verify behavior of individual members and connection assemblies within the context of the entire moment frame system. Member and subassemblage studies are limited in that boundary conditions representing the potential interaction with other elements in the system must be imposed. This is accurate to the extent that these interactions are known. System-level investigations should be used to help confirm that boundary condition assumptions are valid. In a complementary way, information gained from subassemblage investigations should be used to improve the accuracy and robustness of system-level simulations.

System-level computational studies will commence with the preliminary work described in Section 3.2 to assess the performance of archetype buildings. The results of the preliminary computation investigations are used in the development of the PJP column splice (Chapter 4) and weak panel zone (Chapter 5) studies. Advanced computational system-level investigations described in this chapter should draw from the results of the column splice and panel zone research to further extend the knowledge base on system-level performance. These detailed computational studies should typically focus on either column splices or panel zones. Some final studies may also address both issues simultaneously. The system-level experimental research program described in this chapter should also draw from the results of the Chapter 4 and 5 research.

Significant coupling exists between component and system response (e.g., fracture in some splices or beam-to-column connections may influence overall frame response and the demands in other components). To this end, the advanced computational and experimental system-level tasks should be conducted in close coordination with each other, as well as the results from the research conducted within the Chapter 4 and 5 research programs.

Figure 6-1 schematically illustrates the anticipated interconnections of these tasks within Chapter 6 and those to the Chapter 4 and 5 research results and recommendations.

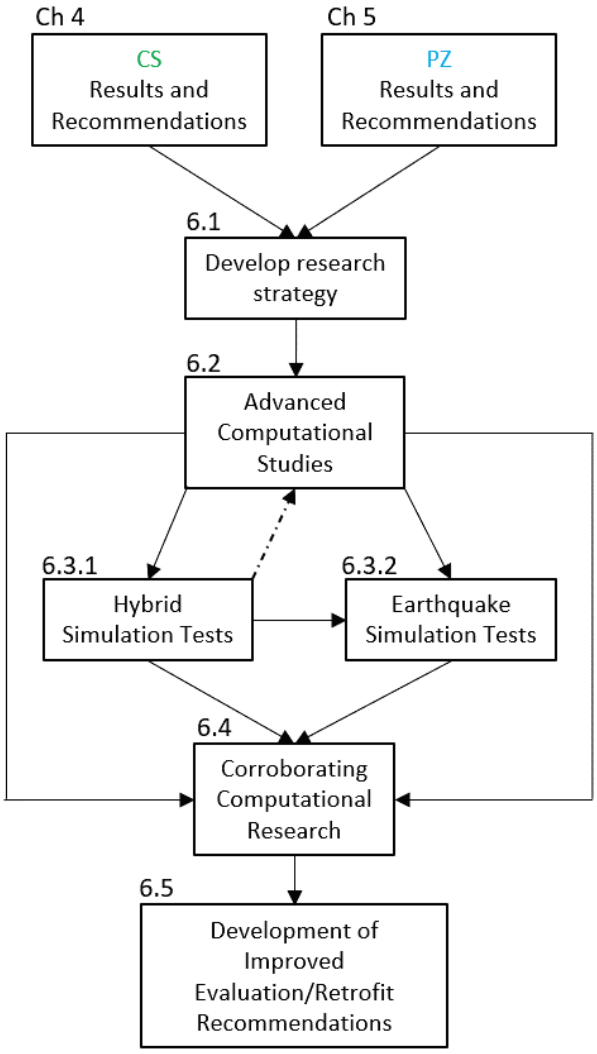

Figure 6-1 System study task interrelationships.

6.2 Advanced Computational Research Plan

The computational research plan consists of two parts: preliminary computational studies and advanced computational studies. For the purposes of developing research

plans described in Chapters 4 and 5, the preliminary computational studies described in Section 3.2 should be conducted on the archetype building design using state-of-the-art simulation models that have been calibrated based on currently available information from past analytical and experimental studies. The advanced computational studies described is this section should narrow the list of important design variables considered in the archetype buildings. Models should be expanded to three-dimensions and updated with refined simulation models calibrated with updated information on composite beams, column splice details, panel zones, column bases, and gravity framing.

System-level analytical work should consist of nonlinear static analyses and NLRHA for evaluation of global behavior. Research analysis programs are available and could be used for this purpose, including OpenSees, *Open System for Earthquake Engineering Simulation* (McKenna, 1997), and FRAME3D. The OpenSees simulation platform is also compatible with the Open-Source Framework for Experimental Setup and Control (Schellenberg, 2008), which could be utilized for hybrid simulation tests.

The advanced computational system studies should narrow the list of important design variables considered in the development of archetype buildings used to investigate the column splice and panel zone evaluation/retrofit issues. This work should build on the two-dimensional and three-dimensional models developed during the preliminary computational research studies. Information from integrated computational and experimental research on subassemblage test specimens and the frame-level computational work done as part of the Chapter 4 and 5 research programs should be used to update the analytical models for simulating member and connection behavior.

Advanced computational system studies should consider the following:

- Re-design (if needed) of the archetype building models based on recommendations from subassemblage-based research on column splices and panel zones.
- Importance of slab effects on cyclic behavior, stability of beam-to-column connections, and dynamic instability of moment frame systems.
- Relative flexural strength between connected beams and column that provide stability of deep beam-to-column connections and delay or prevent local story mechanisms, particularly in the bottom stories of multistory frames. This includes considering the effects of dynamic axial load ratios on behavior.
- Cyclic behavior of columns including three-dimensional effects. This requires member-based experimental tests to determine the effect of coupling of axial load and biaxial bending on columns. Three-dimensional column models should

be developed and calibrated with available experimental data and incorporated into three-dimensional nonlinear archetype models.

- The use of advanced panel zone models that are able to simulate shear buckling in panel zones. This will require extensive calibration with experimental data from past studies and the subassemblage-based experimental research (Chapter 5). For panel zone design, material strength variability between the column flange and web, and the additional strength of beams with composite slabs, should be considered.
- Incorporation of column base modeling in cases where preliminary computational studies demonstrate this effect to be important. This will require calibration with experimental data from member-based tests that include alternative column base conditions.
- Incorporation of gravity framing in the numerical models taking advantage of available information such as from the SAC Project tests related to shear connections (Liu and Astaneh-Asl, 2000). The contributions of gravity framing to lateral stiffness and strength of moment frames should be quantified.

6.3 Experimental Research Plan

System-level experimental research is intended to investigate issues that cannot be addressed through component-based testing alone. System-level specimens consist of full-scale complete frame systems or subsystems consisting of multi-bay, multi-story portions of a complete frame. As a result, the system-level testing matrix is limited due to the size of the specimens and complexity of the test set-up. System-level experimental testing includes the use of hybrid simulation techniques on partial frame specimens and shake table tests on full-scale complete frame specimens. Ultimately, shake table testing is recommended to confirm the overall integrated results of all elements of the recommended research plan, but recognition of the high cost of such tests must be considered. System-level experimental testing should be initiated after the completion of all proposed subassemblage tests, and after the completion of system-based computational research as a validation tool. Systems tests on pre-Northridge configurations should be retested after repair whenever possible. In addition, system tests on retrofitted moment frames should be included in the program with the retrofit techniques to be implemented taken from successful results of subassemblage testing and analytical results from both the column splice and panel zone studies. Design of test specimens and test set-up should be informed by the computational research results.

6.3.1 Hybrid Simulation Tests

The hybrid simulation technique should be used in the first experimental test series to reduce potential cost. Before utilizing the hybrid simulation technique, past and

ongoing experimental studies should be reviewed to assess the potential limitations of this experimental method relative to shake table tests. Relevant studies include Schellenberg (2008), Wang et al. (2011), and Lignos et al. (2011b), as well as the NEES Research project, *Collapse Simulation of Multi-Story Buildings through Hybrid Testing* (Eads et al., 2013).

At least four system-level specimens are envisioned for hybrid simulation testing. These partial frame specimens should each include at least two columns and should represent the bottom stories of selected archetype buildings described in Section 3.1. Steel members used in some of these specimens should be nominally identical to selected subassemblage-based specimens to allow for direct comparison and design verification. A slab should be included in all system-level specimens.

The first series of system-level testing has several purposes:

- Quantify the axial restraint provided by a composite slab and the reduction in the modification in maximum demand and post-buckling deterioration of beam-to-column connections.
- Demonstrate potential differences between boundary conditions assumed in cruciform and T-shaped subassemblies versus the influence of surrounding elements in the structural system.
- Evaluate the stability of columns and demands on column splices considering story-level behavior, fluctuation of points of inflection, and combined axial load and cyclic deformations.
- Evaluate the effect of column base connections on the general stability of columns as part of the first story of an entire system.
- Investigate the effects of panel zone design as part of overall system response, considering information gained from subassemblage-based research and the effects of web doubler plates and continuity plates.

Testing should include at least one quasi-static test with a symmetric loading protocol to allow for comparison with subassemblage-based experimental results. Other tests should be used to investigate the effect of loading history on the seismic response of moment frame systems. All system-level specimens should be pushed to large inelastic deformations to investigate dynamic response near collapse. Second-order effects should be considered in the analytical portion of the hybrid simulation model since this effect is expected to dominate response at large deformations.

6.3.2 Earthquake Simulation Tests

Earthquake simulation testing on full-scale, full-frame specimens should be used to investigate effects that cannot be addressed through hybrid simulation techniques,

and to confirm the integrated results of the entire research program. Weight and global overturning will become an issue in full-scale specimens of archetype buildings more than five stories tall. A substructuring technique discussed in Chung et al. (2010) may be employed to simulate the upper stories in lieu of complete frame specimens. Earthquake simulation testing on complete frame specimens should permit further investigation of three-dimensional effects:

- Biaxial bending and cyclic drift coupled with axial load at columns with four-way moment connections and corner columns in perimeter moment frames due to three-dimensional motion. This may be critical for weak column systems due to limitations in weak-axis buckling capacity.
- Validation and identification of limitations for advanced and simplified numerical models and modeling platforms (commercial and research).

This test series should include scaled intensities of ground motions that are representative of design level and maximum considered earthquake (MCE) events in regions of moderate and high seismicity.

6.4 Corroborating Computational Research

Corroborating computational research should be performed using updated analytical models from the advanced computational studies. Models should be updated based on information that becomes available from subassemblage and system research. The system-level experimental program should be used to validate and further refine the integrated use of all numerical models for moment frame behavior considered and developed as part of the overall research program. A major issue for corroboration will be to validate modeling capabilities of systems at large deformations where complex nonlinear response is expected.

6.5 Development of Improved Evaluation and Retrofit Recommendations

Research elements described in Chapter 4 and 5 will contribute to the development of recommendations for improved evaluation and retrofit provisions (e.g., ASCE/SEI 41 and AISC 342). The system-level research is intended to confirm these recommendations through the investigation and confirmation of system behavior. In the last stage of overall research plan, improved evaluation and retrofit provisions should be developed, calibrated, and verified for adoption in seismic evaluation standards. It is envisioned that this research program will provide many valuable contributions to seismic design practice for the evaluation and retrofit of pre-Northridge steel moment frame buildings:

- Implications of varying panel zone strength ratios on performance of pre-Northridge moment connections and systems

- Implications of fracture-sensitive PJP column splices on performance of pre-Northridge moment frames
- Improved modeling procedures, both simplified and detailed, for addressing the interrelationship of the weak panel zone behavior and overall pre-Northridge connection response.
- Improved modeling procedures, both simplified and detailed, for the response of PJP column splices.
- Procedures for design of retrofit procedures for PJP column splices.
- Procedures for design of retrofit procedures to improve the seismic performance of connections with weak panel zones.

Chapter 7

Task Plan, Schedule, and Budget

This chapter lists the recommended tasks, approximate schedule, and order of magnitude budget for the research plan investigating the seismic behavior of pre-Northridge PJP column splices and weak panel zones.

Although the elements of this plan are highly structured and specifically identified, it is understood that the program will evolve as implementation occurs. Wherever possible during implementation, innovative ideas for new experimental and analytical approaches should be encouraged to resolve technical issues that cannot be addressed with present techniques or could not have been foreseen with present knowledge.

Activities in the research plan could be combined with research activities supporting NIST GCR 11-917-13, *Research Plan for the Study of Seismic Behavior and Design of Deep, Slender Wide Flange Structural Steel Beam-Column Members* (NIST, 2011b).

7.1 Research Plan Overview

A multi-phase, multi-year effort is needed to complete all recommended research tasks. Figure 1-6 provides an overview of the entire research plan. Work is split into five major activities: identification of archetype buildings and preliminary computational studies (AR), column splice studies (CS), panel zone studies (PZ), system studies (SM), and final product development (PR).

The first activity involves the identification of archetype buildings and preliminary computational system studies to explore the archetypes. Once the archetypes are identified, the two major activity tracks can begin: column splice studies and panel zone studies. The system studies can begin after both the column splice studies and panel zone studies are underway and have generated significant results. After the main research elements have been completed, a follow-on activity is planned to finalize the recommendations and products.

Although the subtasks have been grouped into tasks and activities, a high level of integration and collaboration across subtasks, tasks, and activities is necessary to meet the objectives of plan.

7.2 List of All Research Tasks

A summary of all tasks is provided in Table 7-1. If funding is limited, it is recommended that the depth of tasks be reduced, rather than any particular tasks being entirely removed. Descriptions are provided in the sections that follow.

Table 7-1 Research Plan – Summary of Tasks

Activity	No.	Name of Activity, Task, or Subtask
Archetype	**AR**	**Identification of Archetype Buildings & Preliminary Computational Studies**
	AR.1	Identify Archetype Building Configurations and Designs
	AR.2	Perform Preliminary Computational Studies
	AR.3	Report on Archetype Buildings and Preliminary Computational Studies
Col Splice	**CS**	**Investigation of Column Splice Behavior**
	CS.1	Develop (and Update) Research Strategy
	CS.2	Conduct Experimental Research
	CS.2.1	*Perform Testing on Large-scale Subassemblage Specimens*
	CS.2.2	*Perform Testing on Subcomponents*
	CS.2.3	*Perform Ancillary Testing*
	CS.3	Conduct Computational Research
	CS.3.1	*Perform NLRHA for Demand Assessment*
	CS.3.2	*Perform CFE Simulation*
	CS.3.3	*Perform NLRHA for Assessment of Mitigation Strategies*
	CS.4	Develop Improved Evaluation and Retrofit Design Recommendations
	CS.4.1	*Develop Best Practices for Evaluation*
	CS.4.2	*Develop Recommendations for Retrofit Practices*
	CS.4.3	*Develop Guidance for Decision Support and Acceptance Criteria*
	CS.5	Develop Improved Repair Design Recommendations
	CS.6	Report on Seismic Behavior and Preliminary Recommendations
Panel Zone	**PZ**	**Investigation of Panel Zone Behavior**
	PZ.1	Develop (and Update) Research Strategy
	PZ.2	Conduct Experimental Research
	PZ.2.1	*Perform Testing on Large-scale Subassemblage Specimens*
	PZ.2.2	*Perform Ancillary Testing*
	PZ.3	Conduct Computational Research
	PZ.3.1	*Calibrate CFE Simulations*
	PZ.3.2	*Perform CFE Simulations to Expand Experimental Program*

Table 7-1 Research Plan – Summary of Tasks (continued)

Activity	No.	Name of Activity, Task, or Subtask
Panel Zone	**PZ**	**Investigation of Panel Zone Behavior (continued)**
	PZ.4	Develop Improved Evaluation and Connection Retrofit/ Repair Recommendations
	PZ.4.1	*Develop Best Practices for Evaluation*
	PZ.4.2	*Develop Recommendations for Retrofit Practices*
	PZ.4.3	*Develop Recommendations for Repair Practices*
	PZ.5	Report on Seismic Behavior and Preliminary Recommendations
System	**SM**	**Investigation of System Behavior**
	SM.1	Develop (and Update) Research Strategy
	SM.2	Conduct Advanced Computational Research
	SM.3	Conduct Experimental Research
	SM.3.1	*Perform Hybrid Simulation Tests*
	SM.3.2	*Perform Earthquake Simulation Test*
	SM.4	Corroborate Computational Research
	SM.5	Develop Improved Evaluation and Retrofit Recommendations
	SM.6	Report on Seismic Behavior and Preliminary Recommendations
Products	**PR**	**Development of Final Products**
	PR.1	Develop Improved Evaluation and Repair/Retrofit Recommendations
	PR.2	Develop Analytical Tools
	PR.3	Implementation in Codes and Standards

7.3 Identification of Archetype Buildings and Preliminary System-Level Computational Studies (AR)

Identification of archetype buildings and preliminary computational studies (designated AR) are an activity that will occur at the start of the research program. Archetype building designs will be used to determine typical member sizes, subassemblages, and system configurations that are studied in the rest of the research plan. Tasks for identification archetype buildings are described below.

Task AR.1: Identify Archetype Building Configurations and Designs. Archetype buildings are intended to be representative of the range of structural configurations that would be expected to have pre-Northridge PJP column splices and weak panel zones. Identification of archetype designs is described in Section 3.1. This task should occur during the first half-year of implementation. The results and recommendations from this task will be inputs into the preliminary system-level computational studies (AR.2), as well as the development of research strategies for column splices (CS.1) and panel zones (PZ.1).

Task AR.2: Perform Preliminary Computational Studies. This subtask will be developed based on considerations in Section 3.2 and the identification of archetypes (AR.1). This subtask will extend over a duration of approximately six months, starting after completion of archetype identification (AR.1). Findings of these studies will be used in the development of the research strategies for column splices and panel zones (CS.1, PZ.1). This subtask may occur concurrently with early stages of column splice and panel zone computational studies (CS.3, PZ.3).

Task AR.3: Report on Archetype Buildings and Preliminary Computational Studies. The resulting archetype buildings, configurations, designs, member sizes, a discussion of preliminary key design variables and assumptions, and a summary of the key findings from the preliminary computational studies will be documented in an interim report for use by other researchers upon completion of task AR.2.

7.4 Investigation of Column Splice Behavior (CS)

Investigation of column splice behavior (designated CS) is an activity that can occur concurrently or non-concurrently with the investigation of panel zone behavior (designated PZ). If optimally organized, the activity is expected to take four years. Tasks for studying column splice behavior are described below.

Task CS.1: Develop (and Update) Research Strategy. This task will be developed based on considerations in Section 4.1, archetype building identification (AR.1), preliminary system-level computational studies (AR.2), and early phases of column splice computational research (CS.3). Work to develop the initial research strategy will extend over a duration of approximately six months, starting after completion of preliminary system-level computational studies (AR.2). The research strategy will be regularly updated over the course of the activity based on interim findings of the experimental research (CS.2) and computational research (CS.3), development of seismic evaluation and retrofit design recommendations (CS.4) and development of post-earthquake repair recommendations (CS.5).

Task CS.2: Conduct Experimental Research. This task will be based on considerations in Section 4.3, the column splice research strategy (CS.1), and interim findings of the computational research (CS.3). Experimental work will extend over a duration of approximately two years, starting later than the computational research (CS.3) but occurring concurrently with later stages of that task. Interim findings of the task will be used to regularly update the column splice research plan (CS.1). Final findings will be incorporated into the evaluation and retrofit research (CS.4), the repair research (CS.5), and the system study research strategy (SM.1). Work will consist of the following subtasks:

- *Subtask CS.2.1: Perform Testing on Large-scale Subassemblage Specimens*. See Section 4.3.3.

- *Subtask CS.2.2: Perform Testing on Subcomponents*. See Section 4.3.4.
- *Subtask CS.2.3: Perform Ancillary Testing*. See Section 4.3.5.

Task CS.3: Conduct Computational Research. This task will be based on considerations in Section 4.4, the column splice research strategy (CS.1), and interim findings of the experimental research (CS.2). Computational work will extend over a duration of approximately two and a half years, starting a year before the experimental research (CS.2) but with later phases occurring concurrently with that task. The early stages of the task may occur concurrently with the preliminary system-level computational studies (AR.2). Interim findings of the task will be used to regularly update the column splice research plan (CS.1). Final findings will be incorporated into the evaluation and retrofit research (CS.4), the repair research (CS.5), and the system study research strategy (SM.1). Work will consist of the following subtasks:

- *Subtask CS.3.1: Perform NLRHA for Demand Assessment.* See Section 4.4.1.
- *Subtask CS.3.2: Perform CFE Simulation*. See Section 4.4.2.
- *Subtask CS.3.3: Perform NLRHA for Assessment of Mitigation Strategies*. Section 4.4.3.

Task CS.4: Develop Improved Evaluation and Retrofit Recommendations. This task will be based on considerations in Section 4.7, findings of the experimental research (CS.2), and findings of the computational research (CS.3). Evaluation and retrofit research will be concurrent with repair research (CS.5) and extend over a duration of approximately one year, starting at the conclusion of the experimental (CS.2) and computational research (CS.3). Work will consist of the following subtasks:

- *Subtask CS.4.1: Develop Best Practices for Evaluation.* See Section 4.7.1.
- *Subtask CS.4.2: Develop Recommendations for Retrofit Practices*. See Section 4.7.2.
- *Subtask CS.4.3: Develop Guidance for Decision Support and Acceptance Criteria*. See Section 4.7.3.

Task CS.5: Develop Improved Repair Design Recommendations. This task will be based on considerations in Section 4.6, findings of the experimental research (CS.2), and findings of the computational research (CS.3). Repair research will be concurrent with the evaluation and retrofit research (CS.4) and extend over a duration of approximately one year, starting at the conclusion of the experimental (CS.2) and computational (CS.3) research tasks.

Task CS.6: Report on Column Splice Behavior and Preliminary Recommendations. Results and findings from tasks CS.2 to CS.5 will be summarized in an interim report

upon completion of the work. Report writing is expected to extend over a duration of half a year, starting at the completion of the evaluation and retrofit research (CS.4) and repair research (CS.5). Results and recommendations in the report will be used to update the system studies research strategy (SM.1) and be integrated into the final products (PR).

7.5 Investigation of Beam-to-Column Panel Zone Behavior (PZ)

Investigation of panel zone behavior (designated PZ) is an activity that can occur concurrently or non-concurrently with the investigation of column splice behavior (CS). If optimally organized, the activity is expected to take four years. Tasks for studying panel zone behavior are described below.

Task PZ.1: Develop (and Update) Research Strategy. This task will be developed based on considerations in Section 5.1, archetype building identification (AR.1), preliminary system-level computational studies (AR.2), and early phases of panel zone computational research (PZ.3). Work to develop the initial research strategy will extend over a duration of approximately six months, starting after completion of preliminary system-level computational studies (SM.1.1). The research strategy will be regularly updated over the course of the activity based on interim findings of the experimental research (PZ.2) and computational research (PZ.3), and development of seismic evaluation and retrofit/repair design recommendations (PZ.4).

Task PZ.2: Conduct Experimental Research. This task will be based on considerations in Section 5.3, the panel zone research strategy (PZ.1), and interim findings of the computational research (PZ.3). Experimental work will extend over a duration of approximately two years, starting later than the computational research (PZ.3) but occurring concurrently with later stages of that task. The early stages of the task may occur concurrently with the preliminary system-level computational studies (AR.2). Interim findings of the task will be used to regularly update the panel zone research plan (PZ.1). Final findings will be incorporated into the evaluation and retrofit/repair research (PZ.4), and the system study research strategy (SM.1). Work will consist of the following subtasks:

- *Subtask PZ.2.1: Perform Testing on Large-scale Subassemblage Specimens.* See Sections 5.3.1 through 5.3.10.
- *Subtask PZ.2.2: Perform Ancillary Testing.* See Section 5.3.11.

Task PZ.3: Conduct Computational Research. This task will be based on considerations in Section 5.4, the panel zone research strategy (PZ.1), and interim findings of the experimental research (PZ.2). Computational work will extend over a duration of approximately two and a half years, starting a year before the experimental research (PZ.2) but with later phases occurring concurrently with that

task. Interim findings of the task will be used to regularly update the panel zone research plan (PZ.1). Final findings will be incorporated into the evaluation and retrofit/ repair research (PZ.4), and the system study research strategy (SM.1). Work will consist of the following subtasks:

- *Subtask PZ.3.1: Calibrate CFE Simulations.* See Section 5.4.1.
- *Subtask PZ.3.2: Perform CFE Simulations to Expand Experimental Program*. See Section 5.4.2.

Task PZ.4: Develop Improved Evaluation, Retrofit, and Repair Recommendations. This task will be based on considerations in Section 5.5 and Section 5.6, findings of the experimental research (PZ.2), and findings of the computational research (PZ.3). Evaluation and retrofit and repair research will extend over a duration of approximately one year, starting at the conclusion of the experimental (PZ.2) and computational research (PZ.3). Work will consist of the following subtasks:

- *Subtask PZ.4.1: Develop Best Practices for Evaluation.* See Section 5.5.1.
- *Subtask PZ.4.2: Develop Recommendations for Retrofit Practices*. See Section 5.5.2
- *Subtask PZ.4.3: Develop Recommendations for Repair Practices. See Section 5.5.3.*

Task PZ.5: Report on Panel Zone Behavior and Preliminary Recommendations. Results and findings from tasks PZ.2 to PZ.4 will be summarized in an interim report upon completion of the work. Report writing is expected to extend over a duration of half a year, starting at the completion of the evaluation and retrofit/repair research (PZ.4). Results and recommendations in the report will be used to update the system studies research strategy (SM.1) and be integrated into the final products (PR).

7.6 Investigation of System Behavior (SM)

Investigation of system behavior (designated SM) is an activity that will occur after the completion of panel zone and column splice experimental research and computational research (PZ.2, PZ.3, CS.2, CS.3). If optimally organized, the activity is expected to take three and a half years. Tasks for studying system behavior are described below.

Task SM.1: Develop (and Update) Research Strategy. This task will be developed based on considerations in Section 6.1, column splice computational and experimental research (CS.2, CS.3), and panel zone computational and experimental research (PZ.2, PZ.3). Work to develop the initial research strategy will extend over a duration of approximately six months, starting after completion of CS.2, CS.3, PZ.2, and PZ.3. The research strategy will be regularly updated over the course of the

activity based on interim findings of the system-level experimental (SM.2) and computational (SM.3) research, and the development of seismic evaluation, retrofit, and repair design recommendations for column splices and panel zones (CS.4, CS.5, PZ.4, and PZ.5).

Task SM.2: Conduct Advanced Computational Studies. This task will be developed based on considerations in Section 6.2 and the system behavior research strategy (SM.1). This subtask will extend over a duration of approximately a year and a half, starting after completion of the system behavior research strategy (SM.1). This subtask is expected to be concurrent with system-level experimental research (SM.3) and the corroboration of computational research (SM.4). Interim findings of the task will be used to regularly update the system behavior research plan (SM.1). Final findings will be incorporated into the system-level evaluation and retrofit research (SM.5).

Task SM.3: Conduct Experimental Research. This task will be based on considerations in Section 6.3 and the system behavior research strategy (SM.1). This task will extend over a duration of approximately two years, starting after completion of the system behavior research strategy (SM.1). This task is expected to be concurrent with system-level computational research (SM.3) and the corroboration of computational research (SM.4). Interim findings of the task will be used to regularly update the system behavior research plan (SM.1). Final findings will be incorporated into the system-level evaluation and retrofit research (SM.5). Work will consist of the following subtasks:

- *Subtask SM.3.1: Perform Hybrid Simulation Tests.* The hybrid simulation experimental research testing program is described in Section 6.3.1. This subtask will occur over a duration of approximately one and a half years. The findings of this subtask will inform and lead into the development of the earthquake simulation (shake table) tests (SM.3.2). It is expected that there will be some overlap in schedule between the completion of the hybrid and start of the shake table testing.
- *Subtask SM.3.2: Perform Earthquake Simulation Tests.* The earthquake simulation experimental research testing program is described in Section 6.3.2. This subtask will occur over a duration of one and a half years. This subtask will be informed by the results of all previous experimental and computational research and will inform the corroboration of the computational research program (SM.4).

Task SM.4: Perform Corroborating Computational Research. This task will be based on considerations in Section 6.4, the system behavior research strategy (SM.1), and findings of the system-level computational (SM.2) and experimental research (SM.3). This task is expected to extend over a duration of 9 months and be concurrent with

system-level computational (SM.3) and the experimental research (SM.4). Findings will be incorporated into the computational research (SM.2).

Task SM.5: Develop Improved Evaluation and Retrofit Recommendations. This task will be based on considerations in Section 6.5, the system behavior research strategy (SM.1), and findings of the experimental (SM.3), and computational (SM.2) research. This task will extend over a duration of approximately one and a half years, starting at the conclusion of the experimental (SM.3) and computational research (SM.2).

Task SM.6: Report on System Behavior and Preliminary Recommendations. Results and findings from tasks SM.2 to SM.5 will be summarized in an interim report upon completion of the work. Report writing is expected to extend over a duration of six months, starting at the completion of the evaluation and retrofit research (SM.5). Results will be integrated into the final products (PR).

7.7 Development of Final Products (PR)

Development of Final Products (designated PR) will bring together all the results of the research program for use by practicing engineers and researchers. If optimally organized, the activity is expected to take two and a half years, starting at the completion of the column splice computational and experimental research (CS.2, CS.3), and panel zone computational and experimental research (PZ.2, PZ.3).

Preliminary recommendations for improved design provisions and practice-based analytical tools will be developed as part of each research activity. These recommendations will be considered preliminary until confirmed by system-level computational and experimental investigations. Upon completion of the system-level studies, results for subassemblage-, and system-based research will be synthesized in the final development stages. Tasks for development of final products are described below.

Task PR.1: Develop Improved Evaluation and Repair/Retrofit Recommendations. This task will be based on considerations described in Sections 4.7, 5.5, and 6.5. Preliminary recommendations and findings from tasks CS.4 to CS.6, PZ.4, and PZ.5. SM.5 and SM.6 will be assimilated together to develop final recommendations for improved evaluation procedures and repair/retrofit techniques. The development of these final recommendations is expected to take two years, starting with the completion of the column splice and panel zone research portions of the plan. They will also be informed by the completion of the system level experimental and computational research.

Task PR.2: Develop Analytical Tools. In parallel with the development of improved evaluation and repair/retrofit recommendations in PR.1, analytical tools to facilitate implementation of the recommendations will be developed for use by practicing

engineers. The development of these final recommendations is expected to take two years, starting with the completion of the column splice and panel zone research portions of the plan. They will also be informed by the completion of the system level experimental and computational research.

Task PR.3: Implementation in Codes and Standards. Recommendations developed under this research plan are intended to be ready for direct integration into federally referenced guidelines, codes, and standards, including ASCE/SEI 41 and AISC 342. A small working group consisting of principal investigators from selected analytical and experimental projects in the research plan can be assigned to work with members of ASCE/SEI 41 Committee (Seismic Evaluation and Retrofit of Existing Buildings) and AISC Task Committee 7 (Evaluation and Repair) to generate proposed modifications to the ASCE/SEI 41 and AISC 342.

7.8 Recommended Schedule

A recommended schedule for the work is shown in Figure 7-1. Based on the scope of the overall program, the estimated overall project schedule is approximately 7 years. Due to complex interrelationships between the tasks and uncertainty in the procurement of contracted experimental research, this schedule must be considered approximate.

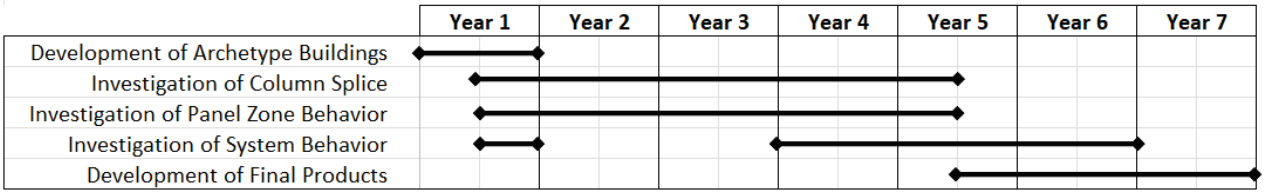

Figure 7-1 Approximate overall schedule

Alternative schedules considering more concurrent or more sequential tasks are possible. Although the major research components can be considered separately, there is expected to be a significant level of interaction and coordination required between many of the tasks to achieve the intended results. Interactions between subtasks are illustrated in Figure 7-2.

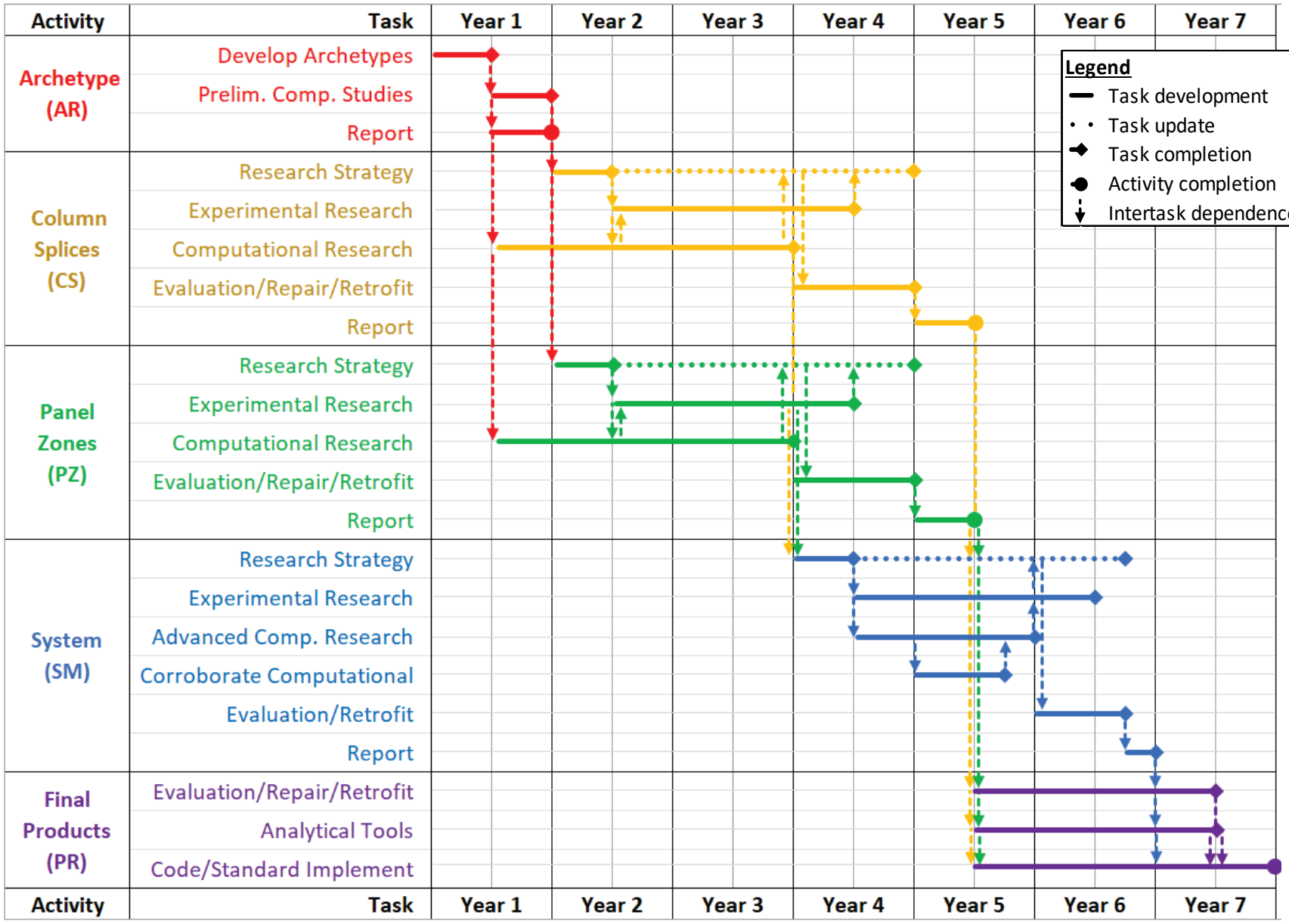

Figure 7-2 Approximate detailed schedule showing tasks and interrelationships between major elements.

7.9 Estimated Budget

It is anticipated that NIST will conduct some subtasks of the research program internally, notably the analytical work. Portions of the analytical work, as well as the experimental work, may well be competitively awarded to outside contractors to perform, contingent on the availability of funds. Due to the competitive nature of the anticipated procurement process, potential variations in material and fabrication costs, and uncertainty in the current economic environment, establishing a precise estimate for each element of the research plan was not feasible. Based on historical expenditures for research on structural steel programs funded by the Federal government in the past, it is estimated that implementation of this program will require up to $11M, of which $4M is estimated for column splice studies, $4M is estimated for panel zones studies, and $3M is estimates for system studies.

It is anticipated that NIST will conduct cost estimating exercises as part of the procurement process to confirm and update the above estimates as the program is implemented.

7.10 Key Collaborators and Potential Funding Sources

Although NIST will manage the overall program and perform selected portions of the work, the objectives of the research program would benefit from support, interaction, and coordination with other agencies of the Federal government, representative industry organizations, and codes and standards development organizations:

- National Science Foundation (NSF)
- Federal Emergency Management Agency (FEMA)
- American Institute of Steel Construction (AISC)
- American Iron and Steel Institute (AISI)
- American Society of Civil Engineers (ASCE)

Opportunities to jointly fund research activities, or collaborate with these organizations, should be pursued.

Appendix A

Literature Review for PJP Column Splices

A.1 Design Guidelines and Practice

This section presents a summary of the past guidelines on PJP column splices over the last six decades. The discussion focuses on pre-Northridge practice (from the 1960s to 1994) during which many of the vulnerable splice details were constructed. Post-Northridge provisions and practices are also discussed for context.

A.1.1 Weld Electrode and Steel Toughness Requirement

Prior to the 1992 AISC *Seismic Provisions for Steel Buildings*, the Uniform Building Code (UBC) and the SEAOC *Recommended Lateral Force Requirements and Commentary* ("Blue Book") served as the primary guidelines for seismic design of steel buildings, along with AISC *Specifications for Structural Steel Buildings*. No requirements for toughness of steel or weld filler material to be used in connections was specified in these historic provisions or even the AISC *Seismic Provisions* of 1992 (AISC, 1992). It is relevant to note that the AISC *Specifications* (AISC 1978; 1986) approved welding electrode specifications AWS A5.20 (AWS, 1979) without regard to filler metal notch toughness requirements, as these were stated to not be critical for building construction. However, the use of steels with superior notch toughness was recommended for demanding service conditions, such as low temperatures with impact loading. A supplement to the AISC *Specifications* issued in 1989 (AISC, 1989) mandated a minimum average CVN toughness requirement of 20 ft-lb at 70°F for steel if heavy rolled members (Groups 4 and 5 of ASTM A6/6M) under primary tensile stresses are spliced using full penetration welds. When notch-toughness of the steel was specified, it required the process consumables for all weld metal, tack welds, root pass and subsequent passes, deposited in a joint to be compatible to assure notch-tough weld metal.

The post-Northridge AISC *Seismic Provisions* of 1997 (AISC, 1997), with the SAC Project ongoing, included a minimum CVN toughness of 20 ft-lb at -20°F for both CJP) and PJP welds in columns splices. The 2002 *Seismic Provisions* (AISC, 2002), after the completion of SAC Project, set a minimum CVN toughness of 20 ft-lb at -20°F for all welds and an additional minimum CVN toughness of 40 ft-lb at 70°F (from tests run at high and low heat input levels) for beam-to-column connections and for column splices. With the categorization of demand-critical welds in 2005

Seismic Provisions (AISC, 2005), only the critical welds such as the beam-to-column connections and column splices in seismic-force resisting systems, were required to meet the dual-toughness standard, while the requirement for non-demand critical welds was relaxed to a minimum CVN toughness of 20 ft-lb at 0°F. The 2010 *Seismic Provisions* (AISC, 2010) simplified the toughness requirement to 20 ft-lb at 0°F for all welds and the additional requirement of 40 ft-lb at 70°F for demand-critical welds. The same requirements are followed in the latest revisions of the AISC *Seismic Provisions* (AISC, 2016a). A requirement of minimum CVN toughness of 20 ft-lb at 70°F for heavy rolled sections, introduced in the supplement issued in 1989, is continued without any change in all the post-Northridge AISC *Seismic Provisions*.

A.1.2 PJP Design Strength Requirement

Pre-Northridge *Uniform Building Code* editions, the SEAOC Blue Book and the AISC *Specifications for Structural Steel Buildings* did not specify any minimum throat thickness (or flange penetration) for PJP column splices subjected to tensile forces or the location of the splices from the floor level. The splice connections were required to be designed to resist any tension developed by specified lateral forces acting in conjunction with 75 percent of the calculated dead load stress and no live load. For splicing of members with plates more than 2 inch thickness subjected to compression and members subjected to tension due to wind or seismic loads, the AISC *Supplement to Specifications for Structural Steel Buildings* issued in 1989 (AISC, 1989) recommended using splice details that do not induce large weld shrinkage strains such as partial penetration flange groove welds with fillet-welded surface lap-plate splices on the web or with bolted or combination bolted/fillet-welded lap plate splices as shown in Figure A-1.

The *Uniform Building Code* of 1988 (UBC, 1988) required the PJP column splices to be located at least 3 ft away from the beam-to-column connections to ensure that splices are located near the inflection point of the column in flexure under first mode response. The splice connections in net tension were required to have a design capacity of 150% of the required strength and the weld in the flange to have a minimum design strength of 50% of the capacity of the smaller column flange. The AISC *Seismic Provisions* immediately preceding the Northridge earthquake (AISC, 1992) mandated the same requirements. Each subsequent edition of the AISC *Seismic Provisions* incrementally updated design requirements for PJP column splices. These restrictions have included requiring the splices to be further away from the beam-to-column connections towards the assumed first-mode point of inflection, the use of expected rather than minimum specified properties to design the splice, the mandatory use of dual web-plates in bolted-web splices, and the requirement for beveled transitions. These are summarized in Table A-1. Furthermore, PJP column splices were explicitly disallowed in SMRF and IMRF systems beginning from the 2002 provisions to mitigate fracture risk. Based on recent experimental and

numerical studies (Shaw et al., 2015; Stillmaker, 2016) PJP welds with a minimum total effective throat of 85% (of the thinner column flange thickness) have been reallowed under special conditions (AISC, 2016a).

The design strength of a PJP joint loaded in any direction, as per AISC 360 (AISC, 2016b) is given by:

$$\phi R_n = 0.8(0.6F_{EXX}A_{we}) \quad \text{(A-1)}$$

in which A_{we} is length of the weld multiplied by the effective groove depth. The factor of 0.6 on F_{EXX} for the tensile strength of PJP groove welds has been used since the early 1960s to compensate for factors such as the notch effect of the unfused area of the joint and uncertain quality in the root of the weld due to the difficulty in performing nondestructive evaluation.

For PJP welds loaded transversely, as in the case of welded column splices (WCS), an additional check for base metal strength evaluation is required, as:

$$\phi R_n = 0.75(F_u A_{BM}) \quad \text{(A-2)}$$

in which A_{BM} is the base metal cross-sectional and F_u is the tensile strength of the base metal. It should be noted that Equation A-1 will generally govern design, provided the penetration ratio (i.e., effective throat relative to plate thickness) of the PJP is low.

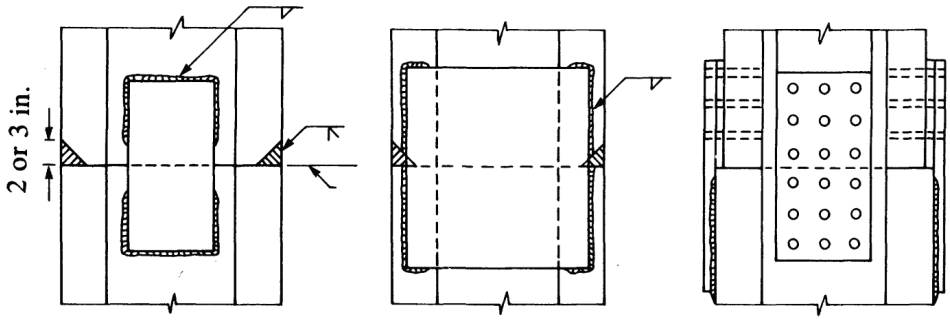

Figure A-1 Splice details to minimize weld restraint tensile stresses (AISC, 1989).

Table A-1 Summary of Seismic Requirements for PJP Column Splices

Provisions	Weld Filler Metal Toughness	Steel Toughness	Design of PJP Column Splices in Tension
UBC 1967-1985	Not specified	Not specified	$\phi R_n \geq R_u$, where R_u is net tension stress developed by lateral forces acting in conjunction with 75% of calculated dead load stress and no live load.
UBC 1988	Not specified	Not specified	$\phi R_n \geq 1.5R_u$ and $(\phi R_n)_{flange\ weld} \geq 0.5f_yA_f$
AISC 341 1992	Not specified	Not specified	Located < 3 ft from beam to column connection. No transitions required.
AISC 341 1997	20 ft-lb @ -20°F	20 ft-lb @ 70°F	$\phi R_n \geq 2.0R_u$ and $(\phi R_n)_{flange\ weld} \geq 0.5R_yf_yA_f$ Located < 4 ft from beam to column connection. No transitions required.
AISC 341 2002	20 ft-lb @ -20°F for all welds. Additional 40 ft-lb @ 70°F for beam-to-column connections & column splices		**PJP prohibited in SMF & IMF.** $\phi R_n \geq 2.0R_u$ and $(\phi R_n)_{flange\ weld} \geq 0.5R_yf_yA_f$ Located < 4 ft from beam to column connection. No transitions required. Dual web plates for bolted web.
AISC 341 2005	20 ft-lb @ 0°F for all welds. 40 ft-lb @ 70°F and 20 ft-lb @ -20°F for demand-critical welds		
AISC 341 2010	20 ft-lb @ 0°F for all welds. Additional 40 ft-lb @ 70°F for demand-critical welds		
AISC 341 2016	20 ft-lb @ 0°F for all welds. Additional 40 ft-lb @ 70°F for demand-critical welds		**PJP with total effective throat > 85% of thickness of thinner column flange permitted in SMF & IMF.** Thicker flange thickness > 1.05 thinner flange thickness. Smooth transition with slope not greater than 1 in 25. $\phi R_n \geq 2.0R_u$ and $(\phi R_n)_{flange\ weld} \geq 0.5R_yf_yA_f$ Located < 4 ft from beam to column connection. Dual web plates for bolted web.

A.1.3 Past Detailing Practice

Jumbo wide flange rolled sections, especially W14 and W24 were extensively used as compression members in the pre-Northridge moment-resisting frames. The provisions in the pre-Northridge era did not mandate CJP welds at column splice location. Consequently, most flanges were welded using single bevel PJP welds.

Based on a review of as-built drawings of a few pre-Northridge buildings, solicitated from various structural engineers in California, the following flange penetration for PJP-welded flanges were found to be typically specified:

- $t_u/3$: This value was found in the details of buildings constructed in early 1960s.
- $\sqrt{t_u / 6}$ + 1/8": This was the minimum throat for pre-qualified PJP connection specified by AWS in 1966 (AWS D1.0, 1966).
- $t_u/2$ + 1/8"
- t_u – 1/8"

In the above values, t_u is the thickness of the upper or thinner connected column flange. The splices were more heavily detailed as t_u minus 1/8 inch at the end of the moment frames where the original engineer assumed uplift and tension could occur (Chisholm et al., 2017). A minimum unfused section thickness of 1/8 inch was specified in nearly all the reviewed details. CJP was also specified in some details, which necessitated web access holes to be provided. No instance of double-bevel PJP was found. Specifically, the following flange penetration for different thickness of the smaller connected flange were found in the as-built drawings of a 7-story building in San Francisco (Figure A-2):

- For $t_u > 2.5$", $t_u/2 – 0.25$"
- For $t_u > 1.5$", 1.25"
- For $t_u < 1.5$", $t_u – 0.25$"

To summarize, the flange penetration in the pre-Northridge splices ranged from 25% ($\sqrt{t_u / 6}$ + 1/8" for t_u = 3.5") to 100% (i.e., CJP).

Both bolted web connections and PJP-welded web connections, were found to be specified at the splice locations in the reviewed drawings. In some details, CJP was also specified in the web. Where PJP-welded, the web penetration ratios were in a similar range as flange penetration ratios. Where bolted, a splice plate was typically fillet welded to the web of the lower column in the shop (this also acted as an erection plate) and bolted to the upper column at site. Figure A-3 shows details of two pre-Northridge WCS with bolted and welded web connection.

It is important to note that beveled transition to the PJP welds when connecting two flanges of unequal thickness in the pre-Northridge splices were neither mandated by

the erstwhile provisions nor it was specified by the original engineer (in the reviewed details). Another aspect of the construction practice is that the columns were surrounded with pre-cast concrete panels, as shown in Figure A-4. This is not a prevalent observation but wherever present, this limits the access to the columns for inspection and retrofit.

Built-up box sections or box sections made using W shapes with longitudinally welded cover plates, as shown in Figure A-5(a), were also used in some pre-Northridge buildings. The splices of these box columns were detailed similar to the W-section splices, as shown in Figure A-5(b). These sections always featured PJP because CJP welds required accessibility to the inside of the box at site.

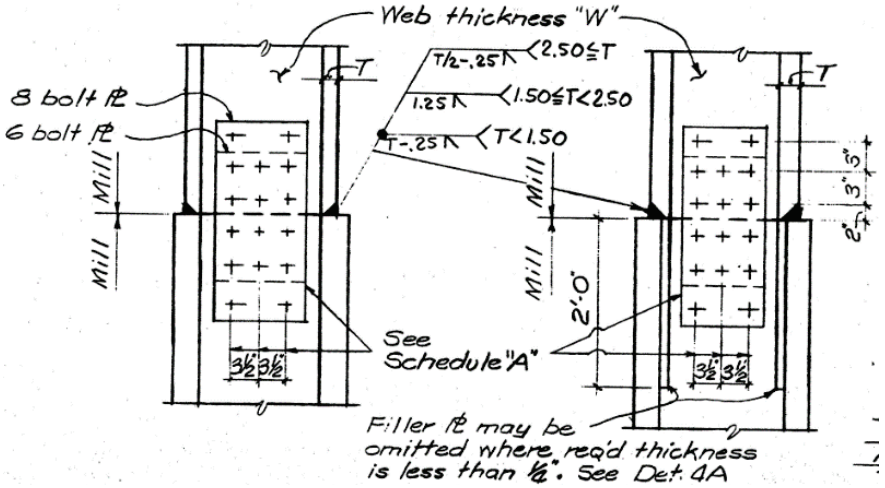

Figure A-2 Existing column splice detail (Nudel et al., 2015).

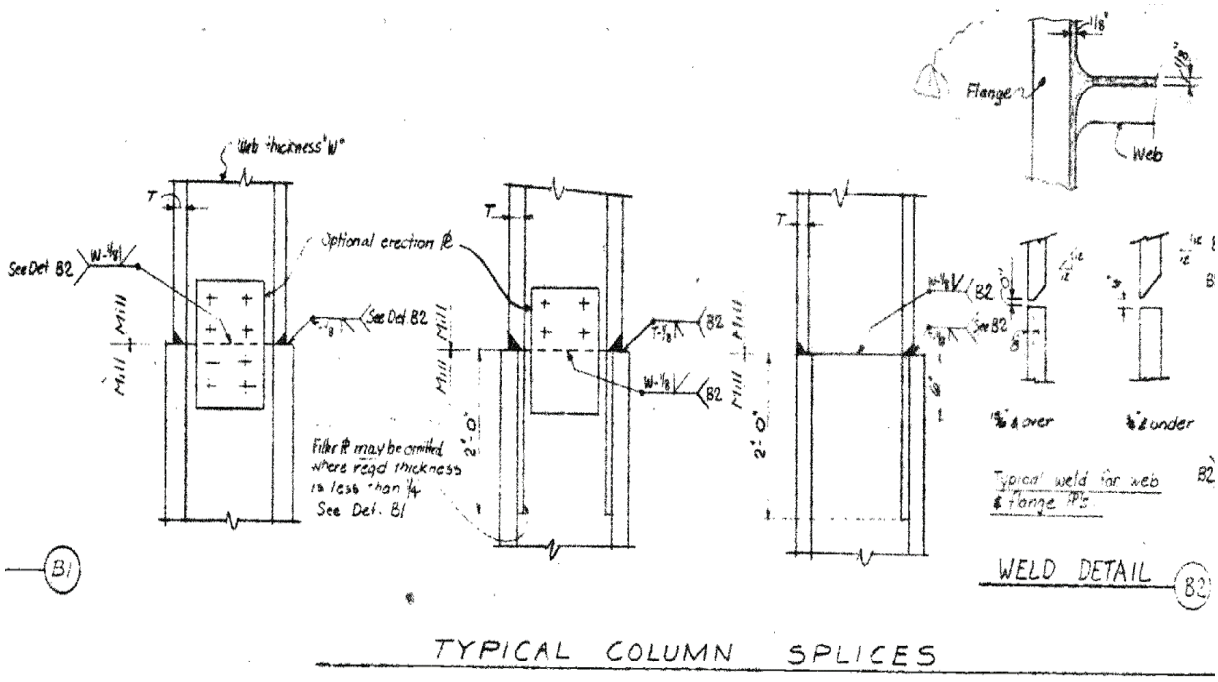

Figure A-3 Pre-Northridge PJP column splice details.

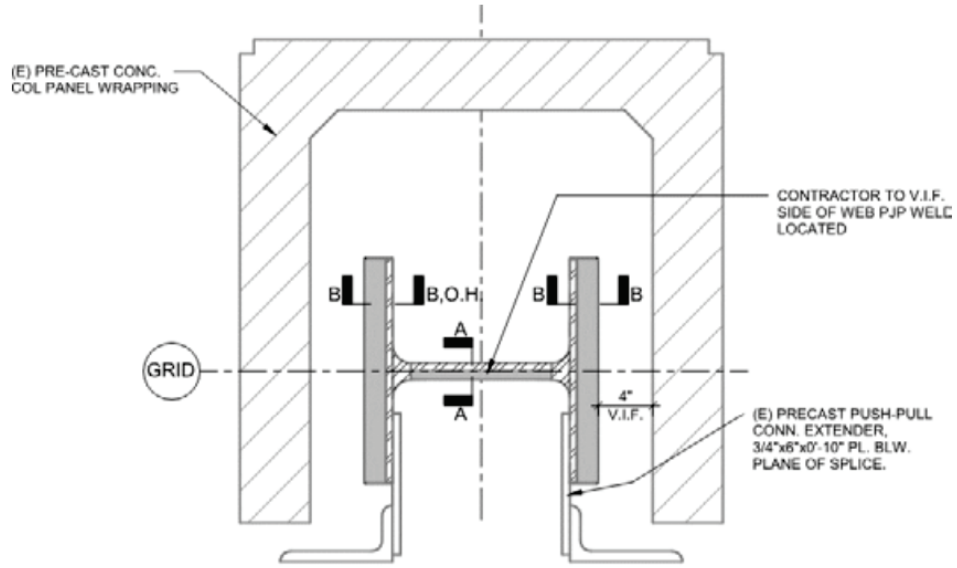

Figure A-4 Existing plan of as-built splice (Chisholm et al., 2017).

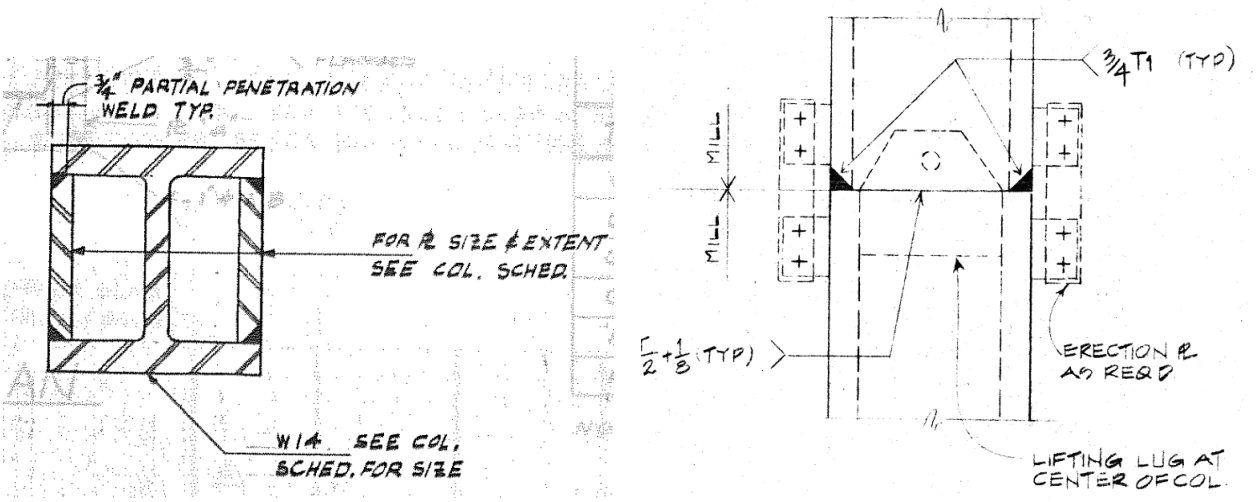

(a) Typical box column detail (b) Box column splice detail

Figure A-5 Box column and box column splice detail.

A.2 Previous Research on WCS and Similar Connections

Based on the brittle fractures at CJP welded splices in tension chords made of jumbo wide flange sections in a truss during construction in 1981, Fisher and Pense (1987) recommended the use of bolted splices in tension members and fillet-welded shear plates attached to the section surface. The fracture was attributed to the low fracture toughness of the base metal, notches provided by flame-cut access copes, and the high residual stresses from CJP welds.

Following the Northridge earthquake of 1994, numerous fractures in CJP-welded beam-column (WBC) connections originating from the beam lower flange and propagating into the beam web or the column flange were reported. Numerous

studies associated with the SAC Project which was initiated to address the issue, and subsequent research examined the factors responsible for the fractures and led to the development of retrofit strategies and major changes in the design guidelines (FEMA, 1995; FEMA, 2000a). Full-scale tests of WBC connections with pre-Northridge weld filler material and base metal were performed (Engelhardt and Sabol, 1998; Popov et al., 1996). All fractures in the CJP welded joints were attributed to high stress/strain demands coupled with the stress-raiser created due to unfused portion of steel backing, deficient field welding, low-toughness weld metal, and design assumptions. The new guidelines mandated strict requirements based on these observations: (a) base metals and weld filler material that satisfied the specified notch toughness; (b) pre-qualification of connections in SMRFs; and (c) limits on material overstrength.

Compared to other structural connections, quantitative research on WCS has been sparse. This section presents a summary of the past experimental and computational studies that have examined the behavior and strength of fracture-critical PJP (or CJP welded) column splices or PJP welds like those in WCS.

A.2.1 Experimental Studies

Only three experimental studies in the United States, and one in Japan had been conducted with a focus exclusively on column splices before the Northridge earthquake (Bruneau and Mahin, 1991; Hayes, 1957; Popov and Stephen, 1976; Yabe et al., 1994). These, along with the more recent experimental studies on PJP column splices and similar connections that feature toughness-rated welds are discussed below.

Popov and Stephen (1976)

The Hayes (1957) study, which focused on evaluating compression capacity of bolted column splices using relatively small sections, motivated Popov and Stephen (1976) to conduct a study on full sized columns featuring welded splices. This study was primarily focused on: (1) the effect of initial imperfections; (2) residual stress; and (3) the behavior of spliced columns in compression. The five specimens in this test series were all W14×320 shapes (flange thickness of $2^{1}/_{16}$") that featured only flange PJP welds with total throat thickness of ½ inch, $^{7}/_{8}$ inch, and $1^{1}/_{8}$ inch (corresponding to flange penetration ratios of 24%, 42%, and 55%). The results of the study indicated that initial imperfections are relatively unimportant and that the behaviors of spliced or un-spliced columns do not differ substantially in compression. The specimens were tested in tension after having been buckled. The spliced joints developed their specified strengths (determined based on the cross-sectional area of weld throat). However, failure in all specimens with PJP welds occurred through the splice exhibiting very limited ductility. It was subsequently pointed out by Bruneau

and Mahin (1991) that: (1) the usefulness of test data from specimens without web connections is limited; and (2) connections without web welds avoided the high residual stresses likely to be present in field welded column splices.

Bruneau and Mahin (1991)

Bruneau and Mahin (1991) conducted an experimental study of column splices several years prior to the 1994 Northridge earthquake. The study featured two column splice specimens: (1) PJP weld connecting W14×665 to W14×500; and (2) CJP weld connecting W14×426 to W14×370. The PJP specimen had a flange penetration ratio of 50% with respect to thickness of top section in both flanges and web. Bevel transition to the PJP weld was provided. The webs of the CJP specimen were connected by PJP weld with 50% penetration. Weld access holes for flange CJP was provided in the webs. The details of the two specimens are shown in Figure A-6. The specimens were constructed to replicate erstwhile construction in terms of material properties, weld and member sizes, residual stresses as well as detailing practice and welding procedures. The specimens were subjected to cyclic loading under a four-point bend configuration, such that the splice region was subjected to pure flexure and no shear. The key findings from this study were: (1) the CJP welded splice sustained moments greater than the cross-sectional strength of the smaller column; and (2) the PJP splice fractured in a brittle manner after the net section strength of the connection was developed (i.e., the strength based on the cross-sectional area, discounting the unfused section). This strength corresponded to a maximum stress of ~85% yield stress in the smaller column flange extreme fibers. The smooth bevel transition between the smaller and larger sections at the splice created an enlarged weld surface which may have been responsible for the observed strength (this detailing is not present in more typical pre-Northridge construction). This implied that the PJP weld had sufficient toughness to allow yielding over the entire weld ligament, but the associated strength was not sufficient to prevent brittle fracture prior to yielding of smaller column section. Post failure, the fracture quickly progressed through the entire section and the erection plates were unable to restrain or stabilize the failure once it initiated, as shown in Figure A-7. The observed brittle behavior is concerning in seismic events where the code calculated forces are largely exceeded.

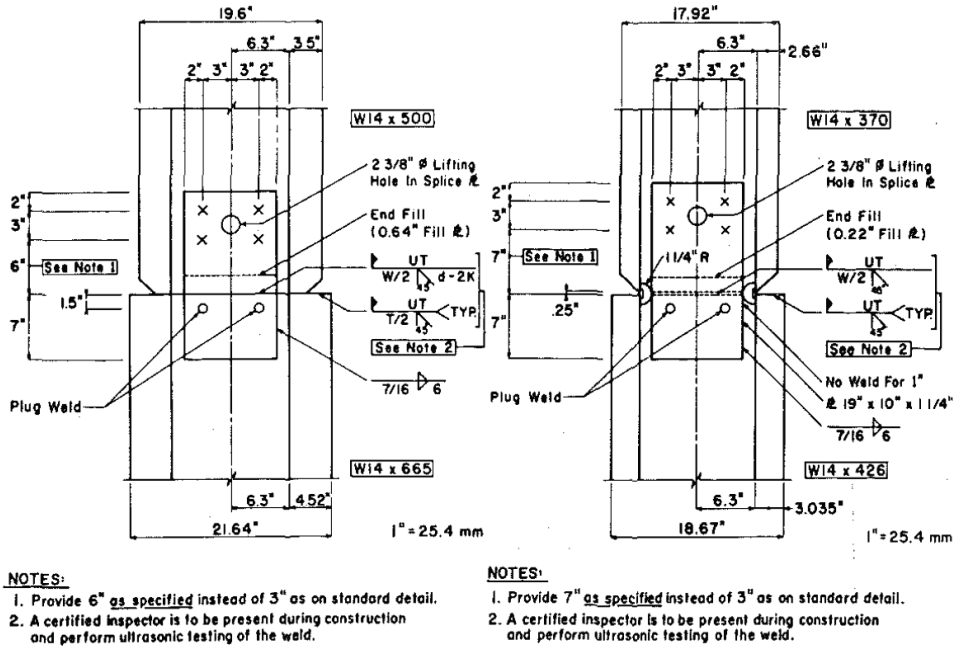

Figure A-6 PJP and CJP test specimens used in Bruneau and Mahin (1991) study.

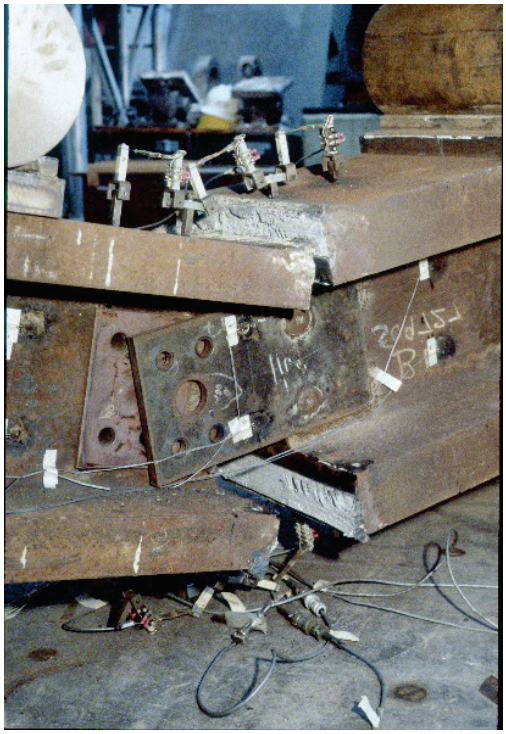

Figure A-7 Failure of a PJP column splice (Courtesy of M. Bruneau).

Gagnon and Kennedy (1989)

Gagnon and Kennedy (1989) conducted a series of 75 tensile tests on PJP steel plates. Test specimens were constructed from two grades of base metal – Grade 300W and

Grade 350A, having specified yield strength of 300 MPa (43.5 ksi) and 350 MPa (50.7 ksi) respectively. Two plates of 25mm (~1 in.) thickness were connected with single bevel PJP welds with flange penetration ranging from 20% to 80% as well as CJP welds using E48018 electrode, a toughness-rated weld filler material with minimum specified tensile strength of 480 MPa (70 ksi). Careful consideration was given to assess the effect of load eccentricity experienced by single bevel welds. The effect of flange penetration ratio, p on the strength of PJP joints was investigated and it was found that the weld strength increases on a unit area basis as the percentage penetration decreases due to an increase of the lateral restraint from the adjacent lesser stressed base material. Based on the findings, the following equation to estimate the nominal PJP weld strength was proposed:

$$R_n = (1.55 - 1.16p + 0.61p^2)pA_pF_u \quad \text{A-3}$$

in which, F_u is the minimum specified tensile strength of base metal and A_p is the plate area. A lower bound to the above equation was given by:

$$R_n = pA_pF_u \quad \text{A-4}$$

To ensure overall member ductility with member yielding before weld fracture, based on the above equations for tensile resistance, limits on PJP flange penetration ratio may be determined through the following:

$$(1.55 - 1.16p + 0.61p^2)p > F_y/F_u \quad \text{A-5}$$
$$p > F_y/F_u \quad \text{(lower bound)}$$

in which F_y is the minimum specified yield strength of steel. Based on the above equation, a lower bound flange penetration ratio of 85% is required for A572 Gr. 50 steels with maximum value of $F_y/F_u = 0.85$.

Yabe et al. (1994)

Full scale testing by Yabe et al. (1994) of PJP column splices of materials typical in Japanese construction subjected to cyclic loading in both the vertical (longitudinal) and horizontal (transverse) direction led to similar findings as the other studies discussed above. Three wide flange specimens with flange penetration ratios $t/4$, $t/2$ and $3t/4$, and details as shown in Figure A-8, were tested. Although the connection strength decreased with decreasing flange penetration ratio, the plastic capacity of the net section could be developed with flange penetrations as low as 25%. Cracks were reported at the weld root along both weld-column interfaces early in the loading protocol but did not propagate until after the apparent plastic strength had been achieved. The presence of axial loads did not appear to have a significant effect on the strength.

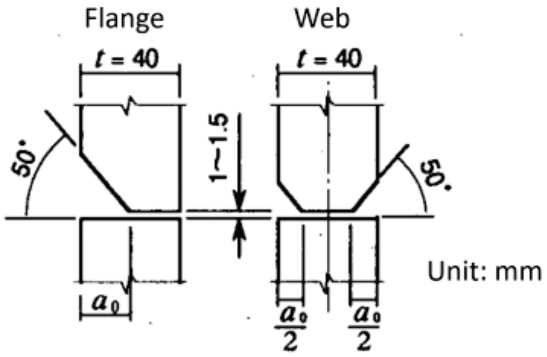

Figure A-8 Details of PJP-welded test specimens used in Yabe et al. (1994) study.

Shaw et al. (2015)

The AISC *Seismic Provisions* of 2002 explicitly disallowed PJP column splices in SMRF and IMRF. Based on the observation that pre-Northridge splices developed strength corresponding to full apparent yielding of the weld and that column splices have modest deformation demand, Shaw et al. (2015) conducted a series of 5 full-scale tests on WCS with PJP welds of toughness-rated filler material (conforming to toughness requirements for demand-critical welds) and high penetration ratios (>80%) in both webs and flanges. The specimens consisted of a larger and smaller column section, made of W14 or W24 shapes, spliced using PJP welds and loaded as a simply supported beam, subjecting the splice to cyclic bending and shear. Two specimens were double bevel PJP welds, whereas the others were single bevel (external PJP welds). All specimens contained a single bevel PJP web splice, except for one, which featured a bolted web splice. All specimen developed yielding in the smaller column and showed significant inelastic deformation prior to fracture. The ratio of moment at fracture to plastic moment capacity of the smaller column were obtained in the range 1.04 to 1.37. The stress in the flanges of smaller column at fracture, was reported to be in the range 1.31 to 1.43 times the measured yield stress, suggesting that significant hardening occurred prior to fracture. The results along with FEFM simulations (Stillmaker, 2016) discussed in section A.2.2, led to PJP welds being permitted for use in WCS under special detailing requirements. The minimum total effective throat is prescribed as 85% of the thinner flange. This assumes that the flange of the larger column is at least 5% thicker than the smaller column and a smooth weld transition is provided between the two flanges.

PJP Welds in Other Connections

Since CJP welds are required for all WBC connections, studies on PJP welds in beam-to-column connections are not available for practice in the United States. An experimental study in Japan (Azuma et al., 2006) on PJP-welded WBC connections demonstrated that PJP welds reinforced with fillet welds, such that the weld

cross-sectional area is greater than the flange cross-sectional area, are adequate in resisting the plastic moment of the member despite the stress-raiser effect created by the unfused section. The configuration of the test specimens used in the study is shown in Figure A-9. Ductile cracks were reported to initiate at weld toes with stable crack growth under cyclic loading. The testing and numerical fracture mechanics assessment indicated that the brittle fracture initiation at the weld roots is unlikely when weld material has sufficient fracture toughness, and the effective throat is large. Similar performance was reported in column to base plate connections with PJP welds reinforced with fillet welds, made of filler material with minimum specified toughness, when tested for cyclic loading by Myers (Myers et al., 2009). The PJP-welded specimens were found to perform better than the CJP welded specimens as the latter involved weld access holes which led to concentration of stresses in the HAZ. The fracture in all the specimens, although occurring at stresses greater than design level stresses, was brittle and led to complete connection failure. However, a significant delay was observed between the initiation of ductile cracks and the transition to brittle fracture. The fracture in fillet reinforced PJP welds initiated at the toe of the weld (on the flange) in the HAZ of the column flange instead of the unfused section between the column flange and base plate. This was attributed to the strength and toughness at the weld root of the reinforced PJP welds, which permitted the development of a fully yielded and strain-hardened column flange.

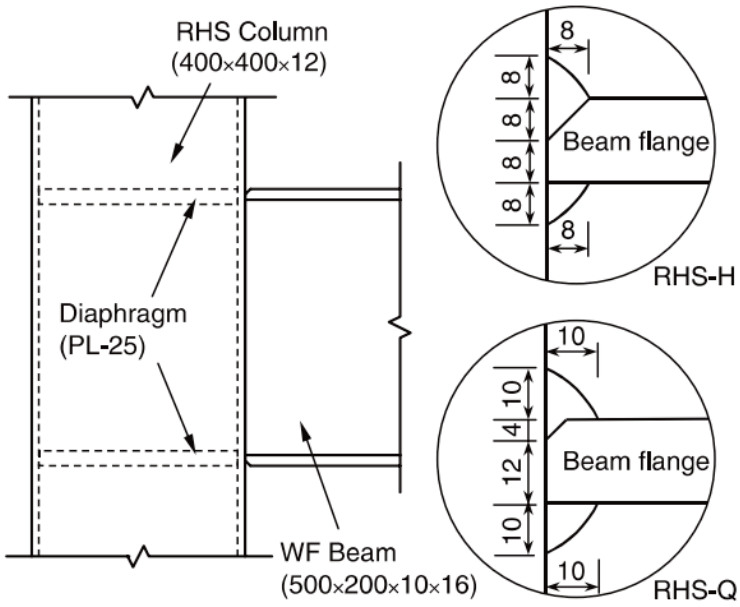

Figure A-9 Details of PJP-welded beam-to-column joint with fillet reinforcement (Azuma et al., 2006).

Strength of PJP Welds

The equations for directional strength increase of PJP welds are not included in AISC 360 (2016). Recent experimental and numerical study by Luo et al. (2020) on the

effect of loading angle on PJP welds with 45% penetration ratio indicates that the AISC formula (See Equation A-1) is conservative when the directionality effect of loading is ignored. However, the strength of PJP welds loaded longitudinally is accurately predicted by the AISC formula. The directionality effect was found to be more significant on the strength of a PJP-welded joint than that of a fillet-welded joint. The strength of a transversely loaded PJP weld, as in the case of WCS, was found to be approximately 1.96 times that of a longitudinally loaded PJP weld. The increase in strength reported by numerical analysis was much lower than the experimentally obtained values, which is as expected due to the presence of a notch and an actual weld defect at the weld root of the specimen considered in the study. Reynolds et al. (2020) further showed that reinforcing fillet did not enhance the strength of the PJP-welded joints with penetration >85% in cruciform orientation. This was attributed to the transition of the tensile fracture surface to shear fracture surface.

To summarize, all experimental studies indicate a brittle fracture in PJP-welded connections with fracture initiating either at the root of the weld (i.e., at the tip of the unfused region of the PJP weld or at the top of the weld in the HAZ of the column flange when significant strain hardening occurs). The stress in the smaller connected column or plate at which this fracture is observed is much lower than the yield stress of the material in the case of pre-Northridge welds.

A.2.2 Analytical and Computational Studies

Conventional Linear Elastic Fracture Mechanics (LEFM) and Elastic Plastic Fracture Mechanics (EPFM) indices have been widely used to characterize the fracture toughness demands and capacity in pre-Northridge connections. This is because pre-Northridge connections, with relatively low-toughness materials and brittle response, usually satisfy the conditions required for the validity of LEFM and EPFM. Three of the most popular indices used for this purpose include the following (detailed theoretical background for these is provided in Anderson, 2017):

1. K_I – Elastic stress intensity factor, a measure of the critical value of stress singularity at the crack tip under elastic conditions (Irwin, 1957). The subscript I indicates Mode-I fracture, corresponding to crack opening.
2. *CTOD* – Inelastic Crack Tip Opening Displacement, whose critical value is a measure of the maximum blunting of the crack tip at the onset of crack initiation and hence provides a direct characterization of the crack-tip stress and deformation fields (Wells, 1969).
3. J_I – Strain energy release associated with crack extension that is applicable for both linear and nonlinear elastic analyses (i.e., deformation theory of plasticity (Rice, 1968)). Under the assumption of proportional loading behavior, the

J-integral is equal to the linear or nonlinear elastic energy release rate, G. The J-integral provides a convenient numerical technique to determine K_I and $CTOD$ from finite element analyses.

The relationship between stress intensity factor K_I , energy release rate J_I and $CTOD$ is given by:

$$CTOD = \frac{K_I}{m\sigma_f E'} = \frac{J_I}{m\sigma_f} \tag{A-6}$$

in which σ_f is the flow stress, E' is the effective modulus of elasticity depending on plane stress/strain and, m is a dimensionless constant that depends upon material strain hardening and the degree of constraint. Due to prevalence of elastic stress intensity factor, K_I in engineering problems, an equivalent elastoplastic stress intensity factor K_I determined from J_I calculated for the elastic-plastic behavior is widely used.

As per LEFM or EPFM, fracture occurs when the fracture toughness demand (the crack-driving force) exceeds the corresponding toughness capacity (Anderson, 2017), i.e., $K_I \geq K_{Ic}$ or $J_I \geq J_{Ic}$ or $COTD > COTD_c$ (the subscript c denotes the critical values or the capacity). While fracture toughness demand may be computed from the analytical formulas for standard cracked geometries or from FE simulations, fracture toughness capacity (assumed a material property) is determined via material testing. Fracture toughness capacity depends not only on the material tested, but also on other factors including temperature, rate of load application, and level of stress constraint. The static linear-elastic fracture toughness capacity for Mode-I loading conditions (i.e., K_{Ic}, under plane-strain conditions), which is typically the relevant capacity for column splice loading conditions, is directly determined through the ASTM Test Method E399 (ASTM, 2020c). The fracture toughness capacity in terms of J_{Ic} or $CTOD_c$ can be determined through the ASTM Test Method E1820 (ASTM, 2020a). The ASTM Test Method E1221 (ASTM, 2018a) is used to determine mode-I fracture toughness capacity under dynamic or impact loads. Within each of these tests, the load application rate and geometry, which governs stress conditions, are mandated, while the test temperature may be varied within a specified range. These tests are costly and difficult to perform. Consequently, toughness capacity is determined indirectly through the CVN impact test (ASTM, 2018b). CVN results provide insight into whether a material behaves in a brittle (low absorbed energy) or ductile (high absorbed energy) manner and relative toughness (compared to other CVN results) but does not directly measure fracture toughness. Instead, empirical relations have been proposed to relate CVN test results with K_{Ic} and K_{Id} test results to allow for the indirect determination of fracture toughness capacity by way of the simpler and less costly CVN impact test. These are discussed in Section A.4.3.

Finite Element Fracture Mechanics (FEFM) simulations are widely used in various spheres of aerospace, mechanical and nuclear engineering to characterize fracture toughness requirements in components with a crack-like flaw. These toughness demands are generally quantified in terms of one of the fracture indices discussed previously depending on the type of loading and material behavior. Previous studies that characterize the toughness demands in PJP column splices and similar connections are discussed next.

Chi et al. (2000)

Chi et al. (2000a; 2000b; 2000c) performed detailed 2D and 3D FEFM analyses to study fracture toughness requirements in pre-Northridge welded beam-to-column connections that featured flanges of the beam connected to the column flange using CJP weld. The CJP weld had weld root flaws and a notch due to unfused portion of the steel backing when it was left in place. Toughness demands were quantified in terms of the elastic stress intensity factor K_I and inelastic crack tip opening displacement. When the beam flanges were loaded beyond the yield stress, which is typically the case for plastic hinge development, the elastic analyses were found to significantly underestimate the fracture toughness demand as yielding concentrated around the weld flaw. The analyses also demonstrated that connections with notch effects created by unfused sections and low-toughness E70T-4 weld metal are likely to fracture from the weld root at or below the plastic moment (i.e., the section yield). This is consistent with field observations from the Northridge earthquake.

Nuttayasakul (2000)

Following the methodology laid out by Chi et al. (2000), Nuttayasakul (2000) performed FEFM simulation of the Bruneau and Mahin (1991) WCS tests. A 2D FEFM model of the PJP column splice was created in ABAQUS (Hibbitt et al., 1998). Fracture toughness capacity of the PJP splice was assessed by computing the J-Integral around the crack tip created by the unfused section while imposing loads corresponding to measured failure loads from the physical test to an elastic model of the splice configuration and subsequently converting the attained J-integral value to a mode-I stress intensity factor. This approach led to a fracture toughness estimate of K_{Ic} = 67 ksi √in, a value slightly lower that the theoretical estimate made by Bruneau and Mahin. Additionally, Nuttayasakul carried out a parametric study comparing loading type (bending versus tension), flange penetration (25% to 75% of the thinner flange), weld material yield strength (55 ksi to 75 ksi), and relative column flange thickness (0.38 to 1.0) holding the section size below the splice constant. The parametric study found that (1) simulating tensile loading caused approximately 14% higher toughness demands than bending, (2) member area based stress capacities for loading increased with increasing flange penetration due to decreasing toughness demands, while weld area based stress capacities tended to increase with decreasing

flange penetration, which confirms a similar experimental finding from Gagnon and Kennedy, (3) member area based stress capacities ranged from 22 ksi to 60 ksi, which provides evidence that the yield strength of the column may not be fully developed by a PJP weld (4) varying weld material yield strength did not have a noticeable effect on splice capacity, and (5) the ratio of the flange thicknesses connected at a splice had a significant inverse relationship to the splice stress capacity. It is important to note that all the simulations involved smooth transition of the PJP from upper to lower column which is typically not the case with pre-Northridge construction practice. Thus, the findings may be non-conservative with respect to erstwhile practice.

Stillmaker et al. (2015)

As the experimental and simulation studies indicated that the failure of PJP splices is controlled by fracture of the flange weld and that the stress state in the flange is predominantly longitudinal tension (with shear stresses carried by webs), Stillmaker et al. (2015) performed 2D FEFM analysis on twenty-five PJP WCS configurations to develop an empirical relation between axial stress in upper connected column flange to the J-integral and geometric characteristics (i.e., the total penetration ratio of PJP and ratio of thickness of upper and lower flange). When utilized with the critical J-integral value, J_{Ic}, the formulas can be used to predict the axial stress at which fracture is expected to occur:

$$\sigma^{flange}_{capacity,\,estimate} = f(J_{Ic}, a, t_{upper}, t_{lower}) \qquad \text{(A-7)}$$

a, t_{upper}, and t_{lower} are shown in Figure A-10. The 25 simulations included both double beveled PJP and single beveled PJP, including the configurations from Shaw et al. (2015b), with flange thickness ratio $\xi = t_{upper}/t_{lower}$ varied between 0.77 and 1.0 and the ratio of unfused section thickness and lower flange thickness $\eta = a/t_{lower}$ varied between 0.1 and 0.5. The η values in the vicinity of 0.1 reflect anticipated unfused section thickness in post-Northridge construction while 0.5 reflect pre-Northridge construction practice. It is relevant that only a small number of simulations (5 out of 25) considered $\eta = 0.5$, which is consistent with pre-Northridge practice. The FE model featured only the flanges with weld as shown in Figure A-10. 2D Plane strain elements were used as (1) through width stress variation in flanges are modest and (2) plane strain approximation represents out of plane constraint in a conservative manner. The steel and weld metal were simulated as elastic-plastic materials with von-mises plasticity and isotropic hardening that followed a linear plus power law stress-strain relationship. The yield stress for steel and weld metal were taken to be 53.65 ksi and 72.50 ksi respectively. The latter being typical value of the post-Northridge filler materials. A typical $\sigma - J_I$ curve for a simulation with equal flanges and $\eta = 0.5$ is shown in Figure A-11. The obtained $\sigma - J_I$ for the 25 simulations is filtered for J values in the range of 0.01 – 0.7 ksi-in which represents

an envelope of anticipated values in construction practice (For e.g., a CVN value of 10 ft-lb @ 70°F corresponds to a J_{Ic} of 0.133 ksi-in at 0°F, obtained using Barsom's two step correlation followed by Master Curve approach). The following algebraic function was selected to represent the flange stress capacity as an analytical function of the input parameters:

$$\sigma_{capacity,\,estimate}^{flange} = \frac{K_{Ic}}{\sqrt{\pi \times (\eta / 2\xi) \times t_{upper}}} \times \frac{1}{\xi\sqrt{a} \times f_1(\eta) \times f_2(\xi) \times g_1(\eta) \times g_2(\xi)} \le F_u^{flange} \tag{A-8}$$

In which, the first term represents the allowable stress in an infinite plate with a center crack from elastic stress intensity factor, K_{Ic} is obtained from J_{Ic} value as (for plane strain conditions):

$$K_{Ic} = \sqrt{J_{Ic} \times E / (1 - \nu^2)} \tag{A-9}$$

The variable α equals 1 for specimens with PJP weld on two sides thus creating a central unfused section (referred as center-cracked) and equals 2 for specimens with PJP on one side only (referred as edge-cracked); the terms $f_1(\eta)$ & $f_2(\xi)$ account for deviation from the center-cracked infinite plate geometry; and $g_1(\eta)$ & $g_2(\xi)$ account for the presence of plasticity around the crack tip. These functions are given by following equations:

$$f_1(\eta) = (A_1\eta^2 + A_2\eta + A_3) \tag{A-10}$$

$$f_2(\xi) = B_1(\xi - 1)^2 + B_2(\xi - 1) + 1 \tag{A-11}$$

$$g_1(\eta) = \left(C_1K_{Ic}^3 + C_2K_{Ic}^2 + C_3K_{Ic}\right)\eta + C_4K_{Ic}^3 + C_5K_{Ic}^2 + C_6K_{Ic} + 1 \tag{A-12}$$

$$g_2(\xi) = \left(D_1K_{Ic}^2 + D_2K_{Ic} + D_3\right)(\xi - 1)^2 + 1 \tag{A-13}$$

It should be noted that if both the flanges are of equal width, $f_2(\xi)$ & $g_2(\xi)$ become 1. The coefficients are calibrated with the data from the simulations for each of the four splice geometry classifications: centre-cracked & equal flange (CC-EF), centre-cracked & unequal flange (CC-UF), edge-cracked & equal flange (EC-EF), edge-cracked & unequal flange (EC-UF). The obtained coefficients for the EC cases, which are of interest for pre-Northridge WCS, are shown in Table A-2. To ensure that the FEFM results represent the physical test data, the finite element models were validated against the physical tests performed by Shaw et al. (2015) by computing $\sigma_{design,\,true}^{flange} / \sigma_{capacity,\,FEM}^{flange}$. The numerator denotes the failure load of the selected specimen obtained from physical tests. Using $\sigma_{capacity,\,true}^{flange}$ and the FEFM simulation results at J_{Ic} value corresponding to CVN values of the specimen, the mean value of $\sigma_{design,\,true}^{flange} / \sigma_{capacity,\,FEM}^{flange}$ is determined to be 1.1475 with a coefficient of variation of 0.0652. This indicates that the FEFM simulations provides an accurate, yet slightly conservative, estimate of the stress capacity.

Design strength values for a given geometry are obtained from the stress estimates using resistance factor, ϕ which is determined by calibration to obtain a target safety level with respect to the design objective:

$$\sigma_{design}^{flange} = \phi \sigma_{capacity,\ estimate}^{flange} \quad \text{(A-14)}$$

Variability inherent in: (1) the sectional geometry; (2) the relationship between material toughness and CVN test results; (3) the fit of the finite element models to the physical reality; and (4) the fit of the predictive model to the finite element data are considered. The reliability analysis is performed for two scenario values of σ_{design}^{flange}: 42 ksi, the stress associated with 2475 year return period earthquake (Galasso et al. 2015) and 55 ksi, the yield stress of the column flanges. Additionally, two mean toughness values are assumed: 20 ft-lb and 40 ft-lb at 70°F. A reliability factor of $\beta = 4$ is used to obtain the ϕ values. The obtained ϕ values for the edge cracked specimen is presented in Table A-3. Based on the reliability analyses, design tables that indicate the maximum unfused section thickness ratio (i.e., a/t_{upper}) permissible for a given pair of flange thicknesses above and below the splice such that yield strength of upper column can be achieved at the two CVN values were proposed and can be obtained from Stillmaker (2016). Based on these outcomes, modifications in the AISC *Seismic Provisions* (AISC, 2010) were made to allow PJP WCS with flange penetration ratio more than 85%, provided a sophisticated non-linear analysis is performed to characterize demands in the splice.

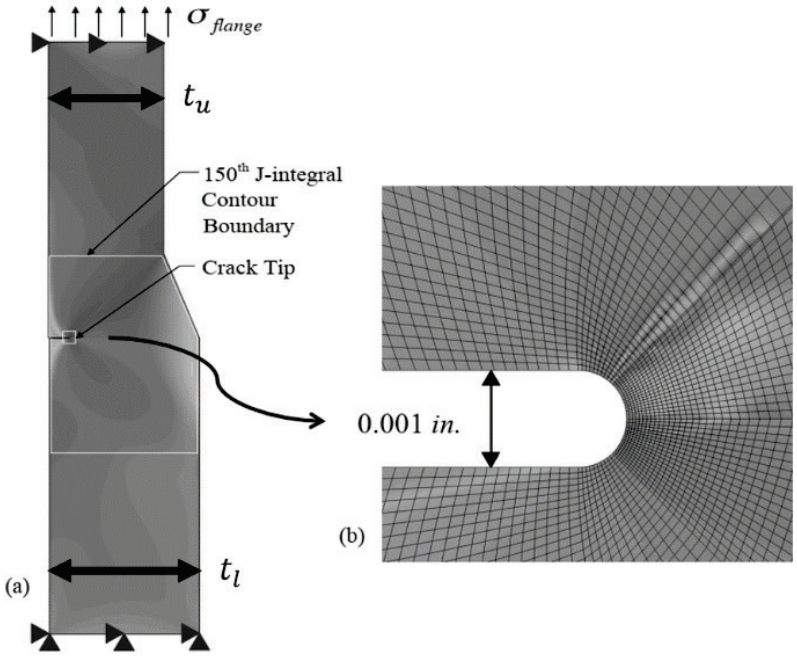

Figure A-10 FEFM simulation model (Stillmaker et al., 2015).

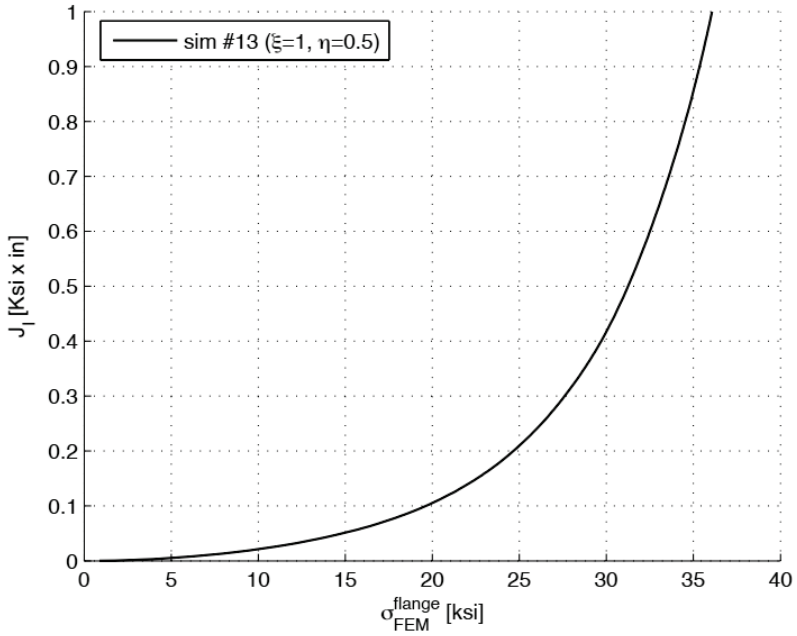

Figure A-11 J-integral vs. tensile stress in upper column flange for a simulation with η = 0.5 and ξ =1 (Stillmaker, 2016).

Table A-2 Calibrated Coefficients and Fitting Metrics (Stillmaker et al., 2015)

Term	Coefficient	EC-EF	EC-UF
$f_1(\eta)$	*A1*	4.310	
	A2	0.247	
	A3	1.120	
$f_2(\xi)$	*B1*		4.250
	B2		0.390
$g_1(\eta)$	*C1*	1.780E-06	
	C2	-4.990E-04	
	C3	1.770E-02	
	C4	-9.170E-07	
	C5	2.720E-04	
	C6	-6.590E-03	
$g_2(\xi)$	*D1*		0.000
	D2		-0.077
	D3		3.460
Mean $\sigma^{flange}_{design,FEM} / \sigma^{flange}_{capacity,estimate}$		1.021	1.024
Standard deviation $\sigma^{flange}_{design,FEM} / \sigma^{flange}_{capacity,estimate}$		0.160	0.123

Table A-3 Calibrated Resistance Factors (Stillmaker et al., 2015)

Scenario	EC-EF	EC-UF
CVN = 20 ft-lb @ 70°F; σ_{design}^{flange} = 42 ksi	0.5	0.6
CVN = 20 ft-lb @ 70°F; σ_{design}^{flange} = 55 ksi	0.5	0.6
CVN = 40 ft-lb @ 70°F; σ_{design}^{flange} = 42 ksi	0.5	0.5
CVN = 40 ft-lb @ 70°F; σ_{design}^{flange} = 55 ksi	0.5	0.5

SEAONC URP Project on Column Splices (2021)

In a recent SEAONC University Research Program project, the fracture susceptibility of a WCS in a pre-Northridge building was examined using component-level finite element analysis (Tam et al., 2021). The von Mises stress at the weld root tip was compared with the stress capacity based on the toughness of weld metal, provided by NIST GCR 17-917-46v2, *Guidelines for Nonlinear Structural Analysis for Design of Buildings Part IIa – Steel Moment Frames* (see Section A.2.3), to determine whether the splices were vulnerable to fracture. Based on this method, the splices fracture before yielding of the column section. The same procedure was repeated for splice connections retrofitted using fin plates, box plates, and extension plates with the plate sizes determined using linear stress distribution. The latter two retrofit techniques were found to reduce the von Mises stress concentrations significantly when compared to splice without retrofit and fin plate retrofit.

A.2.3 Available Guidance on Estimating Strength of Column Splices

Appendix A of NIST GCR 17-917-46v2, *Guidelines for Nonlinear Structural Analysis for Design of Buildings Part IIa – Steel Moment Frames* (NIST, 2017), provides guidance for modeling and checking the pre-Northridge (fracture-critical) welded connections and column splices using critical fiber stress limits based on fracture mechanics.

The critical stress in the upper column flange, which depends on the PJP weld configuration, is given by:

$$\sigma_{cr} = \frac{K_{Ic}}{F\left(\frac{a_o}{t_f}\right)\sqrt{\pi a_o}} \le F_{u,exp}\left(1-\frac{a_o}{t_f}\right) \le F_{y,exp} \qquad \text{(A-15)}$$

in which:

$$F\left(\frac{a_o}{t_f}\right) = \left(2.3-1.6\frac{a_o}{t_f}\right)\times\left(4.6\frac{a_o}{t_f}\right) \qquad \text{(A-16)}$$

and K_{Ic} is the fracture toughness at the operating temperature, t_f is the thickness of the column flange. a_o is the unfused section thickness of the flange, $F_{u,exp}$ is the lesser of the weld or base metal ultimate strength, and $F_{y,exp}$ is the expected yield strength of the base metal (See Figure A-12). It is important to note that the above equations are valid where the thickness of the two connected flanges are same. For a more generalized form of the equation, which involves both dependence on the PJP penetration and the ratio of upper and lower column flange width, Stillmaker et al. (2015) is referred (See Section A.2.2.).

The guideline recommends using Barsom's two step correlation followed by Master Curve approach (Wallin, 1998) to determine K_{Ic} values from the CVN tests, which is discussed in Section A.4.3. Median as well as the 5-percentile, and 95-percentile values of K_{Ic} assuming room temperature (70ºF) CVN toughness of 5, 10, and 20 ft-lb are indicated in Table A-4. The critical fracture stress corresponding to median and 5-percentile values of K_{Ic} estimated for a CVN value of 10 ft-lb, which is typical of pre-Northridge weld filler material (See Section A.4.2), for different a/t_f ratio, are shown in Table A-5. These stresses would govern the capacity of the column at splice with Grade 50 steel ($F_{y,exp}$ = 55 ksi) and E70XX electrodes. The stress demand obtained from the combination of axial load, P, and biaxial bending moments, M_x and M_y may be compared with this critical fracture stress to assess the potential for fracture.

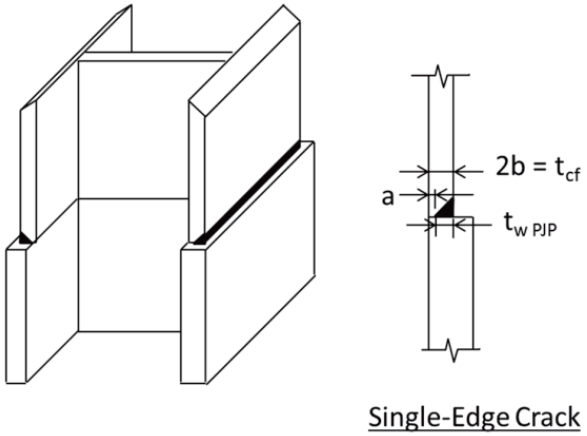

Figure A-12 Typical pre-Northridge column splice (NIST, 2017).

Table A-4 Fracture Toughness Values at 70º F

CVN (ft-lb)	K_{Ic} (ksi $\sqrt{\text{in.}}$)		
	5 percentile	*Median*	*95 percentile*
5	36	51	66
10	65	107	147
20	106	186	261

Table A-5 Fracture Stress Corresponding to Median and 5 Percentile Toughness Capacity for Various a/t_f Ratio (Corresponding to CVN of 10 ft-lb at 70°F and Flange Thickness of 2 inch)

a/t_f	0.3	0.5	0.7
5 percentile K_{Ic}	18.9 ksi	10.6 ksi	8.2 ksi
Median K_{Ic}	31.0 ksi	17.5 ksi	13.4 ksi

A.2.4 Knowledge Gaps

- Although one large scale test on a PJP column splice was performed by Bruneau and Mahin (1991), it is not indicative of the response of all the welded column splices of the pre-Northridge era which have flange penetration as low as 30% and different connection conditions for the webs – PJP-welded or bolted. The recent large scale tests by Shaw et al. (2015) high penetration (>85%) and weld filler material with minimum specified toughness are not representative of the splices in question. More large scale tests on various configurations based on survey of the pre-Northridge splices are required to characterize the behavior and fracture tendency accurately.
- The stress capacity estimates of the PJP-welded flanges, made available by Stillmaker et al. (2015) using FEFM simulations, may overestimate the capacity of pre-Northridge splices as the simulations were conditioned for large penetration ratio (with some simulations of 50% flange penetration). A more specific capacity estimate of the pre-Northridge splice geometries based on the framework developed by Stillmaker et al. is required. Also, the effect of lateral restraint provided at the web location needs to be quantified based on 3D FEFM simulations.
- The effect of stress gradient, under either uniaxial or biaxial bending of the columns, on the fracture capacity of the PJP splices has not been addressed previously. The simulations performed by Stillmaker et al. (2015) included uniform stress across the flange. The stress gradient may imply an increased or lower fracture capacity than using the peak or averaged stress in the flange.
- In previous computational works, it has been considered that the fracture initiates at the PJP weld root and completely severs the section. Although this is corroborated by certain experimental observations, the crack propagation effects need to be investigated more comprehensively. The influence of crack growth direction on fracture toughness (varying thickness encountered by crack front changes the fracture toughness capacity) and the phenomena of crack arrest due to features such as cope holes and bolted web connections are important issues that need to be addressed.

A.3 Performance Under Previous Earthquakes

Numerous welded steel moment frame buildings were damaged in the Northridge Earthquake of 1994 in the Los Angeles area (FEMA, 2000c). Structural damage observed in these buildings included yielding, buckling, and fracture in beams and columns. Damaged elements included beam and column flanges, column panel zones, welds connecting beam flanges to column flanges, and the shear tabs connecting beam webs to column flanges. While fracture at beam-to-column connection was the most dominant damage mode that raised concerns, no instance of column splice fracture was reported in the buildings damaged by the Northridge earthquake (FEMA, 1995). However, several column splice fractures in buildings affected by the 1995 Kobe (Great Hanshin), Japan earthquake were reported (AIJ, 1995). Figure A-13 shows the fracture at splice location in a cold-formed hollow square steel column of 5-story building damaged in Kobe earthquake. In many cases where PJP welds were provided, the fracture completely severed the section, and the two connected columns were misaligned after the earthquake. Figure A-14 shows fracture in the upper column flange at welded splice location in a high-rise structure. Fractures at column splices originating both in the plane of splice (at the unfused section of PJP welds) as well as in the HAZ of the top column flange were observed. The fracture surfaces were reported to be highly rough, involving shear lips and tear ridges. It is relevant to mention here that the typical welding process used in Japan at the time featured GMAW electrodes and required minimum CVN toughness.

(a) Column with fracture

(b) Close-up view

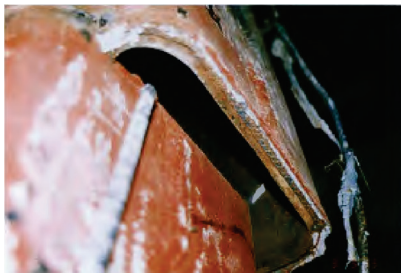

(c) Fracture surface and backup plate inside of column

Figure A-13 Fracture of cold-formed square-tube column at CJP-welded splice (AIJ, 1995).

Figure A-14 Fracture of column at welded column splice location (AIJ, 1995).

The post-Northridge investigations on demands in column flanges at splice location and the capacity of the typical pre-Northridge splices (See Sections A.2 and A.5) reveal a high susceptibility to fracture of these connections. However, the reported inspections and surveys do not mention any column splice fractures. The lack of data on splice fractures after the Northridge earthquake may be attributed to insufficient inspections of column splices, or because assumptions in fracture mechanics simulations that predict such fractures are incorrect. Most of the surveys in the years after the earthquake were performed by engineering firms on an ad hoc basis (mandated by the local ordinances) and were extremely limited (Weinberg and Goltz, 1999). Many owners were not compelled to undertake substantial voluntary inspections in the absence of severe non-structural damage. Consequently, many buildings remained uninspected or only minimally inspected (Youssef et al., 1995). Where the inspections were performed, the center of attention was primarily the fractured beam-to-column connections. For example, the survey form used for inspection of 51 steel moment frames for damage after the earthquake as a part of the NIST survey (Youssef et al., 1995) did not explicitly mention column splices as potential site of fracture, thereby limiting the data to beam-to-column fractures.

A.4 Material Characterization

The material properties of pre-Northridge filler metal and column steel material are discussed in this section. Hot-rolled W-shapes of A36 (ASTM A36/A36M 2019) and A572 grade 50 (ASTM A572/A572M 2021) steel material were extensively used as columns in pre-Northridge buildings and the welds in the connections (both beam-to-column connections and column splices) were commonly made with the self-shielded flux-cored arc welding (FCAW-SS) process using an E70T-4 or E70T-7 weld wire. A brief overview of the post-Northridge weld material is also presented. Tools to convert the material toughness to fracture toughness criteria are discussed later.

A.4.1 Column Steel

First introduced in 1960, ASTM A36 was the prominent steel material used in building construction in 1960s and 1970s. Both beams and columns were generally specified with ASTM A36 steel. The columns were occasionally specified with

ASTM A572, Grade 50 or Grade 42 steel, which was first issued in 1966. During the 1980s, it became a common practice to specify beams of ASTM A36 steel and columns of A572, Grade 50 steel to develop economical designs with a strong-column-weak-beam configuration (FEMA, 2000c). Kaufmann et al. (1997) performed tensile tests on coupons extracted from column flanges and beam flanges of 5 pre-Northridge buildings. The mechanical properties of all beam material tested satisfied the mechanical property requirements of A36 steel. The column material in all samples was found to satisfy the strength requirements of A36 steel with column material in three buildings also satisfying the strength requirements of A572 Gr. 50 steel. So, for three of the buildings sampled, the yield strength of the columns exceeded that of the beams, whereas the opposite was found in the other two buildings. This necessitates sample extraction from column flanges for accurate strength quantification of the pre-Northridge buildings to be re-evaluated. FEMA 351 (FEMA, 2000b) recommends beams and columns to be conservatively considered of the same grade of material with lower bound and expected material properties as given in Table A-6. It is important to note that for wide-flange shapes, produced before 1997, indicated values are representative of material extracted from the web of the section rather than the flanges. (ASTM A6 was revised in 1998 to specify that tensile coupons be taken from the flange of wide flange shapes.)

Table A-6 Lower Bound and Expected Material Properties for Structural Steel Shapes of Various Grades (FEMA, 2000c)

			Yield Strength (ksi)		Tensile Strength (ksi)	
Material Specification		Year of Construction	*Lower Bound*	*Expected*	*Lower Bound*	*Expected*
ASTM, A7, A373		pre-1960	30	35	60	70
ASTM, A36	Group 1	1961-1990	41	51	60	70
	Group 2		39	47	58	67
	Group 3		36	46	58	68
	Group 4		34	44	60	71
	Group 5		39	47	68	80
ASTM, A572	Group 1	1970-1997	47	58	62	75
	Group 2		48	58	64	75
	Group 3		50	57	67	77
	Group 4		49	57	70	81
	Group 5		50	55	79	84
A36 and Dual Grade 50	Group 1	1990-1997	48	55	66	73
	Group 2		48	58	67	75
	Group 3		52	57	72	76
	Group 4		50	54	71	76

CVN values were also reported for specimen extracted from intersection of the web and flange of the columns for different temperatures by Kaufmann et al. (1997). Except for one building, the CVN values exceeded 20 ft-lb at 70°F. The AISC mill survey (Cattan, 1996), which studied the production data of various manufacturers to provide data on steel toughness, also reported high mean CVN values which ranged from 33 ft-lb at 70°F for ASTM A572 Gr. 50 steel to 200 ft-lb at 70°F for ASTM A36 steel.

A.4.2 Weld Material Properties

Early structural welding typically used the SMAW process and stick filler metals. Although a variety of weld filler metals were available, the most employed filler metal in the 1950s and early 1960s conformed to the E6012 designation which corresponds to a filler metal with a minimum specified tensile strength of 60 ksi. In the 1960s, as higher strength steels came on the market, there was a gradual shift to the E7024 weld filler metal, which was capable of depositing metal with a higher minimum specified tensile strength of 70 ksi. Neither of these filler metals had minimum specified notch toughness. A switch to FCAW, which permitted more rapid deposition of filler metal and therefore, more economical construction of welded structures, occurred in the mid-1960s (FEMA, 2000c).

E70T-4 and E70T-7, which are FCAW with a minimum specified tensile strength of 70 ksi, were commonly used in welded steel moment connections before the 1994 Northridge earthquake. These filler metals were also not specified any notch toughness. E71T-8, E70T-6, and E70T7-K2 are all FCAW that satisfy the specified minimum notch-toughness and have been replacing E70T-4 and E70T-7 since then. Many weld metal samples extracted from the fractured beam-to-column connections of the pre-Northridge buildings have been tested for CVN toughness after the earthquake (Fisher et al., 1995; Kaufmann et al., 1996, 1997).

As a part of the SAC Project, Fisher et al. (1995) investigated CVN values of weld samples taken from beam-to-column connections that fractured in the Northridge earthquake as well as shop-welded samples that followed the recommended pre-Northridge welding procedure. The lower bound impact energy obtained in the former was between 3 and 10 ft-lb for temperatures up to 120°F. For shop-welded samples, the fracture toughness increased slightly but remained low as also indicated in Figure A-15. It is important to note that the values lie in the lower shelf or lower-transition regions.

A similar and low level of weld metal toughness was reported by the NIST study at Lehigh (Kaufmann et al., 1996, 1997) shown in Figure A-15. The room temperature toughness of the weld specimen, extracted from the pre-Northridge beam-to-column connections, was in the range of 7 ft-lb to 15 ft-lb and reached an upper shelf

toughness of 34 ft-lbs to 61 ft-lbs at 212 °C. The base metal toughness and strength were found to be similar in both fractured and intact samples. Low weld toughness was found to be the only consistent factor in the connection fractures. Four weld metal compact tension tests (ASTM E399, 1990) to determine the plain strain fracture toughness of E70T-4 weld metal were also carried out as a part of the study. The static fracture toughness at room temperature was found to be in the range of 60 ksi $\sqrt{\text{in.}}$ to 65 ksi $\sqrt{\text{in.}}$ and was reduced to 55 ksi $\sqrt{\text{in.}}$ to 60 ksi $\sqrt{\text{in.}}$ at intermediate loading rates.

CVN test results of E70T-6, E70T-1, and E71T-8, which are weld filler materials used post-Northridge, in an AISC sponsored study at Lehigh (Ricles et al., 2004) showed that these satisfied the toughness requirements of 20 ft-lb at -20°F and 40 ft-lb at 70°F as shown in Figure A-16. The CVN specimens were taken from both AWS standard test plates and connection mock-ups and manufactured in accordance with AWS A5.20-95 (AWS A5.20, 1995). Similar high toughness, well above the specified requirements, was reported by Shaw et al. (2015) for E70T-6 weld material. The CVN requirement of 40 ft-lb at 70° F was met at 0° F for samples extracted from specimen with qualified weld procedures. The study also reported two CVN values at 70° F of samples taken from the HAZ of flange – 38 ft-lb and 55 ft-lb. These samples were extracted from unfractured flanges of the tested columns so these CVN values indicate the original weld HAZ to be sufficiently tough.

In a more recent AISC study (Gomez et al., 2008) that aimed to evaluate the strength and ductility of fillet welded connections subjected to out-of-plane bending, two CVN tests at three temperatures (-20°F, 70°F, and 212°F) were conducted to establish the temperature transition behavior of E70T-7 and E70T7-K2 weld filler material. The E70T7-K2 electrode exceeded the minimum toughness requirements of 20 ft-lb at -20°F and 40 ft-lb at 70°F required by AISC 341 (2002). The E70T-7 electrode (without minimum specified toughness), used in the pre-Northridge era, did not meet the toughness criteria, and showed CVN values consistent with values reported in previous studies, as shown in Figure A-15. On performing the spectrochemical analysis of the two weld materials, it was reported that the E70T7-K2 electrode had a substantially higher nickel and manganese content and a lower carbon and aluminum content as compared to E70T-7 electrode. A comparison of the two along with the chemical composition of E70T-4 as reported by Kaufmann et al. (1997) is shown in Table A-7.

As part of the SAC Project, yield strength, F_y and ultimate strength, F_u of several weld metals were evaluated using tensile tests (Chi and Deierlein, 2000). The average yield strengths of all welds were found in the range of about 70 to 75 ksi, except for E70T-4, which exhibited an average yield strength of 55 ksi (the minimum yield strength requirement for these electrodes is 58 ksi). Ultimate strengths of all welds were reported in the range of F_u = 80 to 90 ksi, thus meeting the minimum

requirements for E70 materials. Similar strength range is reported by various researchers for the welds with minimum specified toughness used after the Northridge earthquake (Kanvinde et al., 2008; Ricles et al., 2004). A high variability in the yield strength of the weld metals, presumably due to variations in welding procedures such as heat input, cooling rates, etc., is observed. The variability can be significant in cases when the behavior is controlled by yielding of the weld or more specifically the relative yield strength of the weld-to-base metal (Chi et al., 2000).

In addition to the weld material mechanical properties, it is important to address the issue of lack of quality control and quality assurance in the pre-Northridge welded connections. The fractured surfaces of beam-to-column connections of the buildings damaged in the Northridge and Kobe Earthquakes revealed evidence of improper use of electrodes and welding procedures. Prominent among the misuses were high production deposition rates. Pass widths of up to one and a half inches and pass heights of a half inch were common. The heat input associated with large passes promotes grain growth in the HAZ and low notch toughness (FEMA, 1995).

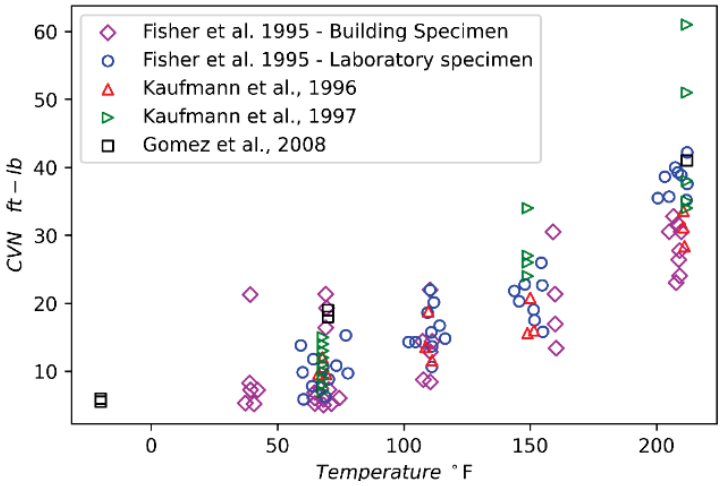

Figure A-15 Typical CVN values of pre-Northridge FCAW-S weld material.

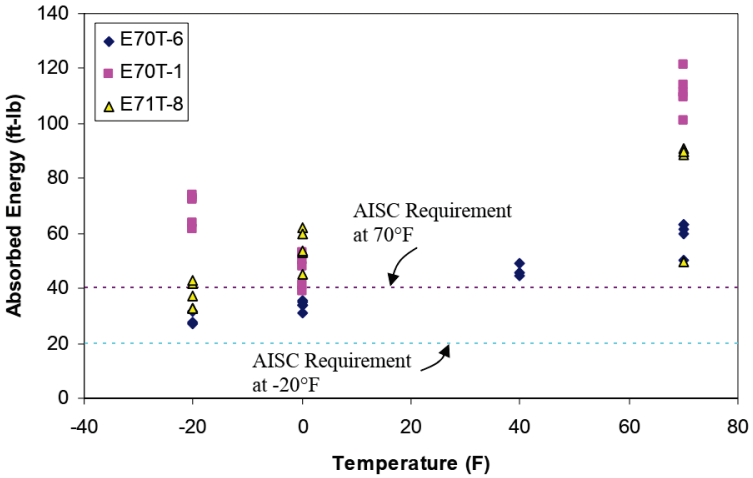

Figure A-16 CVN test results for weld metal (Ricles et al., 2004).

Table A-7 Chemical Composition of the Weld Filler Materials (NR: Not Reported)

	Filler Metal		
	E70T7-K2	*E70T-7*	*E70T-4*
Element	*(Gomez et al., 2008)*		*(Kaufmann et al., 1997)*
Al	1.16	1.74	1.38
C	0.08	0.33	0.24
Cr	0.03	0.02	NR
Cu	0.03	0.02	NR
Mn	1.27	0.37	0.55
Mo	0.02	0.01	NR
Ni	1.68	0.01	NR
P	0.009	0.006	0.008
Si	0.24	0.08	0.25
S	0.005	0.005	0.008

A.4.3 CVN-K_{Ic} Correlations in Structural Engineering

While CVN data provides a qualitative check on fracture toughness, these do not directly relate to fracture indices calculated by analysis. Empirical relations have been derived to relate CVN test results with static fracture toughness, K_{Ic} and dynamic fracture toughness, K_{Id} test results to allow for the indirect determination of fracture toughness capacity by way of the simpler and less costly CVN impact test. Based on comparison of CVN and K_{Ic} test data in the upper shelf region, Barsom proposed the following upper shelf correlation (Barsom and Rolfe, 1970):

$$K_{Ic} = \sqrt{5F_y\left(\mathrm{CVN} - \frac{F_y}{20}\right)} \tag{A-17}$$

in which K_{Ic} is in ksi√in., the yield stress, F_y, is in ksi, and CVN is in ft-lb. CVN, which is a measure of dynamic toughness, is related to K_{Ic}, which is a measurement of static toughness, in the upper shelf region, because the loading rate has little effect on fracture toughness in this region. However, when relating CVN and K_{Ic} in the lower transition region, a direct relationship is not easily accomplished because of the large loading rate effect. Instead, a two-step correlation that first converts CVN toughness values to K_{Id} values at the CVN test temperature is used, using the relationship (Barsom, 1975):

$$K_{Id} = \sqrt{5 \times E \times \mathrm{CVN}} \tag{A-18}$$

in which K_{Id} is in psi $\sqrt{\text{in.}}$, E is in psi, and CVN is in ft-lb. The dynamic toughness curve is then shifted horizontally to the left, referred to as the temperature shift, such

that when compared at a constant temperature, static fracture toughness, K_{Ic} is higher than K_{Id}. The static and dynamic fracture toughness tests are performed at strain application rates of around 10-5 in/in/s and 10 in/in/s, respectively. The temperature shift, measured in °F between these rates of loading for steels with yield stress less than 140 ksi, is a function of yield stress, given by (Barsom and Rolfe, 1970):

$$T_{shift} = 215 - 1.5\sigma_{ys} \tag{A-19}$$

Thus, K_{Ic} at a temperature T_o can be determined from CVN value at temperature $T_o + T_{shift}$:

$$K_{Ic,T_o} = \sqrt{5E\left(\text{CVN}\right)_{T_o+T_{shift}}} \tag{A-20}$$

A more generalized version of temperature shift equation allows for the temperature shift to be calculated between static loading and a service strain application rate, $\dot{\varepsilon}$, that is less than the dynamic loading rate:

$$T_{shift} = (150 - F_y)(\dot{\varepsilon})^{0.17} \tag{A-21}$$

It is important to note that the CVN – K_{Id} correlation was determined using test data for various grades of steel ranging in yield strength from about 36 to 140 ksi, and eight heats of SA 533B, Class 1 steel. Also, the correlation is a lower bound correlation, intended to specify conservative, minimum toughness requirements. A best fit to the same data is given by (Stillmaker, 2016):

$$K_{Id} = \sqrt{7.576 \times E \times \text{CVN}} \tag{A-22}$$

The use of the lower-shelf Barsom correlation between CVN toughness and K_{Ic} is conservative primarily because it does not explicitly consider the rate shift (dynamic toughness values are significantly lower, in general, as compared to static values). This serves the purpose in the current industrial practice where only minimum, and not the actual material, toughness values are known at only one (or possibly two) temperatures. It remains unclear, with one or two data points, where on the CVN-temperature transition curve the minimum required toughness occurs.

Hoffman (1980) proposed a lower bound CVN-K_{Ic} correlation at lower shelf and transition region behaviors to all the existing CVN-K_{Ic} correlations. The lower bound is given by:

$$K_{Ic} = 9.35 \times \text{CVN}^{0.63} \tag{A-23}$$

BS 7910 (BSI, 2019) gives two methods to predict static fracture toughness of ferrite steels. The lower bound static fracture toughness at service temperature is given by:

$$K = \left[\left(12\sqrt{\text{CVN}} - 20\right)\left(\frac{25}{B}\right)^{0.25}\right] + 20 \tag{A-24}$$

in which, K is material toughness in MPa $\sqrt{\text{m}}$, B is component thickness in mm and CVN value is taken at service temperature in Joules. A cap on the above value, for material exhibiting low upper shelf toughness, is put by the following correlation:

$$K = 0.54 \times \text{CVN} + 55 \ \text{MPa}\sqrt{\text{m}} \tag{A-25}$$

The Master Curve approach (Wallin, 1998) provides a rational framework for characterization of statistical variations in fracture toughness at a given temperature for lower shelf and lower-transition toughness. ASTM E-1921 (ASTM, 2020) standardizes procedures for characterizing the Master Curve of ferritic steels that experience onset of cleavage cracking (brittle fracture) at elastic, or elastic-plastic instabilities, or both. The basic expression for the macroscopic failure probability of a 1 inch thick (1T) cracked specimen is given as:

$$P_f = 1 - \exp\left\{-\left(\frac{K_{Jc} - K_{min}}{K_0 - K_{min}}\right)^4\right\} \tag{A-26}$$

in which, K_{Jc} is elastoplastic equivalent critical fracture toughness based on J integral or the effective toughness following plasticity correction, K_0 is temperature dependent scale parameter (or the reference curve) which corresponds to a 63.2% fracture probability, K_{min} is a lower limiting K_{Jc} value below which cleavage fracture is impossible. The above expression is based on a 3 parameter Weibull distribution with scale parameter K_0, threshold of K_{min} and slope of 4. For test specimens of steel, the value of K_{min} is approximated as 20 MPa $\sqrt{\text{m}}$ (18.2 ksi $\sqrt{\text{in.}}$) (Wallin, 1993) and the reference curve is given by:

$$K_0 = 31 + 77e^{0.019(T - T_o)} \ \text{MPa}\sqrt{\text{m}} \ (T,\ T_o \text{ is in °C}) \tag{A-27}$$

$$K_0 = 28.2 + 70.1e^{0.0105(T - T_o)} \ \text{ksi}\sqrt{\text{in.}} \ (T,\ T_o \text{ is in °F}) \tag{A-28}$$

in which T_o is the reference temperature. The reference temperature represents the temperature at which the median (50% fracture probability) fracture toughness value of the exponential master curve is equal to 100 MPa $\sqrt{\text{m}}$ (91 ksi $\sqrt{\text{in.}}$). The value of K_{Jc} can be written as:

$$K_{Jc,0.xx} = 20 + \left[\ln\left(\frac{1}{1 - 0.xx}\right)\right]^{\frac{1}{4}} \left\{11 + 77e^{0.019(T - T_o)}\right\} \ \text{MPa}\sqrt{\text{m}} \ (T,\ T_o \text{ is in °C}) \tag{A-29}$$

$$K_{Jc,0.xx} = 18.2 + \left[\ln\left(\frac{1}{1 - 0.xx}\right)\right]^{\frac{1}{4}} \left\{10.0 + 70.1e^{0.0105(T - T_o)}\right\} \ \text{ksi}\sqrt{\text{in.}} \ (T,\ T_o \text{ is in °F}) \tag{A-30}$$

in which, 0.*xx* to the fracture probability or bounds to the toughness. The temperature dependence of median toughness (50% fracture probability) in the ductile–brittle transition region is thus given by:

$$K_{Jc(median)} = 30 + 70e^{0.019(T-T_o)} \text{ MPa}\sqrt{\text{m}} \ (T,\ T_o \text{ is in °C}) \qquad \text{(A-31)}$$

$$K_{Jc(median)} = 27.3 + 63.7e^{0.0105(T-T_o)} \text{ ksi}\sqrt{\text{in.}} \ (T,\ T_o \text{ is in °F}) \qquad \text{(A-32)}$$

The Master Curve is normalized to 1T specimen; K_{Jc} for a specimen of thickness, B_x may be obtained from:

$$K_{Jc(Bx)} = K_{min} + \left[K_{Jc(1T)} - K_{min}\right]\left(\frac{1.0}{B_x}\right)^{0.25} \qquad \text{(A-33)}$$

As J integral provides an estimate of the energy release rate, G, during an elastoplastic fracture or ductile tearing, critical J integral values for static tests can be converted to K_{Jc}, by using the relationship (Anderson, 2017):

$$K_{Jc} = \sqrt{\frac{J_{Ic}E}{1-\nu^2}} \text{ for plain strain \& } K_{Jc} = \sqrt{J_{Ic}E} \text{ for plain stress} \qquad \text{(A-34)}$$

Figure A-17 schematically shows the steps used to characterize the Master Curve given CVN values at a single lower shelf temperature (typically T = 0° F). The subsequent discussion describes each of the steps:

1. Determine K_{Id} for the CVN values at lower shelf (temperature = T_i) using the Barsom lower bound correlation. $K_{Id} = \sqrt{5 \times E \times \text{CVN}}$
2. Determine the median value of the K_{Id} data points assuming a Weibull distribution with threshold of K_{min} and a scale of 4.
3. Shift the median K_{Id} to the left to account for the temperature dependent rate shift. Thus, K_{Ic} at $T = T_i + T_{shift}$ is obtained. $T_{shift} = 215 - 1.5\sigma_{ys}$
4. The data point (K_{Ic}, T) falls on the median Master Curve prescribed in ASTM E1921 (Equation A-31 and A-32). Determine the reference temperature, T_o from the equation.
5. The bounds around the median curve can also be obtained now using Equation A-30.

If CVN values at multiple temperatures are known, the method for evaluation of reference temperature, T_o, as per ASTM E1921 is followed. Additionally, ASTM E1921 places a toughness limit on K_{Ic} for use with the master curve methodology, given by:

$$K_{Ic} = \sqrt{\frac{Eb_o\sigma_{ys}}{30\left(1-\nu^2\right)}} \quad \text{(A-33)}$$

in which b_o is the difference between the specimen width and the initial crack and σ_{ys} is the yield stress. Any toughness value exceeding this limit is censored in Step 1.

With the master curve well established for the ferrite steels, recent developments have focused on relating CVN toughness with the master curve reference temperature, T_o, directly (BSI, 2019; Collins et al., 2016a; Wallin, 2011). The correlation proposed by Wallin (2011) includes the effects of material yield stress and upper shelf toughness as:

$$T_o = T_{28J} - C + \frac{\sigma_{ys}}{12} + \frac{1000}{\text{CVN}_{\text{US}}} \quad \text{(A-34)}$$

in which T_{28J} is the temperature corresponding to a CVN value of 28 J (21 ft-lb), C is a constant depending on fracture specimen type; σ_{ys} is material yield stress in MPa and CVN_{US} is CVN corresponding to upper shelf. The upper shelf energy values are included in the correlation to account for low upper shelf toughness materials, in which 28 J (21 ft-lb) does not correspond with cleavage fracture behavior. Constant C is 77 and 87°C for compact tension and single edge bend specimens, respectively.

The standard BS 7910 (BSI 2019) provides a method to establish the reference temperature when data for a full CVN temperature transition curve are available. Test temperatures corresponding to CVN impact test values of 27 and 40 J (20 and 30 ft-lb) are adjusted to provide an estimated reference temperature, given by:

$$\begin{aligned} T_o &= T_{27J} - 18°\text{C} + T_k \\ T_o &= T_{40J} - 24°\text{C} + T_k \end{aligned} \quad \text{(A-35)}$$

in which, T_o is reference temperature, T_{27J} and T_{40J} are test temperatures at CVN energy levels of 27 and 40 J, respectively and T_K is a temperature term to account for scatter in CVN data. All temperatures are in degrees Celsius. A value of $T_k = 25°\text{C}$ is recommended unless experimental data support the use of a lower value. The BS 7910 correlation is found to be preferable amongst all lower shelf correlations for evaluation of bridge steel toughness based on analysis of the legacy bridge fracture database (Collins et al., 2016a; 2016b).

It is important to note that the application of the Master Curve method to an inhomogeneous material may result in an inaccurate estimate of the transition reference value T_o and nonconservative confidence bounds (ASTM, 2020b). Multi-pass welds, as is the case with column PJP or CJP welded splices, may often generate heat-affected and brittle zones with localized properties that are quite different from either the base or weld materials. Consequently, the method should be used with

caution. Additionally, it is necessary to identify the temperature above which upper shelf behavior is expected for a material. This becomes especially important for materials exhibiting a low upper shelf fracture toughness which limits the applicability of the Master Curve approach. ASTM E1921 establishes an upper limit of T_o + 50°C as the temperature above which K_{Ic} values may not be used to estimate T_o. Using empirical and physical basis, the temperature at onset of upper shelf behavior, T_{US} was shown to be dependent on the transition temperature, T_o, for ferrite steels by EricksonKirk and EricksonKirk (2006). The linear relationship is given by:

$$T_{US} = 0.7985T_o + 48.843 \text{ (Temperature in °C)} \quad \text{(A-36)}$$

The relationship was determined using the intersection of lower-shelf Master Curve (ASTM E1921 approach) and a proposed upper-shelf master curve (EricksonKirk and EricksonKirk, 2006b) as shown in Figure A-18.5 The comparison of the proposed T_{US} with the ASTM E1921 bound of T_o + 50°C showed that the ASTM E1921 upper temperature limit is too restrictive for materials having T_o below -5°C and is not restrictive enough for materials having higher T_o values. Thus, caution should be exercised while employing the Master Curve to determine fracture toughness of inhomogeneous materials which generally exhibit high T_o values.

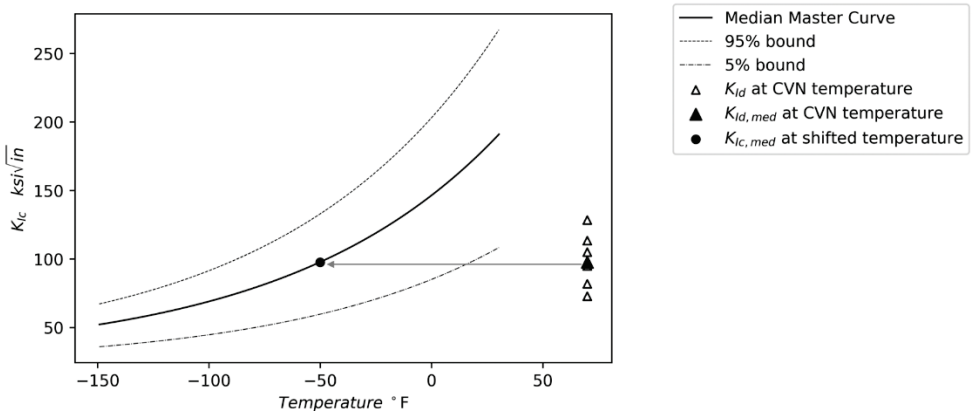

Figure A-17 Process for determining toughness using the Master Curve method.

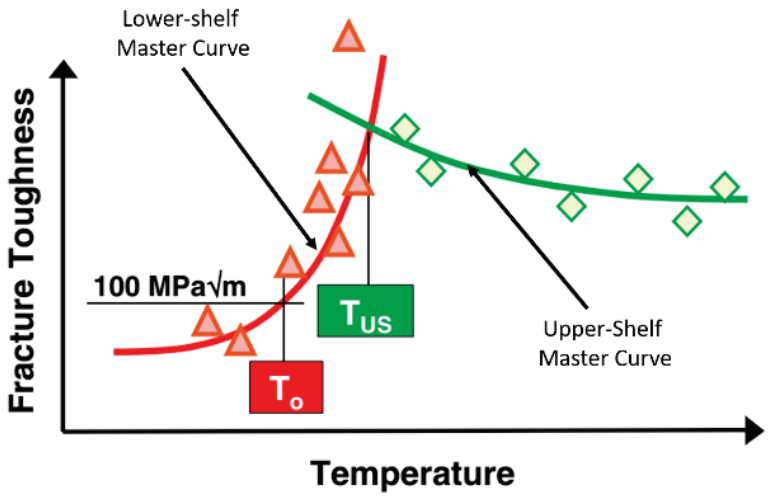

Figure A-18 T_{US} as the intersection of the ASTM E1921 lower shelf Master Curve and the upper shelf Master Curve (EricksonKirk and EricksonKirk, 2006a).

A.4.4 Knowledge Gaps

- Although data on the CVN toughness of weld material extracted from the failed pre-Northridge beam-to-column connection is available, confidence in using this data as a representative toughness of weld material in the PJP WCS has not been independently verified. This is because the *in situ* toughness may differ from the CVN toughness determined from filler metal assemblies (AWS A5.20 filler metal classification tests) owing to different deposition rates, number of weld passes, and heat input.
- Moreover, the CVN toughness in itself cannot be used in a quantitative manner in fracture mechanics analysis – for this, toughness values measured in terms of J_{Ic} or K_{Ic} at operating temperatures are needed. These are not known and must be indirectly estimated through empirical correlations. While well established, these correlations have been general developed using only base material data, and not the materials used in pre-Northridge WCS. These correlations have not been verified in the context of the actual materials used in pre-Northridge splices.

A.5 Seismic Demands in Splices and Post-Fracture Simulation Tools

A.5.1 Demand in Splices Based on Performance Assessment

As part of the SAC Project, three consulting firms were commissioned to perform designs for 3-, 9-, and 20-story model buildings, following all local code requirements for the following three cities: Los Angeles, Seattle, and Boston. The buildings were to be designed as standard office buildings situated on stiff soil. The consulting firms were asked to perform three designs:

- Pre-Northridge design (i.e., without consideration of FEMA 267),
- Post-Northridge design following the FEMA 267 recommendations, and
- Special designs for the 9-story building with reduced beam sections and higher strength columns.

Building orientation and member sizes similar to these pre-Northridge buildings have been used by numerous researchers to evaluate the demands in the columns at the column splice location (Galasso et al., 2015; Gupta and Krawinkler 1999; Shaw et al., 2015; Shen et al., 2010). Actual buildings that needed re-evaluation and retrofitting have been analyzed by practicing engineers for the demands at splice location and similar range of demands have been found (Chisholm et al., 2017; Nudel et al., 2013, 2015). The methodology adopted in these studies and the outcomes are discussed in this section. The ASCE/SEI 41 evaluation procedure for the column splices in existing buildings is also discussed.

Gupta and Krawinkler (1999)

Gupta and Krawinkler (1999) with a primary objective to quantify the overall behavior of SMRFs in a statistical manner, evaluated the moment and axial load demands corresponding to drift demands based on non-linear time history analysis (NLTHA) at column splice locations on the 5th floor of the 20 story LA building using pushover analysis of the 2D non-linear model. The splices being located 6 ft above the floor centerline were expected to lie closely to the inflection point, but significant displacement of inflection point from mid-height location was observed. The bending moments in the exterior splices were found to be as high as 30% of plastic moment capacity of the columns at 6% drift demands as the columns deformed in single curvature with plastic hinge forming at the top of the column. The tensile force in the interior and exterior columns differed significantly, the latter remaining in compression at all anticipated drift ratios. Tensile axial forces, as high as 30% of yield tensile capacity, in the exterior columns was reported even at modest drift demands. A summary of the demands in the splices when the building is subjected to ground motions with 2% probability of exceedance in 50 years (MCE) is presented in Table A-8. More detailed analysis was recommended to quantify the demands in splices as pushover analysis may severely underestimate the demands based on drift ratio due to contributions from higher modes (and thus single curvature response in columns).

Table A-8 Axial Force and Bending Moment Demand in Splices of 5th Floor for the 20-Story Los Angeles Building (Gupta and Krawinkler, 1999)

		Maximum	84th percentile	Median	Minimum	Std. Dev.
Story 5 Drift Angle		0.1185	0.0628	0.0309	0.0099	0.71
Exterior Column	M/M_p	0.47	0.32	0.21	0.11	0.43
	$P(compression)/P_y$	0.7	0.65	0.59	0.44	0.1
	$P(tension)/P_y$	-0.37	-0.3	-0.25	-0.19	0.19
Interior Column	M/M_p	0.78	0.55	0.38	0.22	0.39
	$P(compression)/P_y$	0.34	0.32	0.3	0.27	0.06
	$P(tension)/P_y$	0	0	0	0	0

Note: The values represent the upper bounds for the observed individual force demands for exterior and interior column splices of 5th floor

Shen et al. (2010)

Shen et al. (2010) conducted a series of NLTHA to directly examine seismic demands in column splices rather than use the indirect approach of pushover analysis. The simulations were conducted for 4-, 9- and 20-story moment frame buildings (2D frame model) subjected to a suite of 20 ground motions (Magnitude > 6.5) with 2% probability of exceedance in 50 years, representative of the Southern California region. The buildings were designed based on the seismic design requirements in ASCE/SEI 7-05 (2005) and AISC 341 (2010). The force demands were characterized in terms of a P-M Interaction Ratio (IR), which reflects the combined effect of the axial tension and bending moment, such that IR = 1 implies tensile yielding of the flange of the smaller (upper) column. As splice fracture is sensitive to a peak tensile stress in the flange of the connection, IR provided an adequate measure of splice demands. The simulations revealed that under the extreme ground motions, the force demands approach the capacity of the smaller connected column. However, the inelastic deformation demand in the splices is negligible, when interpreted at the cross-sectional level of the smaller column. The demands reported were as high as IR of 1.0 for the 20-story building. This is attributed to (1) higher overturning moments increasing the axial tension in the exterior columns and (2) the pronounced participation of higher dynamic modes, resulting in single-curvature bending of columns. For the 4- and 9-story frames, the force demands ranged from an IR of 0.35-0.8 and 0.5-0.9 respectively which, although lower than the upper column cross-sectional capacity, are concerning for pre-Northridge splices where the stress capacity of the PJP-welded section is determined to be significantly lower than yield stress depending on the penetration of PJP and toughness of weld metal. A summary of the splice demands in the three buildings at different ground motion levels is summarized in Table A-9. The study also compared the effect of splice location on

the demands using two variations: (1) splice located at 4 ft from the finished floor level and (2) splice located at 4 ft from the beam-to-column connection centerline. When the seismic response of the frame is low to moderate, the demands in the splice closer to the mid-height of column was lower than the splice away from mid height (ratio of former to latter ranging from 0.67 to 0.95). This difference was negligible when the frames experienced significant inelastic deformation as the axial tension in the columns, which remains constant through the height of column, is the significant contributor to IR. On comparing the demands at splice location with rotations at beam-to-column connections, it was found that the two quantities are closely related and the demand on the splice can be of the order of the smaller column's strength when the beam-to-column connection reaches expected maximum deformation capacity. The authors recommend that the splices in special moment-resisting frames (SMRF) and intermediate moment-resisting frames (IMRF) to be designed such that they can develop the capacity of the smaller connected column.

Table A-9 Summary of Seismic Response (Shen et al., 2010)

Ground Motion Group	Range of story drift ratio	Building Type	Plastic rotation * $\mu \pm \sigma$	IR = P/P_y + M/M_p $\mu \pm \sigma$
1	0.01 to 0.02	4-story	0.013 ± 0.007	0.338 ± 0.141
		9-story	0.017 ± 0.008	0.339 ± 0.020
		20-story	0.010 ± 0.002	0.492 ± 0.048
2	0.02 to 0.04	4-story	0.035 ± 0.004	0.650 ± 0.085
		9-story	0.030 ± 0.007	0.512 ± 0.080
		20-story	0.023 ± 0.007	0.666 ± 0.089
3	0.04 to 0.05	4-story	Not Applicable	
		9-story	0.050 ± 0.009	0.651 ± 0.090
		20-story	0.070 ± 0.012	0.924 ± 0.125

*Maximum plastic rotation at beam-to-column connection

Shaw et al. (2015)

NLTHA of buildings similar to the previous study was conducted by Shaw et al. (2015) to characterize demands in splices and develop the loading protocols for testing the full-scale specimens of column splices. The 4-, 9-, and 20-story frames were subjected to a suite of 20 ground motions based on recordings from the 1994 Northridge, 1995 Kobe, 1989 Loma Prieta, and the 1974 Tabas earthquake, in addition to simulated motions. The ground motions were scaled to match the spectra at 10% and 2% probability of exceedance in 50 years. Some salient features of the modeling strategy used are: (1) use of fiber sections for beam-column to capture axial-moment interaction and spread of plasticity in a more sophisticated manner, (2)

finite joint sizes as the demands at splice are sensitive to the distance from ends of column, and (3) geometric non-linearity effects were modelled. The stress in the extreme fiber of the smaller connected column at the splice location was monitored and reported after normalizing with the yield strength of flange material (i.e., σ_{max}/σ_y). This value is the same as interaction ratio (IR) given by Shen et al. (2010). A summary of the IR for the different buildings along with the maximum interstory drift ratio (MIDR) is given in Table A-10. The maximum values fall in similar range to those given by Shen et al. (2010). It is important to note that the maximum demands are generally observed in the exterior columns which can be ascribed to a combination of net axial tension due to large overturning moments, and higher mode effects that result in single curvature bending of the columns.

Although the buildings used in this study and by Shen et al. (2010) were designed based on post-Northridge considerations, the demands in column splices are a fair representation of those in pre-Northridge buildings. This can be ascribed to similar global response and member force demands in pre-Northridge and post-Northridge frames (Gupta and Krawinkler, 1999). The significant differences between the two are limited only to local moment distribution in the beam and beam column connections, owing to detailing such as the use of reduced beam sections or local flange reinforcements.

Table A-10 Summary of Seismic Response (Shaw et al. 2015)

Hazard level	Building Type	Median IR_{peak}	Max IR_{peak}[a]	Median *MIDR*	Max *MIDR*[b]
10% PE in 50 years	4-story	0.16	0.30 (3E)	1.10%	2.9% (2)
	9-story	0.11	0.30 (2E)	0.80%	1.6% (3)
	20-story	0.18	0.72 (5E)	0.60%	1.5%(16)
2% PE in 50 years	4-story	0.3	0.54 (3E)	2.40%	6.1% (2)
	9-story	0.23	0.72 (2I)	2.00%	5.4% (4)
	20-story	0.22	0.95 (5E)	1.10%	2.5%(2)

[a] Value in parentheses indicate location of occurrence of IR_{peak} (e.g., "3E" indicates 3rd story exterior column while "2I" indicated the 2nd story interior column).

[b] Value in parentheses indicates location of occurrence of IDR_{peak} (e.g., "4" indicates 4th story).

Galasso et al. (2015)

Galasso et al. (2015) assessed the performance of the 4- and 20-story frame buildings, used in the previous studies, in a probabilistic manner to characterize the seismic demands in the column splices and determine the annual probability of fracture of splices in the buildings. With the modelling strategy same as Shaw et al. (2015b), Probabilistic Seismic Demand Models (PSDM) of the maximum tensile stress in the smaller connected column, σ_D, and spectral acceleration, S_a, as Intensity

Measure were generated using Incremental Dynamic Analysis (IDA). The far field ground motion set of FEMA P-695 (FEMA, 2009) were used. The IDA curves for the splice in exterior column on 5th floor of the 20-story frame and for the splice in interior column on 4th floor of the 4-story frame is shown in Figure A-19. The stress demands increase rapidly at low intensities and then saturate at higher intensities. The saturation suggests that yielding the beams (formation of plastic hinge at beam-to-column connection) at higher intensities limits the maximum stress in splices which prevents inelastic deformations at splice location. These demands are used to generate fragility functions for the splices, with the capacity value obtained from splice capacity equations developed by Stillmaker et al. (2015) considering a CVN of 10 ft-lb and a penetration ratio of 50% in the PJP welds (typical of pre-Northridge splice connection). A temperature for the CVN value was not specified and instead the dynamic toughness capacity, K_{Id} obtained from Barsom's lower shelf lower bound relationship was conservatively used as the static toughness capacity, J_{Ic} or K_{Ic}. The following points based on the fragility functions (See Figure A-20) developed by Galasso et al., are especially concerning:

1. For the 4-story frame (fundamental time period of 0.93s), at design level S_a (= 0.67g), the fracture probability of the splices in exterior column is as high as 70% and the corresponding value for the interior splices is 10%. Even when a toughness of 20 ft-lb is considered for capacity calculation, the fracture probability is 30%.

2. For the 20-story frame (fundamental time period of 2.33s), at design level S_a (= 0.26g), the fracture probability of the splices in the exterior column approaches 100% and the corresponding value for interior splices is 50%. For an increased toughness of 20 ft-lb, the fracture probability in the exterior splices is same and reduces to 20% for interior splices.

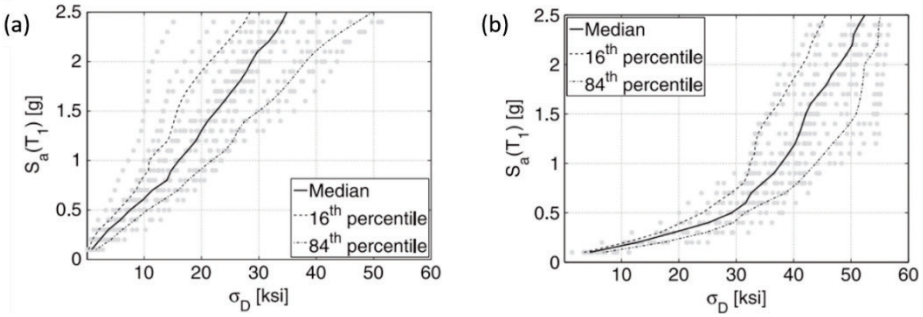

(a) interior splice on 4th floor of 4-story frame

(b) exterior splice on 5th floor of 20-story frame

Figure A-19 IDA results in terms of stress demands at splice location (Galasso et al., 2015).

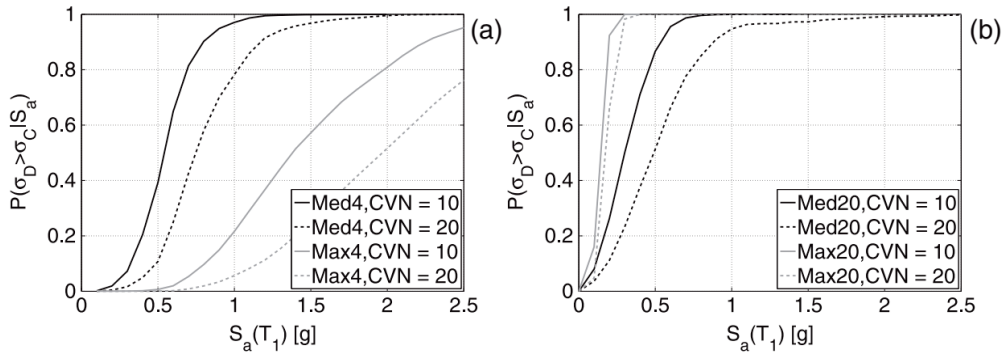

Figure A-20 Fracture fragility functions for (a) 4-story frame splices and (b) 20-story building splices (Galasso et al., 2015).

Convoluting the fragility functions with the seismic hazard data, the annual fracture risk is reported. The return periods for fracture of various splices are generally low across all splices and frames. A summary of the return period of fracture is presented in Table A-11. Except for the interior splices in the 4-story frame, the return periods are significantly lower than the return period of the design earthquake (475 years). The return periods are expectedly higher for the higher CVN, but not greater than 475 years. The disaggregation of the risk, shown in Figure A-21, revealed that the motions with lower intensity (and thus lower return periods) contributed disproportionately to the risk of fracture because they produced demands that are not significantly lower as compared with motions with higher intensity. Nearly half of fracture probability was attributed to S_a values lower than the design S_a (marked with dashed lines in the figure). This exacerbates the concern of fracture criticality of the pre-Northridge splices.

Table A-11 Return Period for Fracture in Selected Splices of 4-Story and 20-Story Frame (Galasso et al., 2015)

	4-story frame		20-story frame	
CVN	*Interior splice*	*Exterior splice*	*Interior splice*	*Exterior splice*
10 ft-lb	417 years	75 years	156 years	87 years
20 ft-lb	909 years	137 years	270 years	103 years

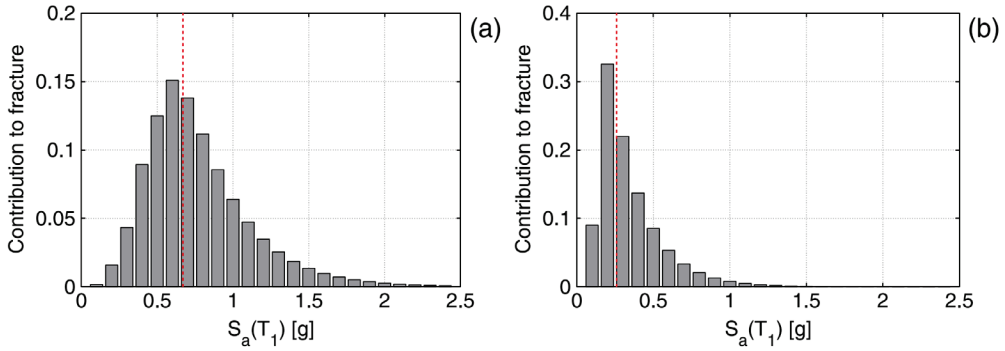

Figure A-21 Distribution of S_a values contributing to annual fracture risk: (a) interior splice of 4-story frame and (b) exterior splice of 20-story frame (Galasso et al., 2015).

Song et al. (2020)

The study by Galasso et al. (2015) did not consider the effect of vertical ground motions on the fracture risk of the splices and used deterministic values of splice capacity based on the FEFM simulations. These issues were addressed in the recent study by Song et al. (2020). An advanced IM similar to geometric mean of S_a values at different time periods with spectral shape correction was used to account for the significant contribution in stress demands at splice location due to involvement of higher mode response. It was observed that the difference in fragility functions with variability in splice capacity and deterministic splice capacity is negligible. However, the former increased the dispersion around mean functions by about 10% which could be significant when determining design equations based on reliability analysis. On comparing fracture fragilities with and without vertical ground motion (Scenario 1 and 2 respectively), higher fracture fragility of 4-story frame was observed in Scenario 1 while the 20-story frame showed higher susceptibility to fracture in both scenarios (fractures at lower intensity). Accounting for the vertical components simultaneously with the corresponding horizontal components of ground motions increases the fracture fragility, through an increase of the peak tensile stress. If the amplitudes of the ground-motion vertical components are comparable to their horizontal components, a significant increase in fracture fragility can be observed.

It is important to emphasize that fracture at splice does not necessarily imply immediate collapse or loss of safety, which is dependent on several factors, including the redundancy in lateral load resisting system and characteristics of the ground motion. The ‘fracture probability of the splices’ is reported and not the ‘collapse probability of the building’ in the studies discussed. The frame models used do not explicitly model the splice fracture and the post-fracture behavior. The effect of splice fracture on demands in other elements and change in overall global response are needed to be evaluated, using sophisticated modelling strategies, to understand the collapse probability of the entire system.

Case Studies on Remediation of Existing Buildings

Case study on remediation of two steel buildings: one mid-rise and one high-rise by Forell/Elsesser Engineers (Nudel et al., 2013, 2015) and a 25-story building constructed in 1985 by Degenkolb Engineers (Chisholm et al., 2017) indicate similar high demands in column splices. The maximum stress level at splice locations in the upper (smaller) column flange, based on NLTHA, exceeded 75% of the yield stress of the flange. The high demands combined with low penetration PJP and low toughness weld necessitated extensive retrofit which involved replacing the PJP welds with CJP welds with minimum specified toughness.

ASCE/SEI 41, *Seismic Evaluation and Retrofit of Existing Buildings*

The ASCE/SEI 41 (ASCE, 2017) three-tiered approach for seismic performance evaluation of existing and retrofitted buildings is widely adopted in the industry. A simplified Tier 1 screening evaluation is required for simple buildings and a systematic Tier 3 evaluation is required for more complex buildings. The basic performance objective for existing structures recommended by ASCE/SEI 41 requires the building to meet the Life Safety performance level. However, the guideline requires the column splices to develop the full strength of the smaller connected column only when the target performance objective is Immediate Occupancy. Most low- to mid-rise steel buildings with regular configuration, even in high seismic zones, qualify for the simplified Tier 1 screening with a target performance objective of Collapse Prevention. This may cause the splices to be overlooked as a potential deficiency. Even when a Tier 3 evaluation is performed, the use of linear-elastic analysis may underestimate the demands in column splices. Thus, more stringent requirements to flag the splices of the pre-Northridge era as critical are required.

A.5.2 Post-Fracture Response and Modeling Strategies

Simulating post-fracture response in welded beam-to-column connections may be accomplished by representing the connection moment-rotation relation (with residual capacity at fracture moment) by a rotational spring at end of the beam element as the shear load carrying capacity is usually not influenced by fracture and the axial load–moment interaction is negligible (Rodgers and Mahin, 2006). A similar strategy using axial springs is often adopted in modeling brittle fracture in brace to gusset connection in braced frames (Hsiao et al., 2014). Simulating post-fracture response in WCS is much more challenging in general, because of various complex physical phenomena – these include the loss of shear capacity after fracture (if the section is completely severed), as well as loss of tensile capacity and issues such as gapping and reseating (possibly in an imperfect manner) under seismic shaking.

As discussed in previous sections, the high likelihood of splice fracture implies that a large majority of splices in pre-Northridge SMRFs require retrofit for compliance with current performance standards. This, however, is based on the assumptions that WCS fracture eventually will lead to undermining the collapse safety of the building. Stillmaker et al. (2017) examined the effect of splice fractures on the seismic response of pre-Northridge frames used in previous studies, in a probabilistic and performance-based engineering framework. The modeling strategy was same as previous studies (Galasso et al., 2015; Shaw et al., 2015) except that splice fracture was modelled explicitly within the constraints of frame-based analysis. The splices were modelled as a beam-to-column frame element of small length. In the cross-section of the element, all fibers were assigned a constitutive model that can replicate the response associated with fracture. The characteristics of the constitutive model are:

- Elastic response in tension until the fracture stress, $\sigma_{fracture}$ is reached. The fracture stress is determined based on the splice capacity equations developed by Stillmaker et al. (2015) considering a K_{Ic} of 38.1 ksi$\sqrt{}$in and a penetration ratio of 50% in the PJP welds (typical of pre-Northridge splice connection). For various splices, $\sigma_{fracture}$ lied in the range of 8.6-25.7 ksi.
- After $\sigma_{fracture}$ is reached in tension, material stress capacity in tension is reduced to zero.
- In compression, the model is elastic up to the expected yield strength, and then hardens indefinitely with a slope 5% of the elastic modulus. It is assumed that the column effectively re-seats, and compressive behavior is unaffected by tension fracture.

The above constitutive model was constructed in OpenSEES (McKenna et al., 2000) by arranging already available material models in series and parallel as shown in Figure A-22. This manner of simulating fracture can simulate "snap-back," wherein the strain returns elastically to zero after fracture, and then increases back up to the applied strain eliminating spurious dissipation. The behavior was modeled at the fiber level, so a splice does not necessarily lose tensile capacity across the entire cross section simultaneously, thus capturing partial fracture of the section. Similar modeling strategy was used by Hall (1998) to primarily study the influence of beam-to-column connection fracture in a custom-built software for analysis. It is important to note that the model can simulate axial gapping (separation) of the column, as well as flexural loss of strength post fracture. However, it cannot directly simulate the loss of shear strength at the splice location, although it does reduce the lateral stiffness of the columns due to introduction of the hinge within the column but at a singular location in the splice element depending on how the model numerically converges. So, the assumptions hold true when – (1) the splices do not fracture completely and (2) splices fracture completely but the relative shear deformations are restricted at

splices (through details as such as full depth web plates welded to one of the connected columns).

Under these highly specific scenarios of no shear loss post-fracture, it was found that splice fracture led to onset of rocking deformations in the portion of the frame above the splice fracture, thus improving the global performance. As more splices fractured, the rocking deformations increased and improved the MIDR performance by mobilizing rotational inertia of rotating body like many passive structural control systems. The results, although counter-intuitive, suggest that a complete retrofit of the splices might not always be necessary. Details that restrain unseating or loss of shear capacity of the column (e.g., through guiding plates on the flanges or a bolted web plate may be deemed sufficient depending on the rigorous NLTHA in performance-based engineering framework of the concerned building).

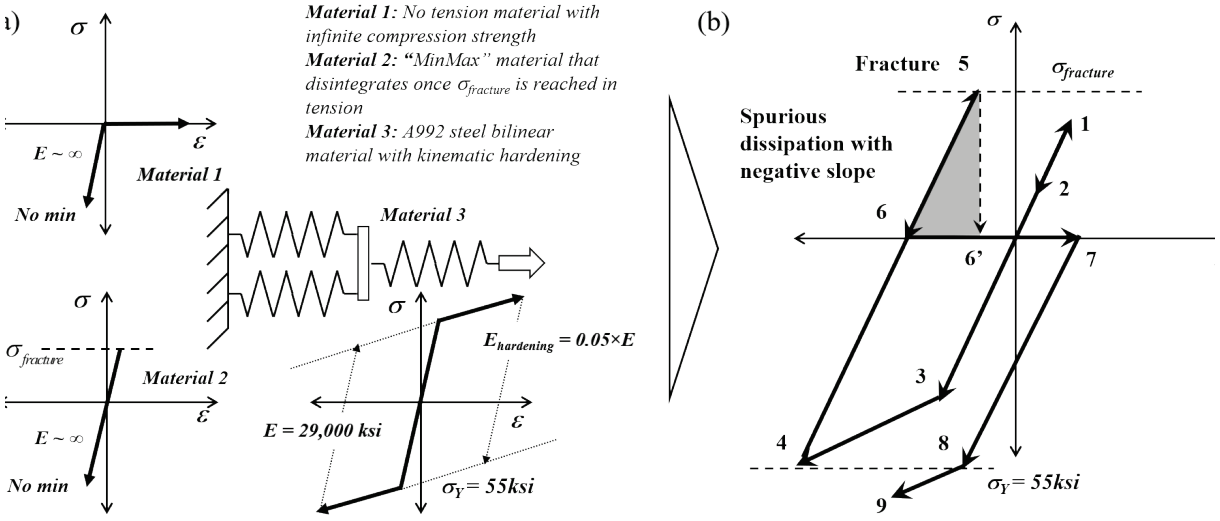

Figure A-22 Constitutive material model for simulating fracture and post fracture response: (a) construction of model using series and parallel springs in OpenSEES, (b) resultant response. (Stillmaker et al., 2017).

The study, despite having its limitations, provides a foundation to develop more rigorous splice element in a frame-element based framework. Based on the challenges posited in modelling shear loss in frame element framework, NIST GCR 17-917-46v2 (NIST, 2017) recommends using the fiber-based element approach used in the study for simulating post fracture behavior.

> *The upper (or smaller) connected column may be modeled in a manner similar to the lower column, with the exception that the tension behavior in the flanges (at the splice location) is defined with a fracture stress σ_{cr} from Eq. A-7. If the stress is calculated in this manner, the width and thickness of the flange in the fiber model should reflect the dimensions of the flange without consideration of the weld flaw or effective throat. Tension behavior in the web may be represented similarly (i.e., using Eq. A-7, and the web thickness, instead of the flange*

thickness) if the web splice is a partial joint penetration (PJP) weld. If the web splice is bolted, then the web fibers may be simulated to reflect load deformation response of the bolts. For both the flange and the web, the compression behavior is defined by the base material.

(Note: *Eq. A-7* referenced in the excerpt is provided as Equation A-15 in this appendix.)

To overcome the inadequacy of the previously discussed approach in modelling of shear loss and inability to reseat in compression (especially in a 3D analysis), modelling strategies from other domains of structural engineering can be investigated and scrutinized for applicability. One such method is the element removal technique to simulate progressive collapse in reinforced concrete structures (Talaat and Mosalam, 2009). Here, the damage level associated with the reinforced concrete frame element is monitored at each step and once damage exceeds the specified index, the element removal procedure is summoned, and the contribution of the element and associated forces is not considered from the next analysis step. This strategy is also adopted in modeling collapse of unreinforced masonry walls where the in-plane and out-of-plane interaction diagram is considered as an element removal trigger (Kadysiewski and Mosalam, 2009). This method is available in the current version of OpenSEES. A similar approach can be used to model splice fracture when considering no reseating of the upper column on the lower column (i.e., no forces are transferred through the splice post-fracture).

A more sophisticated approach to model the shear loss, post fracture, when the column is in tension is the use of non-local approach. Non-local approach is widely used to regularize the softening problem by introduction of a length scale where the mesh dependence is high (Kolwankar et al., 2017; Wu and Wang, 2010). For modeling the shear loss, the fracture trigger at any fiber in a cross-section of splice element should trigger fracture at the same fiber locations in all other cross-sections (i.e., the integration points) of the element. This would create hinges at both extremities of the element when the section is completely fractured and in tension, rather than at a singular location, thus preventing any transfer of shear.

A.5.3 Knowledge Gaps

- All of the studies that characterized demands and fracture risk of the pre-Northridge WCS did not consider the effect of fracture in the un-retrofitted pre-Northridge beam-to-column connections or the degrading cyclic behavior of the retrofitted beam-to-column connections (e.g., reduced beam section), which can lead to significant deviations in outcomes. Moreover, 3D simulations are needed to quantify the stress demands due to biaxial bending that may be of consequence, especially in corner columns.

- Approaches that simulate various physical phenomena that occur after splice fracture need to be developed and implemented in commercially available or open-source software architecture to inform more accurate risk-based decision support frameworks for splice retrofit. These phenomena include more accurate characterization of post-fracture response, including the effects of shear loss and reseating and impact in compression.

A.6 Retrofit Strategies

FEMA 352 (FEMA, 2000c) recommends using the vee-and-weld procedure to repair any fractures that are detected in the welded column splices. The vee-and-weld procedure has for long been a method of weld repair for long and through-thickness cracks in steel bridges (FHWA, 2013). The weld material is removed along the crack length, through three-quarter the thickness of the flange in the shape of a U. The U-shaped groove is then filled with weld metal and the process is repeated on the other side of the flange if CJP weld is to be provided as shown in Figure A-23. Alternatively, if the column loads are safely resisted with the entire section of column flange removed, or if suitable shoring is provided, it is recommended to use a single bevel weld.

Due to lack of guidance on the required level of retrofit to assure adequacy of the pre-Northridge PJP column splices, the dominant retrofit practice is to replace the PJP welds with double beveled CJPs. This is challenging for numerous reasons (Chisholm et al., 2017; Nudel et al., 2013, 2015):

1. If the contact in the flanges after making the V shaped bevel from one side is not sufficient to carry the gravity load, which is at times the case for bottom story splices in tall buildings, the removal of material requires temporary shoring. This usually entails a temporary shutdown of building operations to ensure safety.
2. Replacing the PJP weld with a CJP weld requires creation of cope holes in the web to allow complete gouging. Flame cut web cope holes, if not ground smooth, often result in locally poor toughness due to martensite transformation and are susceptible to crack initiation due to stress concentration due to subsequent welding.
3. Access from all sides of the column is required to successfully perform the through-thickness replacement operation. The columns are usually covered from at least one side with concrete panels or façade which makes the task time consuming if not difficult.

To address issue (3), the façade/ panels must be removed, which is difficult in exterior columns. For a retrofit project in San Francisco, an access window was cut out in the column web at splice location to access the inaccessible part of the flange (Chisholm et al., 2017). This allowed access to the unwelded portion of the original

PJP-welded column flange. The unwelded portion of the flange was gouged in V shape, penetrating sufficiently into the existing weld. This groove was then filled with the weld filler material with minimum specified toughness. This resembled a double beveled CJP with the outside bevels filled with original E70T-4 weld filler material and the inside filled with filler material that had minimum specified toughness. The detail of the procedure is shown in Figure A-24. The removal of web at splice location along with partial flange due to gouging, necessitated the use of shoring. Permanent shoring splints, designed to supplement the removed portions of the cross-section, were added in the 4-inch gap between column flanges and façade as shown in Figure A-25. It is important to note that any retrofit operation involving arc air gouging and new weld deposition entails probable issues of distortion, stress concentration and strength reduction of the column flange material which needs to be accounted for during performance assessment of the repaired structure.

Another technique to repair through-thickness cracks is attaching cover plates to the inside (as well as outside) of column flanges using welding or high-strength bolts as shown in Figure A-26. These plates add material to the column flanges, thus reducing the stress in the flanges. They also provide continuity in the section in case of fracture. This system is widely used to splice bridge girders on-site.

Some of the retrofitted welded column splices of the buildings damaged in the Kobe earthquake are shown in Figure A-27 to Figure A-29 (AIJ, 1995). The columns in these images are made of cold formed steel hollow square sections. In Figure A-27, vertical ribs (fin plates) were welded to the fractured splice to achieve continuity of the section. In Figure A-28, splice plates were welded on all four sides of the column to repair the column splice. Figure A-29 shows retrofitting of a splice fracture that led to a separation of 28 cm (11 in.) between the two connected columns. The two columns were connected in the misaligned position by welding wide flange studs with stiffened angle connection.

An alternate approach is to develop details that arrest crack propagation like those used in bridge applications (Connor and Lloyd, 2017). For example, a dog bone detail directly in line with the PJP welds, as shown in Figure A-30, to ensure crack arrest in webs may be provided. These kinds of repair do not add any strength or continuity to the section and should be used only if the adequacy of the remaining section, after crack arrest, can be established.

A.6.1 Knowledge Gaps

- Complete replacement of the PJP welds with CJP welds is a complex and costly process with the possibility of severe disruptions to building operability. Consequently, a robust decision support framework is required to balance the trade-offs of splice retrofit versus non-intervention in a risk-based manner. This framework requires (1) accurate assessment of the fracture potential of existing

splices, (2) assessment of building response assuming splice fracture, and (3) quantitative characterization of the efficacy of various retrofit strategies.

- Previous sections (see Sections A.2.2 and A.5.2) suggest that there is limited progress in the former two areas, but there is essentially no research on retrofit strategies. Without this research, it is not possible to make informed decisions regarding the cost-benefit of retrofit. This is a major knowledge gap that needs to be addressed using elaborate analytical and experimental studies. In addition to the characterization of the efficacy, various secondary effects of each retrofit technique such as mixing of weld materials, distortion, stress concentration, and strength reduction are required to be studied.

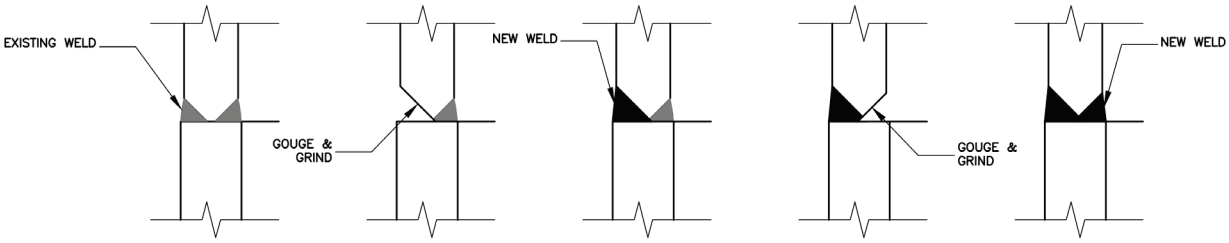

Figure A-23 Vee-and-weld procedure for complete replacement of double bevel PJP with CJP.

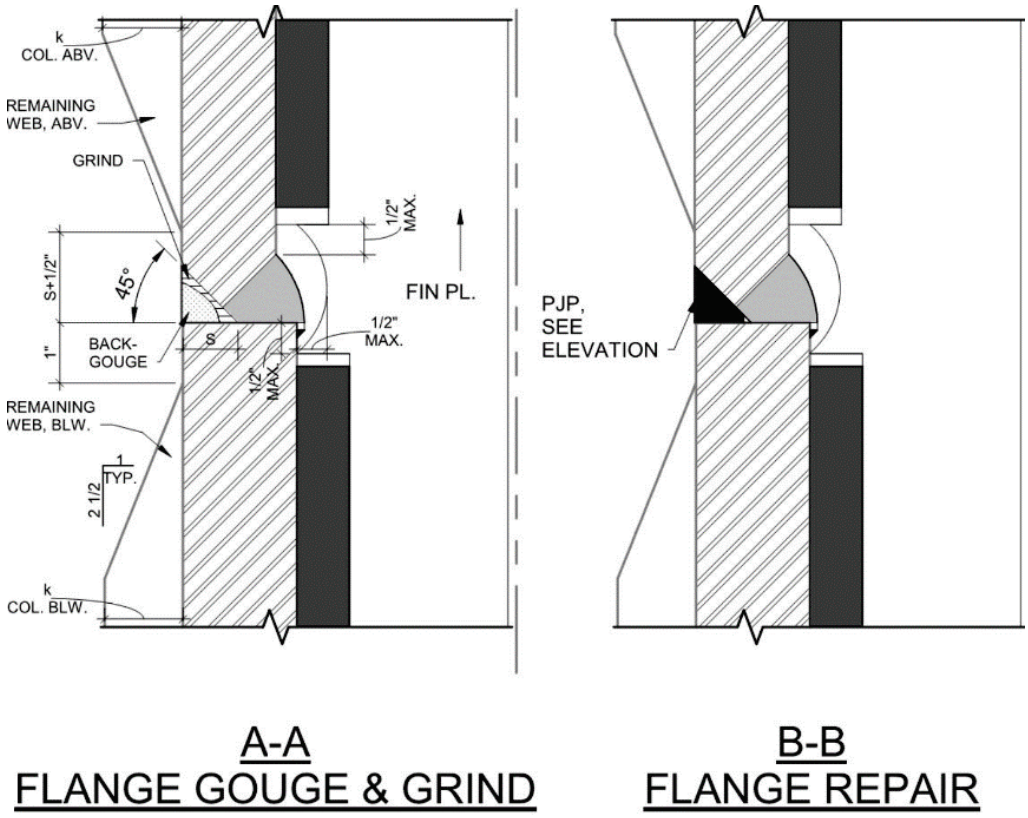

Figure A-24 Gouging of flange and re-welding (Chisholm et al., 2017).

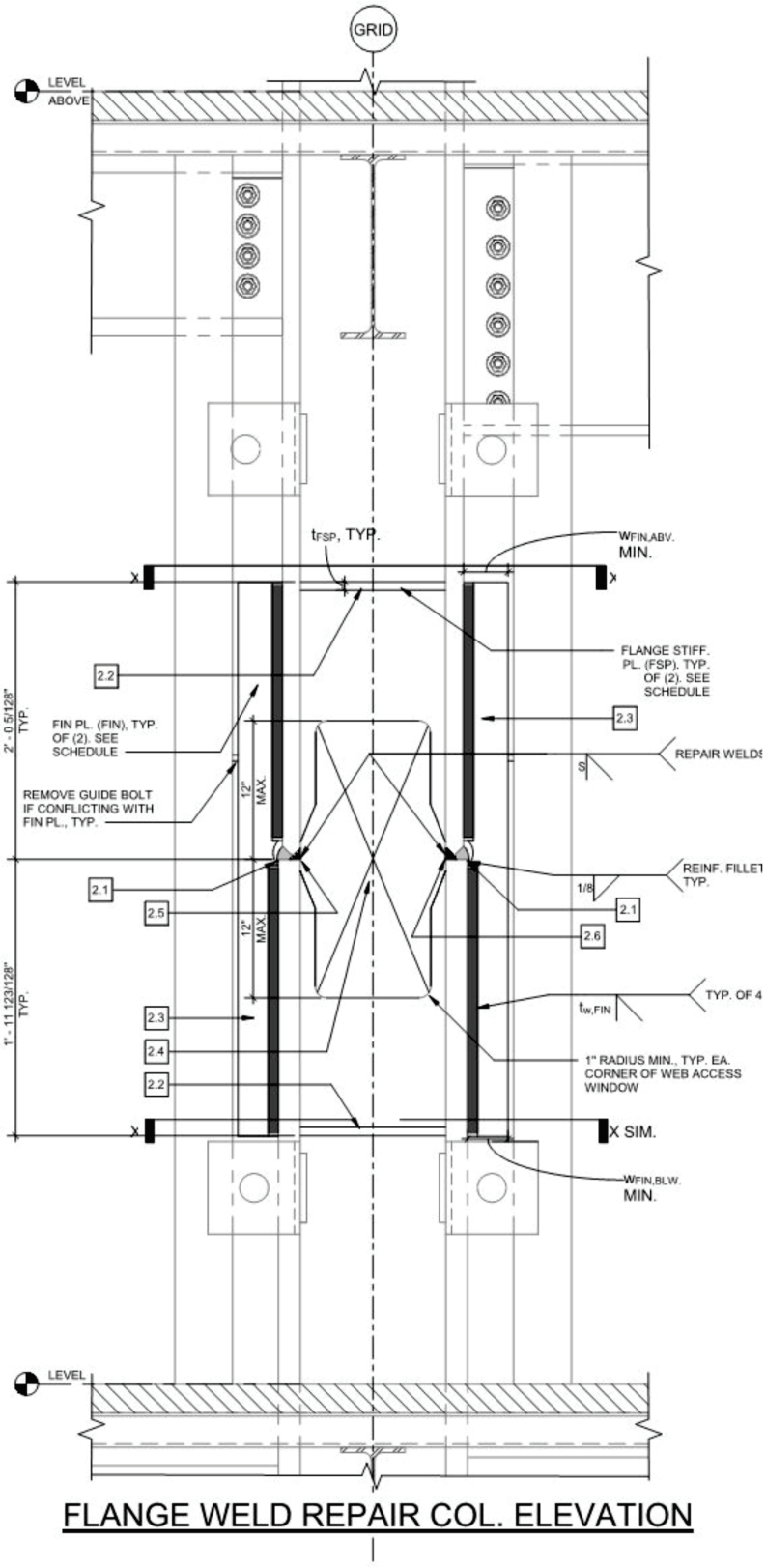

Figure A-25 Column splice retrofit detail showing access hole in web (Chisholm et al., 2017).

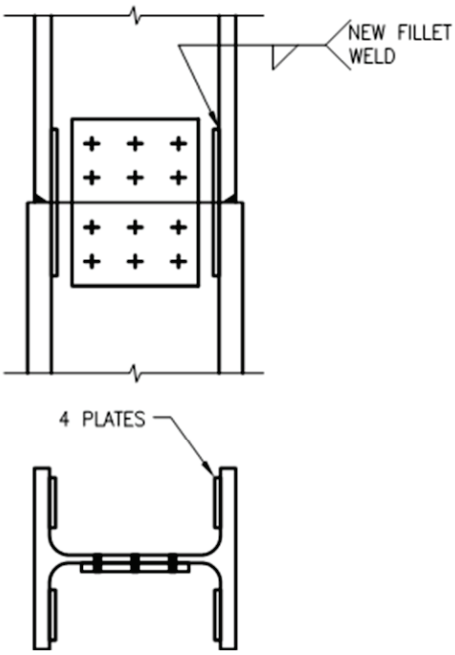

Figure A-26 Addition of doubler or splice plates to column flanges (Nudel et al., 2015).

Figure A-27 Retrofit of fractured CJP WCS using welded vertical ribs (AIJ, 1995).

Figure A-28 Retrofit of fractured CJP WCS by welding splice plates on all flanges (AIJ, 1995).

Figure A-29 Retrofit of fractured CJP WCS by welding wide flange studs with stiffened base plates (AIJ, 1995).

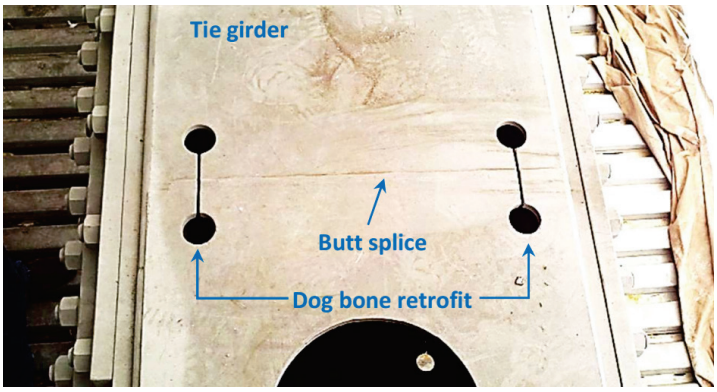

Figure A-30 Dog bone retrofit of butt weld (CJP) on the web of a tie girder (Connor and Lloyd, 2017).

Appendix B
Literature Review for Panel Zones

B.1 Introduction

Panel zones are integral components to moment frame systems acting to transfer the beam end moments to the columns (Figure B-1). This zone is the portion of the column between the beam flange elevations. Figure B-2(a) shows an idealized moment diagram between inflection points of the beams and columns for a moment frame system subjected to a lateral force pattern. When the finite size of the panel zone is considered, the moment diagram transitions over the height of the panel zone instead of instantaneously at the working point of the frame (Figure B-2(b)). This high moment gradient is accomplished by a high shear force in the panel zone (Figure B-2(c)). This diagram is made by the common assumption that the beam end moments can be resolved into a force couple between the centers of the beam flanges, resulting in a constant panel zone shear over the depth of the panel.

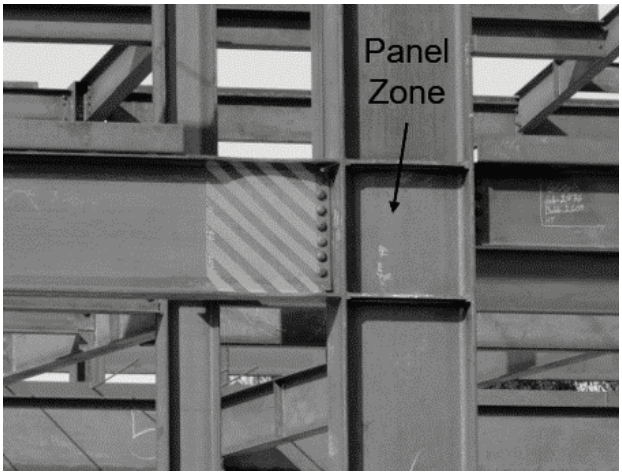

Figure B-1 Panel zone in a moment connection.

The high shear forces that exist in the column between the beam flange force couple may require reinforcing of the column web. This was traditionally done through the installation of an inclined plate between corners of the panel zone or through a plate that sisters the column web. The latter doubler plate which doubles up the column web thickness and reinforces its shear strength is the common method to reinforce the panel zone for seismic applications. Additionally, resisting the concentrated beam flange forces may require local stiffening details to prevent the exceedance of a column limit state, for example, web local yielding or flange local bending. This

reinforcing is provided through continuity plates, which are stiffener plates aligned with the beam flanges to provide continuity to the beam flanges.

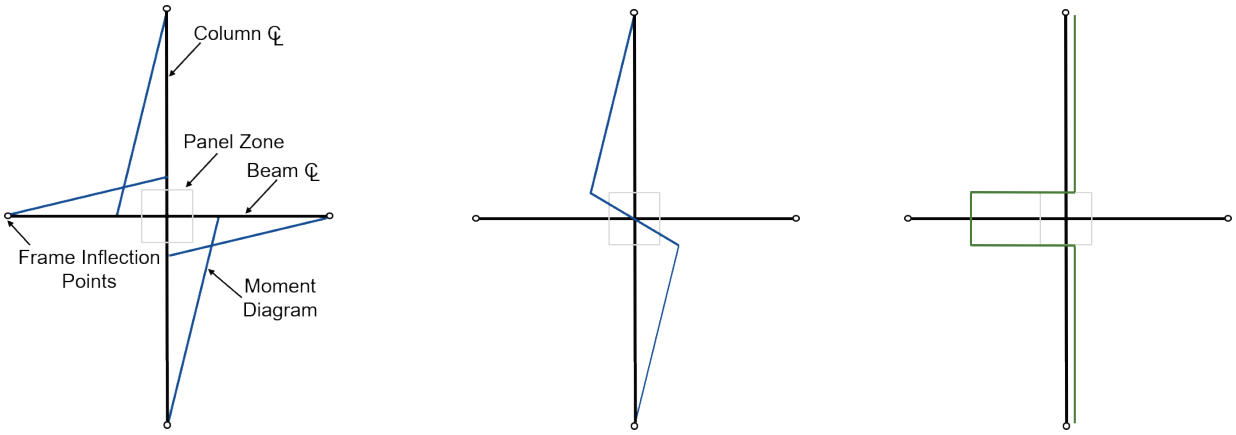

(a) Idealized moment diagram (b) Column moment diagram (c) Column shear diagram

Figure B-2 Frame moment and shear diagrams.

The design requirements of panel zones developed over the last five decades resulted in scenarios that can cause significant panel zone yielding when subjected to a seismic demand. When the majority of the inelastic behavior is anticipated in the panel zone such that it becomes the primary ductile mechanism, it is called a *weak* panel zone. This is contrasted to a *strong* panel zone which uses the flexural hinging in the beam as the primary source of ductility. There are merits to both philosophies, which has given rise to the concept of a *balanced* panel zone which distributes the ductility demands between the beam and panel zone. The column deformations associated with weak panel zones may impose significant secondary demands on the fracture-sensitive beam flange-to-column flange CJP welds. A strong panel zone, on the other hand imposes all of the deformation demands to the beams, imposes a larger primary force on the CJP weld. This literature review summarizes the design requirements and available research on weak panel zones, implications of their use, and identifies gaps in the current knowledge base.

B.2 Historical Development of Panel Zone Design Provisions

This section discusses the historical development of the design requirements of panel zones for seismic application of steel moment frames. In the early 1970s, engineers started to use a connection type known today as the welded unreinforced flange-bolted web connection, or WUF-B (Figure B-1). Prior to that, gusseted connections with (riveted) built-up beams and columns or I-shaped members with bolted seat angles were used (NIST, 2016). This code review is based on the former construction type.

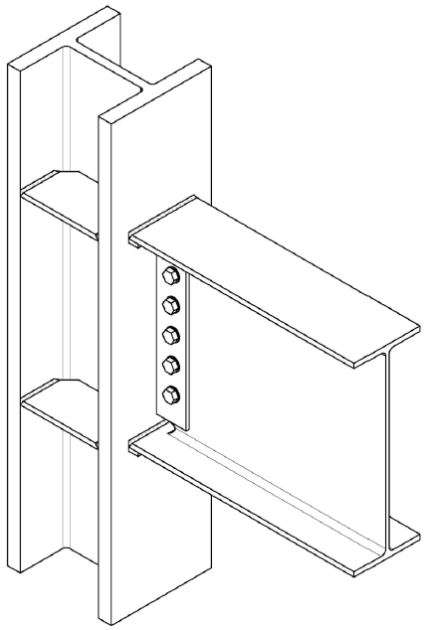

Figure B-3 Welded unreinforced flange – bolted web connection (NIST, 2016).

B.2.1 Design Practice Prior to 1988 UBC

Prior to the 1988 Uniform Building Code (UBC), design requirements on panel zones were limited. For example, the 1985 UBC states the following in Section 2722(d) for steel ductile moment-resisting space frames in high seismic regions:

> *"Connections: Each beam or girder moment connection to a column shall be capable of developing in the beam the full plastic capacity of the beam or girder.*
>
> *Exception: The connection need not develop the full plastic capacity of the beam, or girder if it can be shown that adequately ductile joint displacement capacity is provided with a lesser connection."*

Although the design requirement is very limited, design engineers during that era quite often would follow the *Recommended Lateral Force Requirements and Commentary* ("Blue Book") published by SEAOC. The Commentary in the 1980 edition (SEAOC, 1980) suggested the following procedure for computing the required panel zone shear for allowable stress design:

$$V_w = \frac{M_{p1}}{0.95d_1} + \frac{M_{p2}}{0.95d_2} - V_{cw} = \sum \frac{M_{pi}}{0.95d_i} - V_{cw} \qquad \text{(B-1)}$$

where the column shear, V_{cw}, nortuals $(M_{p1} + M_{p2})/H_c$, with H_c being the effective story height.

According to Teal (1975), however, another common practice at the time was to use the earthquake load-produced beam moment (M_{Ei}), not the full beam plastic moment in Equation B-1, to compute the required panel zone shear:

$$V_w = \sum \frac{M_{Ei}}{0.95 d_i} - V_{cw} \tag{B-2}$$

Note that the prescribed design earthquake forces for computing M_{Ei} was for allowable stress design; this seismic force level was approximately two thirds of that required for strength design. The panel zone design strength was computed as $0.4F_v(d_c t_w)$ (1.33), where the allowable shear stress is increased by the 1.33 factor for earthquake load combinations. Since full plastic moment of the beam is not used in computing the required panel zone shear, this design practice is likely to produce a weak panel zone.

B.2.2 1988 UBC

The prescribed seismic forces (E) based on a Response Modification Factor R_w (= 12 for SMF) was used for Allowable Stress Design (ASD), where the basic seismic load combination ($D + L + E$) was used to design panel zones. It was stated that the panel zone shall be capable of resisting the shear induced by beam bending moments due to gravity loads plus 1.85 times the prescribed seismic forces, but the shear strength need not exceed that required to develop $0.8\sum M_p$ of the girders framing into the column flanges at the connection with an implicit resistance factor (ϕ) of 1.0. The required panel zone shear strength is:

$$V_u = 1.85\left[\frac{\Delta M_w}{\left(d_b - t_{bf}\right)}\right] \le \frac{0.8\sum M_p}{\left(d_b - t_{bf}\right)} \tag{B-3}$$

where ΔM_w is the unbalanced moment of the beam(s) framing into the column, determined based on the basic seismic load combinations for the R_w-based ASD. According to the commentary of the SEAOC Recommendations (SEAOC, 1988), the 1.85 factor represents a compromise of two schools of thoughts as the average between 2.0 and 1.7. Note that the unbalanced moment for computing the required shear strength has an upper bound value of $0.8\sum M_p$ to acknowledge that, in some cases, gravity loads might inhibit the development of plastic hinges on both sides of a column. Later research would find that the 80% upper limit applied to the beam moments is unconservative for many exterior connections in steel moment frames and systems which use only a few bays of moment frames such that the gravity load on the beams is minor compared to the lateral forces carried by the system (El-Tawil, 2000). The design shear strength of the connection was given by the following formula (Krawinkler, 1978):

$$V_n = 0.55F_y d_c t\left[1 + \frac{3b_c t_{cf}^2}{d_b d_{bc} t}\right] \quad \text{(B-4)}$$

B.2.3 1990 AISC Seismic Provisions

The 1990 AISC *Seismic Provisions* were based on the UBC prescribed seismic forces for ASD, but were adjusted with a seismic load factor of 1.5 with the following basic seismic load combination for strength design of panel zones:

$$1.2D + 0.5L + 1.5E \quad \text{(B-5)}$$

Like the UBC, these provisions did not use the concept of "horizontal seismic load effect including overstrength" for panel zone design. Equation B-4 was used as the panel zone strength. In order to match the same panel zone design as that produced from 1988 UBC, however, a seismic resistance factor of 0.8 was introduced from the following calibration for the design strength of panel zone, ϕV_n:

$$\phi = 1.5/1.85 = 0.8 \quad \text{(B-6)}$$

B.2.4 1992 AISC Seismic Provisions

The 1992 AISC *Seismic Provisions* based the determination of the prescribed seismic forces on the 1991 NEHRP Recommended Provisions instead of UBC (FEMA, 1991). Since an R factor, not R_w, was used to determine the seismic effects, the 1.5 seismic load factor was replaced by 1.0:

$$1.2D + 0.5L + 1.0E \quad \text{(B-7)}$$

Expressing in a way similar to Equation B-3, the required design shear is:

$$V_u = \frac{\Delta M}{\left(d_b - t_{bf}\right)} \le \frac{0.9\sum M_p}{\left(d_b - t_{bf}\right)} \quad \text{(B-8)}$$

The design shear strength of the panel zone was first introduced in the 1993 AISC LRFD Specification, with $\phi = 0.9$ and V_n similar to Equation B-4:

$$V_n = 0.6F_y d_c t\left[1 + \frac{3b_c t_{cf}^2}{d_b d_{bc} t}\right] \quad \text{(B-9)}$$

The *Provisions* used the above equation to compute V_n. To match the same panel zone design as that produced from the 1990 AISC *Seismic Provisions*, however, the resistance factor was adjusted from 0.8 to 0.75 based on the following calibration:

$$\phi = 0.8(0.55)/(0.6) = 0.73 \approx 0.75 \quad \text{(B-10)}$$

B.2.5 1997 AISC Seismic Provisions

The 1997 AISC *Seismic Provisions*, for the first time, referred to ANSI/ASCE 7-95 (ASCE, 1995) for the seismic load combination with overstrength to compute the required design shear, V_u, for the panel zones:

$$1.2D + 0.5L + 0.2S + \Omega_o Q_E \tag{B-11}$$

which is very similar to the seismic load combination with overstrength adopted in ASCE/SEI 7-16 (ASCE, 2016). The only difference is that the required panel zone design shear was capped as shown below:

$$V_u = \frac{\Delta M}{\left(d_b - t_{bf}\right)} - V_c \le \frac{0.8\sum R_y M_p}{\left(d_b - t_{bf}\right)} \tag{B-12}$$

With a value of 1.1 for R_y, the cap value is practically the same as that in Equation B-8. The Commentary provided the following justification for this upper bound V_u value:

> *"As an upper limit, the design panel-zone shear strength need not exceed that due to 80 percent of the summation of the expected plastic moments $R_y M_p$ of the beam(s) framing into the panel-zone. The factor of 80 percent is intended to recognize that because of gravity loads and the variation in inflection point locations observed in inelastic analysis, it is unlikely that the full M_p will occur on both sides of a given column at the same time. Additionally, since panel-zone yielding within limits is a relatively benign event, and since web doubler plates are expensive and contribute to possibly undesirable shrinkage, distortion and residual stress conditions, it would be too conservative to use the full summation of M_p."*

B.2.6 Supplements to 1997 AISC Seismic Provisions

Supplement No. 1 published in 1999 made a minor modification:

$$V_u = \frac{\Delta M}{\left(d_b - t_{bf}\right)} - V_c \le \frac{0.8\sum M^*_{pb}}{\left(d_b - t_{bf}\right)} \tag{B-13}$$

where $\sum M^*_{pb}$ is determined by summing the projections of the expected beam flexural strength(s) at the plastic hinge location(s) to the column centerline. Significant changes were introduced in the Supplement No. 2 published in 2000. The first major change was to not rely on the seismic load combination in Equation B-11 to compute V_u. Instead, it is to be determined from the summation of the moments at the column faces as determined by projecting the expected moments at the plastic hinge points to the column. The justification for deleting the 0.8 factor was that *"…there is no assurance that (gravity loads might inhibit the development of plastic hinges on both sides of a column) will be the case, especially for one-sided*

connections and at perimeter frames where gravity loads may be relatively very small." This change ended the practice of promoting a very weak panel zone design introduced since 1988 UBC. The second major change was that the value of ϕ in Equation B-10 was changed from 0.75 to 1.0.

B.2.7 AISC Seismic Provisions Since 2002

The 2002, 2005, 2010, and 2016 editions of AISC *Seismic Provisions* had the same requirement as that in Supplement No. 2 of 1997 edition. The panel zone design strength given as Equation B-9 is now found in the *Specifications* (AISC, 2016b) with the *Seismic Provisions* overriding the resistance factor of 0.7 in AISC 341 (AISC, 2016a) to be equal to 1.0.

B.2.8 ASCE/SEI 41: Seismic Evaluation and Retrofit of Existing Buildings

ASCE/SEI 41 (ASCE, 2017) is the standard for seismic evaluation and retrofit of building structures. Chapter 9 provides information on modeling steel structures, including pre-Northridge steel moment frames. Both linear and nonlinear procedures are provided. For the latter, beams, columns, panel zones, and beam-to-column fully restrained (FR) connections are modeled based on the generalized force-deformation relationship shown in Fig. B.4. Values of a, b, c, and the yield force Q_y are provided for each structural component. The provided parameters for beam, column, and panel zone assume that each of these three structural components would behave independently. Parameters a and b for the pre-Northridge FR connection are a function of the beam depth.

For the panel zone, the values of a, b, and c are $12\gamma_y$, $12\gamma_y$, and 1.0, respectively, which imply that the panel zone is very ductile and strength degradation will not occur up to the deformation level $12\gamma_y$. Similarly, highly ductile beams also have large ductility ($a = 9\theta_y$, $b = 11\theta_y$, and $c = 0.6$). The nonductile nature of the welded pre-Northridge connection is handled in the model of FR connections with $a = 0.051 - 0.0013d_b$ (rad), and $b = 0.043 - 0.0006d_b$ (rad), where d_b is the beam depth. (The value of a varies from 0.0276 rad for W18 beams to 0.0 rad for W36 beams.) Therefore, the FR connection model includes the effect of beam depth, but the effect of panel zone deformation on aggravating the brittle fracture of beam flange CJP welds is not reflected in the ASCE/SEI 41 modeling procedure.

Although ASCE/SEI 41 specifies large plastic deformations for the panel zone, the usable deformation capacity is actually less due to the vulnerability of low-toughness beam flange CJP welds. Based on Kim et al. (2015), ASCE/SEI 41 in its 2017 edition provides usable panel zone deformation capacities, depending on the level of notch toughness of the CJP welds.

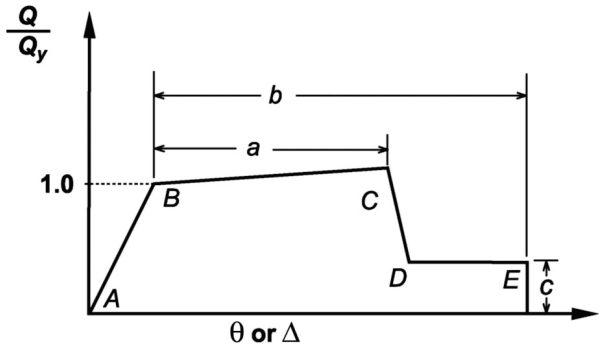

Figure B-4 Generalized force-deformation relation for steel components (ASCE, 2017).

B.3 Previous Research on Panel Zones

This section describes the previous research focusing on panel zone behavior starting from subassemblage testing during the late 1960s and early 1970s which demonstrated the strength and deformation capacities of the panel zone. A common sentiment at the time was that panel zones have significant inelastic potential, but that large shear deformations have the potential to generate high curvatures in the column flanges at the edges of the panel zone. These regions of high curvature are referred to as column *kinks* (Figure B-5) which were postulated to contribute to the eventual failure of the beam flange-to-column flange weld. Continued analysis in the 1970s worked to refine a force-displacement description that is still used in the AISC *Specifications* today. The 1980s saw continued experimentation and recommendations to increase the resolved flange forces to account for strain hardening.

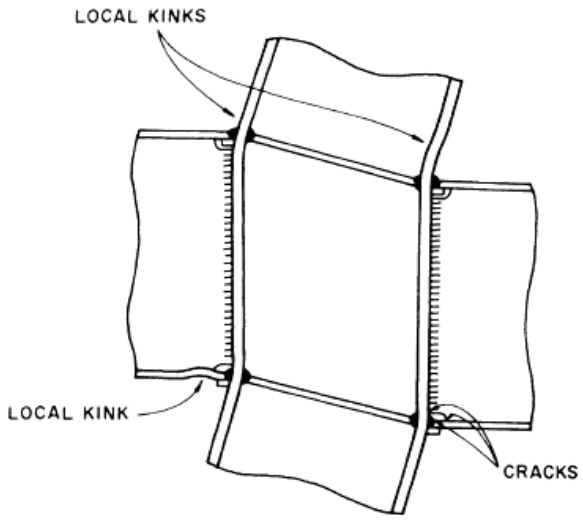

Figure B-5 Column behavior when subjected to large panel zone displacements (Krawinkler et al., 1971).

After brittle fractures were observed from the 1994 Northridge Earthquake, a significant amount of research was conducted on the behavior of moment frames as

part of the SAC Project. One of the parameters investigated during this time was the implications of a weak panel zone as it was believed to possibly be one of the root causes of the observed damage. The quantitative definition of a weak versus strong panel zone has not been consistent among researchers; however, a shared qualitative descriptor of "weak" is when the panel zone is the primary mechanism of inelastic behavior. A strong panel zone is the opposite, where the beams act as the primary mechanism of inelastic behavior. The work in this period led to substantial changes in the design of seismic moment frame connections and defines a transition between the pre-Northridge and post-Northridge type connections. Post-Northridge moment connections improve the connection by using weld electrodes with specified toughness, amended weld details, and connection parameters that have been identified to achieve at a minimum story drift angle (SDA) during testing.

During this research program and subsequent research in the early 2000s, the concept of a balanced panel zone rose to prominence. This concept was initially discussed in the 1970s as a way of spreading out the ductility demands instead of concentrating large inelastic strains on a few structural elements. The concept of a balanced connection design sought to leverage the observed stable hysteretic behavior of an inelastic panel zone combined with the benefits of a flexural beam hinge. A balanced approach can be realized by initiating yielding in the beam as a flexural hinge. When inelastically cycled, the probable plastic moment of the beam that develops through strain hardening of the flanges eventually lead to panel zone yielding. This sequence can also be reversed, achieving a balanced system by yielding the panel zone first. Several approaches that have been proposed in the literature to achieve a balanced system are discussed in this section.

This section also discusses post-Northridge analytical work applying fracture mechanics to the beam flange CJP welds to understand the observed Northridge fractures. This research found that weak panel zones negatively influenced derived fracture metrics at the beam flange CJP weld. This observation led to a stigma in the engineering community against weak panel zones. For example, the AISC *Seismic Provisions* have taken the approach that beam yielding should still be the primary source of inelastic deformation, but that limited yielding of panel zone is acceptable (AISC, 2016a). Research in the last decade has reinvestigated the issue of weak panel zones. Some of this research was performed as projects to evaluate and rehabilitate existing moment frame connections for improved seismic performance. The research shows that connections implementing some of the attributes of a post-Northridge connection with a weak panel zone have adequate to excellent performance.

B.3.1 Early Research

Fielding and Huang (1971) and Fielding et al. (1972)

Early experimental research at Lehigh University on panel zones performed by Fielding and Huang (1971) demonstrated significant deformation capacity under monotonic loading (Figure B-6). These specimens were welded with the SMAW welding process and an E7018 electrode. This testing showed that panel zone deformations were amplified when the column was exposed to a large compressive axial force. They determined that incorporating a von Mises yield criterion to amend the shear strength of the panel zone was an appropriate approach to incorporate the axial load into the strength of the panel zone. This research also defined a width-to-thickness limit of either the column web or doubler plate to preclude buckling:

$$(d_c - 2t_{cf})/(t_w) \leq 70 \quad \text{(B-14)}$$

It is noted that the beam webs of these specimens were fabricated with a welded shear tab, which is known now to improve the ductile performance of the connections versus a bolted shear tab. The researchers also derived a bilinear force-displacement relationship for the panel zone with the panel zone acting as a shear deformable element for the elastic stiffness of the panel zone and a post-elastic stiffness that incorporates the column flanges acting as cantilever elements.

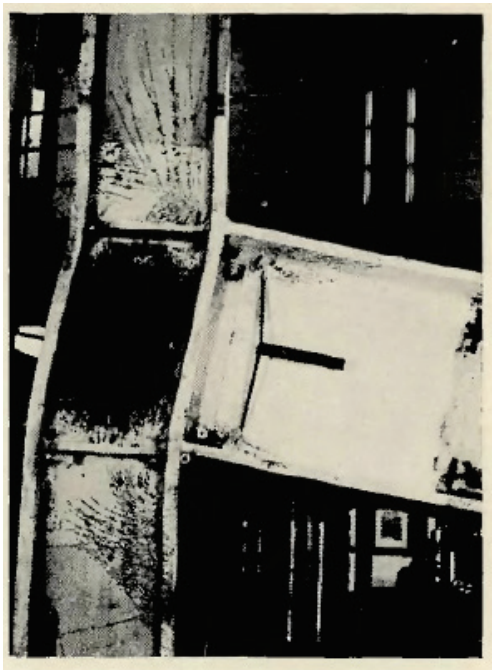

Figure B-6 Large panel zone deformation (Fielding and Huang, 1971).

Continued analytical work by Fielding et al. (1972) explored the implications of panel zone deformations. Their analysis demonstrated that connection stiffness has a significant impact on overall system strength and stiffness. Conversely, modeling the

connection as a rigid set of elements overestimates the stiffness. Their research found that modeling the panel zone regions with a rotational hinge with a specified stiffness was an appropriate methodology to model the behavior accurately.

Krawinkler et al. (1971) and Bertero et al. (1973)

Cyclical experimental testing at the University of California, Berkeley by Krawinkler et al. (1971) demonstrated significant inelastic panel zone capacity. It was not reported what welding process or electrode was used in this research program. But given the period it was likely performed with the SMAW process. These specimens also utilized a welded beam web instead of the common bolted shear tab of the typical pre-Northridge connection. The researchers mapped the deformation pattern of a panel zone and observed primarily shear deformations within the panel zone with substantial curvatures at the top and bottom ends (Figure B-7(a)). The curvatures at each end of the panel zones are referred to as column kinks and were reported to have a detrimental effect on the adjacent beam flange-to-column flange weld. It was suggested that the maximum ductility of the panel zone be limited to $4\gamma_y$, where γ_y is the shear deformation at first yield of the panel, to prevent excessive deformation and column kinking from fracturing the beam flange CJP welds. The researchers also mapped the yield front as it progressed through the panel zone with strain gauges (Figure B-7(b)). The yielding in the panel zone was first recorded at load point 7 (LP-7) in the center of the panel zone. This was attributed to the location of maximum delivery of shear force from beam coupled with the well-known shear flow distribution in the web of a wide-flanged shape. Yielding progresses from this point towards the corners of the panel zone. Finally, the authors derived a set of force-displacement relationships which was a precursor to the one in use in the AISC *Specifications.* It was also observed that large column axial forces contribute to secondary distortions of the panel zones and result in less overall hysteretic energy dissipation of the panel zone.

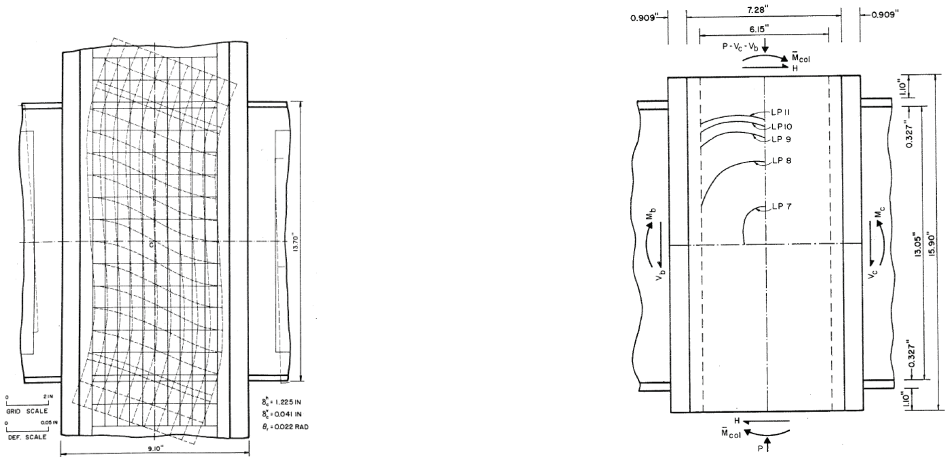

(a) Deformation pattern (b) Distribution of yielding

Figure B-7 Panel zone deformation and yielding (Krawinkler et al., 1971).

This work was continued by further testing by Bertero et al. (1973), who proposed that the best moment frame performance would be achieved by systems that spread out the inelastic demands to as many elements as possible to prevent large inelastic strains from concentrating to a few elements. The authors argued that this could be achieved by designing the yield capacity of the panel zone to match the yielding moment of the beam. The authors also studied the effect of doubler plate reinforcement. If a doubler plate was flush mounted to the column web, it was found that the reinforced web was equal to the sum of its parts once the panel zone developed its inelastic capability (Specimen A-3 in Figure B-8(b)). However, it was found that doubler plates offset from the column web were not able to be fully effective (Specimen A-4 in Figure B-8(b)). Specimen A-2 was the control specimen with an unreinforced web. In contrast to this conclusion, Lee et al. (2002) observed that an offset doubler plate located at 2/3 of the half flange width from the column web had compatible deformations and strains. It was suggested in this latter study that the plates be no more than 2/3 of the half flange width from the column web (a value exceeded by Bertero et al., 1973).

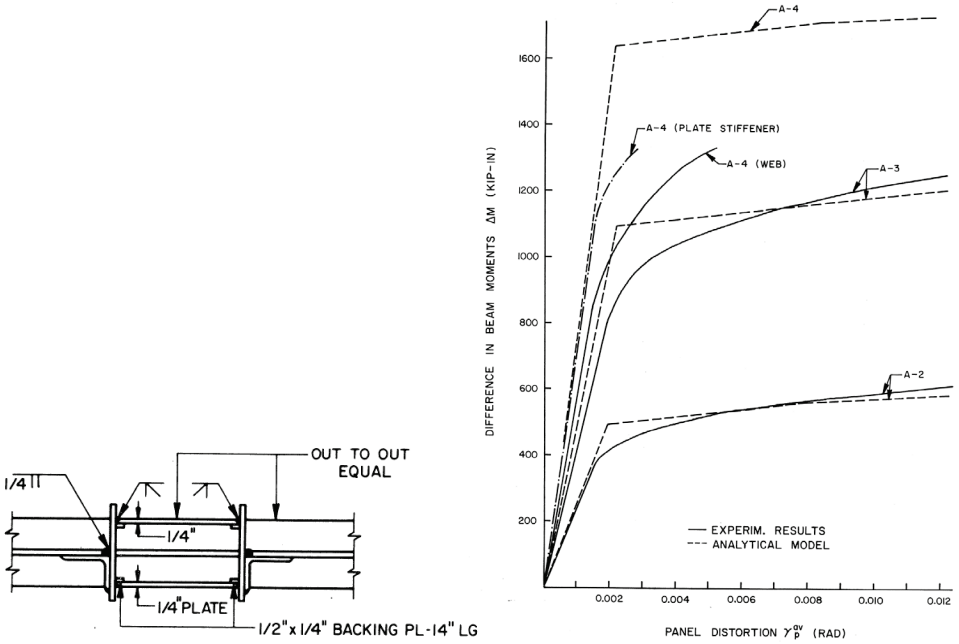

(a) Offset doubler plate (Spec. A-4) (b) Panel zone response

Figure B-8 Doubler plate effectiveness (Bertero et al., 1973).

Becker (1975)

Becker (1975) reported cyclic testing of three specimens at the University of Southern California. The welding process used during these tests was SMAW with E70 electrodes. He observed that under-sizing the welds attaching the doubler plate to the column results in the incomplete transfer of shear to the plate. He also found that the recorded strains in a doubler plate with adequate welds lagged behind the

column web. This lag diminished gradually as the doubler plate was loaded beyond yield and converged when the full inelastic strength of the panel zone was realized (Figure B-9). Skiadopoulos et al. (2021a; 2021b) had the same conclusion investigating this issue using finite element analysis.

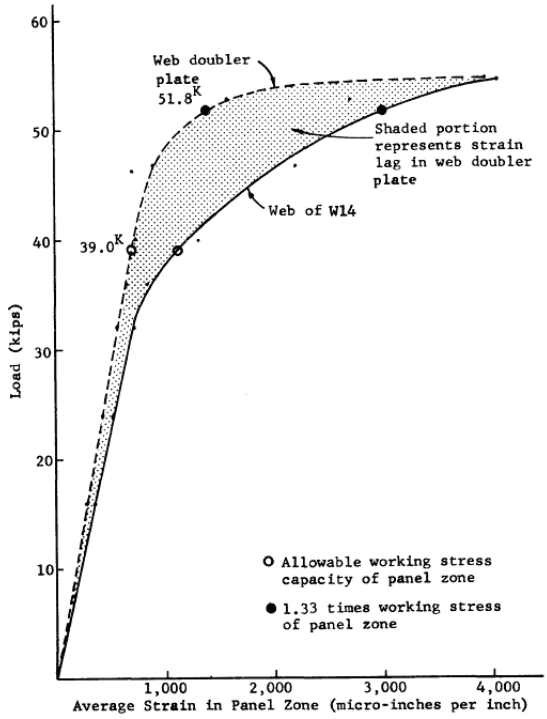

Figure B-9 Doubler plate strain lag (Becker, 1975).

Krawinkler (1978)

In 1978, Krawinkler published a summary of the research completed at the University of California, Berkeley in the 1970s. This paper explains that the panel zone shear force can be adequately determined by

$$V_{pz} = \frac{\Delta M}{0.95 d_b} - V_c \tag{B-15}$$

where ΔM is the sum of beam flange moments and $0.95 d_b$ is the assumed effective depth of the beam. The column shear V_c is found through static equilibrium of the frame. The yield strength of the panel zone was defined in the Specification at the time as $V_y = 0.55 F_y d_c t_w$, which originated from assuming that 95% of the column depth is effective in shear multiplied by $1/\sqrt{3}$ for the von Mises shear strength of the web. It is noted that yielding at the center of the panel zone appears to initiate at 75% of this value, which explains the earlier than expected softening of the panel zone. The panel zone behavior is described by a force-displacement relationship that forms the basis of the current panel zone strength expression in today's Specification. This

force-displacement relationship is described as an elastic slope of the panel zone and is equal to V_y/γ_y, where $\gamma_y = F_y/(G\sqrt{3})$. The resulting elastic spring constant is given by

$$K_e = 0.95 d_c t_w G \tag{B-16}$$

where F_y represents the yield strength of the steel, while G is the shear modulus. The post-elastic stiffness is dominated by the bending strength of the column flanges and is derived in the Krawinkler et al. (1971):

$$K_p = \frac{1.095 d_c t_{cf}^2 G}{d_b} \tag{B-17}$$

This is derived from the flexural stiffness of the column flanges at each corner of the panel zone (Figure B-10(a)). The stiffness term is assumed equal to zero when $\gamma < \gamma_y$. This expression was developed for modest thickness of column flanges, and the author recommended additional research be done to validate the expression for thick column flanges. Based on the observed column kinking and failures in the beam flange CJP welds, a maximum panel zone distortion of $4\gamma_y$ was selected. This gives the total strength of the panel zone as:

$$V_u = K_e \gamma_y + 3K_p \gamma_y = V_y \left(1 + \frac{3K_p}{K_e}\right) = 0.55 F_y d_c t_w \left(1 + \frac{3.45 b_c t_{cf}^2}{d_b d_c t_w}\right) \tag{B-18}$$

Note the similarity to the modern equation in Equation B-9. The contribution to story drift of the panel zone is derived from the portal frame method assuming inflection points at the centers of each beam span and column story as:

$$\delta_p = \frac{h(h - d_b)}{d_b d_c t_w G} H \tag{B-19}$$

where h is the story height, and H is the applied horizontal shear to the column. This expression was also derived by Becker (1975). Dashed lines of Figure B-10(b) show agreement with the experimental results when using this force-displacement rule. The gradual transition between elastic and post-elastic stiffness was attributed to the progressive yielding of the panel zone and participation of other elements within the joint (i.e., continuity plates). It was noted that Specimen A-2 demonstrated shear buckling of the unreinforced column web, which did not appear to degrade the strength of the panel zone.

Krawinkler (1978) also discussed the implication of axial loads on the columns. As the panel zone yields, the axial force in the column is transferred to the column flanges. He further concludes that this can contribute to the early yielding of the panel zone when the axial loads in the column are relatively high. Similar to Fielding and Haung (1971), it was proposed that a von Mises yield criterion be adopted as a

correction factor to reduce the strength of panel zones exposed to high column axial forces.

As an evaluation of the drift induced by panel zone distortion, Krawinkler evaluated the simplification of modeling the beams and columns using their centerline dimensions. This approach artificially increases the flexural compliance of the system to compensate for the complexity of modeling the panel zone with a finite stiffness. He found that the centerline approach was conservative with overestimates as high as 21%.

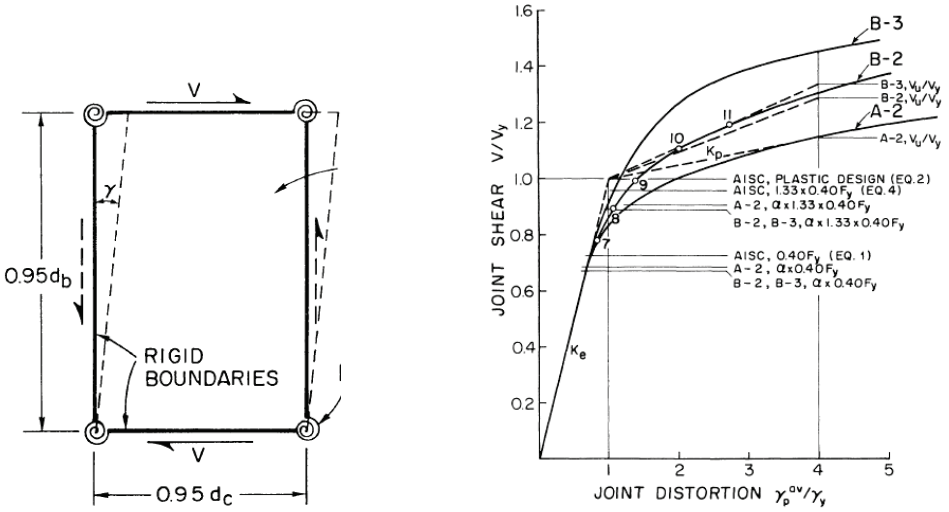

(a) Model (b) Force-displacement relationship

Figure B-10 Panel zone behavior (Krawinkler, 1978).

Popov et al. (1986), Popov (1987), and Tsai and Popov (1988)

Popov et al. (1986) conducted a testing program of eight half-scale subassemblages for a new high-rise building in San Francisco. The testing was performed to determine the need to use costly joint stiffening elements like continuity and doubler plates in ductile moment frames. To investigate this issue, some specimens were designed with weak panel zones, where doubler plates were intentionally omitted to encourage inelastic behavior in the joint. It was found that a “delicate balance” between panel zone yielding and beam flexural yielding exists, and that excessive panel zone deformation results in column kinking which was hypothesized to be a contributor to the abrupt failures observed in the beam flange CJP welds. The researchers found that stiffening the specimens with continuity plates and doubler plates such that inelastic behavior is forced to initiate in the beams improves the overall ductility of the system. The research also revealed that the selection of stiffeners based on the nominal yielding strength of the beam flanges was unconservative because they undergo appreciable strain hardening.

Popov (1987) continued to explore panel zone flexibility by investigating previous experimental work at the University of California, Berkeley during the early 1970s. He observed that flange local bending failures in the beam-flange-to-column-flange weld were caused by the combined effect of an unreinforced column flange and column flange kinking. It was predicted that a very weak panel zone with inadequate reinforcing may result in such high compliance that the beams fail to achieve their strengths before the failure of the connection. This approach was recommended by Kawano (1984), who demonstrated through testing a limited number of specimens that relying on the panel zones entirely as the ductile mechanism was a viable approach. Thus, adequately reinforcing the column flange to resist a flange local bending failure may permit weaker panel zones to be used. To this end an ultimate flange force of $1.8F_y bt_f$ that accounts for expected material properties and strain hardening of an A36 steel flange was deemed appropriate.

Tsai and Popov (1988) performed experimental testing and numerical analysis on 19 full-scale specimens with varying connection details. In particular, the implications of using the FCAW welding process for the welding of the beam flange CJP welds were compared to the SMAW welding process. Specimens using either process demonstrated low drift capacities; however, on average the specimens welded with the FCAW weld process achieved an SDA of 0.015 rad, while those with SMAW weld process achieved an SDA of 0.03 rad. The testing also demonstrated the importance of welding the beam web, which was suggested for beams with webs that contributed more than 30% to the plastic moment capacity of the beam.

Ghobarah et al. (1992) and Schneider et al. (1993)

Ghobarah et al. (1992) performed a series of full-scale subassembledges of bolted end plate moment connections where the panel zone strength was varied. It was observed that panel zones that share the inelastic burden with the beams tend to perform better as these frames delay strength degradation due to the onset of the local beam buckling. The researchers determined that the end plates increased the apparent strength of the panel zone. Schneider et al. (1993) observed that even though weak panel zones demonstrated stable hysteretic behavior that their use should be investigated further because the decrease in stiffness leads to larger second-order effects and story drift. The authors also cautioned that combining panel zone mechanisms with flexural hinging at the base of a column could trigger a soft story mechanism similar to frames made with weak column-strong beam philosophies.

Panel Zone Width-to-Thickness Requirement

In the AISC *Seismic Provisions*, there is a requirement that the thickness of the panel zone meet the follow requirement:

$$t \geq (w_z + d_z)/90 \qquad \text{(B-20)}$$

where w_z is the width of the panel zone between column flanges, and $d_z = d - 2t_{bf}$ of the deeper beam at the connection. This is different from the requirement originally proposed by Fielding and Haung (1971) as it includes the depth of the panel zone. Lee et al. (2002) discussed the origin of this expression as first being published in the 1988 SEAOC Blue Book and has not been amended since. The commentary of this document refers to the work done by Krawinkler (1978), which leverages experimental testing from Krawinkler and Bertero (1971), and states that the buckling of the panel zone will not reduce the shear capacity below $F_y d_c t_{cw}$ even under cyclic loading. It appears that the limit was based on Specimen A-2, which used a W8x24 column that had a panel zone thickness of $(w_z + d_z)/68$. This panel zone buckled but did not demonstrate strength degradation. It is reasoned that the SEAOC committee at the time made the criteria more stringent than this specimen in efforts of precluding strength degradation of the panel zone. Recent analytical work performed found that buckling of doubler plates in panel zones may not result in a loss of strength of stiffness (Gupta, 2013). Research by Chen et al. (2017) confirmed this by observing stable hysteretic responses after panel zone buckling in specimens with a panel zone thickness less than $(w_z + d_z)/90$. These specimens demonstrated significant panel zone buckling which resulted in eventual fracture of the panel zone in regions of repeated high cyclic strains associated with tight curvatures due to shear buckling.

B.3.2 SAC Steel Project Research

Before 1994, steel moment frames and their typical connection details were believed to be an optimal connection with excellent ductile behavior. However, brittle fractures were observed following the 1994 M6.7 Northridge Earthquake in the San Fernando Valley and the 1995 M6.9 Kobe Earthquake at drift levels below the expected capacity. These events triggered a significant research project called the SAC Project in the six years following the earthquake with further studies extending into the following decade. The joint venture consisted of SEAOC, ATC, and CUREe with coordination and funding provided by FEMA, NSF, and NIST. One of the parameters investigated during this time was the implications of a weak panel zone, as it was believed to be one of the root causes of the observed damage. The primary findings of the SAC Project are published in a series of reports through FEMA (FEMA, 2000a-g) and are summarized in many research papers and guidelines (i.e., Malley, 1998; Roeder, 2002; NIST, 2016). Ultimately, it was determined that observed damage was a result of several key factors.

First, the requirement that connections be qualified to demonstrate adequate ductility through a prescribed story drift ratio for use as either special or intermediate moment frames prevents connections with undesirable geometries or details. For example, the WUF-B detail does not demonstrate adequate ductility, even with notch-tough electrodes, because the compliance of a bolted web does not adequately transfer the

beam shear resulting in an overloading of the beam flange welds (Stojadinovic et al., 2000).

Second, in the 1970s the dominant welding process changed from SMAW to the wire feed FCAW process. Eventually, the large diameter E70T-4 electrode became the desired weld electrode for field welded beam flange-to-column flange connections. This electrode did not have specified CVN toughness, and typically demonstrated low toughness (FEMA, 2000f). This resulted in the SAC Project concluding that the weld filler metal toughness was the single most critical welding parameter controlling the observed fractures (Malley, 1998). It was also found that modifying welding details like the backing bar and run-off tabs decreased the potential number of flaws that become sites of strain localization in the weld. Eliminating these defects were found to incrementally improve the ductility of the connections.

It was identified that the design practice through the use of Equation B-1 to Equation B-10 encouraged weak panel zones that would generate the high column curvatures at the corners associated with column kinking. A summary of testing prior to 1994 by Roeder and Foutch (1996) found that weak panel zones may generate acceptable ductility but are susceptible to early fracture of the beam-flange-to-column-flange CJP welds.

A review of the testing performed during the SAC Project is seen in Figure B-11, where V_{pz} is the panel zone demand determined from testing and V_p is the panel zone demand given by Equation B-9. This plot includes both pre- and post-Northridge connections. Although the data has significant scatter, it is apparent that tested specimens that did not develop V_p had a marginally higher probability of achieving plastic rotations beyond 0.03 rad. Part of the complication of comparing this data is that panel zone yielding and beam flexural yielding are interrelated. Another comparison performed contrasts the panel zone demand, V_{pz}, to the panel zone shear force at first yield of the beam, V_y determined from S_xF_y of the beam (Figure B-12). This figure suggests a minor trend that increased plastic rotation capacity occurs if flexural yielding occurred first in the beam. It is noted that even these comparisons are limited, as even a strong panel zone can eventually develop moderate inelastic deformation as strain hardening of the beam flexural hinge gradually increases the flange forces.

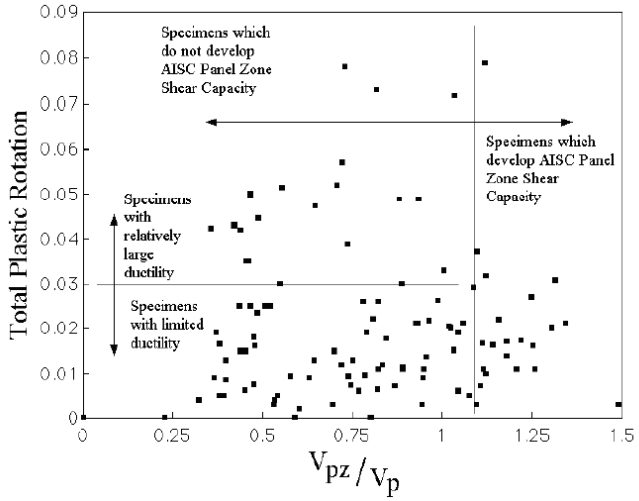

Figure B-11 Plastic rotation capacity versus panel zone strength of SAC Project era tests (FEMA, 2000f).

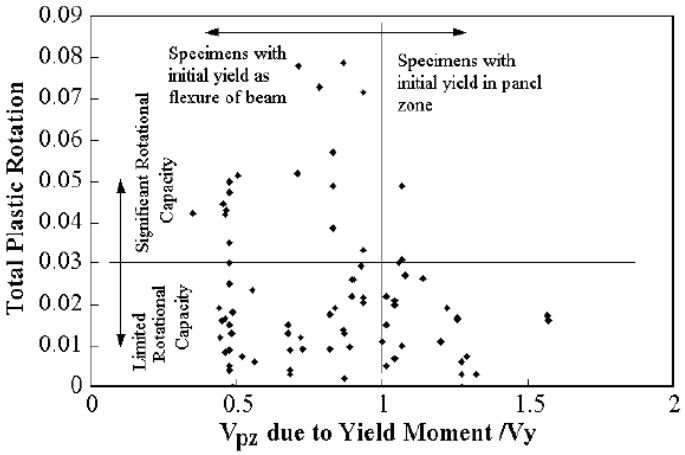

Figure B-12 Plastic rotation capacity versus panel zone balance of SAC Project era tests (FEMA, 2000f).

The SAC Project recommended that the panel zone be proportioned such that shear yielding in the panel zone occurs at the same time as flexural yielding of the beam elements or that the flexural yielding should occur only in the beam. FEMA 351 recommended the following equation to size a balanced panel zone (FEMA, 2000b):

$$t_{pz} \geq \frac{M_c\left(h - \frac{d_b}{h}\right)\left(\frac{S_x}{Z_x}\right)}{0.9(0.55)F_y R_y C_{pr} d_c (d_b - t_{bf})} \quad \text{(B-21)}$$

where R_y and C_{pr} are the expected material property coefficient and the peak connection strength factor, respectively. It was recommended that panel zones in retrofitted or repaired connections be reinforced to this limit such that some yielding of the panel zone would occur and that the panel zone should not be over-reinforced. Note that Jin and El-Tawil (2005) found that this approach, using the prescribed

resistance factor of 0.9 and the 0.55 coefficient for the shear capacity, results in an underutilized panel zone.

B.3.3 Post-Northridge Research on Panel Zone Behavior

Lin et al. (2000) tested four full-scale WUF-W specimens with composite slabs and weak panel zones. These specimens generated excellent performance with maximum drifts above 0.05 rad and panel zone ductility ratios (γ/γ_y) between 13 and 20. All of these specimens failed in the beam flanges with fractures originating at the intersection of the weld access hole and beam flange. The author attributed the eventual failure to the large distortions induced by column kinking and the length of the free flange at the weld access hole. The use of notch-tough electrodes and post-Northridge detailing also attributed to the specimen's ductility.

Testing of eight full-scale specimens with composite slabs and a Reduced Beam Section (RBS) with varying panel zone strength was performed by Jones et al. (2002) at the University of Texas at Austin and Texas A&M University. The relevant tested specimens, including those with weak panel zones, achieved at least 0.04 rad of story drift. It was observed that strong panel zones tested dissipated less energy relative to their balanced or weak counterparts and eventually failed in the beam flanges near the RBS. The specimens which used a balanced panel zone developed the stable hysteretic behavior until flange local buckling of the RBS resulted in strength degradation of the beam hinge which further localizes the strain demands. These specimens failed in either the beam flanges at the RBS or adjacent to the beam flange weld. The two specimens tested with weak panel zones developed the highest total drift and exhibited the most stable hysteretic behavior. These specimens failed in the beam flange just outside of the beam flange weld (Figure B-13). A comparison of the load-displacement response of three specimen types is shown in Figure B-14.

Figure B-13 Typical weak panel zone beam flange failure (Jones et al., 2002).

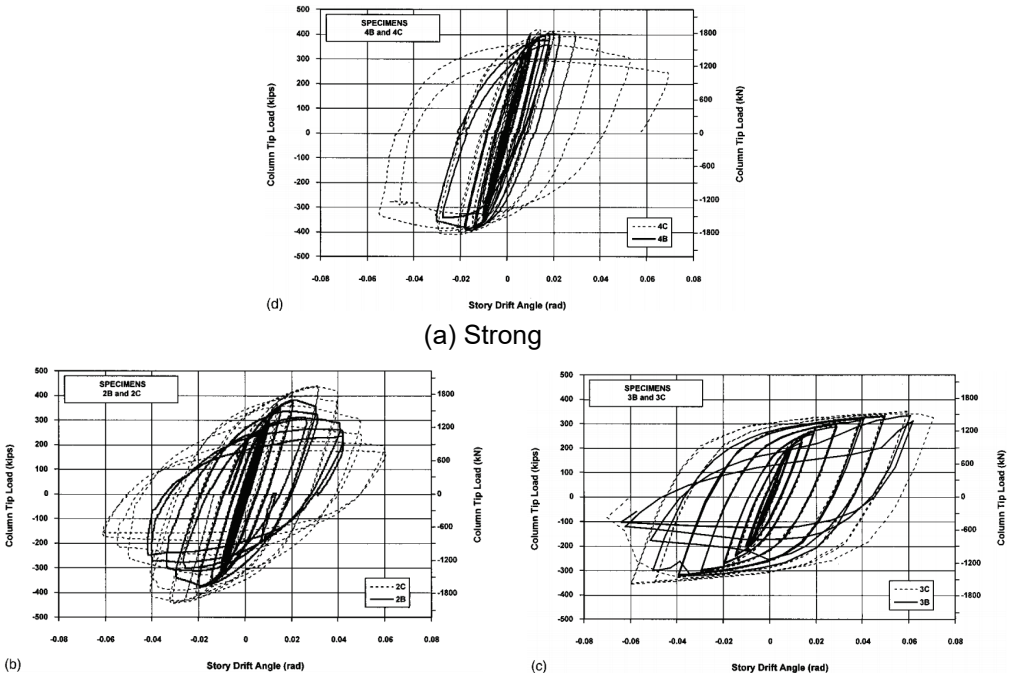

(a) Strong

(b) Balanced

(c) Weak

Figure B-14 Load-displacement response of RBS connections with varying panel zone strengths (Jones et al., 2002).

Testing at the University of Minnesota (Lee et al., 2002; and Lee et al., 2005b) on full-scale interior post-Northridge WUF-W connections explored limit states around continuity and doubler plate details. Their testing program consisted of five specimens using weak panel zones. The specimens were designed with panel zone demand-to-capacity ratio between 1.2 and 1.4 using the probable maximum moment at the face of the column for the demand and Equation B-9 for the capacity. All of the specimens performed adequately, completing multiple cycles at 0.04 rad drift before fracture of the beam flanges. The weak panel zones performed well with stable hysteretic behavior up to $12\gamma_y$. Similar fractures to Jones et al. were observed with occasional tearing at the toe of the beam web weld near the weld access holes.

Testing at Lehigh University (Ricles et al., 2002a; and Ricles, 2002b) tested 11 full-scale WUF-W style connections using post-Northridge connection details. The testing program included exterior ‘T’ type connections and interior cruciform ‘C’ type connections. These tests are the first that used the amended weld access hole as required by the Provisions for WUF-W connections which was determined through finite element analysis by Mao et al. (2001). One of the parameters the researchers focused on was the influence of panel zone strength. Specimens T1 through T4 used a weaker panel zone, while Specimens T5 and C1 through C5 used a stronger panel zone. Note that although Ricles et al. used the term “weak” to describe Specimens T1 through T4, these panel zones were designed using a balanced approach and

demonstrated nearly equal inelastic drift components in the panel zone and beam (Figure B-15).

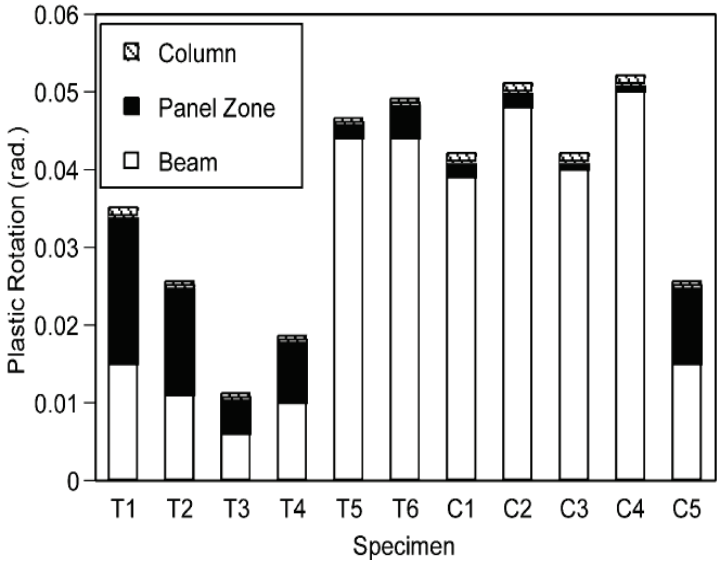

Figure B-15 Comparison of panel zone strength (Ricles et al., 2002a).

Based on the observed decrease in performance of the weaker panel zones, the authors concluded that frames with a stronger panel zone had superior performance. It is identified that Specimens T2 through T4 all varied the web connection detail significantly and would not meet modern WUF-W shear tab connection requirements. Specimen T2 lacked the supplemental fillet weld required between the shear tab and beam web, Specimen T3 used only the supplemental fillet weld and did not weld the beam web to the column, and Specimen T4 used a bolted shear tab. Therefore, the conclusions of this study may be pessimistic given the compounding effect of other parameters known to decrease the ductility of moment connections. Additional testing at Lehigh on interior RBS connections (Zhang and Ricles, 2006) found that balanced and weak panel zones can perform adequately with maximum SDA between 0.04 rad and 0.05 rad. One specimen which was designed as a balanced specimen with a panel zone strength using Equation B-9 equal to probable maximum shear force delivered by the flexural hinge demonstrated weak panel zone behavior. This was hypothesized to be a result of Equation B-9 overestimating the strength of some panel zones due to bending deformations that were observed earlier by Lee et al. (2002).

Further study by Lee et al. (2005a) tested eight full-scale exterior RBS connections with varying web connection details and varying panel zone strengths. The testing reinforced the unsatisfactory performance of a bolted web connection but found the adequate performance of balanced and strong panel zone designs for RBS type connections that used a welded web. It is found that specimens that used a strong

panel zone developed earlier beam instabilities leading to pronounced lateral-torsional buckling of the beam, a conclusion shared by Zhang and Ricles (2006). It is noted that these specimens were bare and did not incorporate a composite slab which has been found to stabilize the beam (Jones et al., 2002). Based on the testing results, the authors propose a balanced design expression where the ratio between probable maximum delivered panel zone shear by the capacity of the panel zone given by Equation B-9 shall be between 0.7 and 0.9. It is believed that in this range the panel zone would dissipate between 30 to 40% of the total energy.

Han et al. (2014) demonstrated that balanced or strong panel zones perform equally based on the testing of four full-scale interior WUF-W specimens. Two specimens in this study are believed to have failed early due to the weld access hole geometry which was more obtuse than similar specimens tested by Ricles et al. (2002) and not because of panel zone strength. Testing by Shin (2017) on nine WUF-W connections and one Bolted Flange Plate connection demonstrated that weak panel zones performed equal or better than strong panel zones. Weak panel zones developed stable hysteretic behavior far beyond $4\gamma_y$ (Figure B-16). The researchers also found that applied axial tension on the columns did not increase the fracture potential. Shin found that the peak connection strength factor, C_{pr}, recorded during testing was 1.21, significantly lower than the 1.4 required in the Provisions for WUF-W connections. This overprediction of the beam flange force results in stronger than anticipated panel zones and may impair future attempts at achieving a balanced panel zone. The higher permissible shear deformation in panel zones is recognized by PEER/ATC (2010) who cite a maximum shear distortion angle of 0.08 rad for connections where column kinking does not contribute to the failure of the beam flange-to-column flange weld. This limit is used for shear links in eccentrically braced frames.

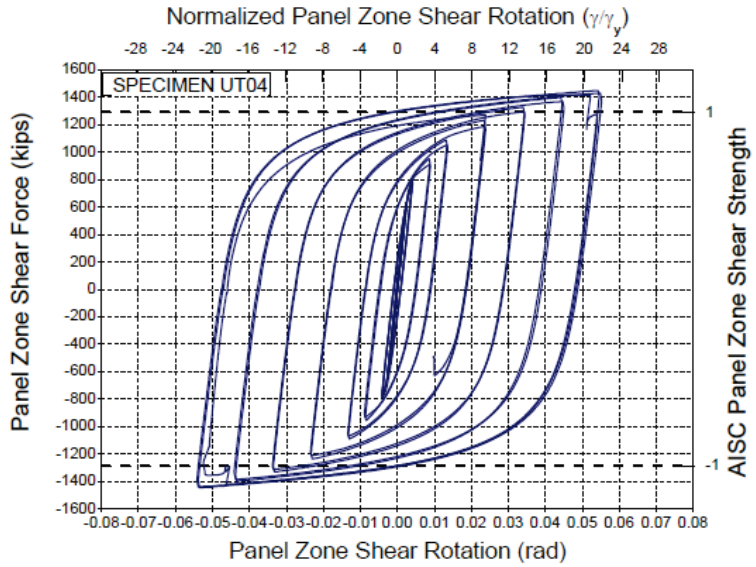

Figure B-16 Weak panel zone test results (Shin, 2017).

Panel Zone (k-area) Fracture

A rarely observed fracture is the brittle rupture of the column web at the beam flange elevations (Figure B-17). This fracture observed by Chi and Uang (2002) during testing of a full-scale RBS connection with a deep column, where the failure of the column web and subsequent propagation into the continuity plate was observed. In this instance, the fracture occurred on a strong panel zone reinforced with a single doubler plate (opposite of the fracture). This type of fracture was originally investigated by Bjorhovde et al. (1999) who investigated the sensitivity of wide flange straightening methods on developing this fracture. The rotary straightening method, commonly used today, develops known regions of low toughness near the fillet of the column due to the amount of cold working that occurs during the process (Tide, 2000). This area has been called the k-area and modern seismic detailing has provisions to minimize the introduction of flaws. Although Bjorhovde et al. (1999) observed fractures in the column outside the fillet, none were attributed to the toughness of the k-area due to the observed stable progression of the fracture. A study by Barsom and Pellegrino (2000) on the fracture observed by Chi and Uang (2002) had the same conclusion. They instead found a flaw induced by the doubler plate weld on the opposite side of the column and attributed the fracture to the overloading of the material in the presence of the flaw.

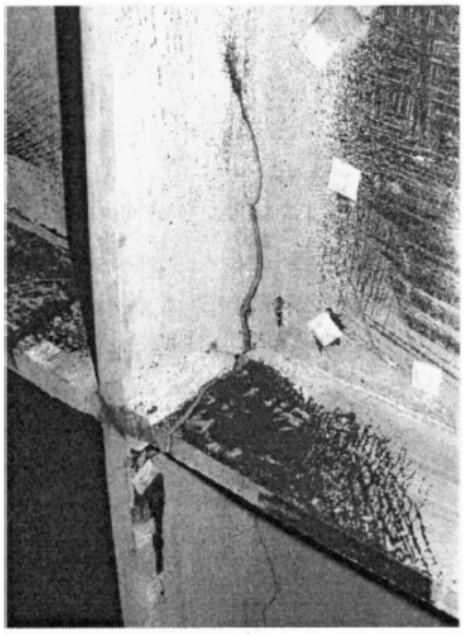

Figure B-17 Column web fracture (Chi and Uang, 2002).

A similar fracture was observed by Stojadinovic et al. (2000) when an undersized fillet-welded continuity plate fractured which led to the fracture propagating into the column web. This specimen was a WUF-B type connection with a weak panel zone. The available research suggests that this type of fracture can occur in strong and

weak panel zones and does not appear to be related to the low toughness of the k-area material. In either case, the fracture seems to occur when another issue is exacerbating the fracture condition in the area, which explains the infrequent observation in the literature.

B.3.4 Post-Northridge Fracture Mechanics Approach

As part of the SAC Project, a minimum set of CVN toughness values for the filler metal were justified using traditional fracture mechanics approaches with a calculated critical stress intensity factor that was subsequently converted to a CVN value through empirical relationships (Johnson et al. 2000). The limitations of this approach are well known as the low-cycle fatigue of a beam flange-to-column flange weld violates many assumptions regarding the development of critical stress intensity factors. One of these violations is the stress field losing its uniqueness due to plastic flow. It is now generally agreed that the flange weld location is exposed to large amounts of plastic strain while being exposed to relatively high levels of triaxial stress (Lee et al., 2002; and Kanvinde, 2017). Therefore, to develop viable fracture metrics researchers have sought to leverage ductile fracture mechanic concepts developed by Rice and Tracey (1969) and Hancock and Mackenzie (1976). These simplified metrics can be extracted from finite element models to evaluate relative fracture potentials. These approaches attempt to capture two key elements in ductile fracture: accumulated plastic strain and triaxial stress. The triaxial stress, *T*, is defined as the ratio of the hydrostatic stress to the equivalent stress. Ductile fracture metrics often used are the plastic equivalent strain index:

$$PEEQ = \frac{\epsilon^p}{\epsilon_y} = \frac{\sqrt{\frac{2}{3}\epsilon_{ij}^p \epsilon_{ij}^p}}{\epsilon_y} \tag{B-22}$$

and the rupture index:

$$RI = \frac{\left(\frac{\epsilon^p}{\epsilon_y}\right)}{e^{-1.5T}} \tag{B-23}$$

where ϵ_y is the yield strain of the material. El-Tawil et al. (1999) and El-Tawil (2000) used these approaches to evaluate the relative fracture potential of the beam flange CJP weld as the panel zone stiffness was varied. Figure B-18a shows the result of the study where a stronger panel zone (CWT5-W) resulted in less *RI* than the weaker panel zone specimen (CWT2-W). El-Tawil also demonstrates the difference in deformation pattern and the bending deformation of the panel zone evident in CWT5-W (Figure B-18b). This type of deformation was more pronounced as the depth-to-width ratio of the panel zone increased and the shear-to-bending strength ratio increased.

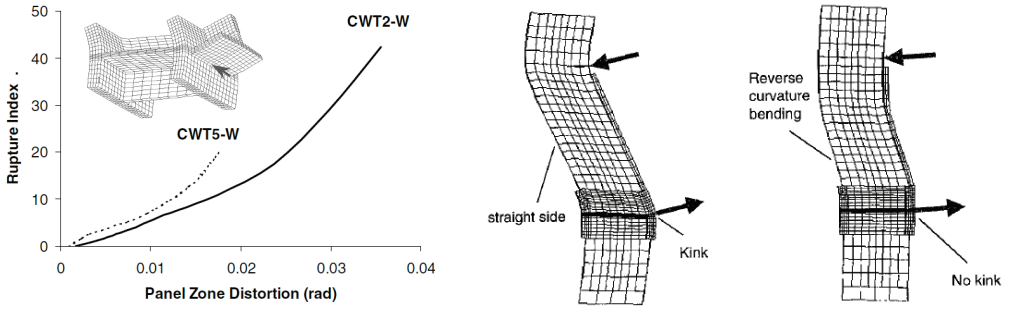

(a) Rupture index (b) Deformation at plastic rotation of 0.03 rad

Figure B-18 Finite element results as panel zone is varied (El-Tawil, 2000; and El-Tawil et al., 1999).

Mao et al. (2001) and Ricles et al. (2002a) investigated fracture metrics at critical locations of unreinforced flange moment connections. Their analysis showed that increasing the panel zone strength reduces the *PEEQ* value, and conversely reduces the *RI* at the toe of the welded beam web. The two sampled locations in the beam flange, at the extreme fiber and the center position of the beam flange CJP weld and the point of tangency of the weld access hole, did not show to be influenced by panel zone strength (Figure B-19). In this figure M_{pz} is the panel zone strength given by the moment required to achieve Equation B-9 and M_{bm} is the predicted moment at the column face. A recent study that compared the *RI* between post-Northridge specimens that developed fractures suggested *RI* might not be a satisfactory metric to predict beam flange CJP weld fractures (Shin, 2017).

Chi and Deierlein (2000) applied a more conventional fracture mechanics approach to the problem when they investigated Crack Tip Opening Displacement (CTOD) to an imposed flaw at the beam flange-to-column flange weld. Their analysis shows that as the panel zone strength is increased, there was a decrease in CTOD and conversely the potential of fracture. The authors also investigate the behavior of connections with and without a continuity plate and observed the beneficial effect of a continuity plate. This same conclusion regarding continuity plates was also found by using the *RI* as a fracture metric by Gupta (2013). This was further explored by Reynolds (2020) who used modern Cyclic Void Growth Models (CVGM) to investigate the sensitivity of beam flange CJP weld fracture as a function of continuity plate thickness. CVGM is discussed in detail, including recommended applications, by Kanvinde (2017).

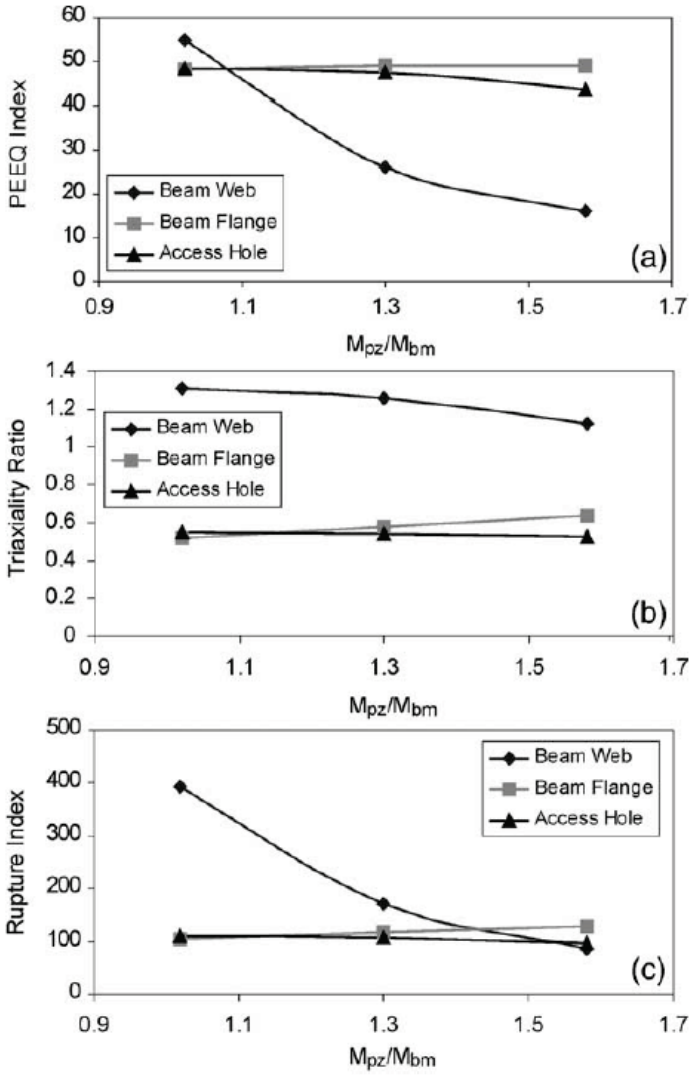

Figure B-19 Fracture metrics versus panel zone strength (Ricles et al., 2002a).

B.3.5 Post-Northridge Research on Force-Deformation Behavior

Panel zone deformation and modeling for structural analysis of moment frames were developed by Fielding and Huang (1971) and Krawinkler et al. (1971). It has been understood since these early studies that the deformation of panel zones increases story drifts. Therefore, since the drift of a moment frame typically governs its design, the deformation of the panel zone is an important consideration. This is exacerbated when panel zones are expected to yield, where the post-elastic deformation of the panel zone can be a significant contributor to frame drift. This is currently recognized for new construction by requiring explicit modeling of the panel zone behavior if the inelastic strength given in Equation B-9 is used in the design.

Liew and Chen (1995) explore a few different modeling options including using a rigid panel zone, a panel zone of an infinitesimal size where the beams and columns are modeled with their centerline dimensions and using springs with calibrated rotational stiffness to capture the behavior. For the rotational stiffness option, the authors also investigated the influence of strong (Type 1) and weak (Type 2) connections. They found that for a typical six-story structure the centerline model approximated the drifts associated with a strong panel zone. However, a 7 percent drop in base shear was observed for a weak panel zone system (Figure B-20). In general, using the centerline dimensions of beams and columns was found to approximate the behavior of a frame with the included deformation of the panel zone unless significant inelastic behavior is anticipated (FEMA, 2000b).

This was attributed to the obvious increase in deformation of the panel zone but also the reduced post-elastic stiffness of the panel zones increasing the second-order effects of the frame. This behavior is further explored by Gupta and Krawinkler (2000), who found that moment frames are already quite sensitive to second-order effects and may approach a critical collapse deflection during time-history analysis if the post-elastic stiffness of the frame is insufficient. Schneider and Amidi (1998) also demonstrated the same unfavorable results but found that the inelastic panel zone behavior tends to demonstrate more stable total structure hysteretic behavior with a more reliable post-elastic stiffness than relying on flexural beam hinging. This was attributed to the strength degradation that typically occurs with beam flexural hinging due to local buckling of the flanges. However, relying solely on panel zones as the ductile mechanism limits the number of mechanisms available. This concept was explored by Biddah and Heidebrecht (1999), who investigated a strong column-weak panel zone (SCWP) and compared the results with strong column-weak beam (SCWB) and weak column-strong beam (WCSB) counterparts. Except for a soft-story mechanism which can occur if a WCSB is used, the SCWP frames showed a reduction in applied base shear during static pushover analysis and higher relative story drifts during time-history analysis.

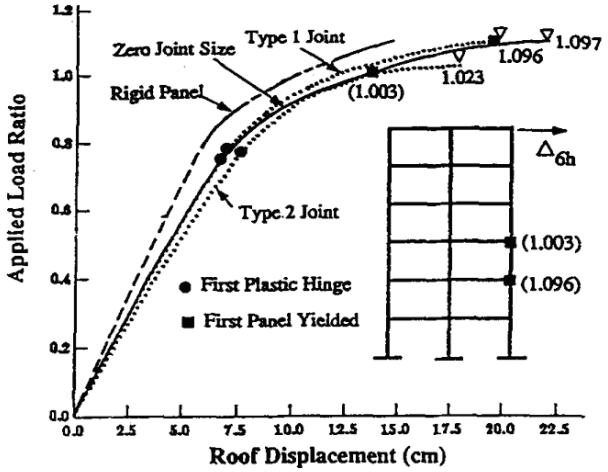

Figure B-20 Influence of panel zone deformation on pushover (Liew and Chen, 1995).

Lee et al. (2002) found from their testing that the force-displacement behavior developed by Krawinkler (1978) is unconservative for stockier column flanges. Based on the observed double curvature deformation of the column flanges, the authors derived an amended force-displacement behavior using the bending stiffness of the column flanges similar to Fielding and Huang (1971). When this new post-elastic term is incorporated into a Krawinkler-like expression at a deformation of $4\gamma_y$, the following panel zone strength is generated:

$$R_n = 0.6F_y d_c t_w \left(1 + \frac{15.6 b_c t_w^3}{d_b^2 b_c t_w}\right) \tag{B-24}$$

The authors conclude that the target panel zone behavior is to permit its inelastic deformation to leverage the robust strain hardening and decreased likelihood of brittle fracture of steel elements loaded in shear. They argue that their results demonstrate $8\gamma_y$ can be used instead as an appropriate limit for the maximum deformation of the panel zone.

Several other researchers have proposed alternative models for the behavior of panel zones. Kim and Engelhardt (2002) developed a model where the panel zone deformation, Δ, as a function of the applied shear force, V, is the shear deformation and bending deformation of the panel zone in series:

$$\Delta = \left(\frac{1}{S_b} + \frac{1}{S_s}\right) V \tag{B-25}$$

where S_b and S_s are the bending and shear stiffnesses, respectively. After calibration, the proposed model appears to offer a closer match to experimental and finite element results of panel zone deformation (Figure B-21). This is most evident on specimens with stocky column flanges where the Krawinkler (1978) model

overestimates the stiffness. Note that in this figure 'Model' is the model proposed by the researchers.

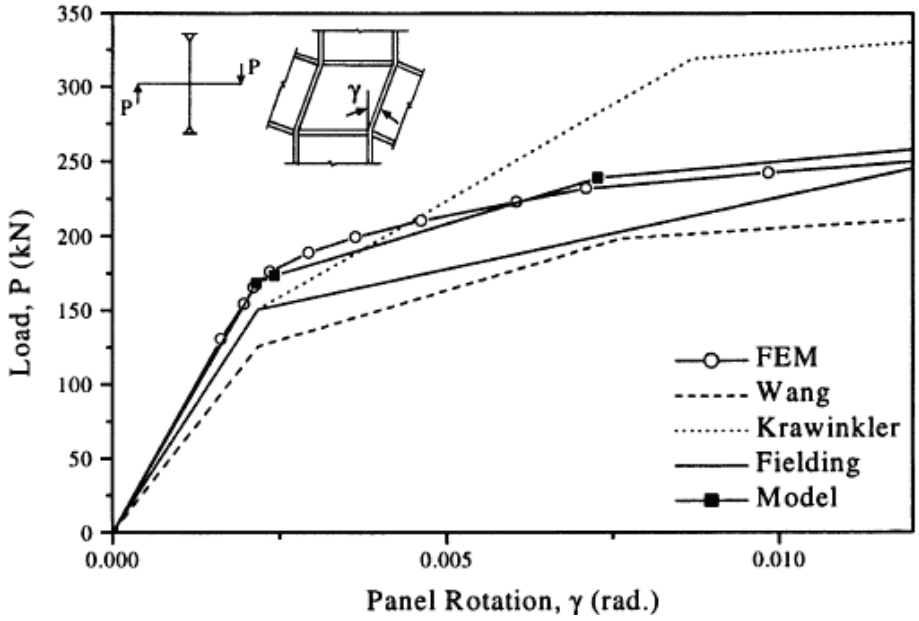

Figure B-21 Comparison of panel zone force-displacement models for specimen with stocky column flanges (Kim and Engelhardt, 2002).

Kim et al. (2015) derived another model which considers flexural and the shear deformation of the column flanges. Their experimental testing of retrofitted connections also demonstrated panel zone capabilities far beyond $4\gamma_y$ for the connections tested. By equating their derived expression to the deformation which achieves complete plastification of the column, the authors derive a panel zone deformation limit:

$$\gamma_{pz} = \frac{0.475F_{yc}}{E}\left(\frac{d_b^2 + 3.45t_{cf}^2}{d_b t_{cf}}\right) \tag{B-26}$$

This limit implies that, after the column flanges have reached their plastic capacity, uncontrolled column kinking will lead to a failure of the beam flange CJP welds. This limit is plotted as a function of the column flange thickness in Figure B-22, note that $\gamma_y \cong 0.012$ rad. It is found that this limit would generate permissible shear distortions less than the current $4\gamma_y$ limit (NIST, 2017). This limit accurately predicted the failure of the two applicable specimens tested by Kim et al. (2015). The researchers also derive a modified expression for the maximum panel zone deformation which accounts for the column axial force.

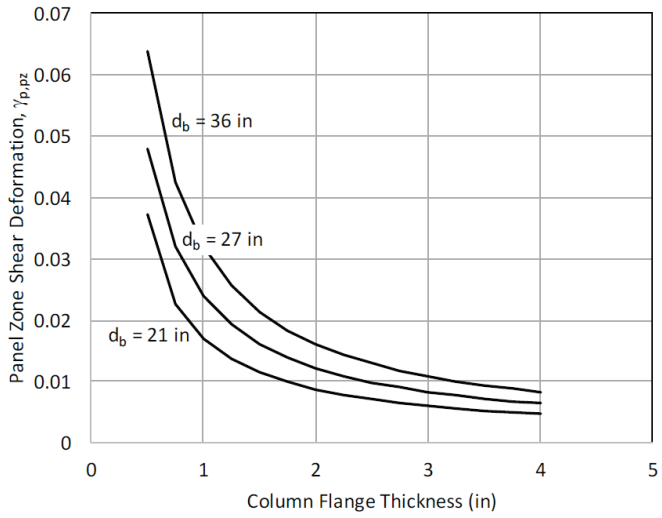

Figure B-22 Panel zone deformation limit (ATC, 2017).

Skiadopoulos et al. (2021) derived another force-displacement rule for the panel zone including the bending stiffness of the panel zone after performing detailed finite element analysis. Their model refines the displacement behavior further by including the shear contribution in the column flanges, which are found to carry a moderate amount of the shear force for stockier columns.

NIST (2017) provides a summary of the available modeling techniques for ductile moment frames. Flexural hinging in beams can be represented with lumped plasticity or fiber models. Panel zones have two important properties to consider when modeling: (1) the finite size of the panel zone which influences the kinematics of the joints, and (2) the elastic and post-elastic stiffness of the panel zone. Figure B-23 demonstrates the kinematics and the resulting offset from the centerline which occurs when modeling the finite size of the panel zone.

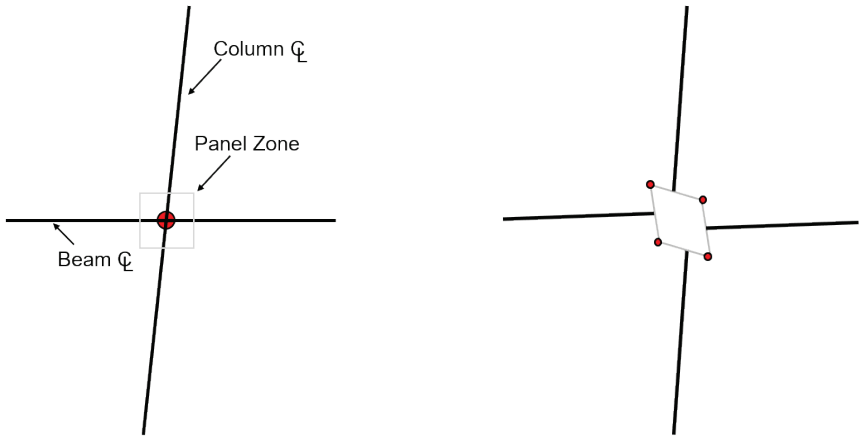

(a) Centerline model (b) Finite size

Figure B-23 Panel zone kinematics.

The three main approaches to modeling the panel zone are as follows:

1. Using centerline models for the beam provides a relatively accurate method if the panel zones are to remain elastic (Figure B-20). Some extra attention to detail is required in this approach when attempting to model non-linear flexural elements in the beams as the beams will be longer than in reality.

2. Rigid or semi-rigid element models where the size and stiffness of the panel zone are captured by members or kinematic coupling. Using rigid offset members without modifying their length is not recommended (Tsai and Popov, 1990; Liew and Chen, 1995; NIST, 2016). The stiffness of these elements or coupling equations can be tuned by modifying their length and/or stiffness to match panel zone force-displacement behaviors from testing (Figure B-24). This technique is commonly used for routine elastic-based design.

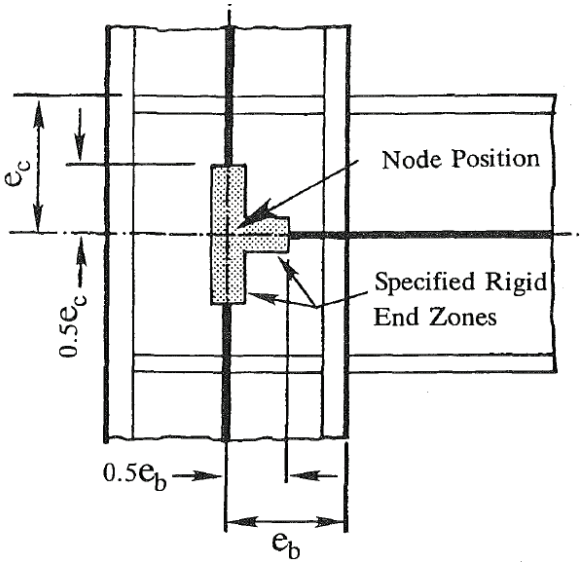

Figure B-24 Rigid end-offsets in end column (Tsai and Popov, 1990).

3. Explicit panel zone modeling can be done where the panel zone size is modeled away from the joint centerline with extra nodes and the stiffness is captured by using non-linear springs. The three common approaches to this are (Figure B-25):

   - The Krawinkler Model uses a deformable shear element to capture the stiffness of the column web and a lumped rotational spring to represent the stiffness of the column flanges,
   - The Modified Krawinkler Model replaces the deformable shear element with a lumped rotational spring, and
   - The Scissors Model uses two nodes at the same location linked with a rotational spring with rigid offsets to capture the finite size of the panel zone. This model is simpler to implement but does not represent the true kinematic

behavior which can be significant when inelastic deformation occurs (Charney and Marshall, 2006).

All models can make concessions to the panel zone stiffness in the presence of high axial loads if required. Charney and Marshall (2006) compare the Krawinkler Model to the Scissors model and find that the Scissors Model underrepresents the stiffness in the inelastic regime (Figure B-25). They also show the significant error that occurs when a designer erroneously uses the Scissors Model with stiffness properties derived from the Krawinkler Model, a situation they claim to occur frequently in the literature.

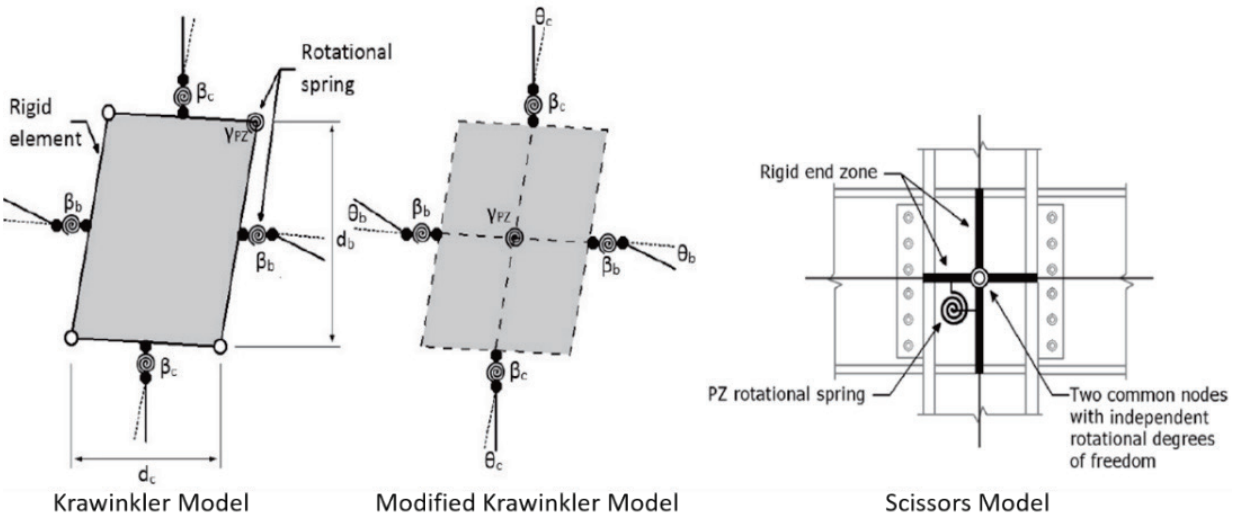

Figure B-25 Explicit panel zone modeling (NIST, 2017).

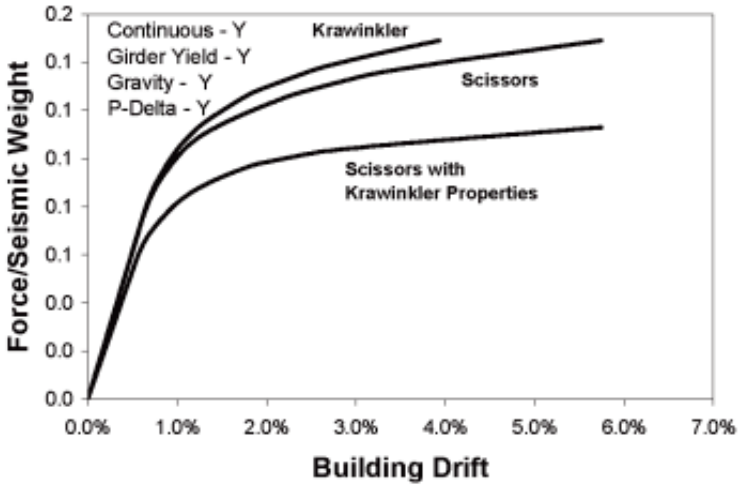

Figure B-26 Comparison of panel zone models (Charney and Marshall, 2006).

B.3.6 Post-Northridge Research on Doubler Plate Design

A common feature of panel zone design is the inclusion of doubler plates which reinforce the column web by increasing its shear strength. Early work on doubler

plates found them effective at reinforcing the column web (Bertero et al., 1973). Becker (1975) found that doubler plates with insufficient welding failed to develop their full shear capacity. This issue is resolved by requiring the doubler plate welding to develop the shear strength of the doubler plate, which has long been the requirement in the AISC *Seismic Provisions*. This often results in substantial amounts of welding, which has raised concerns regarding economy and the influence of welding near and on k-area material.

Shirsat and Engelhardt (2012) and Gupta (2013) performed finite element analysis and found that welding on the horizontal edges of a doubler plate when it is extended beyond the beam flange elevations has no benefit other than to stabilize the plate. In the case of a non-extended doubler plate, the horizontal weld reduces the fracture potential of the vertical doubler plate weld. Finite element models confirmed there was no impact to panel zone strength and stiffness if a thick doubler plate was split into two thinner ones on either side of the column; this technique can be used to decrease required weld volumes. The finite element analysis also found that stresses as high as $1.3F_y$ were observed in the doubler plate welds which was attributed to strain hardening of the doubler plate. The authors argue that doubler plates expected to deform inelasticity might require consideration of strain hardening to design the welds. It was also noted that large transverse stresses exist across the doubler plate weld at the beam flange elevations, which may suggest that additional consideration is required for the doubler plate weld if continuity plates at omitted. Shin (2017) tested a vertical doubler plate groove weld with an embedded tungsten rod to artificially generate an imperfection in the weld of a specimen designed with a balanced panel zone. This specimen (UT05) fractured during its first cycle of 0.04 rad; fracture initiation occurred at the bottom edge of the shear tab-to-column flange weld (Figure B-27). Based on the fracture initiation site it was not believed that this fracture was caused by the intentionally placed defect in the doubler plate weld.

Figure B-27 Column flange fracture (Shin, 2017).

B.3.7 Post-Northridge Research on Retrofitted and Repaired Connections

Over the years, several researchers have explored retrofitting of pre-Northridge connections to improve their ductile performance. While there are no known studies on retrofitted connections which aim to resolve weak panel zones, the strength and stiffness of panel zones are influenced through other retrofit strategies. These strategies consist of reinforcing the beam flanges or cutting an RBS into the beam to relocate the beam plastic hinge location. Usually, these schemes are focused on the beam bottom flange weld of a connection because concrete slabs usually prohibit access to the beam top flanges. Retrofitted connections may still generate inelastic hysteretic behaviors in the panel zones, which can be leveraged to develop the requisite system ductility.

Phase 1 of the SAC Project investigated several repair schemes at the three universities (FEMA, 1997). For example, Uang et al. (1998) tested repaired specimens that included a triangular haunch welded to the bottom flange of the beam to shift the location of the plastic hinge. In situations where the preliminarily tested specimen experienced a beam top flange fracture, the weld was replaced with a notch-tough weld electrode (Figure B-28(a)). To reinforce a beam top flange weld that was not repaired, a set of vertically orientated ribs were added under the top flange (Figure B-28(b)). All of the repaired and retrofitted connections performed better than their pre-Northridge counterparts. The authors concluded that when a pre-Northridge connection is retrofitted with a beam bottom flange haunch, the beam top flange weld should be rewelded with a notch-tough electrode or reinforced with ribs. These retrofitted connections developed a dual-panel zone behavior which can be represented using an equivalent secant stiffness (Figure B-29). A dual-panel zone due to the presence of a haunch results in less panel zone shear because of the deeper effective depth of the beams (Gross et al., 2003). Kim et al (2015) also observed the dual panel zone behavior while testing retrofitted moment connections which used a Kaiser Bolted Bracket on the beam bottom flange. Lee and Uang (2001) performed analytical studies and confirmed that the dual panel zone procedure developed previously for triangular haunch specimens can be applied to connections retrofitted with a straight haunch.

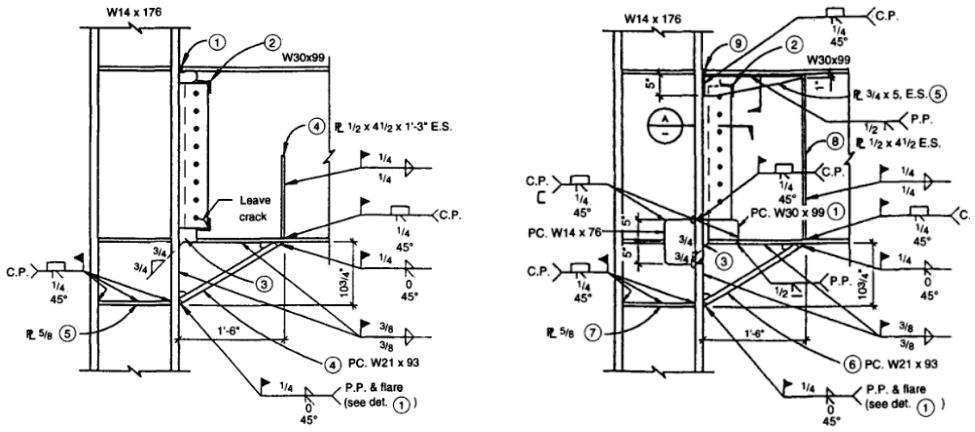

(a) Repair (b) Repair with vertically oriented ribs

Figure B-28 Retrofitted pre-Northridge connection with haunch (Uang et al., 1998).

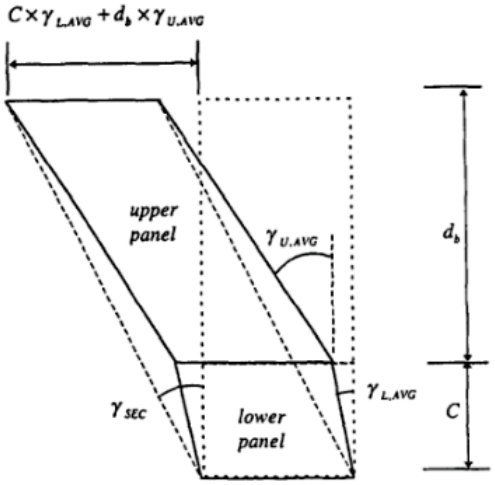

Figure B-29 Dual panel zone behavior (Lee and Uang, 1997).

Gross et al. (2003) reported a research project at three universities that investigated retrofit of pre-Northridge connections. For example, Uang et al. (2000) performed cyclic tested of a series of tests on retrofitted pre-Northridge moment connections using either a welded triangular haunch or an RBS cut of the beam bottom flange. The testing program found that introducing an RBS to the beam bottom flange and removing the beam top flange backing bar and weld root pass (while keeping the bulk of the pre-Northridge weld filler metal made with the E70T-4 weld electrode intact) still developed brittle fractures in the beam top flange weld with little inelastic behavior. Introducing the RBS cut in the beam bottom flange and replacing the beam top flange weld with notch-tough electrode resulted in an improved performance. Introducing the RBS cut to the beam as a retrofit reduces the panel zone shear because of the reduction to the maximum beam flange force. It is concluded that that the welded triangular haunch performed better than the RBS cut; however, it is noted

that no fractures were observed in the beam flange weld of the beam flange with the RBS cut as this beam flange is force limited.

Newell and Uang (2006) performed additional testing on retrofitted moment frame connections intended for a 15-story special moment frame building (Malley et al., 2009). These retrofits consisted of adding haunches to either the beam bottom flange or both beam flanges, adding bolted brackets to both beam flanges, or adding large gusset plates to the connection. Only the backing bar and root pass of the original E70T-4 weld electrode was replaced with notch-tough weld electrodes. In this testing program, the specimen that was retrofitted with beam bottom flange haunches performed poorly with brittle fractures at 0.02 rad story drift. The other retrofit schemes performed well. All specimens demonstrated significant panel zone shear deformations with some of the existing slender doubler plates buckling (Figure B-30). The buckling of the doubler plates did not appear to result in strength degradation of the specimen, which may be attributed to the sistering column web which did not demonstrate bucking. The doubler plate slenderness ratio, $(d_z + w_z)/t_{dp}$, of these specimens were above 150 far greater than the limit of 90 imposed by the AISC *Seismic Provisions*.

Figure B-30 Doubler plate buckling (Newell and Uang, 2006).

Kim and Lee (2017) tested retrofitting of highly composite pre-Northridge moment connections with straight and triangular haunches, or the addition of a welded heavy shear tab placed on either side of the beam web. In this testing program, which used notch-tough electrodes, the retrofit and control specimens performed well with inelastic story drifts exceeding 0.05 rad. It is noted that the heavy shear tab specimen increased the panel zone distortion. It was also observed that shallow beams may be influenced sufficiently by the composite slab to warrant its inclusion in computing the probable maximum moment at the column face.

B.3.8 Weak Panel Zone Database

Skiadopoulos and Lignos (2021b) assembled the testing results from 100 tests conducted over the last 50 years on inelastic panel zones. The testing results were digitized, and meta-information associated with each test was recorded to produce an indexable database. The database includes testing results from pre-Northridge connections using the traditional E70T-4 weld electrodes, retrofitted connections, and modern post-Northridge connections. Using their database, the authors developed cumulative probabilities demonstrating the probability of failure as a function of the normalized panel zone distortion and the SDA (Figure B-31). This figure also compares the performance of reinforced connections like the Bolted Flange Plate (BFP) and the Welded Flange Plate (WFP) connections. Several conclusions regarding the performance of the connections are observed: (1) post-Northridge connections perform remarkably better than pre-Northridge connections; (2) there appears to be a minor correlation between increased panel zone distortion and the probability of failure at the special moment frame qualification SDA of 0.04 rad (Figure B-31(b)); (3) for a given SDA an increase in inelastic behavior of the panel zone does not decrease the probability of failure; and (4) reinforced connections perform better than unreinforced connections.

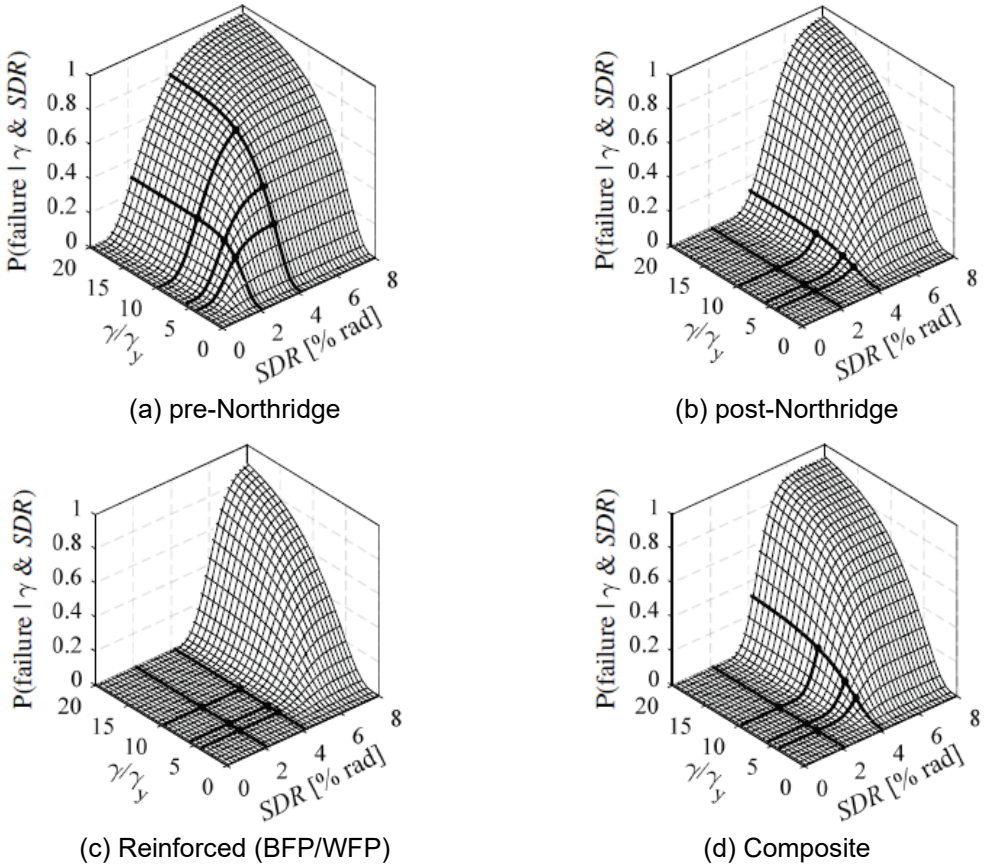

(a) pre-Northridge

(b) post-Northridge

(c) Reinforced (BFP/WFP)

(d) Composite

Figure B-31 Specimen probability of failure (Skiadopoulos and Lignos, 2021b).

The author's analysis of panel zone behavior also demonstrated that as the panel zone is progressively more overloaded, and the recorded moment at the face of the column drops below the probable maximum moment when using existing peak connection strength, C_{pr}, factors. This arises because the additional compliance of the panel zone limits the strain hardening in the beam flexural hinge as the drift concentrates into panel zone distortion. It was found that as the demand-to-capacity ratio of the panel zone using Equation B-9 exceeds 1.2, the full value of C_{pr} is not reached.

B.4 Conclusions

Panel zones in steel moment connections are a ductile component that can be leveraged to provide inelastic deformation and stable hysteretic response under cyclic loading. Based on the early work by Krawinkler et al. (1971), the force-deformation relationship of the panel zone, at an assumed maximum shear deformation of $4\gamma_y$, has been used to define the design shear strength of the panel zone. The original force-deformation derivations were remarkably accurate, and the refinements by other researchers better capture the behavior of thick column flanges and a broader range of panel zone aspect ratios. The classical mathematical models or their updated renditions are used to model the inelastic response of the panel zones in static or time-history analysis for new designs or seismic retrofit of steel moment frames. Capturing the accurate behavior of the panel zone is crucial for an accurate estimate of drift, an issue which is further exacerbated by geometric non-linearities.

A panel zone can be categorized as weak, strong, or balanced, depending on the required shear force and shear capacity used in design. A weak or strong panel zone design refers to that where inelastic action (i.e., energy dissipation) is concentrated in the panel zone or beam, respectively. A balanced design would have both the panel zone and beam participating in energy dissipation. The post-Northridge design procedure contained in the modern AISC *Seismic Provisions* (AISC, 2016a) falls in this category, which has the design intent that the beam flexural yielding be the primary source of inelastic deformation, but that limited yielding of panel zones is acceptable. Nevertheless, a weak panel zone condition may exist in many existing steel moment frames that were design and constructed before the 1994 Northridge Earthquake. This event triggered significant research efforts on finding the source of observed premature fracturing of the beam-flange-to-column-flange CJP welds of steel moment frames. Subsequent code revisions have resolved and clarified the direction to design panel zones.

First, consider the design strength of the panel zone. It is based on shear yielding of the panel zone without or with the contribution from column flange local bending (i.e., kinking); the latter was first introduced in the 1988 edition of UBC. On the required design shear of the panel zone, design codes in the pre-Northridge era were not based on rigorous capacity design principles and, thus, tended to underestimate

the required shear. The 1988 UBC further lowered the required panel zone shear in order to promote a weak panel zone design. This condition is compounded by known issues of pre-Northridge moment connections, especially the beam flange CJP-welded joint, with low notch-toughness weld metal and poor detailing (e.g., left-in-place steel backing at the beam bottom flange CJP weld).

Following the post-Northridge design and construction practice, experimental testing of moment connections with a balanced panel zone design has shown satisfactory performance. Even when a weak panel zone is used, testing showed that column flange kinking due to large panel zone deformation (e.g., greater than $0.04\gamma_y$) would not cause fracture of well detailed beam flange with notch-tough CJP-welded joints. However, this is not the case for pre-Northridge connections. Despite its large inelastic deformation capacity, a panel zone in a pre-Northridge connection will lack the opportunity to develop its full ductility before the beam flange CJP weld fracture occurs. There are no known experimental programs which sought to retrofit, or leverage, a weak panel zone. But panel zone deformations demand can be reduced by, for example, adding a haunch at the connection level or installing damping devices to reduce drift at the system level.

For seismic evaluation and retrofit, the coupling effect between the panel zone and pre-Northridge beam flange CJP welds needs to be established. This interaction also includes other variables like the presence and relative stiffness of other elements in the connection, and the notch-toughness of the filler metal used to perform the beam flange CJP weld. This key knowledge gap can be explored by a robust analytical study that defines a maximum permissible panel zone deformation as a function of the key variables. Analytical studies are required to be validated by thoughtful experimental studies which act to build confidence in the simulations. The experimental program may also explore retrofit strategies which resolve, or leverage, a weak panel to achieve a satisfactory system level performance.

Appendix C

Guidance for Development of Continuum Finite Element Simulations

Both the PJP column splice studies (Chapter 4) and the weak panel zone studies (Chapter 5) rely on continuum finite element (CFE) simulations for test planning and generalization of test results. Consequently, CFE simulations should reflect important effects and physical phenomena that control key aspects of column splice and panel zone performance. This Appendix summarizes important characteristics that should be included in the finite element simulations.

C.1 Physical Phenomena and Effects to be Investigated by CFE Simulations

The CFE should be able to characterize splice or panel zone performance under a given set of loadings (which will usually be applied at the connected members, either in terms of load or displacement control). At a high level, it is important for the CFE simulations to be able to replicate the strength and stiffness characteristics, as well as the spatial distributions of stresses and strains through the component of interest (i.e., splice or panel zone). Most importantly, the CFE simulations should be able to estimate the fracture toughness demands in the components, especially at the critical locations. For the splices, fracture toughness demands at the PJP root flaws in the flanges and the web of the welded column splice connection are important. For the panel zones, fracture toughness demands at the beam-flange-to-column-flange weld is important. This includes the effect of weld detailing (e.g., era appropriate modelling of the weld backing bar) and the effect of local deformations including kinking of the column flanges and deformations of the continuity plates. Additional modes of response, local buckling, fracture propagation, and the overall response of the connection should also be simulated where appropriate. Specifically, the following should be considered:

- Inelastic response of all materials including base materials, welds, and HAZs, along with large deformation kinematics. In this regard, it is important to note that constitutive model calibration for weld materials is especially challenging. Consequently, the use of material coupons extracted from weld assemblies is desirable.
- Appropriate selection of fracture or fatigue toughness indices depending on the specific condition being investigated (e.g., linear elastic fracture mechanics may

not be valid under situations of large-scale yielding). Similarly, elastic plastic fracture mechanics may not be valid under cyclic seismic loading. The dependence of these fracture toughness measures on temperature and strain rate should be considered.

- The simulations should ideally seek to represent three-dimensional response of the full details, including the flange and web connections, as well as out-of-plane bending effects. The CFE model should be large enough to mitigate the influence of any edge/boundary effects on the stress or strain fields at the component. However, it may not be feasible to construct such models for every situation. In such cases, two-dimensional models may be sufficient if their suitability is adequately established through comparison to three-dimensional models.
- The models should feature expected (or measured) detail geometries when available, rather than nominal or specified. This includes the expected geometries of the root pass and surface.
- The models should simulate residual stress patterns to the extent feasible, as well as loading rate effects, both in terms of loading/constitutive response and fracture toughness measures. Residual stresses are difficult to measure and characterize. Consequently, if these cannot be directly measured; the insensitivity of model response to residual stresses should be demonstrated parametrically.
- In addition to the objective of assessing fracture risk, a subset of models should address the consequences of fracture, by modeling crack propagation and subsequent response. For column splices this may include crack arrest (e.g., at the flange-web transition in splices) and other effects such as unseating and loss of shear capacity of the splice. For beam-to-column joints this may include the latent moment capacity after a beam flange fracture has arrested at the weld access hole in the beam web.
- The simulations (and the framework within which they are conducted) should rigorously consider the uncertainty in their predictions of fracture. These uncertainties may arise from several sources, including aleatory and epistemic source. Examples of aleatory sources include: (1) uncertainties and error in measurement of CVN toughness and (2) uncertainties in material property and geometry measurements. Examples of epistemic sources include: (1) errors in converting CVN toughness to fracture indices such as K_{IC} or J_{IC}, (2) errors in representing stress/strain states due to inadequacy of the CFE models and (3) the various assumptions made within them. In addition, the simulation framework should explicitly address the issue of volume sampling in brittle fracture when transferring results from lab scale fracture tests to full-scale. The size effect is demonstrated in large components which show lower effective toughness due to weakest-link sampling.

- The models should include geometric nonlinearity with an appropriate set of applied imperfections. Imperfections are commonly assumed to a superposition of the prevailing mode shapes of the system. Amplitudes of these applied imperfections may be inferred by using sampled geometries.

C.2 Assessment of CFE Simulation Approach

The CFE simulations should be validated against previous experiments as well as experiments that will be conducted as part of the research program. Specifically, existing data sets for PJP column splices include experimental work by Bruneau and Mahin (1991) and Shaw et al. (2015). Of these, Bruneau and Mahin (1991) represent pre-Northridge construction in terms of materials as well as geometry, whereas Shaw et al. (2015) represent prospective splice details with tougher materials and larger weld penetration. While the latter dataset is not directly pertinent to the overall aims of this research plan, it provides a rigorous testbed for validation of the CFE simulations.

Data sets for the cyclic response of panel zones include Krawinkler et al. (1971), Lin et al. (2000), Jones et al. (2002), Lee et al. (2002), Ricles et al. (2002b), Han et al. (2014), and Shin (2017). See Appendix B for details. A database of inelastic panel zones has been developed by Skiadopoulos and Lignos (2021b). Examples of high-fidelity simulations of panel zones and the adjacent beam-column connections include Chi and Deierlein (2000), Gupta (2013), and (Shin, 2017).

For both splices and panel zones, the CFE simulations and the associated framework should be validated through their ability to simulate the deterministic and stochastic response of the specimens and their fracture potential. This can be accomplished by comparison through replicate test data from physical specimens.

Acronyms

AISC	American Institute for Steel Construction
ASD	Allowable stress design
ASTM	American Society for Testing and Material
ATC	Applied Technology Council
AWS	American Welding Society
CFE	Continuum finite element
CJP	Complete joint penetration groove weld
CTOD	Crack Tip Opening Displacement
CUREe	California Universities for Research in Earthquake Engineering
CVGM	Cyclic Void Growth Model
CVN	Charpy V-notch
EDP	Engineering Demand Parameter
EPFM	Elastic plastic fracture mechanics
FCAW	Flux-cored arc welding
FEMA	Federal Emergency Management Agency
FR	Fully restrained
GMAW	Gas metal arc welding
HAZ	Heat-affected zone
IMRF	Intermediate moment-resisting frame
IDA	Incremental dynamic analysis
IR	Interaction ratio
LEFM	Linear elastic fracture mechanics

MIDR	Maximum interstory drift ratio
MCE	Maximum Considered Earthquake
MTR	Material Testing Reports
NIST	National Institute of Standards and Technology
NEHRP	National Earthquake Hazard Reduction Program
NLRHA	Nonlinear response history analysis
NLTHA	Nonlinear time history analysis
NSF	National Science Foundation
PJP	Partial joint penetration groove weld
PQR	Procedure Qualification Record
RBS	Reduced beam section
SEAOC	Structural Engineers Association of California
SEAONC	Structural Engineers Association of Northern California
SCWB	Strong column – weak beam
SDA	Story drift angle
SMAW	Shielded metal arc welding
SMRF	Special moment-resisting frame
UBC	Uniform Building Code
UT	Ultrasonic testing
WBC	Welded beam-column
WCS	Welded column splice
WPS	Welding Procedure Specification
WUF-B	Welded Unreinforced Flanges – Bolted Web
WUF-W	Welded Unreinforced Flanges – Welded Web

Terminology

Charpy V-notch test: A standardized test (ASTM E23) that can be used to measure the notch toughness of a metal.

Connection: Combination of structural members and joints used to transfer forces between two or more members.

Filler metal: Metal added in the welding process to fill the joint between two elements.

Flange penetration: Specified PJP weld size relative to the thickness of the upper flange, typically expressed as a percentage or fraction of the thickness of the upper flange.

Joint: An area where two or more ends, surfaces, or edges are attached.

Kinking: Local column flange bending caused by deformation of a weak panel zone.

Member: An individual beam or column element, excluding connections to other members in a building frame.

Notch toughness: Amount of energy absorbed by a material when subjected to a Charpy V-notch test.

Pre-Northridge: Having key characteristics representative of steel moment frame seismic design and construction that do not reflect improved practices adopted since the 1994 Northridge Earthquake.

PJP column splice: A type of splice common in pre-Northridge frames that uses partial joint penetration groove welds to join the upper and lower column flanges.

Post-Northridge: Having key characteristics representative of steel moment frame seismic design and construction that reflect improved practices adopted since the 1994 Northridge Earthquake.

Root pass: The first weld pass in a welded joint.

Runoff tabs: Tabs placed at the ends of the gap between two elements so weld passes can extend past the joint.

SAC Project: A FEMA-funded research program by SEAOC, ATC, and CUREe that investigated steel moment frame damage in the 1994 Northridge Earthquake and developed recommendations to improve the design and construction of

new steel moment frames, as well as limited guidance on evaluation, retrofit, and repair of existing pre-Northridge steel moment frames.

Subassemblage: A combination of elements and connections representing a portion of the building frame.

System: Overall building frame.

Weak panel zone: A condition in some beam-to-column steel moment connections in which the panel zone yields before the adjacent beams.

Weld backing: Backing placed along the length of the gap between two elements to ensure fusion of the root pass to the connected members and contain molten weld metal.

Weld metal: Metal in a welded joint that has been molten in the welding process and then solidified, usually a mixture of filler metal and base metal.

References

AIJ, 1995, *Reconnaissance Report on Damage to Steel Building Structures Observed from the 1995 Hyogoken-Nanbu (Hanshin/Awaji) Earthquake,* Steel Committee of Kinki Branch, The Architectural Institute of Japan.

AISC, 1961, 1969, 1978, *Specification for the Design, Fabrication and Erection of Structural Steel for Buildings,* American Institute of Steel Construction, Chicago, Illinois.

AISC, 1986, *Load and Resistance Factor Design Specification for Structural Steel Buildings*, American Institute of Steel Construction, Chicago, Illinois.

AISC, 1989, *Supplement No. 1 to the Load and Resistance Factor Design Specification for Structural Steel Buildings*, American Institute of Steel Construction, Chicago, Illinois.

AISC, 1990, *Seismic Provisions for Structural Steel Buildings*, AISC 341-90, American Institute of Steel Construction, Chicago, Illinois.

AISC, 1992, *Seismic Provisions for Structural Steel Buildings,* AISC 341-92, American Institute of Steel Construction, Chicago, Illinois.

AISC, 1997, *Seismic Provisions for Structural Steel Buildings*, AISC 341-97, American Institute of Steel Construction, Chicago, Illinois.

AISC, 1999a, *Supplement No. 1, Seismic Provisions for Structural Steel Building*, AISC 341-97, American Institute of Steel Construction, Chicago, Illinois.

AISC, 1999b, *Steel Design Guide 12: Modification of Existing Steel Welded Moment Frame Connections for Seismic*, American Institute of Steel Construction, Chicago, Illinois.

AISC, 2000, *Supplement No. 2, Seismic Provisions for Structural Steel Building*, AISC 341-97, American Institute of Steel Construction, Chicago, Illinois.

AISC, 2002, *Seismic Provisions for Structural Steel Buildings*, AISC 341-02, American Institute of Steel Construction, Chicago, Illinois.

AISC, 2005, *Seismic Provisions for Structural Steel Buildings*, AISC 341-05, American Institute of Steel Construction, Chicago, Illinois.

AISC, 2010, *Seismic Provisions for Structural Steel Buildings*, AISC 341-10, American Institute of Steel Construction, Chicago, Illinois.

AISC, 2016a, *Seismic Provisions for Structural Steel Buildings*, ANSI/AISC 341-16, American Institute of Steel Construction, Chicago, Illinois.

AISC, 2016b, *Specification for Structural Steel Buildings*, ANSI/AISC 360-16, American Institute of Steel Construction, Chicago, Illinois.

AISC, expected 2022, *Seismic Provisions for Evaluation and Retrofit of Existing Structural Steel Buildings*, AISC 342-22, American Institute of Steel Construction, Chicago, Illinois.

Anderson, T.L., 2017*, Fracture Mechanics: Fundamentals and Applications*, CRC Press.

ASCE, 1995, *Minimum Design Loads for Buildings and Other Structures*, ANSI/ASCE 7-95, American Society of Civil Engineers, Reston, Virginia.

ASCE, 2005, *Minimum Design Loads for Buildings and Other Structures,* ASCE/SEI 7-05, Structural Engineering Institute of the American Society of Civil Engineers, Reston, Virginia.

ASCE, 2016, *Minimum Design Loads for Buildings and Other Structures,* ASCE/SEI 7-16, Structural Engineering Institute of the American Society of Civil Engineers, Reston, Virginia.

ASCE, 2017, *Seismic Evaluation and Retrofit of Existing Buildings*, ASCE/SEI 41-17, Structural Engineering Institute of the American Society of Civil Engineers, Reston, Virginia.

ASCE, expected 2023, *Seismic Evaluation and Retrofit of Existing Buildings*, ASCE/SEI 41-23, Structural Engineering Institute of the American Society of Civil Engineers, Reston, Virginia.

ASTM, 1998, *General Requirements for Rolled Steel Plates, Shapes, Sheet Piling, and Bars for Structural Use*, ASTM A6/6M, ASTM International, West Conshohocken, Pennsylvania.

ASTM, 2013, *Standard Test Method for Determination of Reference Temperature, T_o, for Ferritic Steels in the Transition Range*, ASTM E399, ASTM International , West Conshohocken, Pennsylvania.

ASTM, 2018a, *Test Method for Determining Plane-Strain Crack-Arrest Fracture Toughness, K_{Ia}, of Ferritic Steels*, ASTM E1221-12A, ASTM International, West Conshohocken, Pennsylvania.

ASTM, 2018b, *Standard Test Methods for Notched Bar Impact Testing of Metallic Materials*, ASTM E23, ASTM International, West Conshohocken, Pennsylvania.

ASTM, 2019, *Standard Specification for Carbon Structural Steel*, ASTM A36/A36M, ASTM International, West Conshohocken, Pennsylvania.

ASTM, 2020a, *Standard Test Method for Measurement of Fracture Toughness*, E1820-20b, ASTM International, ASTM E1820-20b, West Conshohocken, Pennsylvania.

ASTM, 2020b, *Standard Test Method for Determination of Reference Temperature, T_o, for Ferritic Steels in the Transition Range*, ASTM E1921, ASTM International, West Conshohocken, Pennsylvania.

ASTM, 2020c, *Standard Test Method for Linear-Elastic Plane-Strain Fracture Toughness of Metallic Materials*, ASTM E399, ASTM International, West Conshohocken, Pennsylvania.

ASTM, 2021, *Standard Specification for High-Strength Low-Alloy Columbium-Vanadium Structural Steel*, ASTM A572/A572M, ASTM International, West Conshohocken, Pennsylvania.

AWS, 1966, *Welding in Building Construction*, AWS D1.0, American Welding Society, Miami, Florida.

AWS, 1979, *Specification for Carbon Steel Electrodes for Flux Cored Arc Welding*, ANSI/AWS A5.20-79, American Welding Society, Miami, Florida.

AWS, 1995, *Specification for Carbon Steel Electrodes for Flux Cored Arc Welding*, ANSI/AWS A5.20-95, American Welding Society, Miami, Florida.

Azuma, K., Kurobane, Y., Iwashita, T., and Dale, K., 2006, "Full-scale testing of beam-to-RHS column connections with partial joint penetration groove welded joints and assessment of safety from brittle fracture," *Welding in the World*, Vol. 50, No. 5, pp. 59-67.

Barsom, J.M., 1975, "Development of the AASHTO fracture-toughness requirements for bridge steels," *Engineering Fracture Mechanics*, Vol. 7, No. 3, pp. 605-618.

Barsom, J.M., and Rolfe, S.T., 1970, "Correlations between K_{Ic} and Charpy V-Notch test results in the transition-temperature range," *Impact Testing of Metals*, D. Driscoll, ed., ASTM International, West Conshohocken, Pennsylvania.

Barsom, J.M., and Pellegrino, J.V., 2000, "Failure analysis of a column *k*-area fracture," *Modern Steel Construction*, Vol. 84, No. 9.

Becker, R., 1975, "Panel zone effect on the strength and stiffness of steel rigid frames," *Engineering Journal*, Vol. 12, No. 1, pp. 19-29.

Beremin, F.M., Pineau, A., Mudry, F., Devaux, J.-C., D'Escatha, Y., and Ledermann, P., 1983, "A local criterion for cleavage fracture of a nuclear pressure vessel steel." *Metallurgical Transactions A*, Vol. 14, No. 11, 2277–2287.

Bertero, V.V., Krawinkler, H., and Popov, E.P., 1973, *Further Studies on Seismic Behavior of Steel Beam-Column Subassemblages*, Report No. EERC-73-27, Earthquake Engineering Research Center.

Biddah, A., and Heidebrecht, A.C., 1999, "Evaluation of the seismic level of protection afforded to steel moment resisting frame structures designed for different design philosophies," *Canadian Journal of Civil Engineering*, Vol. 26, pp. 35-54.

Bjorhovde, R., Goland, L.J., and Benac, D.J., 1999, *Tests of Full-Scale Beam-to-Column Connections*, Southwest Research Institute, San Antonio, Texas.

Bruneau, M., and Mahin, S.A., 1991, "Full-scale tests of butt-welded splices in heavy-rolled steel sections subjected to primary tensile stresses," *Engineering Journal*, Vol. 28, No. 1, pp. 1-17.

BSI, 2019, *Guide on Methods for Assessing the Acceptability of Flaws in Metallic Structures*, BS 7910, British Standards Institution.

Cattan, J., 1996, "Statistical analysis of Charpy V-notch toughness for steel wide flange structural shapes," *Modern Steel Construction*, Vol. 36, No.5, pp. 38-44.

Charney, F.A., and Marshall, J., 2006, "A comparison of the Krawinkler and scissors models for including beam-column joint deformations in the analysis of moment resisting steel frames," *Engineering Journal*, Vol. 43, No. 1, pp. 31-48.

Chen, Y., Pan, L., and Jia, L.-J., 2017, "Post-buckling ductile fracture analysis of panel zones in welded steel beam-to-column connections," *Journal of Constructional Steel Research*, Vol. 132, No. 5, pp. 117-129.

Chi, B., and Uang, C.-M., 2002, "Cyclic response and design recommendations of reduced beam section moment connections with deep columns," *Journal of Structural Engineering*, Vol. 128, No. 4, pp. 464-473.

Chi, W.-M., and Deierlein, G.G., 2000*, Integration of Analytical Investigations on the Fracture Behavior of Welded Moment Resisting Connections*, John A. Blume Earthquake Engineering Center, Report No. 136, Stanford University, Stanford, California.

Chi, W.-M., Deierlein, G.G., and Ingraffea, A., 2000, "Fracture toughness demands in welded beam-column moment connections," *Journal of Structural Engineering*, Vol. 126, No. 1, pp. 88-97.

Chisholm, M.P., Pekelnicky, R.G., and Malley, J.O., 2017, "High-rise pre-Northridge partial joint penetration column splice repair," *Proceedings*, 2017 Structural Engineers Association of California Annual Convention.

Chung, Y.L., Nagae, T., Hitaka, T., and Nakashima, M., 2010, "Seismic resistance capacity of high-rise buildings subjected to long-period ground motions: E-Defense shaking table test," *Journal of Structural Engineering*, Vol. 136, No. 6, pp. 637-644.

Collins, W., Sherman, R., Leon, R., and Connor, R., 2016a, "State-of-the-art fracture characterization. II: Correlations between Charpy V-Notch and the master curve reference temperature," *Journal of Bridge Engineering*, American Society of Civil Engineers, Vol. 21, No. 12.

Collins, W., Sherman, R., Leon, R., and Connor, R., 2016b, "State-of-the-Art fracture characterization. I: Master curve analysis of legacy bridge steels," *Journal of Bridge Engineering*, American Society of Civil Engineers, Vol. 21, No. 12.

Connor, R.J., and Lloyd, J.B., 2017, *Maintenance Actions to Address Fatigue Cracking in Steel Bridge Structures: Proposed Guidelines and Commentary*, Purdue University, West Lafayette, Indiana.

Eads, L., Miranda, E., Krawinkler, H., and Lignos, D.G., "An efficient method for estimating the collapse risk of structures in seismic regions," *Earthquake Engineering & Structural Dynamics*, Vol. 42, No. 1.

El-Tawil, S., 2000, "Panel zone yielding in steel moment connections," *Engineering Journal*, Vol. 37, No. 3, pp. 120-131.

El-Tawil, S., Vidarsson, E., Mikesell, T., and Kunnath, S.K., 1999, "Inelastic behavior and design of steel panel zones," *Journal of Structural Engineering*, Vol 125, No. 2, pp. 183-193.

Elkady, A., and Lignos, D.G., 2018, "Full-scale testing of deep wide-flange steel columns under multi-axis cyclic loading: Loading sequence, boundary effects and out-of-plane brace force demands," *Journal of Structural Engineering*, Vol. 144, No. 2.

Engelhardt, M.D., and Sabol, T.A., 1998, "Reinforcing of steel moment connections with cover plates: benefits and limitations, *Engineering Structures*, Vol. 20, No. 4, pp. 510-520.

Engelhardt, M.D., Fry, G.T., Jones, S., Venti, M. and Holliday, S., 2000, *Behavior and Design of Radius-Cut Reduced Beam Section Connections*, Report No. SAC/BD-00/17, prepared by the SAC Joint Venture, a partnership of the Structural Engineers Association of California (SEAOC), Applied Technology Council (ATC), and California Universities for Research in

Earthquake Engineering (CUREe), for the Federal Emergency Management Agency, Washington, D.C.

EricksonKirk, M., and EricksonKirk, M., 2006a, "The relationship between the transition and upper-shelf fracture toughness of ferritic steels," *Fatigue Fracture of Engineering Materials and Structures*, Vol. 29, pp. 672-684.

EricksonKirk, M., and EricksonKirk, M., 2006b, "An upper-shelf fracture toughness master curve for ferritic steels," *International Journal of Pressure Vessels and Piping*, Vol. 83, No. 8, pp. 571-583.

FEMA, 1991, *NEHRP Recommended Provisions for the Development of Seismic Regulations for New Buildings Part 1: Provisions*, FEMA 222, prepared by Building Seismic Safety Council for Federal Emergency Management Agency, Washington, D.C.

FEMA, 1995, *Interim Guidelines: Evaluation, Repair, Modification and Design of Welded Steel Moment Frame Structures*, FEMA 267, Federal Emergency Management Agency, Washington, D.C.

FEMA, 1997, *Connection Test Summaries*, Report No. FEMA 289, prepared by the SAC Joint Venture, a partnership of the Structural Engineers Association of California (SEAOC), Applied Technology Council (ATC), and California Universities for Research in Earthquake Engineering (CUREe), for the Federal Emergency Management Agency, Washington, D.C.

FEMA, 2000a, *Recommended Seismic Design Criteria for New Steel Moment Frame Buildings*, FEMA 350 Report, prepared by the SAC Joint Venture, a partnership of the Structural Engineers Association of California (SEAOC), Applied Technology Council (ATC), and California Universities for Research in Earthquake Engineering (CUREe), for the Federal Emergency Management Agency, Washington, D.C.

FEMA, 2000b, *Recommended Seismic Evaluation and Upgrade Criteria for Existing Welded Steel Moment-Frame Buildings*, FEMA 351 Report, prepared by the SAC Joint Venture, a partnership of the Structural Engineers Association of California (SEAOC), Applied Technology Council (ATC), and California Universities for Research in Earthquake Engineering (CUREe), for the Federal Emergency Management Agency, Washington, D.C.

FEMA, 2000c, *Recommended Postearthquake Evaluation and Repair Criteria for Welded Steel Moment-Frame Buildings*, FEMA 352 Report, prepared by the SAC Joint Venture, a partnership of the Structural Engineers Association of California (SEAOC), Applied Technology Council (ATC), and California Universities for Research in Earthquake Engineering (CUREe), for the Federal Emergency Management Agency, Washington, D.C.

FEMA, 2000d, *A Policy Guide to Steel Moment Frame Construction*, FEMA 354 Report, prepared by the SAC Joint Venture, a partnership of the Structural Engineers Association of California (SEAOC), Applied Technology Council (ATC), and California Universities for Research in Earthquake Engineering (CUREe), for the Federal Emergency Management Agency, Washington, D.C.

FEMA, 2000e, *State of the Art Report on Systems Performance of Moment Steel Frame Buildings in Earthquakes*, FEMA 355C Report, prepared by the SAC Joint Venture, a partnership of the Structural Engineers Association of California (SEAOC), Applied Technology Council (ATC), and California Universities for Research in Earthquake Engineering (CUREe), for the Federal Emergency Management Agency, Washington, D.C.

FEMA, 2000f, *State of the Art Report on Connection Performance*, FEMA 355D Report, prepared by the SAC Joint Venture, a partnership of the Structural Engineers Association of California (SEAOC), Applied Technology Council (ATC), and California Universities for Research in Earthquake Engineering (CUREe), for the Federal Emergency Management Agency, Washington, D.C.

FEMA, 2000g, *State of the Art Report on Past Performance of Steel Moment-Frame Buildings in Earthquakes*, FEMA 355E Report, prepared by the SAC Joint Venture, a partnership of the Structural Engineers Association of California (SEAOC), Applied Technology Council (ATC), and California Universities for Research in Earthquake Engineering (CUREe), for the Federal Emergency Management Agency, Washington, D.C.

FEMA, 2009, *Quantification of Building Seismic Performance Factors*, FEMA P-695 Report, prepared by the Applied Technology Council for the Federal Emergency Management Agency, Washington, D.C.

FHWA, 2013, *Manual for Repair and Retrofit of Fatigue Cracks in Steel Bridges*, Report No. FHWA-IF-13-020, prepared by the University of Minnesota for the Federal Highway Administration.

Fielding, D.J., Chen, W.F., and Beedle, L.S., 1972, *Frame Analysis and Connection Shear Deformation*, Fritz Engineering Laboratory Report No. 333.16, Lehigh University, Bethlehem, Pennsylvania.

Fielding D.J., and Huang, J.S., 1971, "Shear in steel beam-to-column connections," *Welding Journal*, Vol. 50, No. 3, pp. 313-326.

Fisher, J.W., and Pense, A.W., 1987, "Experience with use of heavy W shapes in tension," *Engineering Journal*, Vol. 24, No. 2.

Fisher, J., Dexter, R., and Kaufmann, E., 1995, "Fracture mechanics of welded structural steel connections," *SAC 95-09, Background Reports: Metallurgy, Fracture Mechanics, Welding, Moment Connections and Frame Systems Behavior*, prepared by the SAC Joint Venture, a partnership of the Structural Engineers Association of California (SEAOC), Applied Technology Council (ATC), and California Universities for Research in Earthquake Engineering (CUREe), for the Federal Emergency Management Agency, Washington, D.C.

Gagnon, D.P., and Kennedy, D.L., 1989, "Behaviour and ultimate tensile strength of partial joint penetration groove welds," *Canadian Journal of Civil Engineering*, NRC Research Press, Vol. 16, No. 3, pp. 384-399.

Galasso, C., Stillmaker, K., Eltit, C., and Kanvinde, A., 2015, "Probabilistic demand and fragility assessment of welded column splices in steel moment frames," *Earthquake Engineering & Structural Dynamics*, Vol. 44, No. 11, pp. 1823-1840.

Ghobarah, A., Korol, R.M., and Osman, A., 1992, "Cyclic behavior of extended end-plate joints," *Journal of Structural Engineering*, Vol. 118, No. 5, pp.1333-1353.

Gomez, I., Kwan, Y., Kanvinde, A., and Grondin, G., 2008, *Strength and Ductility of Welded Joints Subjected to Out-Of-Plane Bending*, University of California, Davis, California, University of Alberta, Canada.

Gross, J.L., Engelhardt, M.D., Uang, C.-M., Kazuhiko, K., and Iwankiw, N.R., 2003, *Design Guide 12: Modifications of Existing Welded Steel Moment Frame Connections for Seismic Resistance*, American Institute of Steel Construction, Chicago, Illinois.

Gupta, U., 2013, *Cyclic Loading Analysis of Doubler Plate Attachment Details for Steel Moment Resisting Frames*, Thesis, University of Texas at Austin, Austin, Texas.

Gupta, A., and Krawinkler, H., 1999, *Prediction of Seismic Demands for SMRFs with Ductile Connections and Elements*, SAC/BD-99/06, SAC Steel Project Background Document, prepared by the SAC Joint Venture, a partnership of the Structural Engineers Association of California (SEAOC), Applied Technology Council (ATC), and California Universities for Research in Earthquake Engineering (CUREe), for the Federal Emergency Management Agency, Washington, D.C.

Gupta, A., and Krawinkler, H., 2000, "Dynamic P-delta effects for flexible inelastic steel structures," *Journal of Structural Engineering*, Vol. 126, No. 1, pp. 145-154.

Hall, J.F., 1998, "Seismic response of steel frame buildings to near-source ground motions," *Earthquake Engineering & Structural Dynamics*, Vol. 27, No. 12, pp. 1445-1464.

Han, S.W., Moon, K.H., and Jung, J., 2014, "Cyclic performance of welded unreinforced flange-welded web moment connections," *Earthquake Spectra*, Vol. 30, No. 4, pp. 1663-1681.

Hancock, J.W., and Mackenzie, A.C., 1976, "On the mechanisms of ductile failure in high-strength steels subjected to multi-axial stress-states," *Journal of the Mechanics and Physics of Solids*, Vol. 24, pp. 147-169.

Hayes, J.M., 1957, "Effect of initial eccentricities in column performance and capacity," *Journal of the Structural Division*, ASCE, Vol. 83, No. 6, pp. 1-40.

Hibbitt, H.D., Karlson, K., and Sorenson, S., 1998, *ABAQUS v5.8*, Dassault Systèmes Simulia Corp., Providence, Rhode Island.

Hoffman, C.R., 1980, *Interpretive Report on Small-Scale Test Correlations with Fracture Toughness Data*, Thesis, Lehigh University, Bethlehem, Pennsylvania.

Hsiao, P.-C., Lehman, D.E., Berman, J.W., Roeder, C.W., and Powell, J., 2014, "Seismic vulnerability of older braced frames," *Journal of Performance of Constructed Facilities*, Vol. 28, No. 1, pp. 108-120.

Irwin, G.R., 1957, "Analysis of stresses and strains near the end of a crack transversing a plate," *Journal of Applied Mechanics*, Vol. 24, pp. 361-364.

Jin, J., and El-Tawil, S., 2005, "Evaluation of FEMA-350 Seismic Provisions for Steel Panel Zones," *Journal of Structural Engineering*, Vol. 131, No. 2, pp. 250-258.

Johnson, M Q., Mohr, B., and Barsom, J., 2000, *Evaluation of Mechanical Properties in Full-Scale Connections and Recommended Minimum Weld Toughness for Moment Resisting Frames*, SAC/BD-00/14, SAC Steel Project Background Document, prepared by the SAC Joint Venture, a partnership of the Structural Engineers Association of California (SEAOC), Applied Technology Council (ATC), and California Universities for Research in Earthquake Engineering (CUREe), for the Federal Emergency Management Agency, Washington, D.C.

Jones, S.L., Fry, G.T., and Engelhardt, M.D., 2002, "Experimental evaluation of cyclically loaded reduced beam section moment connections," *Journal of Structural Engineering*, Vol. 128, No. 4, pp. 441-451.

Kadysiewski, S., and Mosalam, K.M., 2009, *Modeling of Unreinforced Masonry Infill Walls Considering In-Plane and Out-Of-Plane Interaction*, Pacific Earthquake Engineering Research Center, Berkeley, California.

Kanvinde, A.M., Fell, B.V., Gomez, I.R., and Roberts, M., 2008, "Predicting fracture in structural fillet welds using traditional and micromechanical fracture models," *Engineering Structures*, Vol. 30, No. 11, pp. 3325-3335.

Kanvinde, A.M., 2017, "Predicting fractures in civil engineering steel structures: state of the art," *Journal of Structural Engineering*, Vol. 143, No. 3.

Kaufmann, E.J., Fisher, J.W., Di Julio, R.M., and Gross, J.L., 1997, *Failure Analysis of Welded Steel Moment Frames Damaged in the Northridge Earthquake*, NISTIR-5944, National Institute of Standards and Technology, Gaithersburg, Maryland.

Kaufmann, E. J., Xue, M., Lu, L.-W., and Fisher, J. W., 1996, "Achieving ductile behavior of moment connections," *Modern Steel Construction*, Vol. 36. No. 1, pp. 30-39.

Kawano, A., 1984, "Inelastic behavior of low-rise steel frame based on a weak beam-to-column connection philosophy to earthquake motion," *Proceedings*, 8th World Conference on Earthquake Engineering, Vol. 4, San Francisco, California.

Kim, D.-W., Blaney, C., and Uang, C.-M., 2015, "Panel zone deformation capacity as affected by weld fracture at column kinking location," *Engineering Journal*, Vol. 53, No. 1, pp. 27-46.

Kim, K.D., and Engelhardt, M.D., 2002, "Monotonic and cyclic loading models for panel zones in steel moment frames," *Journal of Constructional Steel Research*, Vol. 58, No. 5, pp. 605-635.

Kim, S.-Y., and Lee, C.-H., 2017, "Seismic retrofit of welded steel moment connections with highly composite floor slabs," *Journal of Constructional Steel Research*, Vol. 139, pp. 62-88.

Kolwankar, S., Kanvinde, A., Kenawy, M., and Kunnath, S., 2017, "Uniaxial nonlocal formulation for geometric nonlinearity–induced necking and buckling localization in a steel bar," *Journal of Structural Engineering*, Vol. 143, No. 9.

Krawinkler, A., 1978, "Shear in beam-column joints in seismic steel design of steel frames," *Engineering Journal*, Vol. 15, No. 3, pp. 82-91.

Krawinkler, H., Bertero, V.V., and Popov, E.P., 1971, *Inelastic Behavior of Steel Beam-to-Column Subassemblages*, Report No. EERC-71-07. Earthquake Engineering Research Center, University of California, Berkeley, California.

Lee, C.-H., and Uang, C.-M., 1997, "Analytical modelling of dual panel zone in haunch repaired steel MRFs," *Journal of Structural Engineering*, Vol. 123, No. 1, pp. 20-29.

Lee, C.-H., and Uang, C.-M., 2001, "Analytical modelling and seismic design of steel moment connections with welded straight haunch," *Journal of Structural Engineering*, Vol. 127, No. 9, pp. 1028-1035.

Lee, D., Cotton, S., Dexter, R.J., Hajjar, J.F., Ye, Y., and Ojard, S.D., 2002, *Column Stiffener Detailing and Panel Zone Behavior of Steel Moment Frame Connections*, Report No. ST-01-3.2, Department of Civil Engineering, University of Minnesota, Minneapolis, Minnesota.

Lee, C.-H., Jeon, S-W., Kim, J-H., and Uang, C.-M., 2005a, "Effects of panel zone strength and beam web connection method on seismic performance of reduced beam section steel moment connections," *Journal of Structural Engineering*, Vol. 131, No. 2, pp. 1854-1865.

Lee, D., Cotton. S. C, Hajjar, J.F., Dexter, R.J., and Ye, Y., 2005b, "Cyclic behavior of steel moment-resisting connections reinforced by alternative column stiffener details II. Panel zone behavior and doubler plate detailing," *Engineering Journal*, Vol. 42, No. 4, pp. 189-214.

Liew, J.Y.R., and Chen W.F., 1995, "Analysis and design of steel frames considering panel joint deformations," *Journal of Structural Engineering*, Vol. 121, No. 10, pp. 1531-1539.

Lignos, D.G., Eads, L., and Krawinkler, H., 2011a, "Effect of composite action on collapse capacity of steel moment frames under cyclic loading," *Proceedings*, Eurosteel, Budapest, Hungary.

Lignos, D.G., Krawinkler, H., and Whittaker, A., 2011b, "Prediction and validation of sidesway collapse of two scale models of a 4-story steel moment frame," *Earthquake Engineering and Structural Dynamics*, Vol. 40, No. 7, pp. 807-825.

Lin, K.C., Tsai, K.C., Kong, S.L., and Hsieh, S.H., 2000, "Effects of panel zone deformations on cyclic performance of welded moment connections," *Proceedings*, 12th World Conference on Earthquake Engineering (WCEE). Auckland, New Zealand.

Liu, J., and Astaneh-Asl., A, 2000, "Cyclic tests on simple connections including effects of the slab", *Journal of Structural Engineering,* Vol. 126, No. 1, pp. 32-39.

Luo, P., Asada, H., Uang, C.-M., and Tanaka, T., 2020, "Directionality effect on strength of partial-joint-penetration groove weld joints," *Journal of Structural Engineering*, Vol. 146, No. 4.

Malley, J.O., 1998, "SAC Steel Project: Summary of Phase 1 testing investigation results," *Engineering Structures*, Vol. 20, No. 4, pp. 300-309.

Malley, J.O., Sinclair, M., Graf, T., Blaney, C., Fraynt, M., Uang, C.-M., Newell, J., and Ahmed, T., 2009, "Seismic upgrade of a 15-story steel moment frame building—Satisfying performance criteria with application of experimental and analytical procedures," *Proceedings,* ATC&SEI Conference on Improving the Seismic Performance of Existing Buildings and Other Structures, organized by the Applied Technology Council and the Structural Engineering Institute of the American Society of Civil Engineers, pp 75-84.

Mao, C., Ricles, J.M., Lu, L., and Fisher, J.W., 2001, "Effect of local details on ductility of welded moment connections," *Journal of Structural Engineering*, Vol. 127, No. 9, pp. 1036-1044.

McKenna, F., 1997, *Object Oriented Finite Element Programming Frameworks for Analysis, Algorithms and Parallel Processing, Ph.D. Dissertation*, Department of Civil and Environmental Engineering, University of California, Berkeley, California.

McKenna, F., Fenves, G., and Scott, M., 2000, *Open System for Earthquake Engineering Simulation (OpenSees)*, Pacific Earthquake Engineering Research Center, University of California, Berkeley.

Myers, A., Kanvinde, A., Deierlein, G., and Fell, B., 2009, "Effect of weld details on the ductility of steel column baseplate connections," *Journal of Constructional Steel Research*, Vol. 65, No. 6, pp. 1366-1373.

Newell J., and Uang, C.-M., 2006, *Cyclic Testing of Steel Moment Connections for the Caltrans District 4 Office Building Seismic Rehabilitation*, Report No. SSRP 05-03, University of California San Diego, San Diego, California.

NIST, 2010, *Evaluation of the FEMA P-695 Methodology for Quantification of Building Seismic Performance Factors,* NIST GCR 10-917-8, prepared by the NEHRP Consultants Joint Venture, a partnership of the Applied Technology Council and the Consortium of Universities for Research in Earthquake Engineering for the National Institute of Standards and Technology, Gaithersburg, Maryland.

NIST, 2011a, *Nonlinear Structural Analysis for Seismic Design: A Guide for Practicing Engineers, NEHRP Seismic Design Technical Brief No. 4*, prepared by the NEHRP Consultants Joint Venture, a partnership of the Applied Technology Council and the Consortium of Universities for

Research in Earthquake Engineering for the National Institute of Standards and Technology, Gaithersburg, Maryland.

NIST, 2011b, *Research Plan for the Study of Seismic Behavior and Design of Deep, Slender Wide Flange Structural Steel Beam-Column Members,* prepared by the NEHRP Consultants Joint Venture, a partnership of the Applied Technology Council and the Consortium of Universities for Research in Earthquake Engineering for the National Institute of Standards and Technology, Gaithersburg, Maryland.

NIST, 2016, *Seismic Design of Steel Special Moment Frames: A Guide for Practicing Engineers*, 2nd Edition, NEHRP Seismic Design Technical Brief No. 2, NIST GCR 16-917-41, National Institute of Standards and Technology, Gaithersburg, Maryland.

NIST, 2017, *Guidelines for Nonlinear Structural Analysis for Design of Buildings, Part IIa – Steel Moment Frames*, GCR 17-917-46v2, prepared by the Applied Technology Council for the National Institute of Standards and Technology, Gaithersburg, Maryland.

NIST, 2021, *Seismic Behavior and Design of Deep, Slender Wide-Flange Structural Steel Beam-Columns*, NIST TN 2169, National Institute of Standards and Technology, Gaithersburg, Maryland.

Nudel, A., Dana, M., and Maclise, L., 2013, "Adaptive reuse: Creating a new school of dentistry in an outdated urban office building," *Proceedings*, 2013 Structural Engineers Association of California Annual Convention .

Nudel, A., Marusich, S., Dana, M., and Roufegarinejad, A., 2015, "Evaluation and remediation of pre-Northridge steel moment frame column splices," *Proceedings,* ATC&SEI Conference on Improving the Seismic Performance of Existing Buildings and Other Structures, organized by the Applied Technology Council and the Structural Engineering Institute of the American Society of Civil Engineers, pp. 287-302.

Nuttayasakul, N., 2000, *Finite Element Fracture Mechanics Study of Partial Penetration Welded Splice*, Thesis, Stanford University, Stanford, California.

Ozkula, G., Uang, C.-M., and Harris, J., 2021, "Development of enhanced seismic compactness requirements for webs in wide-flange steel columns," *Journal of Structural Engineering*, Vol. 147, No. 7.

PEER/ATC, 2010, *Modeling and Acceptance Criteria for Seismic Design and Analysis of Tall Buildings*, PEER/ATC 72-1, prepared by the Applied Technology Council for the Pacific Earthquake Engineering Research Center, Berkeley, California.

Pekelnicky, R., and Malley. J, 2019, "Seismic performance of tall steel framed buildings built between 1960 and 1994," *Proceedings*, 2019 Structural Engineers Association of California Annual Convention.

Popov, E.P., 1987, "Panel zone flexibility in seismic moment joints," *Journal of Constructional Steel Research*, Vol. 8, pp. 91-118.

Popov, E.P., and Pinkney, R.B., 1969, "Cyclic yield reversals in steel building connections," *Journal of Structural Engineering*, Vol. 95, No. ST3, pp 327-353.

Popov, E.P., and Stephen, R.M., 1970, *Cyclic Loading of Full Size Steel Connections*, Report EERC-70-3, University of California, Berkeley, California.

Popov, E.P., and Stephen, R.M., 1976, *Tensile Capacity of Partial Penetration Welds*, Report No. EERC 76,28, Earthquake Engineering Research Center, University of California.

Popov, E.P., Amin, N.R., Louie, J.J.C., and Stephen, R. M., 1986, "Cyclic behavior of large beam-column assemblies," *Engineering Journal*, Vol. 23, No. 1, pp. 9-23.

Popov, E.P., Blondet, M., Stepanov, L., and Stojadinovic, B., 1996, *Full Scale Steel Beam-Column Connection Tests*, SAC 96-01, Technical Report: Experimental Investigations of Beam-Column Subassemblies, prepared by the SAC Joint Venture, a partnership of the Structural Engineers Association of California (SEAOC), Applied Technology Council (ATC), and California Universities for Research in Earthquake Engineering (CUREe), for the Federal Emergency Management Agency, Washington, D.C.

Reynolds M., 2020, *Alternative Weld Details and Design for Continuity Plates and Doubler Plates for Applications in Special Moment Frames*, Doctoral Thesis, University of California San Diego, San Diego, California.

Reynolds, M., Huynh, Q., Rafezy, B., and Uang, C.-M., 2020, "Strength of partial-joint-penetration groove welds as affected by root opening, reinforcing, and loading direction," *Journal of Structural Engineering*, Vol. 146, No. 8.

Reynolds M., and Uang, C.-M., 2021, "Economical weld details and design for continuity and doubler plates in steel special moment frames," *Journal of Structural Engineering*, Vol. 148, No. 1.

Rice, J.R., 1968, "A path independent integral and the approximate analysis of strain concentration by notches and cracks," *Journal of Applied Mechanics*, Vol. 35, No. 2, pp. 379-386.

Rice, J.R., and Tracey, D.M., 1969, "On the ductile enlargement of voids in triaxial stress fields," *Journal of the Mechanics and Physics of Solids*, Vol. 17, pp. 201-217.

Ricles, J.M., Fisher, J.W., Lu, L.-W., and Kaufman, E.J., 2002a, "Development of improved welded moment connections for earthquake-resistant design," *Journal of Constructional Steel Research*, Vol. 58, pp. 565-604.

Ricles, J.M., Mao, C., Lu, L., and Fisher, J.W., 2002b, "Inelastic cyclic testing of welded unreinforced moment connections," *Journal of Structural Engineering*, Vol. 128, No. 4, pp. 429-440.

Ricles, J.M., Zhang, X., Lu, L.-W., and Fisher, J.W., 2004, *Development of Seismic Guidelines for Deep-Column Steel Moment Connections*, ATLSS Report No. 04-13, Lehigh University, Bethlehem, Pennsylvania.

Rodgers, J.E., and Mahin, S.A., 2006, "Effects of connection fractures on global behavior of steel moment frames subjected to earthquakes," *Journal of Structural Engineering*, Vol. 132, No. 1, pp. 78-88.

Roeder, C.W., 2002, "General issues influencing connection performance," *Journal of Structural Engineering*, Vol. 128, No. 4, pp. 420-428.

Roeder, C.W., and Foutch, D.A., 1996, "Experimental results for seismic resistant steel moment frame construction," *Journal of Structural Engineering*, Vol. 122, No. 6, pp. 581-588.

Schellenberg, A.H., 2008, *Advanced Implementation of Hybrid Simulation*, Ph.D. Dissertation, Department of Civil and Environmental Engineering, University of California, Berkeley, California.

Schneider, S.P. and Amidi, A., 1998, "Seismic behavior of steel frames with deformable panel zones," *Journal of Structural Engineering*, Vol. 124, No. 1, pp. 35-42.

Schneider, S.P., Roeder, C.W., and Carpenter, J.E., 1993, "Seismic behavior of moment-resisting steel frames: Experimental study," *Journal of Structural Engineering*, Vol. 119, No. 6, pp. 1885-1902.

SEAOC, 1980, *Recommended Lateral-Force Requirements and Commentary*, Seismology Committee of Structural Engineers Association of California, San Francisco, California.

SEAOC, 1988, *Recommended Lateral-Force Requirements and Commentary*, Seismology Committee of Structural Engineers Association of California, San Francisco, California.

Shaw, S.M., Stillmaker, K., and Kanvinde, A.M., 2015, "Seismic response of partial-joint-penetration welded column splices in moment-resisting frames," *Engineering Journal*, Vol. 52, No. 2, pp 87-108.

Shen, J., Sabol, T.A., Akbas, B., Sutchiewcharn, N., and Cai, W., 2010, "Seismic demand on column splices in steel moment frames, " *Engineering Journal*, Vol. 47, No. 4.

Shin, S., 2017, *Experimental and Analytical Investigation of Panel Zone Behavior in Steel Moment Frames*, Doctoral Thesis, University of Texas at Austin, Austin, Texas.

Shirsat, P.S., and Engelhardt, M.D., 2012, "Preliminary analysis of doubler plate attachment details for steel moment frames," *Proceedings*, 15th World Conference on Earthquake Engineering (WCEE), Lisbon, Portugal.

Skiadopoulos, A., Elkady, A., and Lignos, D., 2021a, "Proposed panel zone model for seismic design of steel moment-resisting frames," *Journal of Structural Engineering*, Vol 147, No. 4.

Skiadopoulos, A., and Lignos, D., 2021b, "Development of inelastic panel zone database," *Journal of Structural Engineering*, Vol 147, No. 4.

Song, B., Galasso, C., and Kanvinde, A., 2020, "Advancing fracture fragility assessment of pre-Northridge welded column splices," *Earthquake Engineering & Structural Dynamics*, Vol. 49 No. 2, pp. 132-154.

Stillmaker, K.R., 2016, *Probabilistic Fracture Mechanics Based Assessment of Welded Column Splices in Steel Moment Frames*, Thesis, University of California Davis, California.

Stillmaker, K., Kanvinde, A., and Galasso, C., 2016, "Fracture mechanics-based design of column splices with partial joint penetration welds," *Journal of Structural Engineering*, Vol. 142, No. 2.

Stillmaker, K., Kanvinde, A. M., and Galasso, C., 2015, "Derivation of fracture mechanics based design formulas for partial joint penetration welded column splices," *Proceedings,* Structures Congress 2015, American Society of Civil Engineers, pp. 2372-2383.

Stillmaker, K., Lao, X., Galasso, C., and Kanvinde, A., 2017, "Column splice fracture effects on the seismic performance of steel moment frames," *Journal of Constructional Steel Research*, Vol. 137, pp .93-101.

Stojadinovic, B., Goel, S.C., Lee, K.-H., Margarian, A.G., and Choi, J.-H., 2000, "Parametric tests on unreinforced steel moment connections," *Journal of Structural Engineering*, Vol. 126, No. 1, pp. 40-49.

Talaat, M., and Mosalam, K. M., 2009, "Modeling progressive collapse in reinforced concrete buildings using direct element removal," *Earthquake Engineering & Structural Dynamics*, Vol. 38, No. 5, pp. 609-634.

Tam, H., Becker, T., Roufegarinejad, A., and Chisholm, M., 2021, *Column splice Retrofits*, SEAONC University Research Program, San Francisco, California.

Teal, E.J., 1975, "Seismic design practice for steel buildings," *Engineering Journal*, Vol. 12, pp. 101-151.

Tide, R.H.R., 2000, "Evaluation of steel properties and cracking in 'k' –area of W shapes," *Engineering Structures*, Vol. 22, No. 2, pp. 128-134.

Tsai, K.C., and Popov, E.P., 1988, *Steel Beam-Column Joints in Seismic Moment Resisting Frames*, Report No. UCB/EERC-88/19, Earthquake Engineering Research Center, University of California, Berkeley, California.

Tsai, K.C., and Popov, E.P., 1990, "Seismic panel zone design effect on elastic story drift in steel frames," *Journal of Structural Engineering*, Vol. 116, No. 2, pp. 3285-3301.

Uang, C.-M., Bondad, D., and Lee, C.-H., 1998, "Cyclic performance of haunch repaired steel moment connections: Experimental testing and analytical modeling," *Engineering Structures*, Vol. 20. No. 4, pp. 552-561.

Uang, C.-M., Yu, Q.-S., Noel, S. and Gross, G., 2000, "Cyclic testing of steel moment connections rehabilitated with RBS or welded haunch," *Journal of Structural Engineering*, Vol. 126, No. 1.

UBC, 1967, *The Uniform Building Code - Volume I*, International Conference of Building Officials, Pasadena, California.

UBC, 1985, *The Uniform Building Code*, International Conference of Building Officials, Pasadena, California.

UBC, 1988, *The Uniform Building Code*, International Conference of Building Officials, Whittier, California.

Wallin, K., 1993, "Irradiation damage effects on the fracture toughness transition curve shape for reactor pressure vessel steels," *International Journal of Pressure Vessels and Piping*, Vol. 55, No. 1, pp. 61-79.

Wallin, K., 1998, *Master Curve Analysis of Ductile to Brittle Transition Region Fracture Toughness Round Robin Data*, VTT Publications 367, VTT manufacturing Technology.

Wallin, K., 2011, *Fracture Toughness of Engineering Materials: Estimation and Application*, EMAS Publishing.

Wang, T., Mosqueda, G., Jacobsen, A., and Delgado, M.C., 2011, "Performance evaluation of a distributed hybrid test framework to reproduce the collapse behavior of a structure," *Earthquake Engineering and Structural Dynamics*, Vol. 41, No. 2, pp. 295-313.

Weinberg, P., and Goltz, J., 1999, *The Impact of Earthquakes on Welded Steel Moment Frame Buildings: Experience in Past Earthquakes*, SAC/BD-99/11, SAC Steel Project Background Document, prepared by the SAC Joint Venture, a partnership of the Structural Engineers Association of California (SEAOC), Applied Technology Council (ATC), and California Universities for Research in Earthquake Engineering (CUREe), for the Federal Emergency Management Agency, Washington, D.C.

Wells, A.A., 1969, "Crack opening displacements from elastic-plastic analyses of externally notched tension bars," *Engineering Fracture Mechanics*, Vol. 1, No. 3, pp. 399-410.

Wu, S., and Wang, X.,2010, "Mesh dependence and nonlocal regularization of one-dimensional strain softening plasticity," *Journal of Engineering Mechanics*, Vol. 136, No. 11, pp. 1354-1365.

Wu, T.Y., El-Tawil, S., and McCormick, J., 2018, "Highly ductile limits for deep steel columns," *Journal of Structural Engineering*, Vol. 144, No. 4.

Yabe, Y., Sakamoto, S., and Yakushiji, K., 1994, "Bending strength of steel column members with partial penetration groove welded joints," *Journal of Structural and Construction Engineering*, Vol. 59. No. 459.

Yu, Q.S., and Uang, C.-M., 2000, "Effects of lateral bracing and system restraint on the behavior of reduced beam section moment frame connections," *Proceedings,* STESSA 2000, International Conference on Behavior of Steel Structures in Seismic Areas, Montreal, Canada.

Youssef, N.F., Bonowitz, D., and Gross, J.L.,1995, *A Survey of Steel Moment-Resisting Frame Buildings Affected by the 1994 Northridge Earthquake*, NISTIR 5624, National Institute of Standards and Technology, Gaithersburg, Maryland.

Zhang, X., and Ricles, J.M., 2006, "Experimental evaluation of reduced beam section connections to deep columns," *Journal of Structural Engineering*, Vol. 132, No. 3, pp. 346-357.

Project Participants

National Institute of Standards and Technology

John (Jay) Harris
Engineering Laboratory (MS8604)
National Institute of Standards and Technology
100 Bureau Drive
Gaithersburg, Maryland 20899

Applied Technology Council

Jon A. Heintz
Applied Technology Council
201 Redwood Shores Parkway, Suite 240
Redwood City, California 94065

Chiara McKenney (Project Manager)
Applied Technology Council
201 Redwood Shores Parkway, Suite 240
Redwood City, California 94065

Ayse Hortacsu
Applied Technology Council
201 Redwood Shores Parkway, Suite 240
Redwood City, California 94065

Project Technical Committee

James O. Malley (Project Director)
Degenkolb Engineers
375 Beale Street, Suite 500
San Francisco, California 94105

Duane Miller
Lincoln Electric
22801 St. Clair Ave.
Cleveland, Ohio 44117

Masume Dana
Forell | Elsesser Engineers
160 Pine Street, Suite 600
San Francisco, California 94111

Robert Pekelnicky
Degenkolb Engineers
375 Beale Street, Suite 500
San Francisco, California 94105

Amit Kanvinde
University of California, Davis
One Shields Avenue
Davis, California 95616

Thomas Sabol
Englekirk Structural Engineers
888 S. Figueroa Street, 18th Floor
Los Angeles, California 90017

Larry Kruth
American Institute of Steel Construction
130 East Randolph, Suite 2000
Chicago, Illinois 60601

Chia-Ming Uang
University of California, San Diego
9500 Gilman Dr.
La Jolla, California 92093

Working Group Members

Aditya Jhunjhunwala
University of California, Davis
One Shields Avenue
Davis, California 95616

Mathew Reynolds
Peter Kiewet Sons ULC
4350 Still Creek Drive, #310
Burnaby, British Columbia V5C 0G5